Nanotherapeutics to Combat Infections

by

Pavan Walvekar

(M. Pharm, Rajiv Gandhi University of Health Sciences, India)

Submitted as fulfilment of the requirements for the degree of Doctor of Philosophy in Pharmaceutics at the Discipline of Pharmaceutical Sciences of the School of Health Sciences at the University of KwaZulu-Natal

Supervisor: Professor Thirumala Govender
(PhD, University of Nottingham, United Kingdom)

Co-supervisor: Dr. Chunderika Mocktar
(PhD, University of KwaZulu-Natal, South Africa)

Date submitted: 9th May 2019

"The capacity to learn is a gift; the ability to learn is a skill; the willingness to learn is a choice"

-Brian Herbert-

"***This thesis is dedicated to my beloved parents for their endless love, support and encouragement”***

Declaration 1-Plagiarism

I, Mr. Pavan Walvekar, declare that

1. The research data reported in this thesis, except where otherwise indicated is my own original work.
2. This thesis has not been submitted for any degree or examination at any other university.
3. This thesis does not contain data, pictures, graphs, or other information belonging to other people, unless specifically acknowledged as being sourced from other people.
4. This thesis does not contain any other person's writing, unless specifically acknowledged as being sources from other researchers. Where other written sources have been quoted, then:
    a. Their words have been rephrased but the general information attributed to them has been referenced;
    b. Where their exact words have been used, their writing has been placed inside quotation marks, and referenced.
5. Where I have reproduced a publication of which I am an author, co-author, or editor, I have indicated in detail which part of the publication was written by myself alone and have fully referenced such publications.
6. This dissertation does not contain any graphics, text or tables copied from the internet, unless specifically acknowledged, and the source being detailed in the reference sections of the dissertation.

Signed: [redacted] Date: **23rd April 2019**

I, Professor Thirumala Govender as supervisor of the Ph.D. studies hereby consent to the submission of this Ph.D. thesis.

Signed: [redacted] Date: **23rd April 2019**

I, Dr. Chunderika Mocktar as co-supervisor of the Ph.D. studies hereby consent to the submission of this Ph.D. thesis.

Signed: [redacted] Date: **23rd April 2019**

Declaration 2-Publications

Details of contribution to publications that form part and/or include research presented in this thesis:

Combination drug therapy via nanocarriers against infectious diseases

Walvekar, P., Gannimani, R., and Govender, T. Combination drug therapy via nanocarriers against infectious diseases. European Journal of Pharmaceutical Sciences, 2018. 127: p. 121-141. (Impact factor 3.466). DOI: 10.1016/j.ejps.2018.10.017

Fatty acid conjugated pyridinium cationic amphiphiles as antibacterial agents and self-assembling nano carriers

Walvekar, P., Gannimani, R., Sanjeev Rambharose., Chunderika Mocktar., and Govender, T. Fatty acid conjugated pyridinium cationic amphiphiles as antibacterial agents and self-assembling nano carriers. Chemistry and Physics of Lipids, 2018. 214: p. 1-10. (Impact factor 2.766). DOI: 10.1016/j.chemphyslip.2018.05.001

Self-assembled oleylamine grafted hyaluronic acid polymersomes for delivery of vancomycin against methicillin resistant *Staphylococcus aureus* (MRSA).

Walvekar, P., Gannimani, R., Salih, M., Makhathini, S., Mocktar, C., and Govender, T. Self-assembled oleylamine grafted hyaluronic acid polymersomes for delivery of vancomycin against methicillin resistant *Staphylococcus aureus* (MRSA). Colloids and Surfaces B: Biointerfaces (manuscript ID: COLSUB-S-19-01124) (Impact factor 3.997).

The published first author manuscripts can be found in Chapters two to four of this thesis.

Mr. Pavan Walvekar contributed to the literature search and evaluations, design and conceptualization of the projects. He contributed to the synthesis of novel molecules/drug carriers and their characterization in terms of Fourier-transform infrared (FT-IR) spectroscopy, proton and carbon nuclear magnetic resonance spectroscopy (^{1}H NMR and ^{13}C NMR), bio-safety assessment and *in vitro* antibacterial potential. He also contributed to the formulation of nano-drug delivery systems, optimization of methods, modification, interpretation of data, and characterization in terms of; particle size, polydispersity index, zeta potential, entrapment efficiency, surface morphology, *in vitro* drug release and both *in vitro and in vivo* antimicrobial activity. Mr. Pavan Walvekar was responsible for analysis and data collection, and wrote entire draft versions of all first authored articles, and revised them according to co-authors comments. Dr. Ramesh Gannimani assisted with the inception, conceptualization, overall design of the projects solving any technical problems and supervision of the studies. Dr. Sanjeev Rambharose assisted in performing *in vitro* cytotoxicity studies of the synthesized novel materials and in the *in vivo* antibacterial studies. Dr. Chunderika Mocktar supervised the *in vitro* and *in vivo* antibacterial studies. Prof. Thirumala Govender served as supervisor and was responsible for project conceptualization, problem-solving, manuscript editing and general supervision of the study.

Research output from the dissertation

1. First authored Publications

The following research papers were published as results generated from specific objectives from this study and they include:

- Walvekar, P., Gannimani, R., and Govender, T. Combination drug therapy via nanocarriers against infectious diseases. European Journal of Pharmaceutical Sciences, 2018. 127: p. 121-141. (Impact factor: 3.466). DOI: 10.1016/j.ejps.2018.10.017
- Walvekar, P., Gannimani, R., Sanjeev Rambharose., Chunderika Mocktar., and Govender, T. Fatty acid conjugated pyridinium cationic amphiphiles as antibacterial agents and self-assembling nano carriers. Chemistry and Physics of Lipids, 2018. 214: p. 1-10. (Impact factor: 2.766). DOI: 10.1016/j.chemphyslip.2018.05.001
- Walvekar, P., Gannimani, R., Salih, M., Makhathini, S., Mocktar, C., and Govender, T. Self-assembled oleylamine grafted hyaluronic acid polymersomes for delivery of vancomycin against methicillin resistant *Staphylococcus aureus* (MRSA). Colloids and

Surfaces B: Biointerfaces (manuscript ID: COLSUB-S-19-01124) (Impact factor: 3.997).

2. Conference Presentations

The following conference presentations were produced from the data generated during doctoral study:

- **Pavan Walvekar**, Ramesh Gannimani, Sanjeev Rambharose, Chunderika Mocktar, Thirumala Govender, Fatty acid conjugated pyridinium cationic amphiphiles as antibacterial agents and self-assembling nano carriers. Nano Africa, 23-25 April 2018, Durban, South Africa (Poster presentation).

- **Pavan Walvekar**, Ramesh Gannimani, Sanjeev Rambharose, Chunderika Mocktar, Thirumala Govender, Fatty acid conjugated pyridinium cationic amphiphiles as antibacterial agents and self-assembling nano carriers. College of Health Sciences Annual Research Symposium, University of KwaZulu Natal, 05-06 October 2017 Durban, South Africa. (Poster presentation).

- **Pavan Walvekar**, Ramesh Gannimani, Sanjeev Rambharose, Chunderika Mocktar, Thirumala Govender, Fatty acid conjugated pyridinium cationic amphiphiles as antibacterial agents and self-assembling nano carriers. College of Health Sciences Annual Research Symposium, University of KwaZulu Natal, 11-12 October 2018 Durban, South Africa. (Oral presentation).

3. Co-authored publications

The following study was also undertaken during the PhD study. This research paper focussed on the supramolecular lipidation of novel antimicrobial peptides for enhanced antimicrobial activity against methicillin-resistant *Staphylococcus aureus* (MRSA). This research revealed that the co-delivery of novel antimicrobial peptides, (AMPs), vancomycin and oleic acid in a liposomal system can potentially be used to enhance activity and penetration of AMPs, as well as offering synergism between the encapsulated materials thereby improving the treatment of bacterial infections.

Mbuso Faya[1], Heba A. Hazzah, Calvin A. Omolo[1], Ruma Maji[1], Pavan Walvekar[1], Chunderika Mocktar[1], Bongani Nkambule[2], Fernando Albericio, Beatriz G. de la Torre, Thirumala Govender*,[1]. Supramolecular Lipidation of Novel Antimicrobial Peptides Enhances

Antimicrobial Activity Against methicillin-resistant *Staphylococcus aureus* (MRSA). Nanotechnology (manuscript ID: NANO-121995) (Impact factor: 3.404).

Abstract

The rise of drug resistant microorganisms is threatening the ability of antimicrobials to treat infectious diseases including bacterial infections, thus becoming a significant cause for premature mortality. Limitations associated with conventional dosage forms are one of the contributing factors for increasing antimicrobial resistance. Novel nano-drug delivery systems are showing considerable potential to combat antimicrobial resistance. The application of advanced novel materials for the efficient delivery of antibiotics is an active research area. The aim of the study was to design and synthesize advanced materials, and explore nano-based strategies for preparations of novel drug-delivery systems to treat MRSA infections. In this study, two sets of novel amphiphiles; fatty acid based pyridinium cationic amphiphiles (FCAs) and novel hyaluronic acid-oleylamine (HA-OLA) conjugates were synthesized and characterized. The synthesized novel amphiphiles were employed to formulate two nano-drug delivery systems for efficient delivery of vancomycin (VCM) to treat *S. aureus* and MRSA infections. The synthesized materials were found to have inherent antibacterial activity on tested bacterial strains and proven to be biosafe after exhibiting cell viability above 75% on all tested mammalian cell lines using MTT assay. The formulated nano-systems were characterized in terms of particle sizes, polydispersity indices (PDI), zeta potential (ZP), surface morphology, *in vitro* and *in vivo* (VCM loaded OCA vesicles) antibacterial activity. Oleic based cationic amphiphile (OCA) was employed to construct VCM loaded OCA vesicles, and had sizes, PDI, ZP and entrapment efficiency of 132.9 ± 2.5 nm, 0.167 ± 0.02, 18.9 ± 1.2 mV and 61.24 ± 1.8%, respectively. VCM loaded polymersomes prepared using HA-OLA6 had sizes, PDI, ZP and entrapment efficiency of 248.7 ± 3.08 nm, 0.189 ± 0.01, -17.6 ± 0.6 mV and. 43.12 ± 2.18%, respectively. The drug release from VCM loaded OCA vesicles and VCM loaded HA-OLA polymersomes (VCM-PS6) was sustained throughout the studied period of 72 h. From *in vitro* antibacterial studies, both FCAs and HA-OLA conjugates showed bactericidal activity against the tested bacterial strains. Both VCM loaded OCA vesicles and VCM-PS6 displayed 4-fold enhanced antibacterial activity against MRSA, when compared to bare VCM. Furthermore, synergism was observed between VCM and synthesized novel amphiphiles (FCAs and HA-OLA conjugates) in nano-formulations against MRSA. An *in vivo* BALB/c mice skin infection model revealed that, treatment with VCM loaded OCA vesicles significantly reduced the MRSA burden compared to bare drugs and untreated groups. There

was 4.2-fold reduction in the MRSA load in mice skin treated with VCM loaded OCA vesicles compared to those treated with bare VCM. In summary, synthesized novel materials showed good biosafety, antibacterial activity and drug delivery potential via nano-systems against bacterial infections. The data from this study has resulted in one first authored review article, two first authored and one co-authored research publications.

Acknowledgements

Firstly, I would like to express my sincere gratitude to my supervisor Prof. Thirumala Govender for the continuous support of my PhD study. Her guidance, motivation, patience and immense knowledge helped me in all the time of research, writing of the articles and this thesis. I could not have imagined having a better supervisor and mentor for my PhD study.

Wholehearted thanks to my co-supervisor, Dr. Chunderika Mocktar for her motivational support and thorough guidance on antimicrobial studies.

Special thanks goes to my post-doctoral mentor Dr. Ramesh Gannimani for your assistance in the design of those projects as well as your continuous guidance and motivation. I will forever be indebted to you, for being with me every step of the way, helping me tackle any problem encountered along the way and instilling invaluable skills that will be crucial in my career ahead.

I would like to thank my colleagues, Dr. Rahul Kalhapure, Dr. Manthesh Jadhav, Dr. Dipak Raut, Dr. Sanjeev Rambharose, Dr. Ayman Waddad, Dr. Calvin Omolo, Dr. Andile Mbuso Faya, Dr. Sandeep Sonawane, Dr. Dhiraj Sikwal, Dr. Ruma Maji, Mr. Danford Mhule, Mr. Sifiso Makhathini, Mr. Mohammed Salih, Mr. Daniel Hassan, Ms. Nawras Abdelmoniem, Ms. Victoria Fasiku, Nobuhle Nkubungu, Leslie Murugan, Charlotte Ramadhin and Melissa Ramtahal for all the support in the lab and life-long friendship.

My sincere thanks go to all the organizations, which gave me their indispensable generous resources, including the National Research Foundation, Medical Research Council of South Africa, UKZN Nanotechnology Platform and the College of Health Sciences at UKZN. Without their support and financial help, it would not have been possible for me to pursue and to complete this thesis project successfully. My appreciation geos to Ms. Carrin Martin for your editorial assistance, Microscopy and Microanalysis Unit and Biomedical Resource Unit at UKZN for your technical support.

Finally, I thank my parents, fiancée and family for their love, motivation and support throughout my PhD journey. Without their support, this would not have been possible. Thank you for giving me strength to reach for the stars and chase my dreams.

TABLE OF CONTENTS

List of Abbreviations

%EE	Entrapment efficiency	LLCA	Linolenic acid based cationic amphiphiles
A549	Adenocarcinoma Human Alveolar Epithelial	MCF-7	Michigan Cancer Foundation-7
ARV	Antiretroviral	MDT	Mean Dissolution Time
CFU	Colony Forming Unit	MHA	Mueller Hinton Agar
DCM	Dichloromethane	MHB	Mueller Hinton Broth
DLS	Dynamic Light Scattering	MIC	Minimum Inhibitory Concentration
DSC	Differential Scanning Calorimetry	MRSA	Methicillin Resistant *Staphylococcus aureus*
E. coli	*Escherichia coli*	MTT	3-(4, 5-Dimethylthiazolyl-2)-2,5-Diphenyltetrazolium Bromide
FBS	Fetal Bovine Serum	NMR	Nuclear Magnetic Resonance Spectroscopy
FCA	Fatty acid based pyridinium cationic amphiphiles	OCA	Oleic acid based cationic amphiphiles
FT-IR	Fourier-Transform Infrared	OLA	Oleylamine
H&E	Hematoxylin and Eosin	PDI	Polydispersity Index
HA	Hyaluronic acid	*P. aeruginosa*	*Pseudomonas aeruginosa*
HA-OLA	Hyaluronic acid-Oleylamine	RMSE	Root Mean Square Error
HEK-293	Human Embryonic Kidney 293 Cells	*S. aureus*	*Staphylococcus Aureus*
HeLa	Human cervix adenocarcinoma	TEM	Transmission Electron Microscopy
Hep-G2	Hepatocellular carcinoma	THF	Tetrahydrofuran
HIV	Human Immunodeficiency Virus	TOF-MS	Time-of-flight Mass Spectrometry
HRMS	High Resolution Mass Spectrometry	VCM	Vancomycin
HRTEM	High Resolution Transmission Electron Microscopy	VCM-PS6	Vancomycin loaded HA-OLA6 polymersomes
LCA	Linoleic acid based cationic amphiphiles	WHO	World Health Organization

List of Figures and Tables

CHAPTER 1
INTRODUCTION

1.1 Introduction

This chapter provides a brief background to the study, which includes the current status of infectious diseases and various limitations associated with current antibiotic therapy. It further emphasizes the role of nano-drug delivery systems to improve antibiotic therapy and provides aims, objectives, novelty and significance of the study.

1.2 Background

Infectious diseases caused by pathogenic microorganisms, such as bacteria, viruses, fungi and parasites, impose a significant threat to global health, and remains a major contributor for premature mortality. According to a recent report, approximately 16 million people die from infectious diseases every year worldwide [1]. Despite impressive scientific advancements and availability of potential antimicrobial agents, these pathogens have found ways to establish themselves firmly within the host by destroying their immune system, achieving dormancy or developing resistance. In addition, the emergence and re-emergence of several pathogens have exacerbated the situation, thus challenging current medical technology [2]. Collectively, these challenges demand for alternative optimised and effective treatment strategies to combat infections.

Amongst various infectious diseases, bacterial infections have risen to be of global concern because of their significantly high numbers and severity [3]. Bacterial infections are usually contagious and infect a variety of cells and tissues within the host ranging from cutaneous (MRSA infections) to deep-seated life-threatening infections such as tuberculosis, pneumonia, chlamydia, endocarditis and other metastatic complications [4]. Since the development of penicillin and sulfonamide in the early 20^{th} century, many antibiotics have come to the market and have become essential to virtually every aspect of modern medicine [5]. Despite the availability of highly potent antibiotics and standard medical facilities, the world is still facing difficulties to effectively prevent, control and treat bacterial infections. Sub-optimal use and abuse of drugs, drug delivery to non-specific sites, poor bioavailability, systemic toxicity and drug resistance acquired by bacteria are considered as main reasons for clinical failure of antibiotics, the latter being one of the major contributing factors. According to a recent review, antibacterial resistance results in an estimated 700,000 deaths every year worldwide and is

expected to rise to 10 million by 2050 if efforts are not made to overcome resistance or develop new antibiotics **(Fig.1)** [6, 7]. In 2013, the Centers for Disease Control and Prevention estimated approximately 2 million antibiotic resistance related cases in the United States alone, at a total annual cost of 50-70 billion USD [8]. Furthermore, Jim O'Neill in a 2016 report stated that the global cost of infections due to antibiotic resistance could reach up to 100 trillion USD over next 35 years [7]. The increasing antibiotic resistance challenge is acutely threatening the ability to treat bacterial infections, and therefore requires immediate attention.

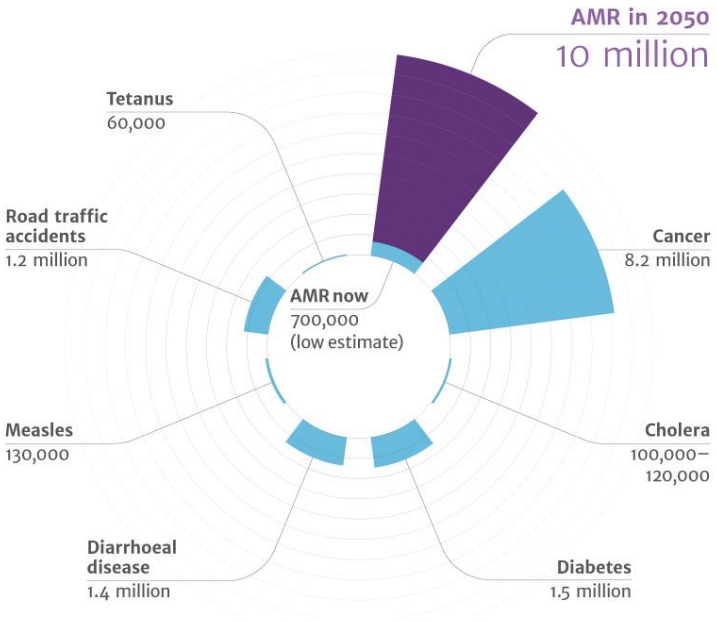

Fig. 1. Deaths attributable to antimicrobial resistance[7].

One of the most serious bacterial strains that has acquired resistance to virtually all potent antibiotics is methicillin resistant *Staphylococcus aureus* (MRSA) [9]. MRSA is responsible for high morbidity and mortality rates, and can cause a variety of organ-specific infections, the most common being skin and soft tissues, followed by invasive infections like osteomyelitis, pneumonia, lung abscess, meningitis, empyema, sepsis and other metastatic complications [10]. An example of MRSA skin infection is illustrated in **Fig.2** [11]. According to a report by R.M Klevens, MRSA accounts for about 19000 deaths every year in the United States alone[12]. Vancomycin is the drug of choice to treat MRSA infections, but some of the MRSA isolates have also acquired resistance to it [13]. As a result, MRSA is on WHO's high priority list for research and development of new antibiotics [9]. Discovering new antibiotics and chemically modifying the existing ones may solve the problem of resistance, however, there is no certainty that these drugs will be potent enough to eradicate the infections completely,

because the eventual development of resistance to these new drugs is also likely to occur. Furthermore, the development and approval of new antibiotics is likely to require several years. Therefore, there is a need for alternative strategies to combat MRSA infections.

Fig. 2. MRSA skin infection [11].

The most common measure used to treat bacterial infections is through delivering antibiotics using conventional therapies, i.e., current drug therapy. Although, conventional dosage forms have provided great outputs over many years by saving millions of lives, they suffer from certain limitations, due to which, inadequate results are obtained. The major limitations of current antibiotic therapy include, drug delivery to non-specific sites, viz., inadequate drug uptake at infection site, sub-optimal therapeutic effects, increased frequency of administration and poor patient compliance due to systemic toxicity. These shortcomings have been recognised as major contributing factors to the development of antibiotic resistance and have ultimately led to the short window period between the introduction of antibiotics and development of resistance **(Fig. 3)** [14]. Furthermore, several pharmaceutical and biotechnology firms are discontinuing investment in research and development of new classes of antibiotics due to low profits and complicated regulatory approval procedures [15, 16]. Therefore, there is an urgent need for novel approaches where, the already available antibiotics can be used in a innovative way to combat these drug resistant strains.

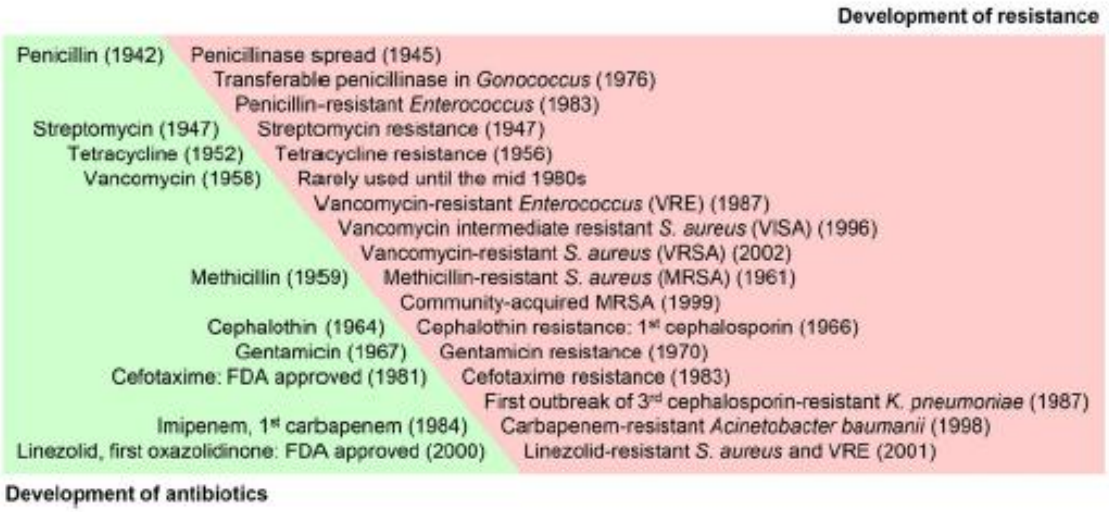

Fig. 3. History of antibiotic development vs. subsequent acquaintance of resistance by bacteria [14].

Over the last few decades, biomedical research has witnessed an unprecedented growth of nanoscience and nanotherapeutics. The potential advantages of nano-drug delivery systems have revolutionized medical technology to an advanced level, where many diseases including bacterial infections can be treated more efficiently with negligible or no adverse effects compared to current drug therapy. The nanoantibiotics offer several advantages, such as, selective and targeted antibiotic delivery to infection site; increased localised drug concentration in bacterial environment; improved solubility, bioavailability and stability of drugs; sustained and controlled drug release; maximum utilization of drugs; treatment of intracellular infections; combination drug therapy; reduced dosing frequency; negligible unwanted side effects; improved patient compliance; and most importantly overcome antibiotic resistance [17, 18]. As a result, numerous antibiotics loaded nano-carrier systems have been demonstrated to treat a variety of bacterial infections, including MRSA infections [14, 18, 19]. Antibiotics such as, vancomycin, fusidic acid, teicoplanin, linezolid, daptomycin, clarithromycin etc, have been encapsulated into various nano-systems to overcome MRSA infections, with the former being recognised as the most explored one [20]. Vancomycin (VCM) is regarded as the last resort for the treatment of MRSA infections, and has been studied with variety of nano-systems. VCM loaded nano-systems made up of advanced novel materials, such as polymers, lipids, amphiphiles etc, have also been reported, and have displayed promising potential in treating MRSA infections both *in vitro* and *in vivo* [21-24]. Therefore, there is increasing optimism that, nano-formulations prepared using novel materials would bring significant advancements in the treatment of bacterial/MRSA infections.

Amongst various nanoparticulated systems, nano-carriers made up of self-assembling amphiphiles are considered as one of the most prominent and promising candidates for drug delivery applications [25]. Under aqueous conditions, the amphiphiles can self-assemble to form various nano-aggregates such as vesicles, micelles, spheres, lamellae, rods and other complex structures [26]. Among various self-assembling aggregates, vesicles have achieved considerable attention because of their versatile nature of encapsulating both hydrophilic as well as hydrophobic payloads including; therapeutic drug molecules, proteins/peptides, dyes and nucleic acids [27]. In the present work, we have developed two different vesicular drug delivery systems using two different sets of novel amphiphiles namely: 1) VCM loaded vesicles prepared using novel fatty acid based pyridinium cationic amphiphiles (FCAs) and 2) VCM loaded polymersomes prepared using novel hyaluronic acid-oleylamine (HA-OLA) conjugates, to effectively target and treat methicillin susceptible and resistant *Staphylococcus aureus* infections.

Cationic compounds, such as pyridiniums have attracted large interest recently due to their abilities to disrupt bacterial cell membrane. In addition to their potential antibacterial activity, these compounds can also make nano-carriers that encapsulate other antibiotics to produce sustained and enhanced/synergistic activity. Unfortunately, their therapeutic application is hampered due to toxicity. To overcome this limitation, these compounds can be conjugated with biosafe and biocompatible molecules such as fatty acids, to develop new promising amphiphiles that could become potential therapeutic agents with low or negligible toxicity. These amphiphiles, in aqueous environment can facilitate self-assembly to form nano-systems to encapsulate therapeutic drugs. Although, there are several reports of pyridinium-based compounds as antibacterial agents, to date, there are no reports on conjugation of unsaturated fatty acids with pyridinium. Furthermore, there are reports on antibiotics such as tetracycline and triclosan being encapsulated into cationic micelles using phosphonium and quaternary ammonium based amphiphiles respectively [28, 29]. The encapsulation of VCM into cationic vesicles and assessing their individual and combined effects against MRSA is yet to be explored. The positively charged cationic vesicles carrying VCM can bind to negatively charged bacterial membranes to induce targeting of bacteria at the infection site and increased localized concentration of drug [30]. Therefore, this study highlights the synthesis and drug delivery applications of novel fatty acid based pyridinium cationic amphiphiles (FCAs) to combat MRSA infections.

Polymersomes are a class of vesicles prepared from synthetic amphiphilic copolymers [31]. In the past decade, polymersomes have attracted immense interest as potential nano-carriers because of their colloidal stability, tunable membrane properties and ability to encapsulate broad range of therapeutic drugs and non-drugs [32]. Various block, branched, alternating and graft copolymers have been demonstrated to make self-assembling nano-polymersomes [31].

Recently, hyaluronic acid (HA), a biodegradable hydrophilic polymer has gained considerable attention in designing various drug delivery vehicles. There are reports on HA being modified with other pharmaceutical ingredients to make self-assembling micelles and polymersomes to deliver anti-cancer drugs [33, 34]. To the best of our knowledge, HA based polymersomes have not been explored to encapsulate and deliver antibiotics. The use of HA based nano-systems to deliver antibiotics can prove to be advantageous because of HA's inherent bacteriostatic and antibiofilm activities against certain strains [35, 36]. Furthermore, HA is known to play a significant role in tissue regeneration and wound healing [37]. These advantages can promote quick healing of dermal infections such as MRSA skin infections. Long fatty chains with strong hydrophobic nature are one class of biosafe and biocompatible compounds, that have been used frequently to make novel materials. HA can be grafted with oleylamine (a long fatty chain) at certain degrees of substitution to synthesize hyaluronic acid-grafted-oleylamine amphiphiles. To date, no HA-fatty amine conjugates have been used to deliver antibiotics. Further, HA-OLA conjugates have not been reported to deliver any class of drugs. These amphiphiles, under aqueous environment can self-assemble to encapsulate active drugs. Furthermore, polymersomes of HA-OLA conjugates can be prepared without using organic solvents, stabilizers or surfactants. This green approach of polymersomes formulation may also circumvent the toxic effects of organic solvents and surfactants. This study therefore highlights the synthesis and drug delivery applications of novel hyaluronic acid-oleylamine (HA-OLA) conjugates to combat MRSA infections.

1.3 Problem statement

Infectious diseases, including bacterial infections, continue to be a major cause of morbidity and pre-mortality globally. Conventional dosage forms have several limitations, which include, inadequate drug concentration at infection/target sites, exposure to normal flora, fast degradation and quick elimination, high frequency of administration, severe adverse effects and poor patient compliance. These factors contribute to suboptimal therapeutic outcomes, thus leading to the current global antimicrobial resistance crisis. Nano-drug delivery systems are

showing significant potential to overcome the limitations associated with conventional dosage forms. The identification of novel nano-based strategies to enhance antibacterial activity and therapy, and to target infection sites, can contribute to enhancing patient therapy and disease treatments. The design and synthesis of advanced materials and nano-based strategies for developing nano-formulations is essential to improve antibacterial activity of currently available antibiotics. Furthermore, synthesis of novel self-assembling amphiphiles having inherent antibacterial effects and their investigation as nano-carriers to improve the activity of encapsulated antibiotics remains to be explored.

1.4 Aims and objectives of this study

The broad aim of this study was to design advanced materials and explore nano-based strategies to formulate nano-drug delivery systems to treat *S. aureus* and MRSA infections. The specific research aims of the two novel nano-formulations developed in this study for enhancing antibacterial activity are highlighted with their respective objectives.

Aim 1

The aim of the study was to synthesize novel fatty acid based pyridinium cationic amphiphiles (FCA) that would serve as nano-drug carriers having intrinsic antibacterial activity, and explore its potential to deliver VCM via vesicles.

In order to achieve this aim, the objectives of the study were to:

1. Use a two-step synthetic scheme to synthesize various FCAs. These included, oleic acid based cationic amphiphile (OCA), linoleic acid based cationic amphiphile (LCA) and linolenic acid based cationic amphiphile (LLCA).
2. Characterise FCAs using structural elucidation techniques such as FTIR, ^{1}H and ^{13}C NMR and HRMS.
3. Determine the *in vitro* toxicity of synthesized FCAs to confirm their use in biological systems.
4. Formulate VCM loaded vesicles using OCA and evaluate the formulated vesicles in terms of particle size, polydispersity index, zeta potential, surface morphology, entrapment efficiency, *in vitro* drug release, *in vitro* and *in vivo* antibacterial activity.

Aim 2

The aim of the study was to synthesize novel hyaluronic acid-oleylamine (HA-OLA) conjugates at various degrees of substitution, that would serve as nano-drug carrier and explore its potential to deliver VCM via polymersomes.

In order to achieve this aim, the objectives of the study were to:

1. Use a single-step synthetic scheme to synthesize various HA-OLA conjugates depending on the degrees of substitution.
2. Characterise HA-OLA conjugates using structural elucidation techniques such as FTIR, ^{1}H NMR and TOF-MS.
3. Determine the *in vitro* toxicity of synthesized HA-OLA conjugates to confirm their use in biological systems.
4. Formulate VCM loaded polymersomes using HA-OLA conjugates and evaluate the formulated polymersomes in terms of particle size, polydispersity index, zeta potential, surface morphology, entrapment efficiency, *in vitro* drug release, *in vitro* antibacterial activity, bacterial cell viability using flow cytometry and bacterial cell morphology.

1.5 Novelty of the study

The novelty of the research work presented in the two experimental chapters is as follows,

Aim 1

The research work performed in this study is novel for the following reasons:

- Few reports on drug delivery using cationic compounds can be found in the literature, this study serves as the first report to employ FCAs for the delivery of any class of drugs. Furthermore, there are no reports on VCM being delivered using cationic molecules. This was the first investigation on the delivery of VCM using fatty acid based pyridinium cationic compounds.

- This article reports the synthesis of three novel fatty acid based pyridinium cationic amphiphiles, which include oleic acid based cationic amphiphile (OCA), linoleic acid based cationic amphiphile (LCA) and linolenic acid based cationic amphiphile (LLCA). These amphiphiles have not been reported in the literature for application in delivering any class of drugs.

- The study serves as the first report to investigate antibacterial potential of FCAs against Gram positive *S. aureus* and MRSA and Gram negative *E. coli* and *P. aeruginosa*.

Aim 2

- This study reports the design and synthesis of novel hyaluronic acid-oleylamine (HA-OLA) conjugates which have not been reported in the literature before.
- HA-OLA conjugates have not been reported in the literature for application in delivering any class of drugs.
- The study serves as the first report to investigate antibacterial potential of HA-OLA conjugates against *S. aureus* and MRSA.
- Whilst, hyaluronic acid based polymersomes have been reported to deliver anti-cancer agents only, this is the first study, that reports the encapsulation and delivery of an antibiotic (VCM) via hyaluronic acid based polymersomes.

1.6 Significance of the study

The nano-drug delivery approaches developed in this study are novel and can contribute to overcoming the problems of bacterial resistance to antibiotics and limitations associated with their conventional dosage forms. The significance of this study is highlighted below:

New pharmaceutical materials/products: The proposed vancomycin loaded FCAs and HA-OLA conjugates are new pharmaceutical products that have not been reported. These products can stimulate the pharmaceutical industries to manufacture cost-effective superior medicines.

Improved patient therapy and disease treatment: Both the proposed formulations can improve patient therapy and treatment of various diseases associated with bacterial infections by enhancing antibacterial performance, reducing doses, lowering side effects and improving patient compliance. The formulations can therefore contribute to improving the quality of patient's lives.

Creation of new knowledge to the scientific community: The studies proposed can lead to new knowledge being generated in pharmaceutical sciences. It can include the following:

- Synthesis schemes for new pharmaceutical materials/new pharmaceutical drug carriers with intrinsic antibacterial activity, formulation optimization procedures for novel drug delivery systems and their properties *in vitro* and *in vivo* can contribute to creation of new scientific knowledge for nano-formulation science.

- The combined effects of these novel antibacterial materials with antibiotics can identify synergistic or additive effects.

- The extensive *in vivo* testing of these novel systems can provide knowledge for *in vitro-in vivo* correlations.

Stimulation of new research: The proposed VCM loaded vesicles and polymersomes holds great promise as nano-delivery systems and therefore can generate new potential research areas for the following reasons:

- Both FCAs and HA-OLA conjugates can be utilized as carriers of other classes of drugs to treat various disease conditions.

- Any class of antibiotics can be encapsulated into FCA and HA-OLA nano-systems to produce/investigate synergistic or additive effects against various bacterial strains.

- Drugs of both hydrophilic as well as hydrophobic properties can be loaded into these vesicular systems with good entrapment efficiencies.

- Since hyaluronic acid has specificity towards some cancer cells, HA-OLA conjugates can be used for targeted drug delivery for cancer therapy.

1.7 Overview of dissertation

The research work performed and presented in this thesis is in the publication format, according to University of Kwa-Zulu Natal, College of Health Sciences guidelines. It specifies the inclusion of a brief introductory chapter, published papers and a final chapter on the conclusions. A PhD study requires at least three first authored papers, two of which must be experimental.

CHAPTER 1. INTRODUCTION: This chapter includes a brief background to the study, indicating the current status of infectious diseases and the various difficulties in antibiotic

therapy. It further provides details on strategic solutions to improve antibiotic therapy, the resulting aims and objectives, novelty and significance of the study pursued.

CHAPTER 2. REVIEW PAPER: This chapter is a first authored review paper published in an ISI international journal i.e. European Journal of Pharmaceutical Sciences (Impact Factor = 3.466). The aim of this article is to review the status and advances of combination drug therapy via nano-drug delivery systems against infectious diseases. This review mainly focuses on lipid and polymer based nano-systems used to co-deliver multiple anti-infectious agents against bacterial, HIV and malarial infections. The review has contributed to the literature on nano-based combination drug therapy against infections, as it has successfully addressed the gap and suggested its use to combat infections more efficiently. The review has also identified key challenges in this area and proposed possible strategies to overcome them. The summary and conclusions provided in this review article could guide formulation scientists to further optimise nano-based co-drug delivery as an approach to fight infections effectively.

CHAPTER 3. EXPERIMENTAL PAPER 1: This chapter addresses Aim 1, Objectives 1-4, and is a first authored experimental article published in an ISI international journal: Chemistry and Physics of Lipids (Impact Factor = 2.766). This article highlights the synthesis of novel FCAs (OCA, LCA and LLCA), *in vitro* toxicity evaluation of synthesized compounds, formulation of VCM loaded OCA vesicles, and characterization of its physical and antibacterial properties both *in vitro* and *in vivo*.

CHAPTER 4. EXPERIMENTAL PAPER 2: This chapter addresses Aim 2, Objectives 1-4, and is a first authored experimental article communicated in an ISI international journal Colloids and Surfaces B: Biointerfaces (manuscript ID: COLSUB-S-19-01124). This article highlights the synthesis of novel HA-OLA conjugates, *in vitro* toxicity evaluation of synthesized compounds, formulation of VCM loaded polymersomes, and characterization of its physical and *in vitro* antibacterial properties.

CHAPTER 5. CO-AUTHORED PAPER: The chapter includes a study that was undertaken during the PhD study. This research paper focussed on the supramolecular lipidation of novel antimicrobial peptides for enhanced antimicrobial activity against methicillin-resistant *Staphylococcus aureus* (MRSA). This research revealed that the co-delivery of novel antimicrobial peptides, (AMPs), vancomycin and oleic acid in a liposomal system can

potentially be used to enhance activity and penetration of AMPs, as well as offering synergism between the encapsulated materials thereby improving the treatment of bacterial infections.

Mbuso Faya[1], Heba A. Hazzah, Calvin A. Omolo[1], Ruma Maji[1], Pavan Walvekar[1], Chunderika Mocktar[1], Bongani Nkambule[2], Fernando Albericio, Beatriz G. de la Torre, Thirumala Govender*,[1]. Supramolecular Lipidation of Novel Antimicrobial Peptides Enhances Antimicrobial Activity Against methicillin-resistant *Staphylococcus aureus* (MRSA). Nanotechnology (manuscript ID: NANO-121995) (Impact factor: 3.404).

CHAPTER 6. CONCLUSION: This chapter includes the overall conclusions from research findings in the study. It further provides information on potential significance of the findings and makes recommendations for future research work in the field of strategic solutions to combat bacterial resistance to antibiotics.

References

[1] Editorial, Microbiology by numbers, Nature Reviews Microbiology, 9 (2011) 628-628.
[2] E. Buliva, M. Elhakim, T. Minh, N. Nguyen, A. Elkholy, P. Mala, A. Abubakar, S.M.M.R. Malik, Emerging and reemerging diseases in the World Health Organization (WHO) Eastern Mediterranean Region-progress, challenges, and WHO initiatives, Front. Public. Health, 5 (2017) 276.
[3] S.J. Lam, E.H. Wong, C. Boyer, G.G. Qiao, Antimicrobial polymeric nanoparticles, Prog. Polym. Sci, 76 (2018) 40-64.
[4] M.-H. Xiong, Y. Bao, X.-Z. Yang, Y.-H. Zhu, J. Wang, Delivery of antibiotics with polymeric particles, Adv. Drug Deliv. Rev, 78 (2014) 63-76.
[5] S.C. Blanchard, A much-needed boost for the dwindling antibiotic pipeline, Mol. Cell, 70 (2018) 3-5.
[6] C. Willyard, The drug-resistant bacteria that pose the greatest health threats, Nature News, 543 (2017) 15.
[7] J. O'Neill, S. Davies, J. Rex, L. White, R. Murray, Review on antimicrobial resistance, tackling drug-resistant infections globally: final report and recommendations, London: Wellcome Trust and UK Government, (2016) 1-84.
[8] Antibiotic resistance threats in the United States., in: C.f.D.C.a. Prevention (Ed.), 2013.
[9] E. Tacconelli, E. Carrara, A. Savoldi, S. Harbarth, M. Mendelson, D.L. Monnet, C. Pulcini, G. Kahlmeter, J. Kluytmans, Y. Carmeli, Discovery, research, and development of new antibiotics: the WHO priority list of antibiotic-resistant bacteria and tuberculosis, Lancet. Infect. Dis, 18 (2018) 318-327.
[10] A. Hassoun, P.K. Linden, B. Friedman, Incidence, prevalence, and management of MRSA bacteremia across patient populations—a review of recent developments in MRSA management and treatment, Crit. Care, 21 (2017) 211.
[11] K.T. Kavanagh, S. Abusalem, L.E. Calderon, The incidence of MRSA infections in the United States: is a more comprehensive tracking system needed?, Antimicrob Resist Infect Control, 6 (2017) 34.

[12] R.M. Klevens, J.R. Edwards, C.L. Richards Jr, T.C. Horan, R.P. Gaynes, D.A. Pollock, D.M. Cardo, Estimating health care-associated infections and deaths in US hospitals, 2002, Public Health Rep, 122 (2007) 160-166.
[13] A. Gupta, S. Mumtaz, C.-H. Li, I. Hussain, V.M. Rotello, Combatting antibiotic-resistant bacteria using nanomaterials, Chem. Soc. Rev, 48 (2019) 415-427.
[14] A.J. Huh, Y.J. Kwon, "Nanoantibiotics": a new paradigm for treating infectious diseases using nanomaterials in the antibiotics resistant era, J. Control. Release, 156 (2011) 128-145.
[15] M.J. Renwick, D.M. Brogan, E. Mossialos, A systematic review and critical assessment of incentive strategies for discovery and development of novel antibiotics, J. Antibiot, 69 (2016) 73.
[16] E. Power, Impact of antibiotic restrictions: the pharmaceutical perspective, Clin. Microbiol. Infect, 12 (2006) 25-34.
[17] W. Gao, S. Thamphiwatana, P. Angsantikul, L. Zhang, Nanoparticle approaches against bacterial infections, Wiley Interdiscip Rev Nanomed Nanobiotechnol, 6 (2014) 532-547.
[18] R.S. Kalhapure, N. Suleman, C. Mocktar, N. Seedat, T. Govender, Nanoengineered drug delivery systems for enhancing antibiotic therapy, J. Pharm. Sci, 104 (2015) 872-905.
[19] L. Sande, M. Sanchez, J. Montes, A.J. Wolf, M.A. Morgan, A. Omri, G.Y. Liu, Liposomal encapsulation of vancomycin improves killing of methicillin-resistant Staphylococcus aureus in a murine infection model, J. Antimicrob. Chemother, 67 (2012) 2191-2194.
[20] A. Hibbitts, C. O'Leary, Emerging nanomedicine therapies to counter the rise of methicillin-resistant Staphylococcus aureus, Materials, 11 (2018) 321.
[21] C.A. Omolo, R.S. Kalhapure, N. Agrawal, M. Jadhav, S. Rambharose, C. Mocktar, T. Govender, A hybrid of mPEG-b-PCL and G1-PEA dendrimer for enhancing delivery of antibiotics, J. Control. Release, 290 (2018) 112-128.
[22] J. Xu, B. Xu, D. Shou, X. Xia, Y. Hu, Preparation and evaluation of vancomycin-loaded N-trimethyl chitosan nanoparticles, Polymers, 7 (2015) 1850-1870.
[23] R.S. Kalhapure, D.R. Sikwal, S. Rambharose, C. Mocktar, S. Singh, L. Bester, J.K. Oh, J. Renukuntla, T. Govender, Enhancing targeted antibiotic therapy via pH responsive solid lipid nanoparticles from an acid cleavable lipid, Nanomedicine, 13 (2017) 2067-2077.
[24] R.S. Kalhapure, M. Jadhav, S. Rambharose, C. Mocktar, S. Singh, J. Renukuntla, T. Govender, pH-responsive chitosan nanoparticles from a novel twin-chain anionic amphiphile for controlled and targeted delivery of vancomycin, Colloids Surf. B Biointerfaces, 158 (2017) 650-657.
[25] A. Rösler, G.W. Vandermeulen, H.-A. Klok, Advanced drug delivery devices via self-assembly of amphiphilic block copolymers, Adv. Drug Deliv. Rev, 64 (2012) 270-279.
[26] J. Du, Y. Chen, Organic–inorganic hybrid nanoparticles with a complex hollow structure, Angew. Chem, 116 (2004) 5194-5197.
[27] J.S. Lee, J. Feijen, Polymersomes for drug delivery: design, formation and characterization, Journal of controlled release, 161 (2012) 473-483.
[28] B. Hisey, P.J. Ragogna, E.R. Gillies, Phosphonium-functionalized polymer micelles with intrinsic antibacterial activity, Biomacromolecules, 18 (2017) 914-923.
[29] M. Leng, S. Hu, A. Lu, M. Cai, X. Luo, The anti-bacterial poly (caprolactone)-poly (quaternary ammonium salt) as drug delivery carriers, Appl. Microbiol. Biotechnol, 100 (2016) 3049-3059.
[30] M.C. Jennings, K.P. Minbiole, W.M. Wuest, Quaternary ammonium compounds: an antimicrobial mainstay and platform for innovation to address bacterial resistance, ACS Infect. Dis, 1 (2015) 288-303.
[31] V. Balasubramanian, B. Herranz-Blanco, P.V. Almeida, J. Hirvonen, H.A. Santos, Multifaceted polymersome platforms: Spanning from self-assembly to drug delivery and protocells, Prog. Polym. Sci, 60 (2016) 51-85.

[32] J.S. Lee, J. Feijen, Polymersomes for drug delivery: design, formation and characterization, J. Control. Release, 161 (2012) 473-483.
[33] L. Qiu, Z. Li, M. Qiao, M. Long, M. Wang, X. Zhang, C. Tian, D. Chen, Self-assembled pH-responsive hyaluronic acid–g-poly (l-histidine) copolymer micelles for targeted intracellular delivery of doxorubicin, Acta Biomater, 10 (2014) 2024-2035.
[34] K.K. Upadhyay, J.-F.L. Meins, A. Misra, P. Voisin, V. Bouchaud, E. Ibarboure, C. Schatz, S. Lecommandoux, Biomimetic doxorubicin loaded polymersomes from hyaluronan-block-poly (γ-benzyl glutamate) copolymers, Biomacromolecules, 10 (2009) 2802-2808.
[35] P. Pirnazar, L. Wolinsky, S. Nachnani, S. Haake, A. Pilloni, G.W. Bernard, Bacteriostatic effects of hyaluronic acid, J. Periodontol, 70 (1999) 370-374.
[36] L. Drago, L. Cappelletti, E. De Vecchi, L. Pignataro, S. Torretta, R. Mattina, Antiadhesive and antibiofilm activity of hyaluronic acid against bacteria responsible for respiratory tract infections, APMIS, 122 (2014) 1013-1019.
[37] J. Zhu, F. Li, X. Wang, J. Yu, D. Wu, Hyaluronic acid and polyethylene glycol hybrid hydrogel encapsulating nanogel with hemostasis and sustainable antibacterial property for wound healing, ACS Appl. Mater. Interfaces, 10 (2018) 13304-13316.

CHAPTER 2. REVIEW PAPER

2.1 Introduction

This chapter is a first authored review paper titled, “Combination drug therapy via nanocarriers against infectious diseases” and had been published in “European Journal of Pharmaceutical Sciences”. The aim of this article is to review the status and advances of combination drug therapy via nano-drug delivery systems against infectious diseases. This review mainly focuses on lipid and polymer based nano-systems used to co-deliver multiple anti-infectious agents against bacterial, HIV and malarial infections. The review has contributed to the literature on nano-based combination drug therapy against infections, as it has successfully addressed the gap and suggested its use to combat infections more efficiently. The review has also identified key challenges in this area and proposed possible strategies to overcome them. The summary and conclusions provided in this review article could guide formulation scientists to further optimise nano-based co-drug delivery as an approach to fight infections effectively.

Graphical abstract

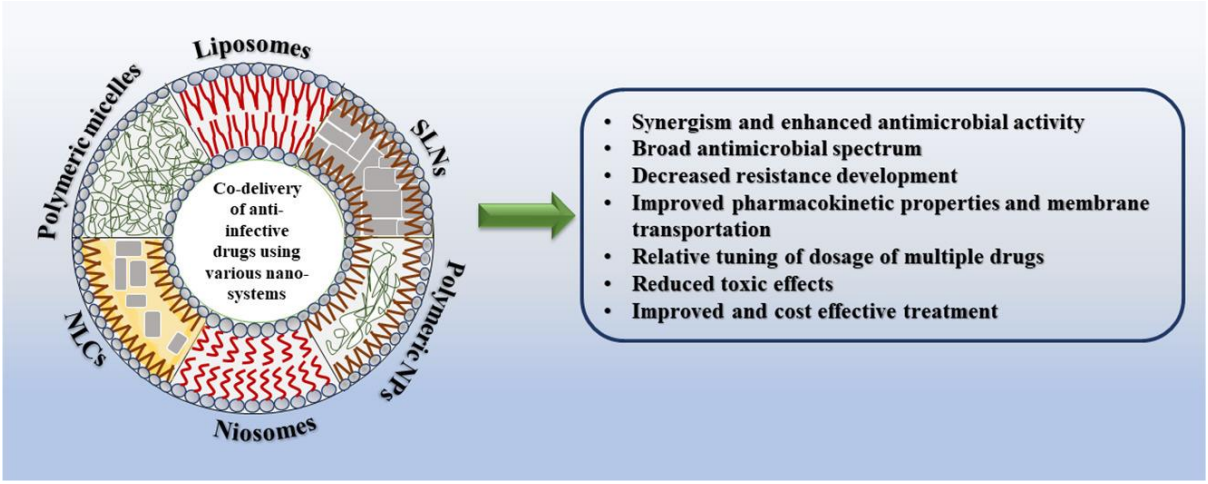

European Journal of Pharmaceutical Sciences 127 (2019) 121–141

Contents lists available at ScienceDirect

European Journal of Pharmaceutical Sciences

journal homepage: www.elsevier.com/locate/ejps

Combination drug therapy *via* nanocarriers against infectious diseases

Pavan Walvekar, Ramesh Gannimani*, Thirumala Govender**

Discipline of Pharmaceutical Sciences, School of Health Sciences, University of KwaZulu-Natal, Private Bag X54001, Durban 4000, South Africa

ARTICLE INFO

Keywords:
Antimicrobial resistance
Nano drug delivery
Nano based combination drug therapy
Antibacterial
Antiviral
Antimalarial
Improved activity

ABSTRACT

Current drug therapy against infections is threatening to become obsolete due to the poor physical, chemical, biological and pharmacokinetic properties of drugs, followed by high risk of acquiring resistance. Taking into account the significant benefits of nanotechnology, nano-based delivery of anti-infectious agents is emerging as a potential approach to combat several lethal infections. Co-delivery of multiple anti-infectious agents in a single nano-based system is beginning to show significant advantages over mono-therapy, such as synergism, enhanced anti-microbial activity, broad anti-microbial spectrum, reduced resistance development, and improved and cost-effective treatment. The current review provides a detailed update on the status of various lipid and polymer based nano-systems used to co-deliver multiple anti-infectious agents against bacterial, HIV and malarial infections. It also identifies current key challenges and suggests strategies to overcome them, thus guiding formulation scientists to further optimize nano-based co-drug delivery as an approach to fight infections effectively.

1. Introduction

Infectious diseases caused by pathogenic microorganisms, such as bacteria, viruses, fungi and parasites, are a significant burden to health and global economics (Signore, 2013), and remain a major current cause for increasing premature mortality rate in humans (Lozano et al., 2013) and other species. The most common measure that is used to treat infections is through the use of anti-microbial agents. Many pathogenic organisms have found a way to establish themselves firmly within the host by destroying their immune system or achieving dormancy or developing resistance to these potent medications challenging modern medical technology. Increasing anti-microbial resistance has become a serious challenge globally, threatening the ability to treat certain infections, such as HIV/AIDS (Pillay and Zambon, 1998), tuberculosis (TB) (WHO, 2000), malaria (White, 2004) and Methicillin resistant *Staphylococcus aureus* (*MRSA*) infections (Kalhapure et al., 2015), resulting in prolonged illness and premature death. In this drug resistant era, scientists have been focussing on eradicating pathogens completely from the host by attempting to invent/discover new drugs and chemically modifying existing ones. Unfortunately, there is no certainty that the newly developed drugs will be potent enough to cure diseases, and the eventual development of resistance to these new drugs also being likely to occur. Therefore, there is a need for innovative approaches to combat infections effectively.

Although, conventional dosage forms are currently used for controlling infectious diseases, poor bioavailability, short half-life, poor patient compliance, sub-optimal therapeutic effects and systemic toxicity are major shortcomings (Aungst, 1993; Sonawane et al., 2017). These are due to poor pharmacokinetic profiles, increased frequency of administration and drug delivery to non-specific sites, *viz.*, inadequate drug uptake at infection site (Sonawane et al., 2017), the latter being one of the major contributing factors to increasing antimicrobial resistance. Researchers are therefore focussing on developing novel and improved strategies for the better management of infectious diseases. Among various novel approaches, the use of nano-drug delivery systems has been proven to be efficient and emerging technique with numerous advantages and applications (Lavan et al., 2002; Farokhzad and Langer, 2009).

The introduction of liposomes (Bangham et al., 1965) by the late pioneer, Alec Bangham and colleagues in 1960s, and their proposal as carriers of drugs and proteins (Gregoriadis and Ryman, 1971; Gregoriadis, 1973) by Gregory Gregoriadis and colleagues in 1970s, has led to a revolutionary change in pharmaceutical research and development process credited to nanotechnology. Researchers have since exhibited considerable interest in delivering active principles to treat various diseases. Numerous advantages of nano-drug delivery systems have been recognised, including better drug solubility and stability, prolonged systemic circulation, the ability to target specific cells or proteins, a controlled and sustained release profile, thus reducing the frequency of dose and systemic toxicity (Zhang et al., 2008).

* Corresponding author.
** Correspondence to: T. Govender, Private Bag X54001, Durban 4000, KwaZulu-Natal, South Africa.
E-mail addresses: gannimanir@ukzn.ac.za (R. Gannimani), govenderth@ukzn.ac.za (T. Govender).

https://doi.org/10.1016/j.ejps.2018.10.017
Received 9 August 2018; Received in revised form 16 September 2018; Accepted 16 October 2018
Available online 17 October 2018

Table 1
Nano drug delivery systems against various infectious agents.

Targeted microorganism	Nanoplatform	Drug	References
A. Bacteria			
Escherichia coli	Solid lipid nanoparticles	Norfloxacin	Wang et al. (2012)
Helicobacter pylori	Polymeric nanoparticles	Amoxicillin	Lin et al. (2013)
Pseudomonas aeruginosa	Liposomes	Gentamicin	Mugabe et al. (2005)
Staphylococcus aureus & methicillin resistant *Staphylococcus aureus*	Vesicles	Vancomycin	Walvekar et al. (2018)
B. Viruses			
Human immunodeficiency virus (HIV)	Nano-emulgel	Tenofovir	Rambharose et al. (2017)
Hepatitis B virus (HBV)	Solid lipid nanoparticles	Adefovir dipivoxil	Xing-Guo et al. (2008)
Hepatitis B virus (HCV)	Nano-emulsion	Silibinin	Liu et al. (2016)
C. Parasites/nematodes			
Plasmodium berghei	Lipid nanoparticles	Artemether	Aditya et al. (2010)
Plasmodium falciparum	Solid lipid nanoparticles	Dihydroartemisinin	Omwoyo et al. (2016)
Brugia malayi	Polymeric nanoparticles	Ivermectin	Ali et al. (2014)
Leishmania donovani	Polymeric nanoparticles	Miltefosine	Kumar et al. (2016)
D. Fungi			
Candida albicans	Solid lipid nanoparticles	Ketoconazole	Ramasamy et al. (2012)
Candida albicans	Nanostructured lipid carriers	Clotrimazole	Ravani et al. (2013)

Furthermore, drug loaded nano-systems have the ability to enter infected cells through endocytosis and release the drugs to treat intracellular infections (Couvreur et al., 1991). As a result, a number of nanoparticulate systems have been reported to treat various infections, some of which are summarized in Table 1.

In the early and mid-20th century, mono-drug therapy was always a first line weapon to treat infectious diseases, until the first drugs started to lose their anti-microbial activity due to resistance acquired by certain microorganisms. These included: 1) Penicillin by *Staphylococcus aureus* (*S. aureus*) (Lowy, 2003), 2) Streptomycin by *Mycobacterium tuberculosis* (*M. tuberculosis*) (Davies and Davies, 2010), 3) Chloroquine by *Plasmodium falciparum* (*P. falciparum*) (White, 2004) and 4) Zidovudine by HIV (Arion and Parniak, 1999). The trend was continued for newer drugs due to the emergence of mutant strains (WHO, 2014). A gradual downfall in mono-drug therapy, due to molecular complexity of these lethal infections and the emergence of drug resistant strains, has led to combination drug therapy becoming a first line treatment for better long-term prognosis (Tamma et al., 2012).

Combination therapy refers to the simultaneous use of multiple pharmacologically active substances called a “drug cocktail” to treat disease conditions. Various diseases, such as cancer, HIV/AIDS, malaria, TB *etc.*, have been regularly treated with combination therapy regimens, with the aim of inducing therapeutic synergistic effects, overcoming drug resistance, broadening antimicrobial spectrum and decreasing side effects (Woodcock et al., 2011). The combination of free drugs has displayed considerable improvements in treating several diseases, their benefits having been well recognised (Komarova and Boland, 2013). However, varying pharmacokinetic profiles and membrane transport properties among different active drugs, intricate dosing and scheduling optimization are challenges with combination drug therapy that could produce outcomes that would be inadequate to produce therapeutic effects (Hu et al., 2010). Furthermore, the co-administration of highly potent drugs in the free form is associated with serious unwanted side effects (Aditya et al., 2010). These limitations have triggered scientists and researchers to explore smarter techniques by combining nano-technology and combination drug therapy by proposing nano-based combinatorial approaches.

Over the past decade, the number of publications reporting on the use of nanomedicines against infectious diseases has grown rapidly. Referring to Table 1, thus far, research on nano-based drug delivery against infections has mainly focussed on mono-drug therapy. In addition, considering several advantages and limitations of nano-drug delivery systems and the co-administration of free drugs respectively, the co-delivery of multiple drugs from nano-systems offer an advanced and superior approach for managing infectious diseases. Co-encapsulation of multiple drugs in a single nano-system for infectious diseases is still in its infancy stage compared to cancer. However, because of their unique advantages, such as tuning relative dosage for more than one drug in a single nano-system, and simultaneously delivering them to target sites with a maintained drug ratio facilitating co-encapsulation of both hydrophilic and hydrophobic drugs, as well as co-delivering a non-drug and a drug (Shi et al., 2010), there has been a surge of interest in nano-based combination drug therapy against infectious diseases. To date, review papers have focussed on nano-based mono-drug delivery systems for infectious diseases (Zhang et al., 2010) and nano-based co-delivery systems for cancer (Mignani et al., 2014). Although, few instances on the co-delivery of anti-infectious drugs were found in some reviews, there is a need for a comprehensive review in order to guide researchers and scientists to optimize this approach as a strategy for overcoming the challenges with current mono-based therapy.

The purpose of the present paper is to review the status and advances of nano-drug delivery systems with combination drug therapy against infectious diseases. The review focuses on bacterial, HIV/AIDS and malarial infections, as these are the most reported areas and are of global interest, and identifies the challenges and future directions for nano-based combination drug therapy against infections.

2. Classes of nano-systems for the co-delivery of anti-infectious agents

The co-delivery of anti-infectious agents using nano-systems can be mainly categorized into lipid and polymer-based systems. Detailed reviews that focus specifically on lipid- and polymer-based nano-systems have been reported previously (Soppimath et al., 2001; Puri et al., 2009). In this review, we briefly highlight the description of each system, with the subsequent sections being structured according to their use for infectious diseases, *i.e.* bacterial, HIV/AIDS and malaria.

In the field of medical nano-technology, biocompatible and biodegradable lipids have been recognised as one of many important materials to be used for preparing nano-based drug delivery systems. Lipid based nano-systems have included, *inter alia*, liposomes, solid lipid nanoparticles (SLNs), nano-structured lipid carriers (NLCs) and niosomes. The advantages of constructing non-toxic carriers that are functionalized with targeting ligands or stealth materials to improve the delivery of multiple drugs (both hydrophobic and hydrophilic), while reducing their side effects, makes them promising candidates to be employed for preparing nano-based combination drug delivery systems to manage infectious diseases. Lipid based nano-systems can prove to be efficient systems to deliver multiple drugs for the treatment of

Table 2
Various nano-systems used to co-deliver anti-infectious agents.

Nano-systems	Structural description	Typical materials used	Typical methods used for preparation	References
1. Lipid based nano-systems				
a. Liposomes	Liposomes are unilamellar or multilamellar vesicles made up of cholesterol and naturally derived phospholipids.	Naturally derived phospholipids *e.g.* phosphatidyl choline (PC), 1,2-Distearoyl-sn-glycero-3-phosphoethanolamine (DSPE), 1,2-dipalmitoyl-sn-glycero-3-phosphocholine (DPPC), 1,2-Dioleoyl-sn-glycero-3-phosphocholine (DOPC), 1,2-distearoyl-sn-glycero-3-phosphocholine (DSPC), 1,2-dioleoyl-3-trimethylammonium-propane (DOTAP) *etc.*, and cholesterol.	• Thin film hydration • Membrane extrusion • Ether injection • Reverse phase evaporation	Akbarzadeh et al. (2013)
b. SLNs	SLNs are lipophilic cored structures made up of biocompatible and biodegradable solid lipids used to deliver lipophilic drugs.	Fatty acids *e.g.* stearic, palmitic & lauric acid, tristearin, tripalmitin, glycerol monostearate, glyceryl dilaurate (GDL), glyceryl behenate, *etc.*	• Hot homogenization • Probe ultrasonication • Solvent evaporation • Spray drying	Mukherjee et al. (2009)
c. NLCs	NLCs are modified version of SLNs, with a core of both solid & liquid lipids to improve stability of encapsulated drugs, loading efficiency & prevent leakage of encapsulated payloads.	Fatty acids *e.g.* stearic palmitic, oleic & linoleic acid, glycerol monostearate, glyceryl dilaurate, soybean oil, *etc.*	• High pressure homogenization • Ultrasonic emulsion evaporation • Solvent evaporation • Film-ultrasonic method	Li et al. (2017)
d. Niosomes	Niosomes are bilayered vesicles made up of biocompatible and biodegradable non-ionic surfactants and cholesterol.	Non-ionic surfactants *e.g.* Tween 20, 60 & 80, Span 20, 40, 60 & 80, Brij 30, 52 *etc.*, cholesterol and charge inducers	• Lipid film hydration • Micro-fluidization • Ether injection • Reverse phase evaporation	Ag Seleci et al. (2016)
2. Polymeric nanoparticles	Polymeric nanoparticles are colloidal particulate systems formed by compact arrangement/aggregation of polymeric molecules in aqueous system where drugs are either adsorbed on the surface or encapsulated inside the matrix.	Poly(lactic-*co*-glycolic acid) (PLGA), chitosan, polyethylene glycol (PEG), methoxypolyethylene glycol (mPEG), polyvinyl alcohol (PVA), polycaprolactone (PCL), polyacrylic, polylactic acid, eudragit, *etc.*	• Solvent evaporation • Solvent diffusion • Salting out • Supercritical fluid technology	Soppimath et al. (2001)

infections. For example, liposomes, due to their lipid bilayer structure that mimic the cell membranes of infectious microbes, can readily facilitate the fusion (Huh and Kwon, 2011). In addition, the advantage of simultaneous encapsulation of both the hydrophilic and hydrophobic drugs makes liposomes one of the ideal candidates for the co-delivery of anti-infectious agents (Zhang et al., 2010). Similarly, SLNs and NLCs can co-encapsulate multiple poorly water soluble payloads in their hydrophobic cores, hence overcoming the limitations of the slow and incomplete dissolution of drugs to improve their bioavailability (Weber et al., 2014; Humberstone and Charman, 1997). Therefore, lipid-based nano-systems present a strong rationale to be used as carriers for the simultaneous delivery of multiple drugs to treat infectious diseases.

Biodegradable polymers to deliver antimicrobials have been in use for several years (Zhang et al., 2010). In contrast to the various beneficial features of lipid based nano-systems, polymeric nano-particles possess some unique advantages for anti-infectious drug delivery. Firstly, they are relatively more stable than lipid-based systems, for example, liposomes tend to lose their integrity on storage, leading to leakage of the encapsulated payloads (Grit and Crommelin, 1993). Secondly, particles with smaller size and narrow polydispersity can be obtained by varying the polymers, length of polymers, surfactants and organic solvents. Furthermore, both hydrophilic and hydrophobic drugs can be loaded in a single particle, depending on the type of polymer and method of preparation. For example, amphiphilic *block-co*-polymers can self-assemble to form polymeric vesicles or polymersomes to co-encapsulate multiple hydrophilic and hydrophobic drugs (Balasubramanian et al., 2016). As with lipid-based systems, polymeric nanoparticles can also be decorated with specific ligands to improve and facilitate targeted drug delivery. For example, Khuller et al. functionalized anti-TB drug loaded Poly(D,L-lactic-co-glycolide) (PLG) nanoparticles with lectin, a bio-adhesive agent, to increase the absorption time of the loaded drugs (Sharma et al., 2004a). These advantages therefore make polymeric nanoparticles a strong contender to be used as carriers of multiple anti-infectious agents. Table 2 depicts various lipid and polymer based nano-systems that have been employed to co-deliver anti-infectious agents, and includes a brief structural description of the systems, typical materials and methods used for their preparation.

3. Nano-systems to co-deliver antibiotics

Despite the considerable success of antibiotics, bacterial infections remain one of the major reasons for premature deaths worldwide, with resistance being one of the major challenges for the failure of antibiotic therapy. According to a recent report, an estimated 700,000 people are affected every year by antibiotic resistance, and if efforts are not made to address the problem, the number could increase to 10 million by 2050 (Willyard, 2017).

In a recent review, Brown and Wright has put on a view on future of antibiotics stating that, after the golden and medicinal chemistry eras in the 20th century, the resistance era in the early 21st century, 2025 would be the narrow spectrum era, where medical research would focus mainly on unconventional drug discovery, diagnostic development, *in vivo* essential targeting, and combinatorial approaches (Brown and Wright, 2016). Discovering new drugs and optimizing novel diagnostic methods is likely to take a long time. Furthermore, there is no guarantee that the new drugs and diagnostic methods would last long, as it is evident that bacteria will continue to acquire resistance unless alternative strategies are employed to develop antibacterials. However, medical nano-technology can satisfy the needs of both *in vivo* essential targeting as well as combinatorial approaches to effectively treat bacterial infections. Fig. 1 indicates that multiple antibiotics loaded in a single nano-system targeting bacteria through various mechanisms may produce synergism and enhanced activity. However, same beneficial outcomes cannot be expected with single antibiotic loaded nano-formulations, as they act through one mechanism only, and may not be as effective as multiple antibiotics loaded nano-systems. Various lipid and polymer based nano-systems for the co-delivery of antibiotics have therefore been reported and are summarized in Table 3.

3.1. Lipid based nano-systems to co-deliver antibiotics

Over the past decade, researchers have shown great interest in the co-delivery of antibiotics using lipid based nano-systems. Liposomes, being a highly versatile platform for co-delivery, have been explored the most, with progress thus far being highlighted. Schiffelers et al. were the first to report the co-encapsulation of antibiotics, gentamicin and ceftazidime, in liposomes (Schiffelers et al., 2001). The study was aimed at comparing the synergistic effects of drugs in free and liposomal form against antibiotic susceptible and resistant *Klebsiella pneumoniae* (*KP*) strains based on the survival of rats after treatment. The liposomes made up of hydrogenated egg PC, DSPE-PEG and cholesterol were prepared using a thin film hydration method and had a mean diameter of 100 nm with > 90% encapsulation achieved for both drugs. From the *in vitro* results, it was found that a combination of free drugs produced synergism against both susceptible and resistant *KP* strains. However, the same was not observed with the *in vivo* results, where only an additive effect was noticed, and prolonged treatment with multiple doses (5-day treatment with dosing at every 12 h) was required. Liposomes loaded with single drugs were relatively more effective compared to the free drugs alone and their combination when tested *in vivo* against both strains. Against susceptible *KP* strain, it was observed that a single dose of gentamicin and ceftazidime co-loaded liposomes produced complete survival of rats at comparable to free gentamicin, 170-fold reduced free ceftazidime body exposures and 10 injections of free drug combination. In contrast, two doses of dual drug loaded formulation were required to achieve complete survival in rats infected with a resistant strain, which was 10 and 40-fold lower gentamicin and ceftazidime body exposures. In addition, the effects were comparable with those of 10 injections of the free drug combination. Therefore, liposomes co-loaded with gentamicin and ceftazidime displayed synergistic activity in both susceptible and resistant *KP* strains, leading to the complete survival of the rats with relatively lower doses than free drugs alone and their combination. This synergistic effect was attributed to targeted and parallel tissue distribution of drugs by liposomes, which was not achieved with free drugs alone or in combination. The authors demonstrated that co-encapsulation of antibiotics in liposomes can synergistically enhance the antibacterial activity with reduced doses. Although drug release studies and particle morphology were not reported in this paper, in our opinion, this study was one of the interesting early studies that served as a building base for the succeeding studies in combating bacterial infections using nanotechnology based combinatorial approach.

The resistant strains of *S. aureus* are another class of bacteria that have become a major clinical threat in recent decades, thus increasing premature mortality rates in humans. A study conducted by Li et al. was aimed at preparing a liposomal nano-carrier system co-encapsulated with daptomycin and clarithromycin (mass ratio of 1:32) to treat *MRSA* infection (Li et al., 2015). A thin film hydration method was employed to prepare the liposomes using hydrogenated soy PC, $mPEG_{2000}$-DSPE and cholesterol, and were found to have an average diameter of 100 nm. The dual drug loaded formulation achieved high entrapment efficiencies of above 90% for both daptomycin and clarithromycin, which was similar to the single drug loaded formulations. Interestingly, similar drug release patterns were observed with single and dual drug loaded formulations, suggesting that a high % entrapment efficiency (% EE) for both drugs in a single formulation did not greatly influence slower release. The *in vitro* antibacterial results revealed that the daptomycin and clarithromycin co-loaded liposomes had greater anti-*MRSA* activity than the formulations containing individual drugs. In addition, the antibacterial results supported the biofilm susceptibility assay, where the dual drug loaded formulation was proven to be more

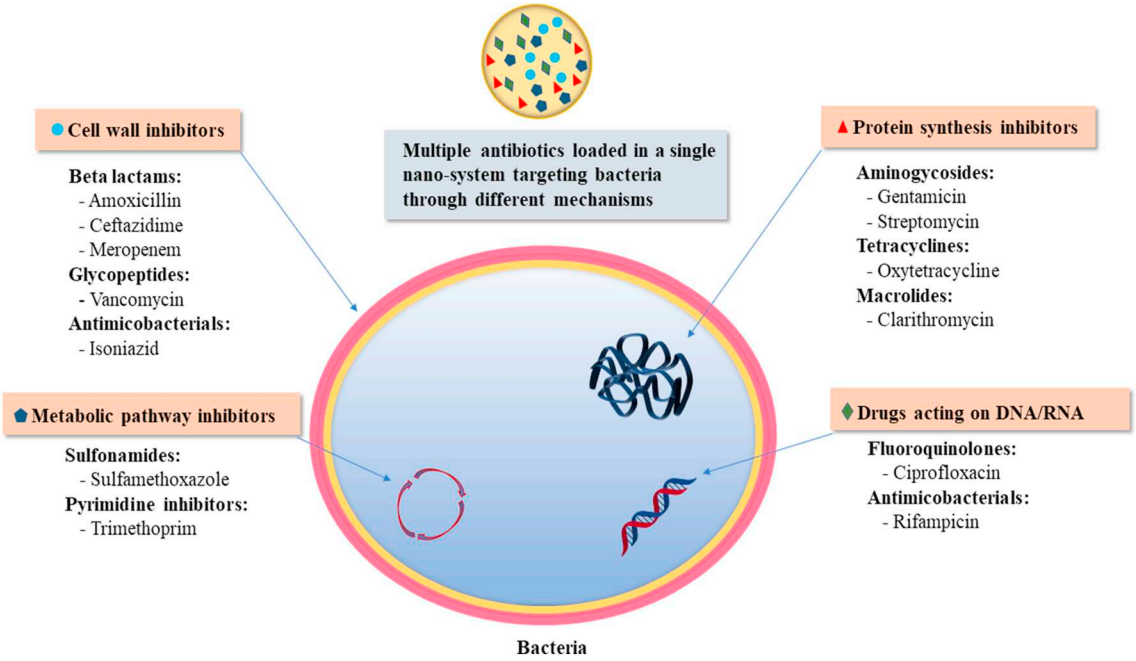

Fig. 1. Simultaneous delivery of various classes of antibiotics using a single nano-system can produce synergistic activity with reduced dose and toxicity.

potent than the formulation loaded with daptomycin only. Furthermore, the *in vivo* antibacterial activity was in complete agreement with *in vitro* results. It was worth noting that the amount of daptomycin in the co-loaded liposomes used was only one thirtieth the dose of the daptomycin alone liposomes, which was sufficient to reduce the *MRSA* load in the major organs and blood of mice. Therefore, daptomycin and clarithromycin co-encapsulated liposomes were dominant compared to the formulations containing individual drugs in lowering the bacterial burden and prolonging the survival rates of infected mice. The co-administration of clarithromycin was found to have markedly reduced the dose of daptomycin without compromising its therapeutic efficacy, which may account for suppressing the risk of potential toxicity of the pharmacologically active drugs. Therefore, the authors showed that the concurrent application of daptomycin and clarithromycin in a liposomal system can prove to be a potential strategy in fighting *MRSA* infection.

Some bacterial infections, mainly TB, are always treated using drug cocktails, which must be administered daily, and may account for the increased risk of toxicity and resistance (Pandey and Khuller, 2006b). Taking into consideration the benefits of nanotechnology and combination therapy, many researchers have co-loaded anti-TB drugs into various lipid based nano-systems to produce potential therapeutic effects. Gursoy et al. fabricated liposomes by co-encapsulating two front-line anti-tubercular drugs, isoniazid and rifampicin (Gürsoy et al., 2004). The liposomes were prepared using two lipids, *i.e.* egg PC and DPPC, to compare the effects on drug loading, entrapment efficiency and drug release. Among both the formulations, liposomes employing DPPC and cholesterol displayed better %EE for isoniazid and rifampicin (73.84 ± 0.78 and 81.53 ± 2.06) than the liposomes with egg PC and cholesterol (64.61 ± 0.51 and 74.45 ± 0.48). These high entrapment efficiencies with DPPC and cholesterol were attributed to the longer carbon chain length of DPPC. Interestingly, rifampicin was found to aid the solubility of isoniazid, and in contrast to the entrapment efficiencies and release behaviour of liposomes encapsulating individual drugs, co-encapsulation of both drugs improved their entrapment efficiencies, and extended their release. While the authors were successful in preparing dual drug loaded liposomes, with high loading efficiencies being achieved for both drugs, the particle size and antibacterial testing, being important aspects of any formulation study, were not reported in this paper. The study would have been strengthened by reporting particle size and antibacterial activity, as these are critical parameters for *in vivo* performance.

In another study, Niu et al. aimed at targeting *M. tuberculosis* infected macrophages with multi-drug loaded PEGylated liposomes, carrying four anti-tubercular drugs, isoniazid, rifampicin, streptomycin and pyrazinamide. Taking into account the marked affinity of TGF-β1 siRNA for THP-1 derived human macrophages, the multi-drug loaded PEGylated liposomes were tailored with TGF-β1 siRNA to target infected macrophages (Niu et al., 2015). Initially, streptomycin was conjugated to amine terminal of DSPE-PEG_{2000}, with the same being used with DOTAP to formulate cationic liposomes encapsulating other three drugs. Thereafter, the negatively charged TGF-β1 siRNA was introduced onto the surface of cationic liposomes. The targeting liposomes had an average diameter of 265 nm with narrow polydispersity index. An MTT assay performed on human macrophages confirmed the bio-safety of the formulation. Through transmission electron microscopy (TEM) imaging, the liposomes were shown as being bound and engulfed by human macrophages. These results indicate that TGF- β1 siRNA conjugated PEGylated liposomes entrapping anti-TB drugs were successfully targeted to THP-1 derived human macrophages to manage TB. Although this study was useful for confirming the targeting potential of TGF- β1 siRNA conjugated PEGylated liposomes to THP-1 derived human macrophages, it is well recognised that %EE is a major challenge with nano-systems due to their small size. This paper would therefore have been strengthened with %EE measurements, which would have been useful to confirm the viability in terms of manufacturing costs and quantity of nanoparticles required to be administered to the patients. Furthermore, the antibacterial efficacy of this formulation is also critical for clinical applications. Similar to the previous report (Gürsoy et al., 2004), antibacterial studies were not performed in this paper.

While researchers were mainly focusing on liposomes to co-deliver anti-TB drugs, Khuller and co-workers co-delivered three front-line anti-TB drugs (rifampicin, isoniazid and pyrazinamide) using stearic acid based SLNs (Pandey et al., 2005). The multi-drug loaded SLNs, prepared by emulsion solvent diffusion method, had the highest entrapment efficiency for hydrophobic rifampicin with 51 ± 5%. Interestingly, the hydrophilic drugs isoniazid and PZ also showed good %EE

Table 3
Various nano-systems to co-deliver antibiotics.

Nanoplatform	Drugs	Formulation ingredients	Targeted bacteria	Route of administration, dose and dosage regimen	Rationale of the study	References
Liposomes	Gentamicin and ceftazidime	PC, DSPE and cholesterol	*K. pneumoniae*	Intravenously to mice; Gentamycin & ceftazidime (various doses tested against both susceptible and resistant strain); administered either as a single dose or as multiple doses every 24 h for 14 days.	Parallel distribution of drugs at infection site & improve synergism.	Schiffelers et al. (2001)
Liposomes	Daptomycin and clarithromycin	mPEG-DSPE, hydrogenated soy PC and cholesterol	*MRSA*	Intravenously to mice; Clarithromycin & daptomycin (51.8 & 1.6 mg/kg); administered once.	To evaluate concurrent use of daptomycin & clarithromycin in liposomal form against MRSA infections.	Li et al. (2015)
Liposomes	Isoniazid and rifampicin	DPPC, Egg PC and cholesterol	*M. tuberculosis*	NA	Encapsulation of two anti-TB drugs in a single liposomal system.	Gürsoy et al. (2004)
Liposomes	Rifampicin, isoniazid, pyrazinamide and streptomycin	DSPE-PEG, DOTAP and cholesterol	*M. tuberculosis*	NA	Targeting *M. tuberculosis* infected human macrophages using TGF-β1 siRNA conjugated liposomes encapsulating anti-TB drugs.	Niu et al. (2015)
SLNs	Rifampicin, isoniazid and pyrazinamide	Stearic acid and PVA	*M. tuberculosis*	Orally to mice; Rifampicin, isoniazid & pyrazinamide (12, 10 & 25 mg/kg); administered once every 10 days for five dosing periods.	To evaluate chemotherapeutic potential of anti-TB drug loaded SLNs in a rat model.	Pandey et al. (2005)
SLNs	LL37 (a peptide with antimicrobial activity) and serpin A1 (an elastase inhibitor with wound-healing properties)	Glycerol mono stearate, PC and PVA	*E. coli* and *S. aureus*	NA	To investigate therapeutic effects of LL37 & serpin A1in SLNs to simultaneously improve wound healing & antibacterial efficacy.	Fumakia and Ho (2016)
Polymeric nanoparticles	Rifampicin, isoniazid and pyrazinamide	PLG and PVA	*M. tuberculosis*	Orally to mice; Rifampicin, isoniazid & pyrazinamide (12, 10 & 25 mg/kg); administered once every 10 days for five dosing periods.	To reduce dosing frequency of anti-TB drugs by encapsulating them in PLG nanoparticles.	Pandey et al. (2003)
Polymeric nanoparticles	Rifampicin, isoniazid and pyrazinamide	PLG, PVA and wheat germ agglutinin	*M. tuberculosis*	Oral/aerosol route to guinea pigs; Rifampicin, isoniazid & pyrazinamide (12, 10 & 25 mg/kg); administered once every 15 days for five dosing periods.	To reduce dosing frequency of anti-TB drugs by encapsulating them in lectin conjugated PLG nanoparticles.	Sharma et al. (2004a)
Polymeric nanoparticles	Rifampicin, isoniazid and pyrazinamide	PLG and PVA	*M. tuberculosis*	Orally to guinea pigs; Rifampicin, isoniazid & pyrazinamide (12, 10 & 25 mg/kg); administered once every 10 days for five dosing periods.	To evaluate chemotherapeutic potency of anti-TB drug loaded PLG nanoparticles at sub-therapeutic dose.	Sharma et al. (2004b)
Polymeric nanoparticles	Rifampicin, isoniazid, pyrazinamide and ethambutol	PLG and PVA	*M. tuberculosis*	Orally to mice; Rifampicin, isoniazid and pyrazinamide & ethambutol (12, 10 and 25 & 16 mg/kg); administered once every 10 days for five dosing periods.	To evaluate the chemotherapeutic efficacy of rifampicin, isoniazid and pyrazinamide loaded formulation along with ethambutol only loaded formulation against *M. tuberculosis* infected mice.	Pandey et al. (2006)
Polymeric nanoparticles	Rifampicin, isoniazid, pyrazinamide and ethambutol	PLG and PVA	*M. tuberculosis*	Orally to mice; Rifampicin, isoniazid, pyrazinamide & ethambutol (12, 10, 25 & 16 mg/kg); administered once every 10 days for five dosing periods.	To evaluate the chemotherapeutic efficacy of rifampicin, isoniazid & pyrazinamide loaded formulation along with ethambutol only loaded formulation to treat cerebral malaria.	Pandey and Khuller (2006a)
Polymeric nanoparticles	Azithromycin and rifampicin	PLGA and PVA	*Chlamydia trachomatis*	NA	Targeting chlamydial inclusion complexes using azithromycin & rifampicin co-loaded formulation.	Toti et al. (2011)

NA = *In vivo* studies not performed.

of between 40 and 50%. This high entrapment for hydrophilic drugs in SLNs could be due to ion pairing between the amine groups of drugs and the carboxyl group of stearic acid. The distribution of drugs in plasma and various organs of mice infected with *M. tuberculosis* $H_{37}Rv$, followed by a single oral administration of triple-drug loaded SLNs, was evaluated using *in vivo* drug disposition studies. The drug concentrations in the plasma and tested organs (lungs, liver and spleen) were detectable for eight and 10 days respectively for multi-drug loaded SLNs, whereas the free drugs were cleared in 24–48 h. Furthermore, there was no evidence of the existence of tubercle bacilli in the lungs/spleen after five oral doses of formulation that was administered every 10th day, while the free drugs had to be administered for 46 days orally to achieve the same beneficial outcome. This multi-drug loaded system displayed its superiority over the free drugs in better management of TB with the potential to reduce the dosing frequency while improving patient compliance. As it is well recognised that particle size does affect the cellular uptake (Gustafson et al., 2015), the size of SLNs should have been reported by the authors.

In the above studies, the research is mainly focused on fighting infections caused by various resistant strains of bacteria. However, it is worth noting that wounds are also prone to get infected by pathogenic microorganisms and may become severe if not taken care of (Bowler et al., 2001). Recognising the biological benefits of LL37 (an endogenous host defence peptide that has antimicrobial activity) and serpin A1 (an elastase inhibitor that possess wound healing properties), Fumakia et al. devised multi-functional SLNs with wound healing, antibacterial and anti-inflammatory properties by simultaneously loading LL37 and serpin A1, intended for topical use (Fumakia and Ho, 2016). Two SLN formulations were prepared, namely prep-1 (final loadings for LL37 and serpin A1 were 8.48 μg and 43.5 μg per mg of SLNs respectively) and prep-2 (final loadings for LL37 and serpin A1 were 16.32 μg and 62.47 μg per mg of SLNs respectively). Both prep-1 and prep-2 had particle sizes below 275 nm, with %EE > 80% being achieved for both LL37 and serpin A1. The results from the *in vitro* drug release studies that were carried out in pH 7.4 artificial wound fluid (AWF) suggested that LL37 and serpin A1 were released in a sustained manner from both prep-1 and prep-2 throughout the study period of 15 days. Interestingly, the free LL37 tended to lose its integrity in AWF beyond 8 h, while encapsulating it in SLNs protected it from degradation. Following the confirmation of synergistic antibacterial activity of LL37 and serpin A1 against *Escherichia coli* (*E. coli*) and *S. aureus in vitro*, antibacterial tests were performed for prep-1 and prep-2 and it was found that, both LL37 and serpin A1 were interdependent for potential synergism against *E. coli* and *S. aureus*. However, the mechanism for synergism was unknown. Both prep-1 and prep-2 displayed accelerated wound healing in BJ fibroblast cells and keratinocytes compared to LL37 and serpin A1 only, with prep-2 being more potent than prep-1 due to higher loadings. Furthermore, both prep-1 and prep-2 were found to attenuate the levels of inflammatory cytokines, and exhibited superior anti-inflammatory responses when tested on BJ fibroblast cells and keratinocytes. These results therefore proved the wound healing, antibacterial and anti-inflammatory potentials of LL37 and serpin A1 co-loaded SLNs (Fig. 2).

The co-delivery of antibiotics *via* lipid-based systems such as liposomes and SLNs, have shown potential for improving activity against various bacterial strains.

3.2. Polymer based nano-systems to co-deliver antibiotics

Polymeric nanoparticles have been explored widely to deliver a variety of antibiotics, and have shown great efficacy against several infections caused by various bacteria. Although polymeric nanoparticles loaded with single therapeutic agents have displayed promising outcomes in treating many bacterial infections, its co-delivery application has been explored to treat TB and chlamydia only. Combination therapy being an essential criterion to treat TB, Khuller and co-workers co-loaded three front line anti-TB drugs; rifampicin, isoniazid and pyrazinamide in PLG nanoparticles (Pandey et al., 2003). While frequent dosing of anti-TB drugs and poor patient compliance are the major limitations associated with TB chemotherapy, the study aimed to overcome these limitations using nanoparticle based combinatorial approach. The particles were formulated using an emulsion solvent evaporation technique, and were found to be in a size range of 186–290 nm, with ~58%, ~65%, ~70% of rifampicin, isoniazid and pyrazinamide being entrapped respectively. Followed by an initial burst release, all three drugs were found to have escaped slowly from the system over a studied period of 42 days. The mice were orally administered with drug loaded particles to study the *in vivo* pharmacokinetics. In plasma, the rifampicin was detectable for six days, whereas isoniazid and pyrazinamide were found at minimum inhibitory concentration (MIC) levels for nine days. In contrast, free drugs were cleared with in a day. When analysed in organs (lungs, liver and spleen), all three drugs were detectable at MIC levels for nine days. It was also noticed that isoniazid continued to have detectable therapeutic concentrations in all tested organs on day 11, whereas the same was not observed for the other two drugs. In contrast, none of the free drugs was detectable in any of the organs after day two. As repeated administration of the formulation can result in progressive accumulation of drugs in the liver, followed by hepatotoxicity, the levels of serum bilirubin, serum alanine amino transferase and serum alkaline phosphatase were examined and found to be in normal range, thus displaying the safety of the formulation. Furthermore, the anti-TB studies performed on the *M. tuberculosis* $H_{37}Rv$ infected mice revealed that 46 oral doses of the free drugs were required to achieve complete bacilli clearance, whereas only five doses of the multi-drug loaded formulation, administered once in 10 days, was sufficient to achieve the same beneficial outcomes. It was noticed that the drug release study was performed in PBS 7.2–7.4 only. While the formulation was intended for oral administration, the initial 2 h of the drug release study should have been performed in PBS 1.2. Despite this criticism, the authors showed that co-loading the multiple anti-TB drugs into a single nano-system can efficiently minimize the dose to improve patient compliance in TB-chemotherapy with a shorter treatment course.

In their subsequent study, the authors functionalized the particles with lectin, a bio-adhesive agent, in order to increase the absorption time and further reduce the dosing frequency of the loaded drugs (Sharma et al., 2004a). A multiple emulsion solvent evaporation method was used to prepare the isoniazid, rifampicin and pyrazinamide co-loaded PLG nanoparticles, followed by a conjugation of the wheat germ agglutinin (an immunogenic lectin) using EDC-NHS chemistry. The lectin coated nanoparticles were distributed in a size range of 350–400 nm, which were considerably larger than the unconjugated nanoparticles that were found to be between 180 and 290 nm. Interestingly, coating of lectin onto the surface of the nanoparticles had no effect on the drug loading and entrapment. High %EE of 64.3 ± 7.4%, 54 ± 2% and 66.8 ± 7.7% were recorded for isoniazid, rifampicin and pyrazinamide respectively. Furthermore, the lectin functionalized formulation was administered into guinea pigs through an oral/aerosol route to study *in vivo* pharmacokinetics. There was no significant difference observed in the distribution of all three encapsulated drugs administered either orally or through the aerosol route, where isoniazid, rifampicin and pyrazinamide were detected for 14, ~7 and ~14 days in plasma respectively, while the free drugs were cleared within a day. Furthermore, the lectin free nanoparticles also showed a short plasma residence time of 8–9 days for isoniazid and pyrazinamide, and 4–6 days for rifampicin. When evaluated in the lungs, liver and spleen, the drugs from the lectin free nanoparticles were un-detectable after day 10. However, all three drugs from the lectin coated nanoparticles were detectable for 15 days, thus displaying the increased bioavailability. The antibacterial studies performed on *M. tuberculosis* $H_{37}Rv$ infected guinea pigs revealed that only three doses, once every 15 days, of oral or nebulized lectin functionalized nanoparticles were required to achieve undetectable bacilli, whereas to achieve the same

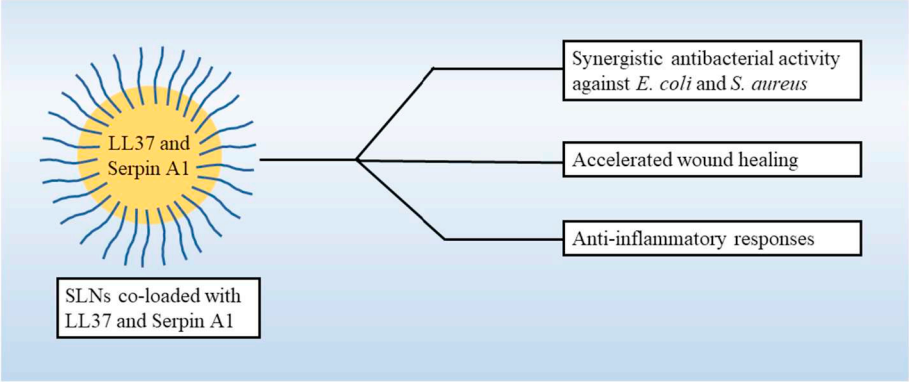

Fig. 2. Potential effects of LL37 and serpin A1 co-loaded SLNs.

beneficial outcome, 45 daily oral doses of free drugs were needed. From these findings, it was observed that the lectin functionalized nanoparticles significantly improved the bioavailability of encapsulated drugs to treat TB with reduced doses.

Encouraged by these results, in a subsequent study by the same research group, the authors examined the effects of isoniazid, rifampicin and pyrazinamide loaded PLG formulation at a sub-therapeutic dose (2/3rd of therapeutic dose) on *M. tuberculosis* $H_{37}Rv$ infected guinea pigs (Sharma et al., 2004b). No difference was observed in the mean residence time at both doses (therapeutic and 2/3rd of therapeutic dose), which was significantly increased for rifampicin (12-folds), isoniazid (24-folds) and pyrazinamide (21-folds) compared to the free drugs. A single dose of the formulation administered orally to the guinea pigs at 2/3rd of the therapeutic dose revealed that all three drugs had attained a sustained plasma levels for 7–12 days and 11–14 days in the tested organs. Furthermore, only five doses of the formulation had to be administered every 10 days to achieve undetectable bacilli, whereas 46 conventional doses were required to achieve the same benefits. Therefore, these results at 2/3rd of therapeutic dose were comparable to the results obtained with therapeutic dose (Pandey et al., 2003).

In another study by the same research group, the triple drug loaded formulation along with ethambutol only loaded PLG nanoparticles were evaluated for chemotherapeutic potential in a murine model (Pandey et al., 2006). Ethambutol, being highly hygroscopic, was shown to adversely affect the stability of the formulation (Bhutani et al., 2004), limiting its co-encapsulation with other drugs. Therefore, recognising this as a major concern, ethambutol was loaded in a distinct formulation and used as a supplement dose to provide enhanced activity. The triple drug loaded formulation along with the ethambutol nanoparticles were administered orally to a group of mice that were infected with *M. tuberculosis* $H_{37}Rv$. The pharmacokinetics study revealed that a single therapeutic dose of the anti-TB drugs loaded formulation displayed sustained levels of the drugs in the plasma for ~5 days, and 7–9 days in the tested organs (lungs, liver and spleen) while the free drugs remained detectable only until day two. In contrast to that of the free drugs, a significant improvement in half-life and mean residence time was observed for the drugs encapsulated in nanoparticles. In *M. tuberculosis* $H_{37}Rv$ infected mice, the formulation showed significantly better activity than the free drugs, with only three oral doses being administered every 10th day to achieve undetectable levels of bacteria, compared to the 28 conventional doses of the free drugs. Therefore, compared to their previous results (Pandey et al., 2003), the addition of the ethambutol nanoparticles to the triple drug loaded formulation improved the activity by reducing the dose and time required for a complete clearance of the bacilli.

Recognising the severity of cerebral tuberculosis, in their following study, the authors administered the same formulation in *M. tuberculosis* H37Rv infected mice orally to evaluate the delivery of the drugs to the brain (Pandey and Khuller, 2006a). Size and %EE were found to resemble those in their previous study (Pandey et al., 2006). To achieve undetectable bacilli in meninges, 46 oral doses of the conventional free drug combination was required, whereas a complete clearance of the bacilli was observed with only five oral doses of the formulation administered once in 10 days. The formulation was proven to cross the blood/brain barrier to deliver the drugs to the brain for treating cerebral tuberculosis, highlighting the potential advantages of nano-based systems in carrying multiple drugs across blood brain barrier.

While research on the co-delivery of drugs using polymeric nanoparticles was mainly focused on tuberculosis, Toti et al. identified the severity of chlamydial infections, and proposed a polymeric nanosystem encapsulating two antibiotics. As the chlamydia strains localise intracellularly, it becomes difficult for the antibiotics to gain access into these inclusion complexes. Taking it as a challenge, the authors devised PLGA nanoparticles co-encapsulating rifampicin and azithromycin for targeting chlamydial inclusion complexes (Toti et al., 2011). An emulsion solvent evaporation method was used to prepare nanoparticles of size 215 nm, with a very low %loading efficiency of 0.5% and 0.1% being achieved for azithromycin and rifampicin respectively. Initially, the authors proved that the nanoparticles loaded with 6-coumarin (dye) were taken up by chlamydial infected cells within 15 min post addition, although the mechanism was unknown. Furthermore, the *in vitro* studies performed using the *Chlamydia trachomatis* infected McCoy cells revealed that the free drugs alone were effective when treated immediately following infection. However, treatment at 24 h and 48 h post infection did not produce potent activity. In contrast, the co-encapsulated nanoparticles were effective even when added at 24 h and 48 h post infection. Although complete killing was not achieved with the drug encapsulated nanoparticles, a significant decrease ($p < 0.05$) in chlamydia inclusion numbers was observed in the dose range tested. A significant improvement in the activity was not observed with the drugs encapsulated in the nanoparticles compared to the combination of drugs in the free form. These insignificant results could be due to very poor drug loadings, thus warranting the need for further optimization of the formulation.

Although the polymeric nanoparticles appear to be limited to co-deliver the antibiotics than the lipid-based systems, it has shown promising outcomes thus far to fight tuberculosis and chlamydia infections.

In addition to the co-delivery of antibiotics using nano-systems, the researchers have also explored the antibacterial metal ions as counterparts to the antibiotics. The combined effects of metal ions, such as gallium and bismuth with other antibiotics, have been studied in liposomal and niosomal forms against a highly resistant bacteria *Pseudomonas aeruginosa* (Halwani et al., 2008a; Halwani et al., 2008b; Halwani et al., 2009; Alipour et al., 2010; Alipour et al., 2011; Alhariri and Omri, 2013; Mahdiun et al., 2017). As these metal ions are not FDA approved antibiotics, the studies presenting co-delivery of metal ions and antibiotics have not been discussed in this review.

4. Nano-systems to co-deliver antiviral drugs

Viral infections are one of the leading causes of the increasing premature mortality worldwide (Singh et al., 2017). Viruses such as HIV, hepatitis B, hepatitis C, influenza, herpes simplex, human papilloma, zika, ebola *etc.*, are known to cause life threatening infections (Singh et al., 2017). Monotherapy using nano drug delivery systems that target different viruses can be found in the literature (Singh et al., 2017). However, to date, among many viruses, HIV appears to be the only focus of interest for prophylaxis using nano-based co-delivery.

HIV is considered to be the most notorious virus among all other viruses, as it has every defensive and offensive strategy to spike the host's obvious immune responses, thus becoming a causative agent for many deaths world-wide. According to a 2016 report by the WHO, approximately 1 million people died from HIV related diseases and 1.8 million people were newly infected with HIV globally (WHO, 2017). Since the discovery of HIV in 1981, scientists have invented many potential antiretrovirals (ARVs) to manage the infection. For efficient prophylaxis, a combination of ARVs, commonly known as combination antiretroviral therapy (cART) or highly active antiretroviral therapy (HAART) is in use to inhibit the multiple steps of the HIV life cycle. Over the years, HAART has become very successful in depleting the viral load to an undetectable level, thus providing hope for HIV infected individuals to extend their lives. However, it does have significant limitations, such as drug resistance, lack of access to tissues and reservoirs, poor bioavailability, long-term drug therapy, toxicity and drug-drug interactions (Mamo et al., 2010). These limitations and pharmacokinetic differences between individuals are believed to be the reasons for poor adherence/non-adherence of the therapy (Mamo et al., 2010). To overcome these limitations, several nano-based approaches employing ARVs can be found in the literature, including co-delivery (Date and Destache, 2013). A schematic was developed to show the influence of multi-ARV loaded nano-systems on the HIV life cycle (Fig. 3). Referring to Fig. 3, the multiple steps of the HIV life cycle can be inhibited using cARV that are loaded into a single nano-system, thereby resulting in an efficient prophylaxis. However, single ARV loaded nano-formulations can inhibit any one of various mechanisms involved in the HIV life cycle, and may not prove to be an effective strategy for HIV prophylaxis. Various nano-systems to co-deliver anti-HIV drugs are summarized in Table 4.

4.1. Lipid based nano-systems to co-deliver antiviral drugs

Various lipid-based nano-systems, such as liposomes, SLNs and lipid nano-emulsions/suspensions, have been investigated to co-deliver anti-HIV agents and achieve efficient prophylaxis for HIV/AIDS. One of the earliest studies on lipid based nano-systems to co-deliver cARV drugs was reported by Sankar et al. in 2012. As colloidal drug carriers can easily be engulfed by opsonin expressed phagocytes, the authors used this as an advantage and co-delivered two nucleoside reverse transcriptase inhibitors (NRTIs), lamivudine and zidovudine, using polymeric and solid lipid nanoparticles to achieve localized high concentrations in the macrophages for targeting HIV (Sankar et al., 2012). The dual drug loaded polymeric nanoparticles that were prepared using the emulsion polymerization method, consisted of PLGA and poloxamer 188. To prepare lamivudine-zidovudine loaded SLNs, a high shear homogenization method was employed when lipids used were stearic acid/cocoa butter/glyceryl monostearate, whereas a solvent evaporation method was employed when lecithin was used as a solid lipid. For both polymeric nanoparticles and the SLNs, poloxamer 188 was chosen as a common surfactant, whereas tween 80 was also screened to optimize the SLNs. From the particle size analysis, it was found that SLNs prepared using glyceryl monostearate and poloxamer 188 had greater particles sizes (~520 nm) than the PLGA nanoparticles (~70 nm). However, the drug release studies revealed that the SLNs were more efficient in sustaining the release of encapsulated drugs compared to the PLGA nanoparticles, and was therefore considered as the optimized formulation. The tissue distribution of the multi drug loaded polymeric nanoparticles and optimized SLNs after intra-peritoneal administration into mice suggested that the SLNs had higher concentrations of the encapsulated drugs than the PLGA nanoparticles in the liver and spleen. In our opinion, screening different polymers and surfactants to prepare polymeric nanoparticles could have given more insight into the characterized studies. Furthermore, the drugs used in this study targeting the same enzyme may result in reduced activity due to the competitiveness for the binding site. Therefore, using a different class of drugs to inhibit the multiple steps of the HIV life cycle may result in effective prophylaxis.

In line with the goal to enhance the therapeutic potency of ARVs and tissue viral clearance, Ho and co-workers developed lipid nanoparticles (LNPs) to co-encapsulate three antiretroviral agents lopinavir, ritonavir, and tenofovir in a ratio of 2:1:3 (Freeling et al., 2015;

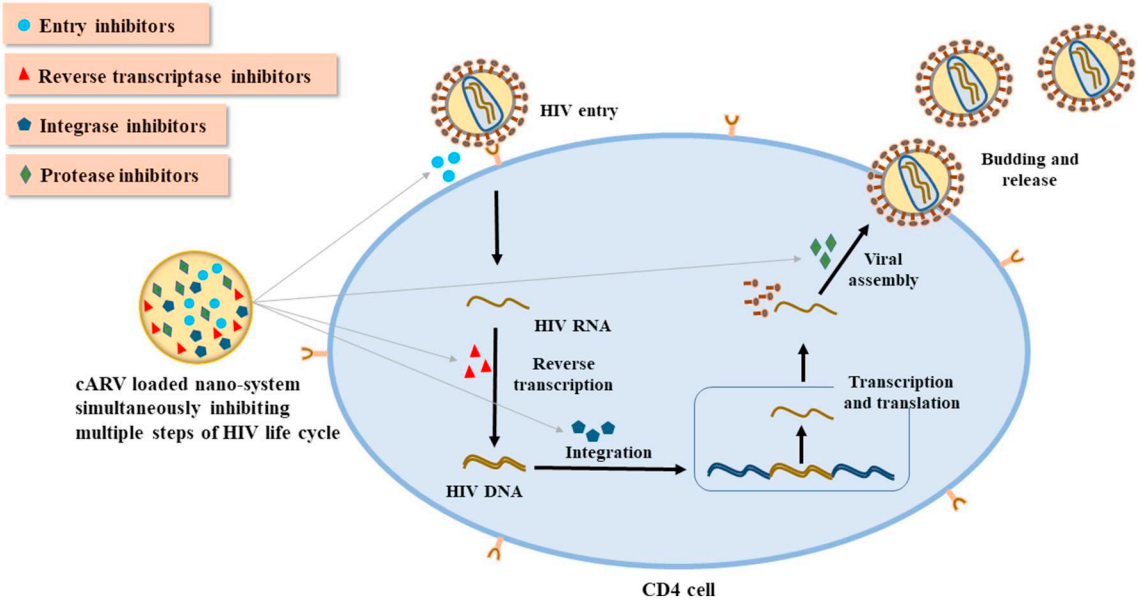

Fig. 3. Schematic representation of nano-based co-delivery of ARVs, simultaneously inhibiting multiple steps of HIV life cycle.

Table 4
Various nano-systems for the co-delivery of antiviral drugs.

Nanoplatform	Drugs	Formulation ingredients	Route of administration, dose and dosage regimen	Major findings	References
SLNs/polymeric nanoparticles	Lamivudine and zidovudine	Glycerol monostearate, PLGA, lutrol F68 and castor oil	Intraperitoneally to mice; 1 mL of each formulation containing lamivudine & zidovudine (0.6 & 1.6 mg); administered once.	• SLNs were more efficient in sustaining the release of encapsulated drugs compared to PLGA nanoparticles. • SLNs had higher concentrations of encapsulated drugs than PLGA nanoparticles in liver and spleen.	Sankar et al. (2012)
LNPs	Lopinavir, ritonavir and tenofovir	DSPC and $MPEG_{2000}$-DSPE	Subcutaneously to macaques; Lopinavir, ritonavir & tenofovir (25.0, 14.3 & 17.1 mg/kg); administered once.	• Enhancement of anti-HIV activity by 3-fold for cARV loaded formulation compared to cARV in free form.	Freeling et al. (2015); Freeling et al. (2014)
LNPs	Lopinavir, ritonavir and tenofovir	DSPC and $MPEG_{2000}$-DSPE	Subcutaneously to macaques; Lopinavir, ritonavir & tenofovir (25.0, 7.0 & 10.6 mg/kg); administered once.	• Enhancement of anti-HIV activity by 30-fold for cARV loaded formulation compared to cARV in free form.	Kraft et al. (2017)
In-situ self-assembly nanoparticles	Lopinavir and ritonavir	Oleic acid, TPGS and aeroperl 300	Orally to rats; Lopinavir (10 mg/kg); administered once.	• > 95% entrapment efficiency for both drugs. • Increased lopinavir concentrations in tested organs compared to kaletra tablet. • Fixed dosage for multiple drugs in a single nano-formulation.	Pham et al. (2016)
Liposomes	Nevirapine and saquinavir	Egg PC, DSPE–PEG and cholesterol	NA	• Overcame incompatibility issues of drugs by encapsulating them in liposomes. • Greater antiviral potency for dual drug loaded formulation compared to single drug loaded formulations.	Ramana et al. (2015)
Polymeric nanoparticles	Lopinavir, ritonavir and efavirenz	PLGA, PVA and pluronic F127	NA	• Increased PBMC concentrations for drugs in nanoparticles compared to free drugs. • Biosafety of the formulation towards MDMs.	Destache et al. (2009)
Polymeric nanoparticles	Lopinavir, ritonavir and efavirenz	PLGA, PVA and pluronic F127	Intraperitoneally to mice; Lyophilized nanoparticle powder (equivalent of 20 mg/kg); administered once.	• Prolonged drug residence time with nanoparticles (detectable for 28 days) compared to free drugs (detectable for 3 days) in mice.	Destache et al. (2010)
Polymeric nanoparticles	Lopinavir, ritonavir and efavirenz	PLGA, PVA and pluronic F127	NA	• Lower molecular weight PLGA and single emulsion solvent evaporation method improved the physical characteristics of particles with greater %entrapment efficiency. • Efficient uptake of drugs loaded nanoparticles in human T cells (H9) and fibroblasts (HeLa).	Shibata et al. (2013)
Polymeric nanoparticles	Raltegravir and efavirenz	PLGA, PVA and pluronic F127	NA	• Enhanced antiviral potency for dual drug loaded formulation compared free drugs against HIV-1 infected TZM-bl cells. • Both formulation and gel were non-toxic towards HeLa.	Date et al. (2012)
Polymeric nanoparticles	Tenofovir, alafenamide and elvitegravir	PLGA, PVA and pluronic F127	Subcutaneously to mice; Tenofovir, alafenamide & elvitegravir (equivalent to 200 mg/kg each); administered at 1, 2, 4, 7, 10 & 14 days.	• Longer residence time for both drugs in plasma and vagina compared to free drugs. • Detectable drug concentrations for nanoparticles were maintained in vaginal tissues for 14 days, while free drugs were cleared within 72 h.	Mandal et al. (2017)
Polymeric nanoparticles	Tenofovir alafenamide and elvitegravir	PLGA, PVA and pluronic F127	Subcutaneously to mice; Tenofovir, alafenamide & elvitegravir (equivalent to 200 mg/kg each); administered at 1, 4, 7, 10 & 14 days.	• Enhanced elimination half-lives for drugs encapsulated in nanoparticles.	Prathipati et al. (2017)
Polymeric nanoparticles	Nonnucleoside reverse transcriptase inhibitor (NNRTI), DAAN-14f and HIV-1 fusion inhibitor, T1144	mPEG-PLA and maleimide-PEG-PLA	Intravenously to rats; DAAN-14f (5 mg/kg); administered once.	• Bypassed P-glycoprotein efflux process of HIV. • Higher cellular uptake and a strong activity against broad-spectrum of HIV-1 strains. • Synergistic activities for drugs loaded in nanoparticles against multiple HIV strains tested.	Li et al. (2016)
Polymeric nanoparticles	Darunavir and atazanavir	Polycaprolactone and TPGS	Orally to rats; Darunavir & Atazanavir (70 & 35 mg/kg); administered once.	• Enhanced plasma concentration of darunavir and atazanavir by ~2-fold compared to free drugs.	Meshram et al. (2015)

NA = *In vivo* studies not performed.

Freeling et al., 2014). A thin-film hydration method, employing DSPC and mPEG-DSPE as lipids, was used to prepare the multi-drug loaded LNPs. These were prepared at laboratory and clinical scale, with the particle sizes being found to be ~70 nm and ~50 nm respectively. High entrapment efficiencies of > 70% and > 90% were achieved for the protease inhibitors at the laboratory and clinical scales respectively, whereas only ~12% of tenofovir was entrapped at either of the scales. While reproducing the results in different scales is not an easy task, in this study, particle size and entrapment efficiency at both scales were similar. An *in vitro* antiviral study on HIV-infected CEM-174 cells revealed that the multi drug loaded LNPs were 3-fold more efficient than the drug combination in free form. To evaluate the total drug exposure in the plasma, both the formulation and free drugs were administered subcutaneously into macaques and it was found that the release of all three drugs from the LPNs was sustained and remained detectable in plasma after seven days. However, the free drugs achieved peak plasma concentrations within 8 h and were undetectable after 24 h. In addition, the multi-drug loaded LNPs showed higher intracellular concentrations for all encapsulated drugs in the lymph nodes, in contrast to the free drugs. In a subsequent study by the same research group, the formulation was customized by increasing the lopinavir:ritonavir ratio to 4:1, while the tenofovir was 17.1 mmol/L (Kraft et al., 2017). A slight increase in the particle size was observed, from 50 nm to 69 nm, with an %EE of > 90% being achieved for lopinavir and ritonavir, and 11.2% for tenofovir. The *in vitro* anti-HIV study proved that higher amounts of lopinavir and tenofovir in this formulation led to 30-fold improvement compared to drug combination in free form. Furthermore, this formulation was found to be 10-fold more potent than their previous formulation. As inhibiting residual HIV that are present in the cells and tissues is extremely challenging, the authors have designed multi-ARV loaded LNPs to address the issue. In yet another report, the authors demonstrated the long acting pharmacokinetic characteristics of the encapsulated drugs, and assumed it to be a combination of following mechanisms, (a) nano-formulation undergoing selective lymphatic uptake from the subcutaneous space (b) retention of drugs in nodes during lymphatic first-pass (c) sustained release of drugs into blood circulation, and (d) limited extravasation of nanoparticles-associated drugs that resulted in prolonged circulation (Kraft et al., 2018).

Pham et al. recently attempted to overcome the challenge of achieving a fixed dosage for multiple drugs in a single nano-system. Using *in situ* self-assembly method, the authors were able to develop children-friendly nanoparticles, with a fixed dose achieved for lopinavir and ritonavir at a ratio of 4:1 (w/w), the same as in the commercially available Kaletra tablets (Pham et al., 2016). In this method, oleic acid and D-α-tocopheryl polyethylene glycol 1000 succinate (TPGS) were selected as suitable lipid and surfactant respectively, due to the high solubility of both drugs in them. The molten mixture of the lipid, surfactant and drugs was loaded onto aeropearl 300 porous granules to prepare fixed-dose granules. The granules when dispersed and vortexed, produced drug-loaded lipid nanoparticles with a size of 158 nm and a > 95% entrapment efficiency for both drugs (Fig. 4). From the *in vivo* kinetics studies performed on rats, it was found that a higher biodistribution for lopinavir was observed in the tested organs than Kaletra (increased lopinavir concentrations by 2.8-fold in liver, 5.1-fold in kidney, 2.7-fold in brain, 6.1-fold in lymph nodes, and 3.4-fold in spleen). Further, higher plasma concertation for lopinavir was observed when it was used in co-delivery form as lopinavir/ritonavir *in situ* self-assembled nanoparticles compared to lopinavir solid granules only. While achieving fixed dosage for multiple drugs in a single nano-system could be challenging with conventional methods, the authors in this study, demonstrated an *in situ* self-assembly strategy to overcome this challenge.

While researchers in the above studies focused on the drugs that are compatible with each other, Ramana et al. aimed to overcome the incompatibility issues of two ARVs by encapsulating them into liposomes (Eagling et al., 1999). One of the limitations of combination drug therapy is inactivation or reduction of bioavailability of one active drug by another. For example, when nevirapine and saquinavir are co-administered in their free forms, the former can increase the metabolization rate of the latter by activating cytochrome enzyme (CYP3A4), resulting in its rapid elimination and poor bioavailability. To address this challenge, the authors co-encapsulated nevirapine and saquinavir into anti-CD4 (an antibody) conjugated liposomes to simultaneously target and co-deliver the encapsulated drugs to HIV infected cells (Fig. 5) (Ramana et al., 2015). These liposomes were prepared by a thin film hydration method using egg PC, DSPE–PEG and cholesterol. Thus formed liposomes were conjugated to alphathiolated anti-CD4 using thiol maleimide chemistry to synthesize the immunoliposomes. These liposomes had a mean diameter of 160 nm, with 45% of nevirapine and 30% of saquinavir being entrapped. An interesting phenomenon was observed by the researchers, where an increase in concentrations of cholesterol and DSPE–PEG led to improved entrapment efficiency of the hydrophobic nevirapine and hydrophilic saquinavir respectively. The release of saquinavir from the liposomes was slower than that of nevirapine, which could be due to the presence of PEG on the outer surfaces of the liposomes, thus not allowing the hydrophobic drug to release easily. Furthermore, the *in vitro* antiviral studies performed on infected human embryonic kidney cells (HEK 293T) proved that the dual drug loaded anti-CD4 conjugated liposomes were more potent than the unconjugated and single drug loaded liposomes. However, it is noteworthy that the anti-CD4 conjugation also increased the toxicity of the drug loaded liposomes due to its higher cellular uptake. The authors therefore demonstrated that drug incompatibilities can be overcome by encapsulating them in a nano-system to achieve maximum utilization of the drugs.

4.2. Polymer based nano-systems to co-deliver antiviral drugs

Polymeric nano-particles have been comprehensively studied to deliver anti-HIV drugs (Khalil et al., 2011). They have gained considerable attention for HIV prophylaxis after Woodrow et al. and Ham et al. demonstrated their application as microbicides (Woodrow et al., 2009; Ham et al., 2009). Until today, PLGA is the most investigated polymer for delivering cARVs. To the best of our knowledge, Destache and co-workers were the first to report on the nano-based co-delivery of ARVs in the late 2000 (Destache et al., 2009). The researchers co-encapsulated efavirenz, lopinavir and ritonavir into commonly used PLGA (Mw 110,000-139,000) nanoparticles and demonstrated their potential applications for the effective management of HIV infection. The polymeric nanoparticles prepared using multiple emulsion-solvent evaporation were ~260 nm, with %EE of 86%, 45% and 38% for efavirenz, lopinavir and ritonavir respectively. As HIV can reside in peripheral blood mononuclear cells (PBMCs), the drug release study was carried out by incubating triple drug loaded PLGA nanoparticles and free drug combination with PBMCs separately. It was found that the intra-cellular concentrations for free drugs peaked at 8 h and were eliminated by the second day, in contrast, the drugs from the PLGA nanoparticles continued to be released for almost a month, demonstrating the sustained behaviour. As visualized by the TEM, the presence of the PLGA nanoparticles in the monocytes-derived macrophages (MDMs) confirmed their uptake. Furthermore, an MTT assay indicated that cellular uptake of the nanoparticles did not interfere with the viability of the MDM_S, confirming the biosafety of the formulation. On the basis of this study, the authors proved that multi ARV-loaded nanoparticles can home phagocytes, such as macrophages, over prolonged periods of time to release drugs. In continuation to the above study, the authors aimed to evaluate the *in vivo* efficacies of cARV loaded PLGA nanoparticles in contrast to free drugs (Destache et al., 2010). The multi ARV loaded nanoparticles and free drugs were administered intra-peritoneally into mice to compare the distribution of the drugs in various organs over the studied time period. It was found that the free drugs were eliminated after 72 h, whereas drugs from the PLGA nanoparticles were detectable

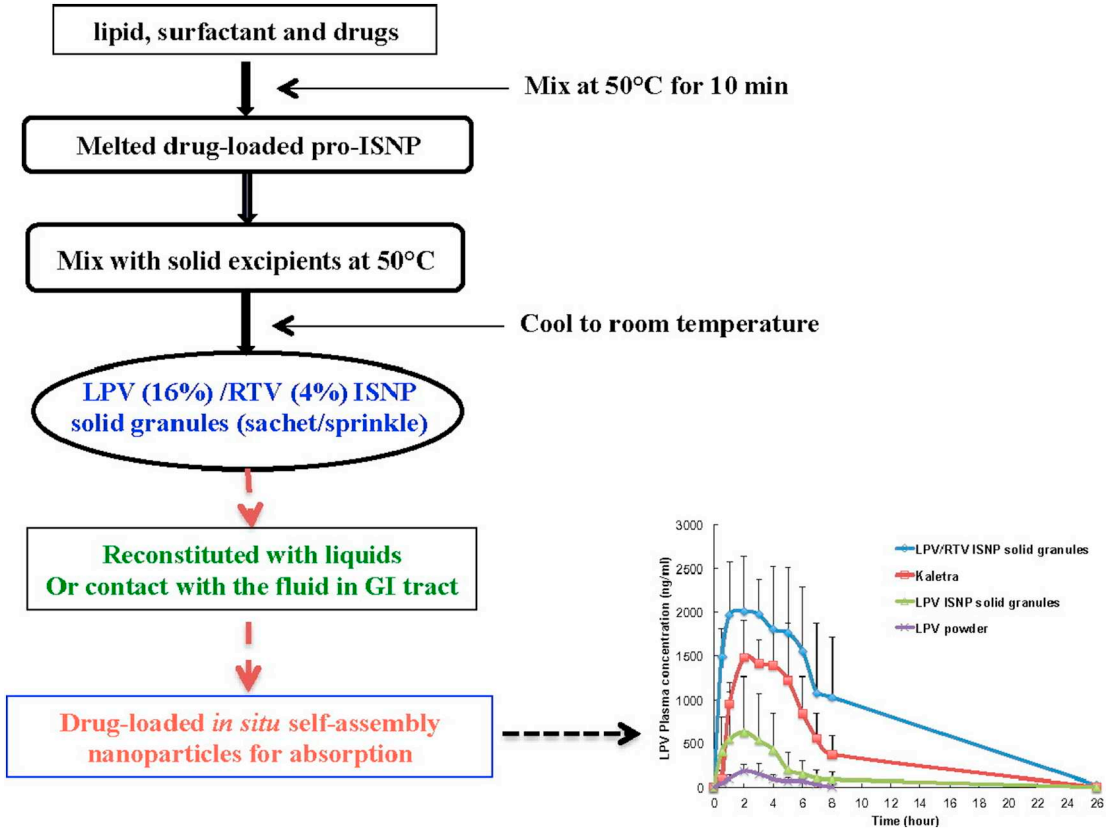

Fig. 4. Formulation and *in vivo* pharmacokinetics of lopinavir/ritonavir co-loaded *in situ* self-assembled nanoparticles. Reprinted from Pham et al. (2016), Copyright (2016), with permission from Elsevier.

until 28 days in the plasma and tested organs, including the brain. In addition, when tested on HIV infected MDMs, the release of the active principles was sustained from the PLGA nano-formulation compared to free ARVs, thus displaying the efficacy and longevity of the therapy.

Following their previous studies on the combination delivery of efavirenz, lopinavir and ritonavir using PLGA nanoparticles, Destache and co-workers formulated PLGA (Mw 52,000 Da) nanoparticles by co-encapsulating same ARVs to demonstrate their biosafety and uptake in both immune (H9 and U937) and nonimmune (HeLa) cells (Shibata et al., 2013). Both blank and multi-ARV loaded formulations did not significantly reduce the viability of the tested cell lines up to the tested period of 28 days. As the authors had proved the formulation's uptake in MDMs in their previous report (Destache et al., 2009), in the present study they were able to display the efficient uptake of multi-ARV loaded formulation in human T cells (H9) and fibroblasts (HeLa), which was confirmed by confocal microscopy. The average size of the particles was 140 nm, with ~80% entrapment efficiency being achieved for all three drugs. It was noteworthy that the authors achieved high %EE for all three drugs, with smaller particle sizes than their previous report (Destache et al., 2009). These improved results were achieved when a single emulsion solvent evaporation technique with low molecular weight polymer, different ratio of surfactant and high-pressure homogenizer were used. The subcellular fractionation study performed on the cARV loaded formulation treated H9 monocyte cells, which were previously infected with HIV-1, had significantly higher nuclear, cytoskeleton and membrane ARV drug levels in contrast to the free drug treated cells. The cARV loaded formulation was found to inhibit HIV-1 infection successfully, with IC_{50} values of 30.73, 14.01 and 16.54 nM being achieved for the encapsulated efavirenz, ritonavir and lopinavir respectively. In this study, the authors were successful in constructing a better formula to achieve smaller size and higher drug loadings. Although the triple drug loaded formulation was effective against HIV, it was noted that the IC_{50} values for the free drugs were not evaluated in this study for comparison.

Encouraged by the success achieved from their earlier studies on efavirenz, lopinavir and ritonavir loaded PLGA nanoparticles, a growing interest led these researchers to evaluate the potential of different ARV combinations for HIV prophylaxis. As, thermosensitive gels have the ability to transform from a liquid state to viscous gels when they meet body temperature (Ruel-Gariepy and Leroux, 2004), the authors developed a thermosensitive gel containing PLGA nanoparticles that was co-loaded with raltegravir and efavirenz, being intended for intra-vaginal delivery (Date et al., 2012). The PLGA (Mw 52,000) nanoparticles that were prepared using an emulsion solvent evaporation technique were ~80 nm, and had an entrapment efficiency of 55.5% and 98.2% for raltegravir and efavirenz respectively. An anti-HIV test on the TZM-bl cells indicated that the dual ARV loaded formulation had lower EC90 values than the free drugs against the tested HIV-1 strain, although a significant difference was not observed ($P > 0.05$). The *in vitro* intracellular drug release performed on the HeLa cells revealed that the efavirenz from formulation was detectable throughout the studied period of two weeks, whereas the raltegravir's concentration had declined by the end of sixth day. Having confirmed the antiviral potential and slow releasing behaviour of the formulation, thermosensitive gels were prepared by adding suitable amounts of pluronic F127 and pluronic F68 into nanoparticle dispersion followed by storing it overnight in a refrigerator. Utilizing fluorescence microscopy, the stained particles from the gel were shown to be transferred through transwell membrane and taken up by the HeLa cells. From the MTT assay, both ARVs containing nanoparticles and blank gel individually proved to be safe on the HeLa cells over a period of 14 days. It was observed that the MTT assays were not performed on the nanoparticle loaded gel itself. In our opinion, as using multiple stabilizers in a single system may produce significant toxicity to human cells, cell viability

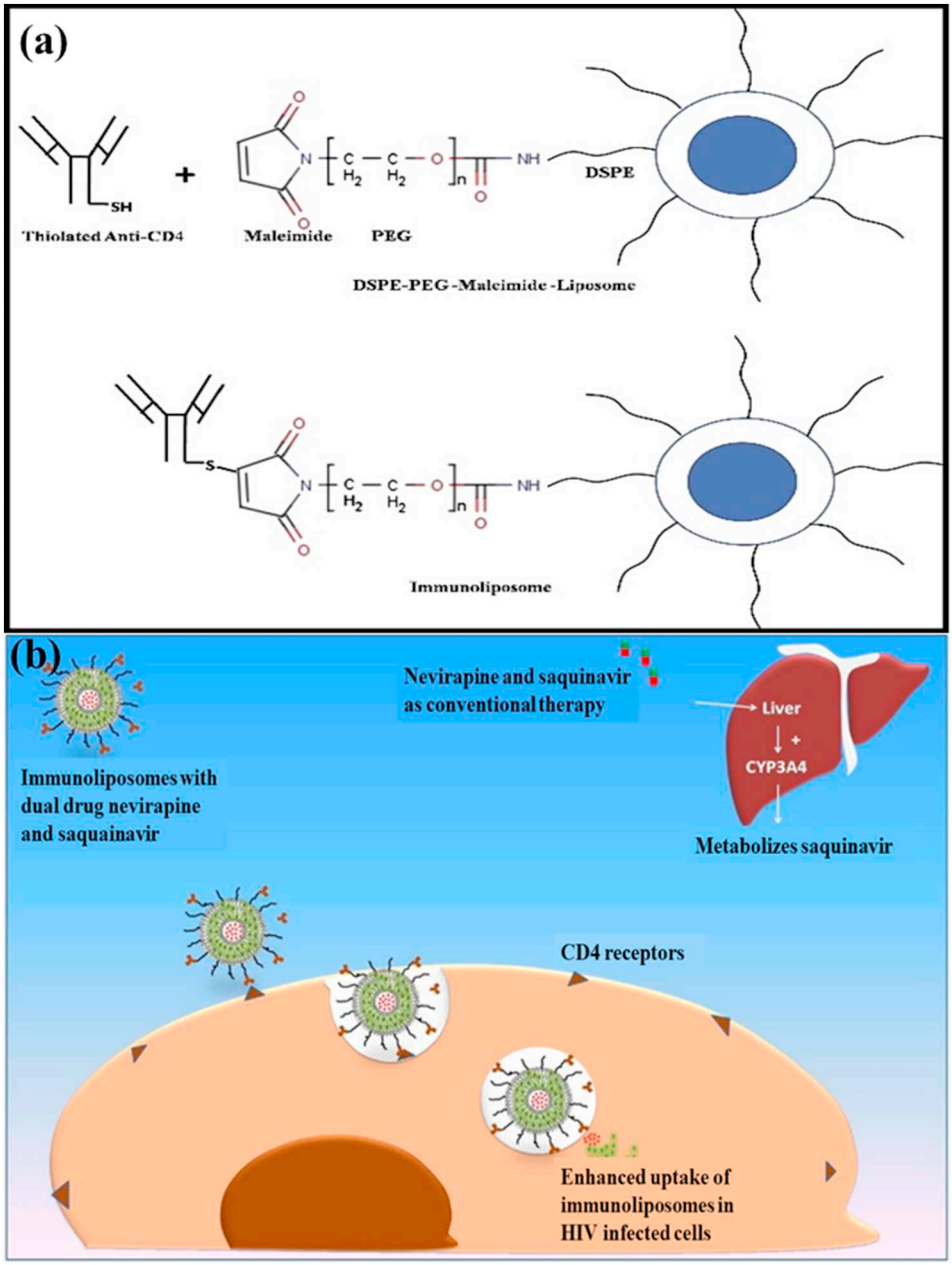

Fig. 5. (**a**) Conjugation of anti-CD4 on dual drug loaded liposomes. (**b**) Targeted delivery of immunoliposomes to enhance their uptake in HIV infected CD4 cells. Reprinted from Ramana et al. (2015), Copyright (2015), with permission from Elsevier.

study should have also been performed for the nanoparticle loaded gel. Despite this criticism, the results from this study provided new avenues for other researchers to use micro-environments as targeting sites to deliver multiple drugs.

Contributing to the concept of pre-exposure prophylaxis, in a subsequent study, the authors encapsulated two different ARVs, tenofovir alafenamide and elvitegravir in PLGA nanoparticles using interfacial polymer deposition technique (Mandal et al., 2017). The particles were 190 nm in size, with %EE of 54.1% and 44.6% being achieved for tenofovir alafenamide and elvitegravir respectively. An *in vitro* anti-HIV study using TZM-bl cells indicated that the co-loaded formulation was 30 times more effective than the free solution. *In vivo* pharmacokinetic experiments showed that when tenofovir alafenamide and elvitegravir were co-administered subcutaneously to Hu-BLT mice in the form of PLGA nanoparticles, detectable concentrations were maintained in vaginal tissues for 14 days, whereas the free drugs cleared within 72 h. This was attributed for the prevention of vaginal transmission of HIV for long periods of time by nano-formulation compared to free drugs. HIV prevention experiments in mice infected with HIV revealed that, all mice were protected for 4 days post nanoparticle injection; however, after 14 days, the authors witnessed a decline in survival rate of mice (60%). In a continuation study, the authors conducted pharmacokinetic and tissue distribution experiments in humanized mice using the same formulation (Prathipati et al., 2017). The subcutaneous administration of the tenofovir alafenamide and elvitegravir formulations resulted in longer residence times for both drugs in the plasma as well as the tested tissue organs, including the vagina and colon. Furthermore, the elimination half-lives were increased for both drugs in the plasma (14.2 h to 5.1 days for tenofovir alafenamide and 10.8 h to 3.3 days for elvitegravir). The tissue distribution studies revealed that the protective drug concentrations were maintained on day 10 for the nano-formulations, which were equal or higher than the concentrations obtained with free drug solution treatments on day 3. Considering the need for a long-acting injectable drug delivery system for pre-exposure HIV

prophylaxis, the tenofovir alafenamide-elvitegravir co-loaded PLGA nano-formulation may prove to be a viable treatment regimen.

Besides PLGA, other polymers, such as poly (lactic acid) and polycaprolactone, have also been investigated to deliver ARVs to control HIV infection. It is well known that functionalizing polymers with therapeutic agents can prove to be an effective strategy to achieve potential outcomes. Recently, an interesting study was published by Li et al. employing maleimide functionalized poly (ethylene glycol) 3400-poly (lactic acid) (Mal-PEG-PLA) to deliver a reverse transcriptase inhibitor DAAN-14f being encapsulated inside the core and HIV-1 entry inhibitor, T1144 being functionalised on the surface of nanoparticles (Li et al., 2016). The first step involved preparing the DAAN-14f loaded Mal-PEG-PLA nanoparticles using an emulsion solvent evaporation technique, which was followed by conjugating the T1144 on the surface of Mal-PEG-PLA nanoparticles using thiol maleimide chemistry. The particles were found to have a mean diameter of 117 nm with an encapsulation efficiency of 48.3% and 47.6% for DAAN-14f and T1144 respectively. This architecture, with the reverse transcriptase inhibitor (DAAN-14f) being entrapped inside nanoparticles, and the HIV-1 entry inhibitor (T1144) being functionalised on the surface of the nanoparticle, was found to facilitate the bypassing of the P-glycoprotein efflux process of HIV, which was attributed for the higher cellular uptake and a strong activity against broad-spectrum of HIV-1 strains (Fig. 6). Furthermore, synergistic activities were observed for the dual drug loaded nanoparticles against the multiple strains tested, improving the efficiency of both drugs by several folds. From the *in vitro* release, 90% of free DAAN-14f was released within 6 h, whereas only ~75% was released from the formulation at the end of 96 h. The *in vivo* pharmacokinetic studies performed on rats indicated that the formulation helped the DAAN-14f to extend its half-life (9.08 h) with a low clearance rate (0.095 L/h). This study demonstrated the application of entry inhibitors in combination therapy. It was observed that HIV entry inhibitors have seldom been used in the co-delivery application using nano-systems. In our opinion, they constitute large area of interest to be scrutinized further, as HIV infection can be controlled from the first step.

In another study, Meshram et al. co-delivered darunavir and atazanavir using polycaprolactone nanoparticle, which were prepared using two different polymers, polycaprolactone/Ɛ-caprolactone (L-PCL), employing the nanoprecipitation method (Meshram et al., 2015). The study aimed to improve the solubility and bioavailability of hydrophobic drugs and to protect them from CYP P450 3A4 enzymatic degradation. Both the PCL and L-PCL nanoparticles had similar size range of below 200 nm. The PCL nanoparticles had higher entrapment efficiencies for darunavir and atazanavir of 91.64% and 83.54% respectively, whereas the L-PCL entrapped 85.2% darunavir and 60.4% atazanavir. In addition, drug release studies have suggested that PCL nanoparticles were more efficient in controlling the release of atazanavir and darunavir than the L-PCL nanoparticles. When administered orally to rats, both formulations were shown to increase the plasma concentration of darunavir and atazanavir by ~2-fold compared to the free drugs. While the authors showed the successful encapsulation of two ARVs in PCL based nanoparticles, the *in vitro/in vivo* antiviral studies were lacking in this report.

It was noticed that, polymeric nanoparticles have been explored more compared to lipid-based systems to co-deliver anti-HIV drugs. Both systems have shown promising outcomes thus far to fight HIV/AIDS.

5. Nano-systems to co-deliver antimalarial drugs

Malaria is still recognised as a life-threatening disease regardless of availability of potential medication. In 2016, 216 million cases of malaria were reported that led to 445,000 deaths word-wide (WHO, 2018). Growing resistance to the existing drugs, accompanied by a scarcity for new drugs, are believed to be the major reasons for the failure of malaria therapy. In 2007, the WHO banned artemisinin-based monotherapy, identifying it as a major contributing factor for increasing resistance, thus obligating the use of artemisinin-based combination therapy (Ujuju et al., 2017). However, artemisinin-based agents suffer from certain limitations, such as poor solubility, erratic absorption, short half-lives, poor intracellular uptake and toxicity (Santos-Magalhães and Mosqueira, 2010; Aditya et al., 2013). To circumvent these challenges, nanotechnology has been used as an essential tool, with several studies on nano-based approaches to fight malaria being reported (Aditya et al., 2013). Table 5 summarizes various nano-systems used to co-deliver antimalarial drugs.

5.1. Lipid based nano-systems to co-deliver antimalarial drugs

As the available antimalarial drugs have poor aqueous solubility, they are extremely difficult to administer through conventional routes. Taking into account the lipophilic nature of these drugs, a few attempts have been made to co-deliver antimalarial drugs using lipid based nano-systems and used as potential strategies to improve their bio-availability. To date, the nano-based co-delivery approach for antimalarial agents has been explored using liposomes, NLCs and lipid nano-emulsion (Table 5), with the strategy and outcomes of each study being discussed below.

As discussed above in the antibacterial and anti-HIV drug delivery sections, liposomes are always good candidates for co-delivery applications. Furthermore, pegylated liposomes are known to increase the half-life and blood circulation time of drugs that undergo quick elimination (Isacchi et al., 2011). Isacchi et al. co-loaded two antimalarial drugs with short half-lives, artemisinin and curcumin, in both conventional (made up of DSPE and cholesterol) and PEGylated (made up of DSPE-PEG_{2000} and cholesterol) liposomes, and compared their *in vivo* efficacy with free artemisinin and its single drug formulation in conventional and PEGylated liposomes (Isacchi et al., 2012). The artemisinin-curcumin co-loaded conventional and PEGylated liposomes prepared using a thin film hydration method were of 202.31 ± 60.59 nm and 137.74 ± 31.17 nm respectively. Conventional liposomes were found to have achieved higher %EE for both artemisinin and curcumin of ~78% and ~62% respectively, which was ~10% more than the PEGylated liposomes. The possible reason for these low loadings of the hydrophobic drugs with PEGylated liposomes could be due to the presence of hydrophilic PEG, minimizing their contact with the hydrophobic bilayer. *In vivo* studies were performed using *P. berghei* infected mice, with artemisinin as a free drug being found to be effective only after the 7th day of treatment. Those treated with a single or co-loaded with curcumin in both conventional and PEGylated liposomes, appeared to have an immediate antimalarial effect, displaying the maximum utilization and availability of drugs in the infected red blood cells (RBCs).

In another study, Marques et al. recognising the antimalarial activity and specific binding ability of heparin to plasmodium-infected RBCs, devised cationic liposomes to co-deliver heparin and primaquine to effectively target and treat malarial infections (Marques et al., 2014). As cationic compounds could lyse RBCs, several lipids were screened in order to prepare an optimal formulation with low toxicity and hemolytic activity. Primaquine loaded liposomes were prepared by lipid film hydration method using the cationic DOTAP to facilitate electrostatic absorption of the negatively charged heparin onto the surface of the liposomes. Thus, formed liposomes were extruded through 200 nm polycarbonate membranes to obtain a uniform size. As, heparin has powerful anti-coagulant properties, it was made sure that the unbound heparin was removed by ultracentrifugation. The formulated liposomes when tested *in vitro* against *P. falciparum* cultures, 3-fold enhancement of activity for the encapsulated primaquine was observed. Furthermore, using anticoagulant study performed on mice, it was shown that only 2.6 μg/mL of the heparin was sufficient to induce targeting of liposomes to infected RBCs, which was well below its anticoagulant concentration

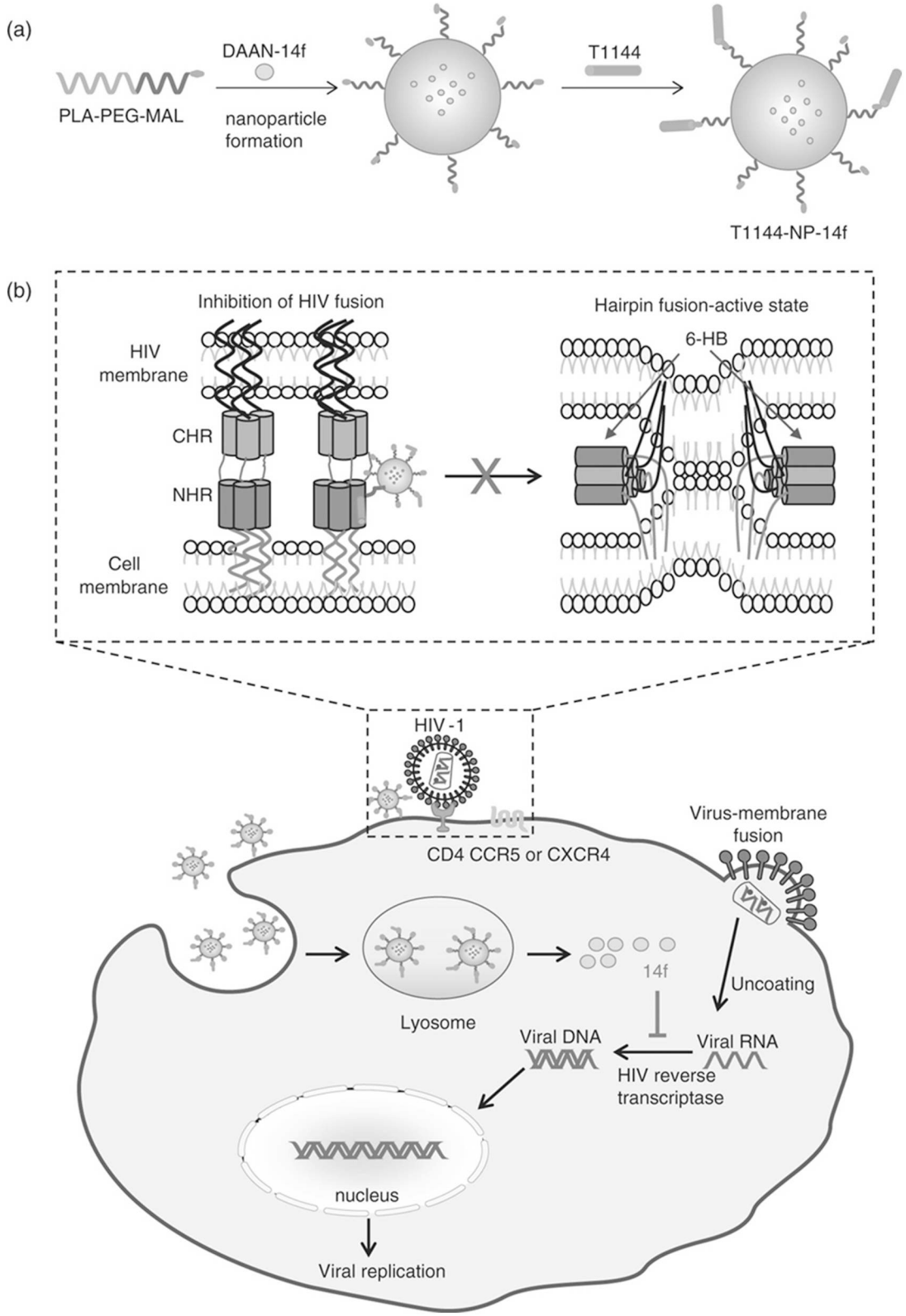

Fig. 6. (**a**) Preparation of Mal-PEG-PLA nanoparticles with DAAN-14f encapsulated inside the core and T1144 functionalised on the surface of nanoparticles. (**b**) Mechanism of action of Mal-PEG-PLA nanoparticles to inhibit HIV-1 infection. Reproduced from Li et al. (Li et al., 2016), with preliminary permissions from Wolters Kluwer.

($\geq 4\,\mu g/mL$). The images obtained from the TEM showed selective binding of the labelled heparin to infected RBCs compared to non-infected RBCs. The authors demonstrated that a heparin mediated targeted drug delivery approach could prove to be a novel alternative strategy compared to the expensive and resistance prone antibody-mediated targeting of plasmodium infected RBCs.

Alongside liposomes, NLCs are another class of lipid-based nanosystems that have been explored to co-deliver antimalarials.

Table 5
Various nano-systems for the co-delivery of antimalarial drugs.

Nanoplatform	Drugs	Formulation ingredients	Targeted parasite	Route of administration, dose and dosage regimen	References
Liposomes	Artemisinin and curcumin	PEG_{2000}-DSPE, Phospholipon90G and cholesterol	*P. berghei*	Intraperitoneally to mice; Artemisinin & curcumin (50 & 100 mg/kg/day); administered for 12 days.	Isacchi et al. (2012)
Liposomes	Primaquine and heparin	DOTAP and cholesterol	*P. falciparum*	NA	Marques et al. (2014)
NLC	Artemether and lumefantrine	Glycerol monostearate, soybean oil and pluronic F68	*P. berghei*	Intraperitoneally to mice; Artemether & lumefantrine (4 & 24 mg/kg); administered once.	Parashar and Rsr (2016)
NLC	Artemether, clindamycin and lumefantrine	Glyceryl dilaurate, and oleic acid, capmul MCM, tween 80, solutol HS 15,	*P. berghei*	Intravenously to mice; Artemether & clindamycin (3.1 & 5.85 mg/kg/day); administered for four consecutive days. Intravenously to mice; Artemether & lumefantrine (0.52 & 3.12 mg/kg/day); administered for four consecutive days.	Jain et al. (2014)
NLC	Artemether and lumefantrine	Glyceryl dilaurate, oleic acid, capmul MCM, tween 80 and solutol HS 15	*P. berghei*	Orally to mice; Artemether & lumefantrine (16 & 96 mg/kg/day); administered for four consecutive days.	Prabhu et al. (2016a)
NLC	Artemether and lumefantrine	Glyceryl dilaurate, oleic acid, capmul MCM, tween 80 and solutol HS 15	*P. berghei*	Intravenously to mice; Artemether (0.0208–0.208 mg/kg/day) & lumefantrine (0.1248–1.248 mg/kg/day); administered for four consecutive days.	Prabhu et al. (2016b)
Lipid emulsion	Artemether and lumefantrine	Soybean oil, sodium oleate, glycerol, pluronic F68 and egg phosphatidylcholine,	*P. berghei*	Intravenously to mice; doses ranging between 0.096 and 0.8 mg/kg/day (corresponding to artesunate); administered for 3 days.	Ma et al. (2014)
Polymeric nano-capsules	Quinine and curcumin	Poly (ε-caprolactone), caprylic/capric triglyceride, tween 80 and lipoid S45	*P. falciparum*	NA	Velasques et al. (2018)

NA = *In vivo* studies not performed.

Recognising the solubilizing behaviour of artemisinin-based compounds in various lipids, several authors have designed nanostructured lipid carriers (NLCs) to deliver these agents. While poor oral bioavailability has always been a major challenge for malaria therapy due to the hydrophobic nature of drugs, Parashar et al. co-loaded two front-line antimalarial drugs, artemether and lumefantrine, into NLCs at a ratio 1:6 (as available in marketed tablets) that was intended for parenteral delivery (Parashar and Rsr, 2016). To formulate the artemether-lumefantrine co-loaded NLCs, glycerol monostearate and soybean oil were used as solid and liquid lipids respectively. The dual drug loaded NLCs were prepared using hot homogenization, followed by an ultrasonication method, and had an average diameter of 145 nm with ~80% of % EE being achieved for both drugs. The authors observed a very similar %EE with the single drug loaded formulations, which indicated that co-loading of the artemether and lumefantrine in the NLCs did not compromise their encapsulation. The release of both drugs from the NLCs was prolonged, with 63% of artemether and 43% of lumefantrine being released over a time period of 30 h. From *in vivo* antimalarial activity performed on *P. berghei* infected mice, it was found that no complete cure was achieved when treated with the free drugs alone or the single drug loaded formulation, thus leading to their death before the studied period of 28 days. However, the mice groups treated with free drugs in combination or dual drug loaded formulation survived beyond 28 days, displaying the potential of combination therapy. Furthermore, the mice treated with the free drug combination had a parasitemia of ~13%, whereas the mice treated with an artemether and lumefantrine co-loaded formulation had only ~4% parasitemia, thus proving its efficiency over the former. As there is no available parenteral combination therapy to treat malaria at present (Prabhu et al., 2016b), this formulation can be a promising alternative to treating malaria effectively.

Pathak and co-workers, in one of their reports had observed a significant anti-plasmodial activity for glyceryl dilaurate (GDL) derived NLCs (no drug present) (Joshi et al., 2008). Although the mechanism of action was unclear, the NLCs were found to have accumulated inside the mitochondria of the parasites. These results were intriguing and led the researchers to extend their work on GDL-NLCs (Jain et al., 2014). The authors found that, GDL-NLCs effectively inhibited the formation of rings and schizonts, whereas trophozoites were still present. Thus, the protection offered by the GDL-NLCs was always partial, suggesting the need for the concurrent use of other antimalarials. Therefore, the GDL-NLCs were loaded with two antimalarial combinations, artemether-clindamycin and artemether-lumefantrine, and evaluated for their anti-plasmodial activity. Both formulations had particle sizes of below 65 nm. As artesunate is the only available drug for intravenous preparation, both formulations were compared with it and were found to exhibit complete parasite clearance at 5–20% of the therapeutic dose of artesunate when tested in *P. berghei* infected mice. Although the %EE was not reported for drugs, in our opinion, it was an interesting study that unveiled the need of antimalarial agents to achieve complete cure when GDL alone is used as an active agent.

While keeping antimalarial drugs in solubilised form is essential for better gastro-intestinal absorption and subsequently to achieve effective therapy (Ezzet et al., 2000), in a follow-up study by the same research group, the authors aimed to improve the gastro-intestinal absorption of hydrophobic drugs (artemether and lumefantrine) by encapsulating them in the GDL-capmul MCM derived NLCs (Prabhu et al., 2016a). The dual drug loaded NLCs were prepared using a microemulsion template technique and were ~68.80 nm in size, with the %EE being 62.11% and 37.09% for artemether and lumefantrine respectively. In contrast to the study by Parashar et al. using glycerol monostearate-soybean based NLCs encapsulated with artemether and lumefantrine (Parashar and Rsr, 2016), the GDL-capmul MCM derived NLCs were found to be of smaller sizes and had lesser amounts of drug being entrapped. However, it is worth noting that using GDL as a lipid in constructing nanocarriers can produce some additive or synergistic effects that may further enhance the antimalarial activity. From *in vivo* antimalarial

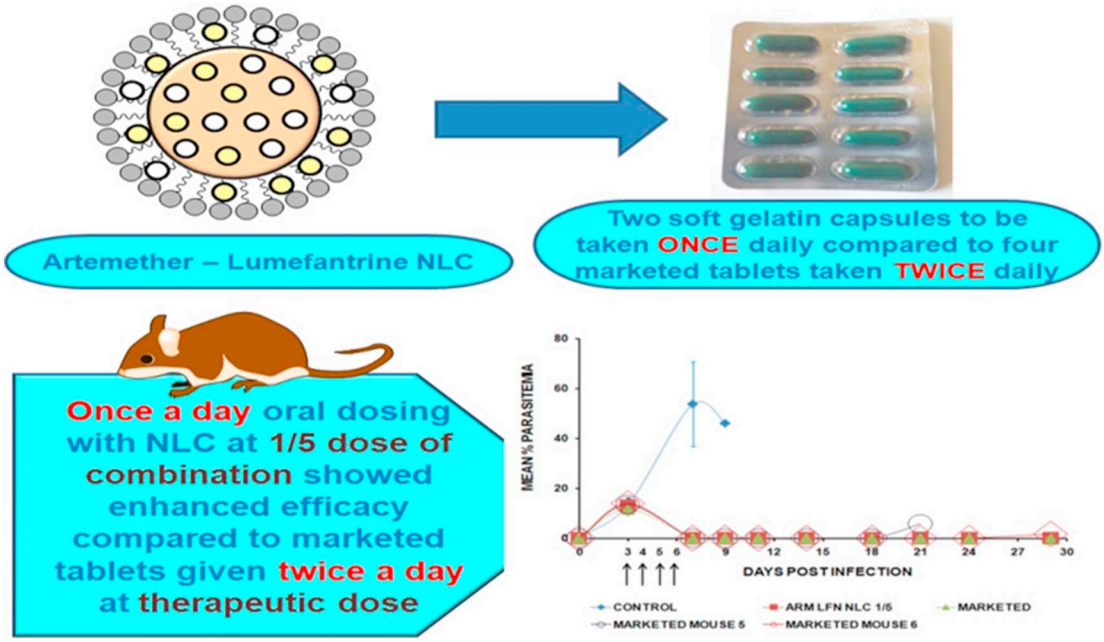

Fig. 7. Enhanced efficacy of artemether-lumefantrine co-loaded NLCs in contrast to conventional tablet form. Reprinted from Prabhu et al. (2016a), Copyright (2016), with permission from Elsevier.

study performed on *P. berghei* infected mice, it was found that an oral dosing with a dual drug loaded formulation at only 1/5th of the dose of combination, administered once a day displayed enhanced efficacy compared to marketed tablets given twice a day at a therapeutic dose (Fig. 7). Furthermore, the NLCs that were filled into soft gelatin capsules were found to be stable for one year at room temperature, with the drug content remaining almost the same as at day one. The authors therefore showed that NLCs can be ideal nano-carriers to overcome poor solubility and bioavailability problems of artemether and lumefantrine.

Cerebral malaria is considered a severe complication, as the infected individuals can experience dreadful symptoms, such as impaired consciousness, convulsions, neurological abnormalities and coma that may last for few days (Pradhan and Ghosh, 2013). Therefore, it becomes extremely challenging to treat patients with cerebral malaria using oral antimalarial therapy. There is no approved antimalarial combination therapy that is intended for parenteral use, considering that the WHO has banned mono-drug therapy to treat malaria (Prabhu et al., 2016b). Taking these shortcomings into account, Prabhu et al., in their subsequent study, aimed to treat mice suffering from cerebral malaria using artemether and lumefantrine co-loaded GDL-capmul MCM derived NLCs (Prabhu et al., 2016b). The formulation was administered intravenously to *P. berghei* infected mice. Sterility being a prerequisite criterion for parenteral preparations, the formulation was autoclaved for 15 min at 121 °C and 15 psi before evaluating its compatibility with the infusion fluids. The formulation was shown to be amenable with no significant changes in globule size and drug loadings, and was compatible with commonly used infusion fluids, such as sterile water for injection, 5% dextrose solution and saline. As free artemether and lumefantrine are not suitable for parenteral delivery due to their poor solubility and life-threatening side effects, the *in vivo* antimalarial study was compared with artesunate. It was found that while artesunate suppressed parasitemia initially, an increase was observed by the second week, followed by the death of the mice. In contrast, the dual drug loaded NLCs resolved the cerebral malarial symptoms, and complete parasite clearance was observed in the mice that survived until the end of studied period (55 days). The authors in this study demonstrated the parenteral application of artemether and lumefantrine co-loaded NLCs to treat cerebral malaria.

With the similar aim of improving the bio-availability of poorly soluble artemether and lumefantrine, Ma et al. prepared a lipid nano-emulsion (Ma et al., 2014). As soybean fat emulsions are known to possess modest anti-plasmodial activity (Deharo et al., 1995), soybean oil was used as one of the formulation ingredients to produce the additive effects. Hot homogenization followed by ultrasonication method was used to prepare the blank and drug loaded lipid emulsions. The artemether and lumefantrine loaded lipid emulsions were prepared by varying the concentrations of both drugs. While all the formulations had particle sizes of ~150 nm and a %EE of > 80% for both drugs, the one with lumefantrine alone and the artemether:lumefantrine (1:6) combination displayed best results in terms of physical and chemical stabilities (studied for 90 days). The *in vivo* antimalarial studies performed on *P. berghei* infected mice revealed that lumefantrine nano-emulsion and artemether-lumefantrine nano-emulsion (1:6) showed better and immediate antimalarial effects among all the other formulations. However, the artemether-lumefantrine nano-emulsion (1:6) was found to possess slightly better activity than the lumefantrine nano-emulsion, indicating the presence of some additive or synergistic effects.

5.2. Polymer based nano-systems to co-deliver antimalarial drugs

To the best of our knowledge, only one study has been reported using polymer based nano-system to co-deliver antimalarial drugs. Recently, Velasques et al. developed polymeric nano-capsules using Poly (ε-caprolactone) as a polymer, and caprylic/capric triglyceride as an oily core, to encapsulate two second-line antimalarial drugs, quinine and curcumin (Velasques et al., 2018). The study aimed to prepare a dual drug loaded nano-system as a possible strategy to overcome drug resistance for malaria treatment. The capsules prepared using the interfacial deposition technique had an average diameter of 200 nm with > 90% of both drugs being entrapped. The *in vitro* antimalarial studies performed against 3D7 and W2 strains of *P. falciparum* revealed that the quinine and curcumin loaded nano-capsules had reduced the parasitemia significantly, in contrast to the free drugs alone and in combination at all tested concentrations. The *in vitro* cytotoxicity study performed on noncancerous human lung fibroblast cell lines proved the bio-safety of the formulation, which was further confirmed by an *in vivo*

nanotoxicology assay performed on *Caenorhabditis elegans*. It was noticed that the authors demonstrated an *in vivo* strategy to confirm the bio-safety of the formulation, which was not performed in the studies discussed above. However, this study would have been strengthened by reporting drug release and *in vivo* antimalarial studies, which are important parameters.

Owing to the lipophilic nature of antimalarial drugs, lipid-based systems have been explored more compared to polymeric nanoparticles. In contrast to combination of free drugs, these systems have displayed significant improvement in the activity.

6. Summary and outlook

Despite the potential activity of many antimicrobial agents, the lack of access to infected tissues/cells, poor solubility, short half-life and toxicity remain significant challenges with conventional dosage forms. In addition, the rapid resistance that is developing to these drugs necessitates smart scientific research. This review highlights the status of the co-delivery of multiple pharmacologically active anti-infectious agents using various nano-drug delivery systems to overcome these challenges. Various lipid and polymeric based nano-systems, such as liposomes, SLNs, NLCs, niosomes, lipid nano-emulsions and polymeric nanoparticles, have been demonstrated for the co-delivery of antibacterial, antiviral and antimalarial agents using various characterization techniques. These nano-systems have displayed outstanding results in treating/controlling various infectious diseases, compared to free drugs and single drug loaded nano-formulations.

This review shows that nano-based combination drug therapy for infectious diseases, although displaying promising and exciting insights, is still far from any clinical applications. The main challenges identified from the literature and possible strategies to optimize further research on the co-delivery of multiple drugs in nano-systems to treat infections more effectively are presented below.

i. *Selection of suitable nano-carrier*: This is the most important challenge of all. Although, co-loaded nano-systems have shown several merits over free drugs and single drug loaded nano-formulations in treating infections, maximizing encapsulation efficiencies of different combination (hydrophobic and/or hydrophilic) of drugs and to achieve their fixed dosages remain a significant challenge. As, the hydrophilic and hydrophobic properties of drugs play a very important role in deciding their loading efficiency, the choice of suitable system becomes crucial. For example, to co-encapsulate both the hydrophilic and hydrophobic payloads, liposomes, niosomes and polymersomes have been identified as the most suitable systems. This special advantage of these systems is credited to their unique structure of having both hydrophilic core and hydrophobic bilayer. These systems can also encapsulate multiple hydrophilic or hydrophobic payloads. Furthermore, SLNs, NLCs and lipid nano-emulsions/suspensions are well suited to co-encapsulate multiple lipophilic and hydrophobic drugs. Good loadings for both hydrophilic and hydrophobic drugs can be achieved with polymeric nanoparticles, depending on the nature of the polymer and the method of preparation. To improve the loadings of the hydrophilic drugs in a hydrophobic system and *vice-versa*, a chemical modification can prove to be a smart alternative. Kalhapure et al. ion paired vancomycin hydrochloride with linoleic acid to improve its entrapment in the compritol 888 ATO based SLNs (Kalhapure et al., 2014). Similarly, hydrophobic drugs can be converted to their salt forms to improve their loadings in hydrophilic systems. Good drug loadings can therefore be achieved using suitable nano-systems and/or making some chemical modifications, which is essential for effective treatment and to progress for their clinical application.

ii. *Achieving fixed doses for multiple drugs*: The doses for drugs in nano-systems do differ from conventional dosage forms. In addition, to achieve fixed doses for multiple drugs in a single nano-system may be difficult; however, dose optimization at clinical levels for a particular disease can prove to be a strategy to overcome this challenge.

iii. *Targeting*: Most of the systems targeted to infectious microbes or infected cells employed passive targeting. While targeted drug delivery systems for infectious diseases are not advanced as cancer therapy, the use of specific ligands, such as peptides, aptamers and antibodies, may produce beneficial results. Furthermore, to reduce the drug loss from nano-systems before entering the infectious sites, the microenvironment of the infection, such as pH, enzyme and temperature, can be used as targeting sites to enhance the activity. These pH, enzyme and temperature responsive systems can facilitate targeting the microbes for the effective delivery of drug payloads.

iv. *Incompatibility of drugs and other formulation ingredients*: Loading multiple pharmacologically active agents with highly hygroscopic drugs in a single formulation may destabilize the system. For example, co-loading ethambutol with other active drugs in a single system destabilizes the system. Exploring advanced architectural designs of nano-systems, such as multi-layered nanoparticles and encapsulating nanoparticle inside another nanoparticle, may prove to overcome this issue.

v. *Same drug combination for a disease*: Most of the studies on tuberculosis are focussed on a similar combination of drugs, while using a different combination in a nano-system may unveil unexpected therapeutic benefits.

vi. *Spectrum of activity*: *In vitro* and *in vivo* antibacterial activities of some broad-spectrum antibiotics have been explored against a single micro-organism only. However, an antibiotic such as gentamycin has great potency against both Gram-positive and Gram-negative bacteria. The concurrent application of such broad-spectrum antibiotics with other antibiotics using nano-systems may lead to potential outcomes against most lethal infections.

vii. *In vivo studies*: In some of the papers, only *in vitro* antimicrobial studies were reported, which provide quick results on the efficacy of nano-systems and encapsulated drugs, but they may not always give accurate outcomes. *In vivo* antimicrobial studies are therefore also essential to verify the activity. In addition, pharmacokinetic and bio-distribution studies were lacking in many of the reports, and would contribute to further optimizing the formulation to clinical level.

viii. *In silico studies*: *In silico* studies are gaining considerable attention due to their accurate predictability, and can assist researchers to understand the mechanisms involved in formation of various nano-systems. Furthermore, binding of nano-systems/drugs/ligands on cell-walls of the microbes or infected cells can also be determined. It was observed that, *in silico* studies were lacking in most of the papers. The application of *in silico* studies may help in better optimization of the formulation.

ix. *Stability studies*: It was observed that physical and chemical stability of many formulations was not correctly studied as per standard regulatory guidelines. A short-term stability study for 3 months at various storage conditions can provide preliminary confirmation of stability and should be included in all future studies.

x. *Neglected diseases*: The current nano-based combinatorial approaches have mainly focussed on bacterial, viral and malarial infections. However, certain diseases such as, fungal infections, HCV/HBV infections, leishmaniasis, filariasis, dengue, trypanosomiasis, schistosomiasis *etc.*, are being neglected regardless of availability of multiple therapeutic agents. Although, these infections may not be of global interest or may not pose significant threat, they still can be life threatening. The potential applications of nano-based combinatorial approaches may prove to treat these infections more effectively.

While most of the potent antimicrobial drugs are becoming resistant to deadly pathogens, thereby leading to life-threatening infections, co-delivery of these drugs in small doses using various nanoplatforms can prove to be a viable strategy to fight resistance and improve therapeutic outcomes. The promising results obtained so far can serve as a platform for further multidisciplinary research to achieve formulation optimization and regulatory approval.

Conflict of interest

The authors declare no conflict of interest.

Acknowledgment

The authors acknowledge the College of Health Sciences, University of KwaZulu-Natal (UKZN) and UKZN Nanotechnology Platform, National Research Foundation of South Africa (Grant No. 106040), Medical Research Council of South Africa for financial support and Ms. Carrin Martin for proof reading.

References

Aditya, N., Patankar, S., Madhusudhan, B., Murthy, R., Souto, E., 2010. Arthemeter-loaded lipid nanoparticles produced by modified thin-film hydration: pharmacokinetics, toxicological and in vivo anti-malarial activity. Eur. J. Pharm. Sci. 40, 448–455.

Aditya, N., Vathsala, P., Vieira, V., Murthy, R., Souto, E., 2013. Advances in nanomedicines for malaria treatment. Adv. Colloid Interf. Sci. 201, 1–17.

Ag Seleci, D., Seleci, M., Walter, J.-G., Stahl, F., Scheper, T., 2016. Niosomes as nanoparticular drug carriers: fundamentals and recent applications. J. Nanomater. 2016, 1–13.

Akbarzadeh, A., Rezaei-Sadabady, R., Davaran, S., Joo, S.W., Zarghami, N., Hanifehpour, Y., Samiei, M., Kouhi, M., Nejati-Koshki, K., 2013. Liposome: classification, preparation, and applications. Nanoscale Res. Lett. 8, 102–110.

Alhariri, M., Omri, A., 2013. Efficacy of liposomal bismuth-ethanedithiol-loaded tobramycin after intratracheal administration in rats with pulmonary *Pseudomonas aeruginosa* infection. Antimicrob. Agents Chemother. 57, 569–578.

Ali, M., Afzal, M., Verma, M., Bhattacharya, S.M., Ahmad, F., Samim, M., Abidin, M., Dinda, A., 2014. Therapeutic efficacy of poly (lactic-co-glycolic acid) nanoparticles encapsulated ivermectin (nano-ivermectin) against brugian filariasis in experimental rodent model. Parasitol. Res. 113, 681–691.

Alipour, M., Suntres, Z.E., Lafrenie, R.M., Omri, A., 2010. Attenuation of *Pseudomonas aeruginosa* virulence factors and biofilms by co-encapsulation of bismuth–ethanedithiol with tobramycin in liposomes. J. Antimicrob. Chemother. 65, 684–693.

Alipour, M., Dorval, C., Suntres, Z.E., Omri, A., 2011. Bismuth-ethanedithiol incorporated in a liposome-loaded tobramycin formulation modulates the alginate levels in mucoid *Pseudomonas aeruginosa*. J. Pharm. Pharmacol. 63, 999–1007.

Arion, D., Parniak, M.A., 1999. HIV resistance to zidovudine: the role of pyrophosphorolysis. Drug Resist. Updat. 2, 91–95.

Aungst, B.J., 1993. Novel formulation strategies for improving oral bioavailability of drugs with poor membrane permeation or presystemic metabolism. J. Pharm. Sci. 82, 979–987.

Balasubramanian, V., Herranz-Blanco, B., Almeida, P.V., Hirvonen, J., Santos, H.A., 2016. Multifaceted polymersome platforms: spanning from self-assembly to drug delivery and protocells. Prog. Polym. Sci. 60, 51–85.

Bangham, A., Standish, M.M., Watkins, J., 1965. Diffusion of univalent ions across the lamellae of swollen phospholipids. J. Mol. Biol. 13, 238–252.

Bhutani, H., Mariappan, T., Singh, S., 2004. An explanation for the physical instability of a marketed fixed dose combination (FDC) formulation containing isoniazid and ethambutol and proposed solutions. Drug Dev. Ind. Pharm. 30, 667–672.

Bowler, P., Duerden, B., Armstrong, D.G., 2001. Wound microbiology and associated approaches to wound management. Clin. Microbiol. Rev. 14, 244–269.

Brown, E.D., Wright, G.D., 2016. Antibacterial drug discovery in the resistance era. Nature 529, 336–343.

Couvreur, P., Fattal, E., Andremont, A., 1991. Liposomes and nanoparticles in the treatment of intracellular bacterial infections. Pharm. Res. 8, 1079–1086.

Date, A.A., Destache, C.J., 2013. A review of nanotechnological approaches for the prophylaxis of HIV/AIDS. Biomaterials 34, 6202–6228.

Date, A.A., Shibata, A., Goede, M., Sanford, B., La Bruzzo, K., Belshan, M., Destache, C.J., 2012. Development and evaluation of a thermosensitive vaginal gel containing raltegravir+ efavirenz loaded nanoparticles for HIV prophylaxis. Antivir. Res. 96, 430–436.

Davies, J., Davies, D., 2010. Origins and evolution of antibiotic resistance. Microbiol. Mol. Biol. Rev. 74, 417–433.

Deharo, E., Krugliak, M., Baccam, D., Ginsburg, H., 1995. Antimalarial properties of soybean fat emulsions. Int. J. Parasitol. 25, 1457–1462.

Destache, C.J., Belgum, T., Christensen, K., Shibata, A., Sharma, A., Dash, A., 2009. Combination antiretroviral drugs in PLGA nanoparticle for HIV-1. BMC Infect. Dis. 9, 198–205.

Destache, C.J., Belgum, T., Goede, M., Shibata, A., Belshan, M.A., 2010. Antiretroviral release from poly (DL-lactide-co-glycolide) nanoparticles in mice. J. Antimicrob. Chemother. 65, 2183–2187.

Eagling, V., Profit, L., Back, D., 1999. Inhibition of the CYP3A4-mediated metabolism and P-glycoprotein-mediated transport of the HIV-1 protease inhibitor saquinavir by grapefruit juice components. Br. J. Clin. Pharmacol. 48, 543.

Ezzet, F., Van Vugt, M., Nosten, F., Looareesuwan, S., White, N., 2000. Pharmacokinetics and pharmacodynamics of lumefantrine (benflumetol) in acute falciparum malaria. Antimicrob. Agents Chemother. 44, 697–704.

Farokhzad, O.C., Langer, R., 2009. Impact of nanotechnology on drug delivery. ACS Nano 3, 16–20.

Freeling, J.P., Koehn, J., Shu, C., Sun, J., Ho, R.J., 2014. Long-acting three-drug combination anti-HIV nanoparticles enhance drug exposure in primate plasma and cells within lymph nodes and blood. AIDS 28, 2625.

Freeling, J.P., Koehn, J., Shu, C., Sun, J., Ho, R.J., 2015. Anti-HIV drug-combination nanoparticles enhance plasma drug exposure duration as well as triple-drug combination levels in cells within lymph nodes and blood in primates. AIDS Res. Hum. Retrovir. 31, 107–114.

Fumakia, M., Ho, E.A., 2016. Nanoparticles encapsulated with LL37 and serpin a1 promotes wound healing and synergistically enhances antibacterial activity. Mol. Pharm. 13, 2318–2331.

Gregoriadis, G., 1973. Drug entrapment in liposomes. FEBS Lett. 36, 292–296.

Gregoriadis, G., Ryman, B., 1971. Liposomes as carriers of enzymes or drugs: a new approach to the treatment of storage diseases. Biochem. J. 124, 58.

Grit, M., Crommelin, D.J., 1993. Chemical stability of liposomes: implications for their physical stability. Chem. Phys. Lipids 64, 3–18.

Gürsoy, A., Kut, E., Özkırımlı, S., 2004. Co-encapsulation of isoniazid and rifampicin in liposomes and characterization of liposomes by derivative spectroscopy. Int. J. Pharm. 271, 115–123.

Gustafson, H.H., Holt-Casper, D., Grainger, D.W., Ghandehari, H., 2015. Nanoparticle uptake: the phagocyte problem. Nano Today 10, 487–510.

Halwani, M., Yebio, B., Suntres, Z., Alipour, M., Azghani, A., Omri, A., 2008a. Co-encapsulation of gallium with gentamicin in liposomes enhances antimicrobial activity of gentamicin against *Pseudomonas aeruginosa*. J. Antimicrob. Chemother. 62, 1291–1297.

Halwani, M., Blomme, S., Suntres, Z.E., Alipour, M., Azghani, A.O., Kumar, A., Omri, A., 2008b. Liposomal bismuth-ethanedithiol formulation enhances antimicrobial activity of tobramycin. Int. J. Pharm. 358, 278–284.

Halwani, M., Hebert, S., Suntres, Z.E., Lafrenie, R.M., Azghani, A.O., Omri, A., 2009. Bismuth–thiol incorporation enhances biological activities of liposomal tobramycin against bacterial biofilm and quorum sensing molecules production by *Pseudomonas aeruginosa*. Int. J. Pharm. 373, 141–146.

Ham, A.S., Cost, M.R., Sassi, A.B., Dezzutti, C.S., Rohan, L.C., 2009. Targeted delivery of PSC-RANTES for HIV-1 prevention using biodegradable nanoparticles. Pharm. Res. 26, 502–511.

Hu, C.-M.J., Aryal, S., Zhang, L., 2010. Nanoparticle-assisted combination therapies for effective cancer treatment. Ther. Deliv. 1, 323–334.

Huh, A.J., Kwon, Y.J., 2011. "Nanoantibiotics": a new paradigm for treating infectious diseases using nanomaterials in the antibiotics resistant era. J. Control. Release 156, 128–145.

Humberstone, A.J., Charman, W.N., 1997. Lipid-based vehicles for the oral delivery of poorly water soluble drugs. Adv. Drug Deliv. Rev. 25, 103–128.

Isacchi, B., Arrigucci, S., Marca, G.l., Bergonzi, M.C., Vannucchi, M.G., Novelli, A., Bilia, A.R., 2011. Conventional and long-circulating liposomes of artemisinin: preparation, characterization, and pharmacokinetic profile in mice. J. Liposome Res. 21, 237–244.

Isacchi, B., Bergonzi, M.C., Grazioso, M., Righeschi, C., Pietretti, A., Severini, C., Bilia, A.R., 2012. Artemisinin and artemisinin plus curcumin liposomal formulations: enhanced antimalarial efficacy against *Plasmodium berghei*-infected mice. Eur. J. Pharm. Biopharm. 80, 528–534.

Jain, S.A., Basu, H., Prabhu, P.S., Soni, U., Joshi, M.D., Mathur, D., Patravale, V.B., Pathak, S., Sharma, S., 2014. Parasite impairment by targeting *Plasmodium*-infected RBCs using glyceryl-dilaurate nanostructured lipid carriers. Biomaterials 35, 6636–6645.

Joshi, M., Pathak, S., Sharma, S., Patravale, V., 2008. Design and in vivo pharmacodynamic evaluation of nanostructured lipid carriers for parenteral delivery of arte-mether: Nanoject. Int. J. Pharm. 364, 119–126.

Kalhapure, R.S., Mocktar, C., Sikwal, D.R., Sonawane, S.J., Kathiravan, M.K., Skelton, A., Govender, T., 2014. Ion pairing with linoleic acid simultaneously enhances encapsulation efficiency and antibacterial activity of vancomycin in solid lipid nanoparticles. Colloids Surf., B 117, 303–311.

Kalhapure, R.S., Suleman, N., Mocktar, C., Seedat, N., Govender, T., 2015. Nanoengineered drug delivery systems for enhancing antibiotic therapy. J. Pharm. Sci. 104, 872–905.

Khalil, N.M., Carraro, E., Cótica, L.F., Mainardes, R.M., 2011. Potential of polymeric nanoparticles in AIDS treatment and prevention. Expert Opin. Drug Deliv. 8, 95–112.

Komarova, N.L., Boland, C.R., 2013. Cancer: calculated treatment. Nature 499, 291–292.

Kraft, J.C., McConnachie, L.A., Koehn, J., Kinman, L., Collins, C., Shen, D.D., Collier, A.C., Ho, R.J., 2017. Long-acting combination anti-HIV drug suspension enhances and sustains higher drug levels in lymph node cells than in blood cells and plasma. AIDS 31, 765–770.

Kraft, J.C., McConnachie, L.A., Koehn, J., Kinman, L., Sun, J., Collier, A.C., Collins, C., Shen, D.D., Ho, R.J., 2018. Mechanism-based pharmacokinetic (MBPK) models describe the complex plasma kinetics of three antiretrovirals delivered by a long-acting anti-HIV drug combination nanoparticle formulation. J. Control. Release 275, 229–241.

Kumar, R., Sahoo, G.C., Pandey, K., Das, V., Topno, R.K., Ansari, M.Y., Rana, S., Das, P.,

2016. Development of PLGA–PEG encapsulated miltefosine based drug delivery system against visceral leishmaniasis. Mater. Sci. Eng. C 59, 748–753.
Lavan, D.A., Lynn, D.M., Langer, R., 2002. Moving smaller in drug discovery and delivery. Nat. Rev. Drug Discov. 1, 77–84.
Li, Y., Su, T., Zhang, Y., Huang, X., Li, J., Li, C., 2015. Liposomal co-delivery of daptomycin and clarithromycin at an optimized ratio for treatment of methicillin-resistant *Staphylococcus aureus* infection. Drug Deliv. 22, 627–637.
Li, W., Yu, F., Wang, Q., Qi, Q., Su, S., Xie, L., Lu, L., Jiang, S., 2016. Co-delivery of HIV-1 entry inhibitor and nonnucleoside reverse transcriptase inhibitor shuttled by nanoparticles: cocktail therapeutic strategy for antiviral therapy. AIDS 30, 827–838.
Li, Q., Cai, T., Huang, Y., Xia, X., Cole, S.P., Cai, Y., 2017. A review of the structure, preparation, and application of NLCs, PNPs, and PLNs. Nano 7, 122–146.
Lin, Y.-H., Tsai, S.-C., Lai, C.-H., Lee, C.-H., He, Z.S., Tseng, G.-C., 2013. Genipin-cross-linked fucose–chitosan/heparin nanoparticles for the eradication of *Helicobacter pylori*. Biomaterials 34, 4466–4479.
Liu, C.-H., Lin, C.-C., Hsu, W.-C., Chung, C.-Y., Lin, C.-C., Jassey, A., Chang, S.-P., Tai, C.-J., Tai, C.-J., Shields, J., 2016. Highly bioavailable silibinin nanoparticles inhibit HCV infection. Gut 0, 1–9.
Lowy, F.D., 2003. Antimicrobial resistance: the example of *Staphylococcus aureus*. J. Clin. Invest. 111, 1265–1273.
Lozano, R., Naghavi, M., Foreman, K., Lim, S., Shibuya, K., Aboyans, V., Abraham, J., Adair, T., Aggarwal, R., Ahn, S.Y., 2013. Global and regional mortality from 235 causes of death for 20 age groups in 1990 and 2010: a systematic analysis for the Global Burden of Disease Study 2010. Lancet 380, 2095–2128.
Ma, Y., Lu, T., Zhao, W., Wang, Y., Chen, T., Mei, Q., Chen, T., 2014. Enhanced antimalarial activity by a novel artemether-lumefantrine lipid emulsion for parenteral administration. Antimicrob. Agents Chemother. 58, 5658–5665.
Mahdiun, F., Mansouri, S., Khazaeli, P., Mirzaei, R., 2017. The effect of tobramycin incorporated with bismuth-ethanedithiol loaded on niosomes on the quorum sensing and biofilm formation of *Pseudomonas aeruginosa*. Microb. Pathog. 107, 129–135.
Mamo, T., Moseman, E.A., Kolishetti, N., Salvador-Morales, C., Shi, J., Kuritzkes, D.R., Langer, R., Andrian, U.V., Farokhzad, O.C., 2010. Emerging nanotechnology approaches for HIV/AIDS treatment and prevention. Nanomedicine (London) 5, 269–285.
Mandal, S., Prathipati, P.K., Kang, G., Zhou, Y., Yuan, Z., Fan, W., Li, Q., Destache, C.J., 2017. Tenofovir alafenamide and elvitegravir loaded nanoparticles for long-acting prevention of HIV-1 vaginal transmission. AIDS 31, 469–476.
Marques, J., Moles, E., Urbán, P., Prohens, R., Busquets, M.A., Sevrin, C., Grandfils, C., Fernàndez-Busquets, X., 2014. Application of heparin as a dual agent with antimalarial and liposome targeting activities toward *Plasmodium*-infected red blood cells. Nanomedicine 10, 1719–1728.
Meshram, S.M., Kumar, Y., Dodoala, S., Sampathi, S., Gera, S., 2015. Biodegradable polymeric nanoparticles for delivery of combination of antiretroviral drugs. Int. J. ChemTech Res. 7, 716–724.
Mignani, S., Bryszewska, M., Klajnert-Maculewicz, B., Zablocka, M., Majoral, J.-P., 2014. Advances in combination therapies based on nanoparticles for efficacious cancer treatment: an analytical report. Biomacromolecules 16, 1–27.
Mugabe, C., Azghani, A.O., Omri, A., 2005. Liposome-mediated gentamicin delivery: development and activity against resistant strains of *Pseudomonas aeruginosa* isolated from cystic fibrosis patients. J. Antimicrob. Chemother. 55, 269–271.
Mukherjee, S., Ray, S., Thakur, R., 2009. Solid lipid nanoparticles: a modern formulation approach in drug delivery system. Indian J. Pharm. Sci. 71, 349–358.
Niu, N.-K., Yin, J.-J., Yang, Y.-X., Wang, Z.-L., Zhou, Z.-W., He, Z.-X., Chen, X.-W., Zhang, X., Duan, W., Yang, T., 2015. Novel targeting of PEGylated liposomes for codelivery of TGF-β1 siRNA and four antitubercular drugs to human macrophages for the treatment of mycobacterial infection: a quantitative proteomic study. Drug Des. Devel. Ther. 9, 4441–4470.
Omwoyo, W.N., Melariri, P., Gathirwa, J.W., Oloo, F., Mahanga, G.M., Kalombo, L., Ogutu, B., Swai, H., 2016. Development, characterization and antimalarial efficacy of dihydroartemisinin loaded solid lipid nanoparticles. Nanomedicine 12, 801–809.
Pandey, R., Khuller, G., 2006a. Oral nanoparticle-based antituberculosis drug delivery to the brain in an experimental model. J. Antimicrob. Chemother. 57, 1146–1152.
Pandey, R., Khuller, G., 2006b. Nanotechnology based drug delivery system (s) for the management of tuberculosis. Indian J. Exp. Biol. 44, 357–366.
Pandey, R., Zahoor, A., Sharma, S., Khuller, G., 2003. Nanoparticle encapsulated antitubercular drugs as a potential oral drug delivery system against murine tuberculosis. Tuberculosis 83, 373–378.
Pandey, R., Sharma, S., Khuller, G., 2005. Oral solid lipid nanoparticle-based antitubercular chemotherapy. Tuberculosis 85, 415–420.
Pandey, R., Sharma, S., Khuller, G., 2006. Chemotherapeutic efficacy of nanoparticle encapsulated antitubercular drugs. Drug Deliv. 13, 287–294.
Parashar, D., Rsr, M., 2016. Development of artemether and lumefantrine co-loaded nanostructured lipid carriers: physicochemical characterization and in vivo antimalarial activity. Drug Deliv. 23, 123–129.
Pham, K., Li, D., Guo, S., Penzak, S., Dong, X., 2016. Development and in vivo evaluation of child-friendly lopinavir/ritonavir pediatric granules utilizing novel in situ self-assembly nanoparticles. J. Control. Release 226, 88–97.
Pillay, D., Zambon, M., 1998. Antiviral drug resistance. BMJ 317, 660–662.
Prabhu, P., Suryavanshi, S., Pathak, S., Sharma, S., Patravale, V., 2016a. Artemether-lumefantrine nanostructured lipid carriers for oral malaria therapy: enhanced efficacy at reduced dose and dosing frequency. Int. J. Pharm. 511, 473–487.
Prabhu, P., Suryavanshi, S., Pathak, S., Patra, A., Sharma, S., Patravale, V., 2016b. Nanostructured lipid carriers of artemether–lumefantrine combination for intravenous therapy of cerebral malaria. Int. J. Pharm. 513, 504–517.
Pradhan, V., Ghosh, K., 2013. Immunological disturbances associated with malarial infection. J. Parasit. Dis. 37, 11–15.
Prathipati, P.K., Mandal, S., Pon, G., Vivekanandan, R., Destache, C.J., 2017. Pharmacokinetic and tissue distribution profile of long acting tenofovir alafenamide and elvitegravir loaded nanoparticles in humanized mice model. Pharm. Res. 34, 2749–2755.
Puri, A., Loomis, K., Smith, B., Lee, J.-H., Yavlovich, A., Heldman, E., Blumenthal, R., 2009. Lipid-based nanoparticles as pharmaceutical drug carriers: from concepts to clinic. Crit. Rev. Ther. Drug Carrier Syst. 26.
Ramana, L.N., Sharma, S., Sethuraman, S., Ranga, U., Krishnan, U.M., 2015. Stealth anti-CD4 conjugated immunoliposomes with dual antiretroviral drugs–modern Trojan horses to combat HIV. Eur. J. Pharm. Biopharm. 89, 300–311.
Ramasamy, T., Khandasami, U.S., Ruttala, H., Shanmugam, S., 2012. Development of solid lipid nanoparticles enriched hydrogels for topical delivery of anti-fungal agent. Macromol. Res. 20, 682–692.
Rambharose, S., Kalhapure, R.S., Govender, T., 2017. Nanoemulgel using a bicephalous heterolipid as a novel approach to enhance transdermal permeation of tenofovir. Colloids Surf., B 154, 221–227.
Ravani, L., Esposito, E., Bories, C., Lievin-Le Moal, V., Loiseau, P.M., Djabourov, M., Cortesi, R., Bouchemal, K., 2013. Clotrimazole-loaded nanostructured lipid carrier hydrogels: thermal analysis and in vitro studies. Int. J. Pharm. 454, 695–702.
Ruel-Gariepy, E., Leroux, J.-C., 2004. In situ-forming hydrogels—review of temperature-sensitive systems. Eur. J. Pharm. Biopharm. 58, 409–426.
Sankar, V., Nilaykumar Nareshkumar, P., Nishit Ajitkumar, G., Devi Penmetsa, S., Hariharan, S., 2012. Comparative studies of lamivudine-zidovudine nanoparticles for the selective uptake by macrophages. Curr. Drug Deliv. 9, 506–514.
Santos-Magalhães, N.S., Mosqueira, V.C.F., 2010. Nanotechnology applied to the treatment of malaria. Adv. Drug Deliv. Rev. 62, 560–575.
Schiffelers, R.M., Storm, G., Marian, T., Stearne-Cullen, L.E., den Hollander, J.G., Verbrugh, H.A., Bakker-Woudenberg, I.A., 2001. In vivo synergistic interaction of liposome-coencapsulated gentamicin and ceftazidime. J. Pharmacol. Exp. Ther. 298, 369–375.
Sharma, A., Sharma, S., Khuller, G., 2004a. Lectin-functionalized poly (lactide-co-glycolide) nanoparticles as oral/aerosolized antitubercular drug carriers for treatment of tuberculosis. J. Antimicrob. Chemother. 54, 761–766.
Sharma, A., Pandey, R., Sharma, S., Khuller, G., 2004b. Chemotherapeutic efficacy of poly (DL-lactide-co-glycolide) nanoparticle encapsulated antitubercular drugs at sub-therapeutic dose against experimental tuberculosis. Int. J. Antimicrob. Agents 24, 599–604.
Shi, J., Votruba, A.R., Farokhzad, O.C., Langer, R., 2010. Nanotechnology in drug delivery and tissue engineering: from discovery to applications. Nano Lett. 10, 3223–3230.
Shibata, A., McMullen, E., Pham, A., Belshan, M., Sanford, B., Zhou, Y., Goede, M., Date, A.A., Destache, C.J., 2013. Polymeric nanoparticles containing combination antiretroviral drugs for HIV type 1 treatment. AIDS Res. Hum. Retrovir. 29, 746–754.
Signore, A., 2013. About inflammation and infection. EJNMMI Res. 3, 1–8.
Singh, L., Kruger, H.G., Maguire, G.E., Govender, T., Parboosing, R., 2017. The role of nanotechnology in the treatment of viral infections. Ther. Adv. Infect. Dis. 4, 105–131.
Sonawane, S.J., Kalhapure, R.S., Govender, T., 2017. Hydrazone linkages in pH responsive drug delivery systems. Eur. J. Pharm. Sci. 99, 45–65.
Soppimath, K.S., Aminabhavi, T.M., Kulkarni, A.R., Rudzinski, W.E., 2001. Biodegradable polymeric nanoparticles as drug delivery devices. J. Control. Release 70, 1–20.
Tamma, P.D., Cosgrove, S.E., Maragakis, L.L., 2012. Combination therapy for treatment of infections with gram-negative bacteria. Clin. Microbiol. Rev. 25, 450–470.
Toti, U.S., Guru, B.R., Hali, M., McPharlin, C.M., Wykes, S.M., Panyam, J., Whittum-Hudson, J.A., 2011. Targeted delivery of antibiotics to intracellular chlamydial infections using PLGA nanoparticles. Biomaterials 32, 6606–6613.
Ujuju, C., Anyanti, J., Newton, P.N., Ntadom, G., 2017. When it just won't go away: oral artemisinin monotherapy in Nigeria, threatening lives, threatening progress. Malar. J. 16, 489.
Velasques, K., Maciel, T.R., Dal Forno, A.H.D.C., Teixeira, F.E.G., da Fonseca, A.L., de Pilla Varotti, F., Fajardo, A.R., Ávila, D.S., Haas, S.E., 2018. Co-nanoencapsulation of antimalarial drugs increases their in vitro efficacy against *Plasmodium falciparum* and decreases their toxicity to *Caenorhabditis elegans*. Eur. J. Pharm. Sci. 118, 1–12.
Walvekar, P., Gannimani, R., Rambharose, S., Mocktar, C., Govender, T., 2018. Fatty acid conjugated pyridinium cationic amphiphiles as antibacterial agents and self-assembling nano carriers. Chem. Phys. Lipids 214, 1–10.
Wang, Y., Zhu, L., Dong, Z., Xie, S., Chen, X., Lu, M., Wang, X., Li, X., Zhou, W., 2012. Preparation and stability study of norfloxacin-loaded solid lipid nanoparticle suspensions. Colloids Surf., B 98, 105–111.
Weber, S., Zimmer, A., Pardeike, J., 2014. Solid lipid nanoparticles (SLN) and nanostructured lipid carriers (NLC) for pulmonary application: a review of the state of the art. Eur. J. Pharm. Biopharm. 86, 7–22.
White, N.J., 2004. Antimalarial drug resistance. J. Clin. Invest. 113, 1084–1092.
WHO, 2000. Anti-tuberculosis drug resistance in the world. World Health Organizationhttp://www.who.int/csr/resources/publications/drugresist/WHO_CDS_TB_2000_278/en/.
WHO, 2014. Antimicrobial resistance: global report on surveillance. World Health Organizationhttp://www.who.int/drugresistance/documents/surveillancereport/en/2014.
WHO, 2017. HIV/AIDS. World Health Organizationhttp://www.who.int/mediacentre/factsheets/fs360/en/.
WHO, 2018. Malaria. World Health Organisationhttp://www.who.int/mediacentre/factsheets/fs094/en/.
Willyard, C., 2017. The drug-resistant bacteria that pose the greatest health threats. Nature 543, 15.
Woodcock, J., Griffin, J.P., Behrman, R.E., 2011. Development of novel combination

therapies. N. Engl. J. Med. 364, 985–987.
Woodrow, K.A., Cu, Y., Booth, C.J., Saucier-Sawyer, J.K., Wood, M.J., Saltzman, W.M., 2009. Intravaginal gene silencing using biodegradable polymer nanoparticles densely loaded with small-interfering RNA. Nat. Mater. 8, 526–533.
Xing-Guo, Z., Jing, M., Min-Wei, L., Sai-Ping, J., Fu-Qiang, H., Yong-Zhong, D., 2008. Solid lipid nanoparticles loading adefovir dipivoxil for antiviral therapy. J Zhejiang Univ Sci B 9, 506–510.
Zhang, L., Gu, F., Chan, J., Wang, A., Langer, R., Farokhzad, O., 2008. Nanoparticles in medicine: therapeutic applications and developments. Clin. Pharmacol. Ther. 83, 761–769.
Zhang, L., Pornpattananangkul, D., Hu, C.-M., Huang, C.-M., 2010. Development of nanoparticles for antimicrobial drug delivery. Curr. Med. Chem. 17, 585–594.

CHAPTER 3. EXPERIMENTAL 1

3.1 Introduction

This chapter addresses Aim 1, Objectives 1-4, and is a first authored experimental article published in an ISI international journal: Chemistry and Physics of Lipids (Impact Factor = 2.766). This article highlights the synthesis of novel FCAs (OCA, LCA and LLCA), in vitro toxicity evaluation of synthesized compounds, formulation of VCM loaded OCA vesicles, and characterization of its physical and antibacterial properties both in vitro and in vivo.

Graphical abstract

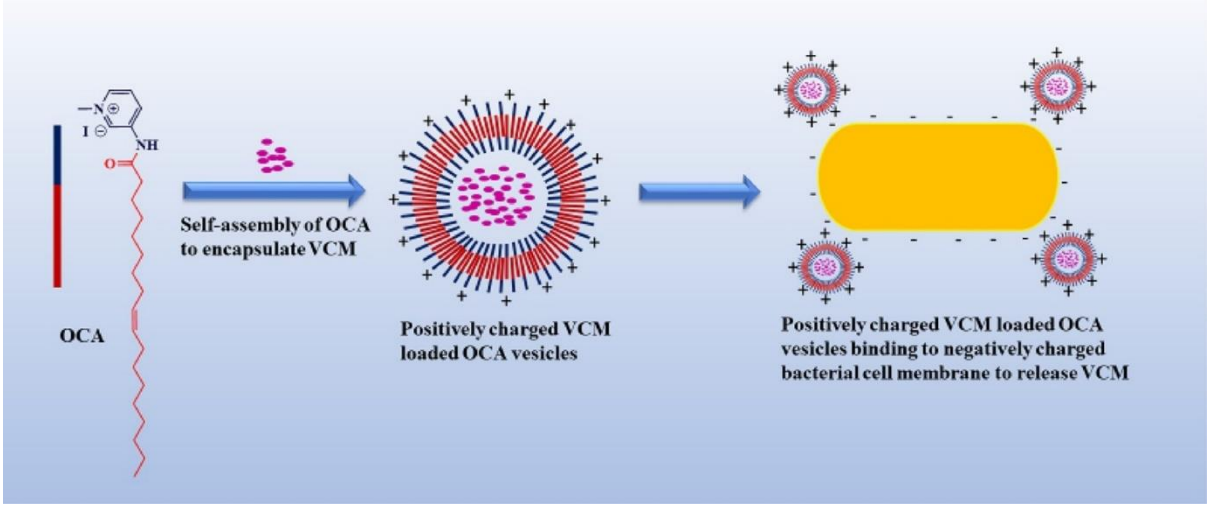

Chemistry and Physics of Lipids 214 (2018) 1–10

Contents lists available at ScienceDirect

Chemistry and Physics of Lipids

journal homepage: www.elsevier.com/locate/chemphyslip

Fatty acid conjugated pyridinium cationic amphiphiles as antibacterial agents and self-assembling nano carriers

Pavan Walvekar[a], Ramesh Gannimani[a,*], Sanjeev Rambharose[a,b], Chunderika Mocktar[a], Thirumala Govender[a,**]

[a] Discipline of Pharmaceutical Sciences, School of Health Sciences, University of KwaZulu-Natal, Private Bag X54001, Durban, 4000, South Africa
[b] Division of Emergency Medicine, Department of Surgery, University of Cape Town, Cape Town, South Africa

ARTICLE INFO

Keywords:
Fatty acid based cationic amphiphiles
Self-assembly
Vancomycin delivery
Enhanced antibacterial activity

ABSTRACT

Most of the bacteria are on the verge of becoming resistant to available potential antibiotics. Novel approaches to combat these drug resistant bacteria are turning out to be crucial. This study aimed to synthesize novel fatty acid based cationic amphiphiles (FCA) that would serve as nano-drug carrier having intrinsic antibacterial activity. Three fatty acids oleic acid, linoleic acid and linolenic acid based cationic amphiphiles were synthesized and evaluated for antibacterial activity and cytotoxicity. The application in the delivery of vancomycin (VCM) was demonstrated using oleic based cationic amphiphilic (OCA). OCA was self-assembled in aqueous media to prepare VCM loaded OCA vesicles. The particle size, polydispersity index, zeta potential and entrapment efficiency were found to be 132.9 ± 2.5 nm, 0.167 ± 0.02, 18.9 ± 1.2 mV and 61.24 ± 1.8% respectively. The images from transmission electron microscopy (TEM) revealed that the vesicles were spherical and bilayered. The release of VCM from OCA vesicles was sustained throughout the studied period of 72 h. From *in vitro* studies, a significant antibacterial activity was observed for all three FCAs and it was found that, VCM loaded OCA vesicles displayed indifference and synergism against Gram positive methicillin susceptible and resistant *staphylococcus aureus* respectively (MRSA). In contrast to minimum inhibitory concentration (MIC) of VCM against Gram negative *Escherichia coli* (*E. coli*) and *Pseudomonas aeruginosa* (*P. aeruginosa*), the synthesized FCAs were more potent against both the strains, further there was no synergism observed against either of the strains when VCM was encapsulated in OCA vesicles. The synergism against MRSA was further confirmed in *in vivo* studies using mouse infection model. These findings therefore suggest that, FCAs can make promising nano-carrier systems for the delivery of antibiotics to treat infections caused by multi drug resistant bacteria.

1. Introduction

The emergence of resistant bacteria continues to be a significant threat, endangering the efficacy of potent antibiotics resulting in increased risk of mortality (Willyard, 2017). Despite impressive scientific advancements, overuse and abuse of antibiotics has led to the rise of multi drug resistant bacteria that are extremely difficult to be eliminated from the body (Kalhapure et al., 2015b). According to a recent report, WHO has ranked twelve different bacteria as a significant threat to human health and stressed the need for newer antibiotics (Willyard, 2017). However, due to slow development of newer antibiotics, the risk of reverting back to a pre-antibiotic era is increasing. In addition, there is also an absolute possibility of development of resistance to the newer drugs too (Kalhapure et al., 2014). Therefore, there is an urgent need for novel approaches to combat these drug resistant strains.

The potential advantages of nanoparticles and their ability to encapsulate therapeutic agents has guided medical technology to an advanced level, where several diseases can be treated more efficiently with negligible or no side effects compared to current dosage forms. Numerous examples of antibiotics being entrapped in various nano-carrier systems can be found in the literature (Kalhapure et al., 2015b). However, in recent years, researchers have shown great interest on antibacterial materials that can be used as excipients in the formulation of nano-systems. The impeccable advantages of entrapping one or more antibiotics and enhancing the antibacterial activity makes these materials more unique when compared to other conventional excipients. Recently, Hisey et al. demonstrated the successful encapsulation of a model antibiotic, tetracycline into phosphonium functionalized polymeric micelles with intrinsic antibacterial activity and demonstrated the sustained release of the drug from the system (Hisey et al., 2017). In

* Corresponding author.
** Corresponding author at: Private Bag X54001, Durban, 4000, KwaZulu-Natal, South Africa.
E-mail addresses: gannimanir@ukzn.ac.za (R. Gannimani), govenderth@ukzn.ac.za (T. Govender).

https://doi.org/10.1016/j.chemphyslip.2018.05.001
Received 13 February 2018; Received in revised form 2 May 2018; Accepted 3 May 2018
Available online 03 May 2018
0009-3084/

another study, Leng and co-workers were successful in loading triclosan, an antibacterial drug into poly(caprolactone)-poly(quaternary ammonium) based micelles having intrinsic antibacterial effects and displayed the synergistic bactericidal activity against *E. coli* (Leng et al., 2016). Hence, fabrication of antibiotics loaded nanoparticles using materials having intrinsic antibacterial effects can exhibit enhanced and synergistic activity in the treatment of infections caused by drug resistant bacteria. The identification of such antimicrobial materials for the preparation of antibiotic loaded nanoparticles is therefore warranted.

Pyridinium based compounds have attracted large interest recently due to their disrupting abilities of the bacterial cell membrane (Eren et al., 2008; Haldar et al., 2005). Among several pyridinium based molecules, compounds having self-assembling abilities are finding significant importance because of their biocompatibility and potential applications as cargoes for the delivery of therapeutic agents. A recent study by Brahmachari et al. demonstrated the application of pyridinium based amphiphilic hydrogelators as antibacterial agents (Brahmachari et al., 2010). Besides, pyridinium residues have also shown promising applications in cell transfection (Ilies et al., 2004). However, the therapeutic use of some of these compounds is hampered due to toxicity and hemolytic activity (Eren et al., 2008). To overcome this problem, pyridiniums could be conjugated to any biosafe/biocompatible molecules to develop new promising compounds that could become potential therapeutic agents with low or negligible toxicity. Fatty acids are another class of compounds that are widely used as pharmaceutical excipients due to their non-toxicity, bio-safety, bio-degradability and easy availability (Kunduru et al., 2016). In addition, fatty acids have been recognised as having some antibacterial activity which makes them attractive substances to be employed in the formulation of nano-antibiotics (Kalhapure et al., 2014).

The self-assembling behaviour of amphiphiles has been extensively studied for the formation of various nanostructures under aqueous conditions (Du and Chen, 2004). The combination of pyridinium cations and fatty acids could produce biocompatible cationic amphiphiles with enhanced antibacterial effects. Further, the long hydrophobic tails of fatty acids may promote self-assembly in aqueous solutions to form nano assemblies (Lee and Feijen, 2012) enabling the encapsulation of antibiotics to produce improved and synergistic antibacterial activity against multi drug resistant bacterial strains. Such combinatorial strategy using cationic amphiphiles with antibiotics could be a viable strategy to overcome the toxicity associated with pyridinium based cationic amphiphiles with the additional advantage of synergistic antibacterial activity.

This study aimed to investigate the antibacterial activity of synthesized novel fatty acid based pyridinium cationic amphiphiles (FCA) alone and in combination with antibiotic, vancomycin (VCM) in the form of self-assembled nano sized vesicles. To the best of our knowledge, there has been no investigation on the delivery of VCM using fatty acid based pyridinium cationic compounds to date. Our hypothesis is that, the positively charged FCA vesicles carrying VCM can bind to the negatively charged bacterial membranes hence potentiating targeting of bacteria at the infection site and increasing localized concentration of drug. The synergistic effects of FCAs and VCM could lead to enhanced activity at low concentrations with reduced toxicity. The present work demonstrates the benefit of combining the advantages of antibacterial vesicles and an antibiotic to develop a multifunctional nano-antibiotic for the treatment of infections caused by multi drug resistant bacteria.

2. Materials and methods

The hydrochloride form of Vancomycin was purchased from Sinobright Import & Export Co. Ltd. (China). Unsaturated fatty acids (oleic acid, linoleic acid and linonenic acid), 3-aminopyridine and Mueller Hinton Broth 2 (MHB 2) were purchased from Sigma-Aldrich (USA). MTT (3-(4, 5-dimethylthiazol-2-yl)-2, 5-diphenyltetrazolium bromide) was purchased from Merck Chemicals (Germany). 1-Ethyl-3-(3-dimethylaminopropyl)carbodiimide hydrochloride (EDC.HCl) was purchased from Carbosynth (UK). For thin layer chromatography (TLC), Merck precoated silica gel $60F_{254}$ plates (Germany) were used. Mueller Hinton Agar (MHA), Nutrient Agar and Nutrient Broth were obtained from Biolab (South Africa). For drug release dialysis tubing of MWCO 14000 DA was obtained from Sigma-Aldrich (USA). Purified water obtained from a Millipore Elix 10 water purification system (Millipore corp., USA) was used throughout the experiment. *Staphylococcus aureus* (*S. aureus*, ATCC 25923) & methicillin resistant *Staphylococcus aureus* (MRSA, *S. aureus* Rosenbach ATCC BAA-1623), *Escherichia coli* (*E. coli,* ATCC 25922), *Pseudomonas aeruginosa* (*P. aeruginosa,* ATCC 27853) strains were used to study the antibacterial activity. ^{1}H and ^{13}C NMR spectra were recorded using a Bruker Avance 400 MHz instrument equipped with BBOZ probe. HRMS (High resolution mass spectrometry) was carried out on a Waters Micromass LCT Premier TOF-MS. All other reagents were of analytical grade and were used without further purification.

2.1. Synthesis and characterization of FCAs

FCAs were synthesized in a two-step procedure as indicated in Scheme 1.

2.1.1. Fatty acid coupling to 3-aminopyridine

In a typical synthesis procedure to a solution of 7.08 mmol of fatty acid in 50 mL of DCM, 8.496 mmol of 3-aminopyridine (1.2 equivalents) and 8.496 mmol of EDC-HCl (1.2 equivalents) were added and stirred for 12 h at room temperature. The reaction mixture was diluted to 100 mL with DCM and washed with 50 mL water and 1 M HCl solution to remove EDC urea, excess EDC-HCl and 3-aminopyridine. Thereafter, DCM fraction was washed with 1 M sodium carbonate solution to neutralise any HCl associated with pyridine structure of the product formed.

2.1.1.1. N-(pyridin-3-yl)oleamide. Yellow solid, yield 79%, Characterization was as follows: IR (ATR): 2918, 1659, 1590, 1536, 1471, 1416, 1281 cm^{-1}; ^{1}H NMR (400 MHz, $CDCl_3$): δ 0.81 (m, 3H), 1.23 (m, 19H), 1.67 (m, 3H), 1.95 (m, 4H), 2.32 (t, 2H), 5.28 (m, 2H), 7.20 (m, 1H), 7.42 (s, 1H), 8.13 (d, 1H), 8.27 (d, 1H), 8.44 (m, 1H); ^{13}C NMR (400 MHz, $CDCl_3$): δ 14.09, 22.66, 25.43, 27.13, 27.20, 29.08,

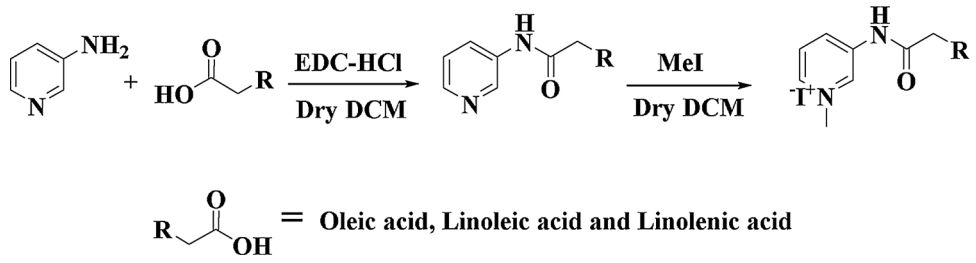

Scheme 1. Synthesis of FCAs.

29.19, 29.24, 29.29, 29.50, 29.67, 29.74, 31.88, 37.58, 123.70, 127.13, 129.66, 130.03, 134.86, 140.93, 145.11, 171.91. HRMS (ESI *m/z*) $[M + H]^+$ calculated for $C_{23}H_{38}N_2O + Na^+$: 381.2882; found 381.2889

2.1.1.2. (9Z,12Z)-N-(pyridin-3-yl)octadeca-9,12-dienamide. Yellow liquid, yield 75%, Characterization was as follows: IR (ATR): 2922, 1669, 1595, 1477, 1417, 1284, 1194 cm^{-1}; ^1H NMR (400 MHz, $CDCl_3$): δ 0.80 (m, 3H), 1.22(m, 16H), 1.65 (m, 2H), 1.96 (m, 4H), 2.32 (t, 2H), 2.69 (m, 1H), 5.27 (m, 3H), 7.20 (m, 1H), 8.16-8.23 (m, 3H), 8.50 (d, 1H); ^{13}C NMR (400 MHz, $CDCl_3$) δ14.03, 22.57, 25.43, 25.57, 27.15, 29.06, 29.18, 29.23, 29.28, 29.55, 29.68, 31.46, 31.84, 123.84, 127.50, 127.83, 128.03, 129.94, 130.19, 135.37, 140.61, 144.39, 172.31. HRMS (ESI *m/z*) $[M + H]^+$ calculated for $C_{23}H_{36}N_2O + Na^+$: 379.2725; found 379.2724

2.1.1.3. (9Z,12Z,15Z)-N-(pyridin-3-yl)octadeca-9,12,15-trienamide. Reddish liquid, yield 72% Characterization was as follows: IR (ATR): 2924, 1670, 1595, 1539, 1477, 1417, 1283, 1193 cm^{-1}; ^1H NMR (400 MHz, $CDCl_3$): δ0.80 (m, 1H), 0.89 (m, 2H), 1.22(m, 10H), 1.63 (m, 2H), 1.97 (m, 4H), 2.32 (t, 2H), 2.71 (m, 3H), 5.27 (m, 5H), 7.20 (m, 1H), 8.14-8.23 (m, 3H), 8.49 (m, 1H); ^{13}C NMR (400 MHz, $CDCl_3$) δ 14.21, 20.48, 22.50, 25.54, 25.56, 27.13, 29.05, 29.52, 29.17, 29.22, 37.42, 123.79, 127.04, 127.40, 127.71, 128.17, 128.25, 130.15, 131.92, 135.31, 140.70, 144.49, 172.30. HRMS (ESI *m/z*) $[M+H]^+$ calculated for $C_{23}H_{34}N_2O + Na^+$: 377.2569; found 377.2567

2.1.2. Conversion of fatty acid coupled 3-Pyridinamine to cationic amphiphile

Fatty acid coupled 3-pyridinamine 5.0 mmol was reacted with excess of methyl iodide (5 equivalents) in DCM, overnight at room temperature (Debnath et al., 2010). After completion of the reaction, excess methyl iodide and solvent where removed by evaporation at reduced pressure to yield the final product.

2.1.2.1. 1-methyl-3-oleamidopyridin-1-ium iodide. Yellow solid, yield 85%, Characterization was as follows: IR (ATR): 2922, 1707, 1549, 1505, 1459, 1318, 1161 cm^{-1}; ^1H NMR (400 MHz, $CDCl_3$): δ 0.80 (m, 3H), 1.21 (m, 21H), 1.65 (m, 3H), 1.93(m, 4H), 2.60 (m, 2H), 4.39 (s, 3H), 5.27 (m, 2H), 7.86 (m, 1H), 8.50 (m, 1H), 9.13 (m, 1H), 9.73 (m, 1H), 10.66 (m,1H); ^{13}C NMR (400 MHz, $CDCl_3$) δ13.11, 21.66, 24.08, 26.21, 28.08, 28.16, 28.30, 28.31, 28.35, 28.51, 28.73, 28.76, 30.88, 36.22, 48.68, 127.04, 128.76, 128.96, 132.97, 133.57, 137.16, 140.01, 173.47; HRMS (ESI *m/z*) $[M+H]^+$ calculated for $C_{24}H_{41}N_2O$: 373.3213; found 373.3219

2.1.2.2. 1-methyl-3-((9Z,12Z)-octadeca-9,12-dienamido)pyridin-1-ium iodide. Yellow solid, yield 87%,Characterization was as follows: IR (ATR): 2922, 1707, 1548, 1504, 1457,1319, 1276, 1161 cm^{-1}; ^1H NMR (400 MHz, $CDCl_3$): δ 0.80 (m, 3H), 1.24 (m, 16H), 1.63 (m, 2H), 1.95(m, 4H), 2.59 (t, 2H), 2.68 (m, 1H), 4.39 (s, 3H), 5.27 (m, 4H), 7.86 (m, 1H), 8.57 (m,1H), 9.09(d, 1H), 9.70 (s, 1H), 10.73 (m, 1H); ^{13}C NMR (400 MHz, $CDCl_3$) δ14.01, 22.49, 22.60, 25.02, 25.56, 27.14, 29.02, 29.09, 29.26, 29.57, 31.43, 31.82, 37.14, 49.68, 127.84, 127.95, 128.03, 129.68, 129.90, 130.00, 133.90, 134.48, 138.45, 140.86, 174.33; HRMS (ESI *m/z*) $[M+H]^+$ calculated for $C_{24}H_{39}N_2O$: 371.3057; found 371.3062

2.1.2.3. 1-methyl-3-((9Z,12Z,15Z)-octadeca-9,12,15-trienamido)pyridin-1-ium iodide. Reddish liquid, yield 92%, Characterization was as follows: IR (ATR): 2924, 1698, 1591, 1547, 1505, 1452, 1322, 1174 cm^{-1}; ^1H NMR (400 MHz, $CDCl_3$): δ0.81(m, 1H), 0.89 (m, 2H), 1.26 (m, 10H), 1.64 (m, 2H), 1.84 (s, 2H), 1.99 (m, 4H), 2.58(t, 2H), 2.73(m, 4H), 4.40(s,3H), 5.28(m, 6H), 7.86 (m, 1H), 8.50(d, 1H), 9.08 (d, 1H) 9.68 (s, 1H) 10.73 (s, 1H); ^{13}C NMR (400 MHz, $CDCl_3$) δ14.23, 20.50, 25.03, 25.47, 25.56, 27.18, 29.03, 29.09, 29.29, 29.56, 37.14, 49.64, 127.11, 127.68, 128.13, 128.26, 128.29, 130.30, 131.96, 134.06, 134.71, 138.33, 140.91, 174.43; HRMS (ESI *m/z*) $[M+H]^+$ calculated for $C_{24}H_{37}N_2O$: 369.2900; found 369.2906

2.2. In vitro cytotoxicity

The influence of synthesized FCAs on the viability of human cells (alveolar basal epithelial cells (A549), embryonic kidney cells (HEK-293) and liver hepatocellular (HEP G2) cells) was evaluated using the MTT assay. The culture medium with cells only was used as a negative control while culture medium without cells was used as a blank. The cells were seeded (2.5×10^3) in 96-well plates and incubated at 37 °C for 24 h. The test samples (FCAs) were added to the wells at different concentrations 20, 40, 60, 80 and 100 µg/mL and incubated for 48h (Kalhapure et al., 2015a). Thereafter, the culture medium was replaced with 100 µL of fresh medium and 5 mg/mL of MTT solution in PBS (100 µL) and allowed to incubate for additional 4 h. The MTT-formazan generated by live cells was dissolved in 100 µL of dimethyl sulfoxide and the absorbance (A540 nm) of each well was measured employing a microplate spectrophotometer (Specrostar nano, Germany) at 540 nm. The experiments were performed in hexaplicates. The percentage cell viability was calculated as follows.

$$\%\text{Cell viability} = \left(\frac{\text{A540 nm treated cells}}{\text{A540 nm untreated cells}}\right) \times 100\%$$

2.3. Fabrication of VCM loaded OCA vesicles

The vesicles were prepared using an o/w emulsion solvent evaporation method (Omolo et al., 2017). Among oleic acid, linoleic acid and linolenic acid based cationic amphiphiles, the oleic acid based cationic amphiphile (OCA) was selected to demonstrate the applicability of these novel materials as nano-carriers. Several formulations were prepared by varying drug and amphiphile concentrations using different solvents. To prepare an optimised formulation, a solution of OCA (50 mg) in THF (5 mL) was added drop-wise to PBS 7.4 (20 mL) containing VCM (5 mg) under continuous stirring. The formed emulsion was stirred for 16 h at room temperature to ensure the complete removal of solvent. Blank vesicles were formulated using the same procedure by omitting VCM in PBS 7.4. All the formulations were prepared separately in triplicate.

2.4. Particle size (PS), polydispersity index (PI), zeta potential (ZP)

The PS, PI and ZP of VCM loaded OCA-vesicles were measured at 25 °C by dynamic light scattering using a Zetasizer Nano ZS90 (Malvern Instruments Ltd., UK) equipped with a laser beam at 633 nm and a 90° scattering angle. FCA-vesicles were analysed for physical properties (PS, PI and ZP) without further dilution. All measurements were performed in triplicate on three different batches prepared separately.

2.5. Entrapment efficiency (%EE) and drug loading capacity (LC)

The%EE of VCM loaded OCA-vesicles was determined by an ultrafiltration method using Amicon® Ultra-4 centrifugal filter tubes (molecular weight cut-off (MWCO) 10,000 Da). A solution of drug loaded vesicles (2 mL) was placed in centrifugal filter tubes and centrifuged at 3000 rpm at 25 °C for 30 min. The amount of free VCM in the filtrate was detected spectrophotometrically at 280 nm using high performance liquid chromatography (HPLC), Shimadzu Prominence DGU-20A3. A reversed-phase C18 column (Nucleosil 120-5 C18; 4 × 150 mm, 5 µm) was used. The mobile phase consisted of acetonitrile:0.1% TFA in water (15:85 v/v). The column temperature, injection volume and flow rate were 25 °C, 100 µL and 1 mL/min respectively. The regression equation used to calculate the unknown amount of VCM was $y = 24598x - 3125.7$ with linearity (R^2) of 0.999. The %EE and LC

were calculated using the following equations (Sonawane et al., 2016).

$$\%EE = \left(\frac{\text{Weight of VCM in vesicles}}{\text{Weight of VCM added}}\right) \times 100\%$$

$$\%LC = \left(\frac{\text{Weight of VCM invesicles}}{\text{Total weight of vesicles}}\right) \times 100\%$$

2.6. Surface morphology

Surface morphology of VCM loaded OCA-vesicles was assessed using Jeol, JEM-1010 (Japan) transmission electron microscopy (TEM). The solution of vesicles was diluted appropriately and a drop of the same was deposited on copper grid (300 mesh) which was allowed to dry under UV lamp to form a thin film. The grid containing thin film was negatively stained with 1% uranyl acetate solution for 30s. The excess stain was removed from the grid by blotting off with filter paper and allowed to dry under UV lamp. The images were captured at an accelerating voltage of 100 kV.

2.7. In vitro drug release

The *in vitro* release of VCM was performed using the dialysis tube technique in PBS at 37 °C. Briefly, 2 mL of VCM loaded OCA vesicles and bare VCM were added into a dialysis bag (MWCO 14,000 Da). The sample loaded tubings were sealed and placed in 50 mL glass bottles containing 40 mL of PBS 7.4 as release medium and incubated at 37 ± 0.5 °C under shaking condition at 100 rpm. 3 mL Samples were withdrawn at specific time intervals from the bottles and an equal amount of fresh PBS was added to maintain a constant volume and sink condition. The obtained samples were analysed spectrophotometrically using HPLC (details are specified in Section 2.5) at 280 nm. The regression equation and linear regression coefficient (R^2) were y = 24598x − 3125.7 and 0.999 respectively.

Various mathematical models can be used to determine the release kinetics of a drug. Most commonly used models such as; (a) Zero order kinetics that explain the release profile of formulation systems which do not disaggregate and release drug slowly and constantly, (b) First order kinetics which describe absorption and/or elimination of drugs from the systems, (c) Higuchi model that describe the release of drugs from matrix systems, (d) Hixson–Crowell model which determine the release of drugs from systems when there is a change in surface area and diameter of particles, (e) Weibull model that describe the process of drug dissolution/release and (f) Korsmeyer-Peppas model that interprets the release of drugs from formulation system based on release exponent (*n*) value (Table 1) were employed to analyse release kinetics of VCM from OCA vesicles (Dash et al., 2010). To explain the release kinetics and mechanism of VCM release, parameters such as correlation coefficient (R^2), root mean square error (RMSE) and mean dissolution time (MDT) were calculated with the help of DDSolver. The experiments were performed in triplicate.

2.8. In vitro antibacterial activity

In vitro antibacterial studies were performed against Gram positive (*S. aureus,* MRSA) and Gram negative (*E. coli* and *P. aeruginosa)* bacteria for the three synthesized fatty acid based cationic amphiphiles, i.e., OCA, linoleic acid based cationic amphiphile (LCA) and linolenic acid based cationic amphiphile (LLCA) by determining minimum inhibitory concentration (MIC) values using broth dilution technique (Balouiri et al., 2016). Since OCA was used as a model carrier of VCM, MIC values were determined for bare VCM and VCM loaded OCA vesicles as well. Briefly, bacterial cultures were grown in Nutrient Broth at 37 °C in a shaking incubator set at 100 rpm. Thereafter, they were diluted with sterile water to achieve a concentration equivalent to 0.5 MacFarland using a densitometer (Latvia). This was further diluted to 1:150 with sterile water to obtain a final concentration equivalent to 5×10^5 colony forming units (CFU)/mL. Bare FCAs, bare VCM and VCM loaded OCA vesicles were serially diluted with MHB-2 in 96 well plates at pH 7.4, inoculated with the bacterial cultures and incubated at 37 °C in a shaking incubator at 100 rpm for 18 h. After incubation, 10 µL from each dilution was spotted on MHA plates and incubated at 37 °C for 18 h to determine the MIC values. The spotting process was repeated every day for 72 h. The experiments were performed in triplicate.

The combined effect of OCA and VCM in VCM loaded OCA vesicles against *S. aureus* and MRSA was evaluated using Σ Fractional Inhibitory Concentration (FIC) based on the results generated by *in vitro* antibacterial activity. A method described by The European Committee for Antimicrobial Susceptibility Testing (EUCAST) was followed to determine FIC (Testing, 2000). The combined effects were categorized as synergy, additive, indifference and antagonism (Testing, 2000). The ΣFIC was calculated using the following equations and Table 2,

FIC (VCM) = MIC of VCM in presence of OCA/MIC of OCA alone

FIC (OCA) = MIC of OCA in presence of VCM/MIC of VCM alone

ΣFIC = FIC (VCM) + FIC (OCA)

2.9. In vivo antibacterial activity

The *in vivo* antibacterial activities of bare VCM, bare OCA, and VCM loaded OCA vesicles were performed and evaluated against MRSA using BALB/c mice. An approved protocol by the Animal Research Committee of the University of KwaZulu-Natal (Approval no. AREC/104/015PD) was followed. The study was performed according to a reported protocol with some modifications (Huang et al., 2011). BALB/c mice weighing 20 g were obtained from the Biomedical Research Unit, University of KwaZulu-Natal. The mice were divided into four groups, negative control (untreated), positive control (bare VCM), treatment A (bare OCA) and treatment B (VCM loaded OCA vesicles). Mice (n = 3 for each group) were shaved to remove back hair and the exposed skin was disinfected with 70% ethanol. 50 µL of MRSA (1.5×10^8 CFU/mL) suspended in sterile saline was injected intradermally. Thirty minutes after infection, 50 µL of bare VCM, bare OCA and VCM loaded OCA vesicles was injected at the site of infection to positive control, treatment A and treatment B respectively, while the negative control was left untreated. The mice were monitored for abscess formation over a period of 48 h and were euthanized for the further study of infected skin tissue.

The infected skin tissue was harvested and homogenised in PBS 7.4 (5 mL) until tiny tissue homogenates were obtained. Further, the obtained homogenates were serially diluted in PBS 7.4 of which 20 µL were spotted on nutrient agar plates. The plates were incubated at 37 °C for 24 h, and the colony forming units (CFU) were quantified. The histological investigations were performed according to a previously

Table 1
Interpretation of diffusional release mechanisms.

Release exponent (*n*)	Drug release mechanism
0.5	Fickian diffusion
0.5 < *n* < 1	Non Fickian/anomalous transport
1	Case II transport
> 1	Super case II transport

Table 2
FIC index interpretation.

Index	Synergy	Additive	Indifference	Antagonism
FIC	≤0.5	> 0.5–1	> 1 to < 2	≥2

reported procedure (Omolo et al., 2017). Briefly, skin samples were fixed in formaldehyde at 25 °C for seven days, dehydrated using ethanol, implanted in paraffin wax. The tissue wax blocks were sectioned using a microtome (Leica RM2235, Leica Biosystems, Germany) and sections were collected on slides, dried and stained with hematoxylin and eosin (H&E). Sections were examined and captured with a Leica Microscope DM 500, fitted with a Leica ICC50 HD camera (Leica Biosystems, Germany).

2.10. Stability studies

VCM loaded FCA vesicles were prepared and examined for physical stability at room temperature (RT) and at 4 °C over a period of 3 months in terms of PS, PI and ZP.

2.11. Statistical analysis

Statistical analysis was performed by using GraphPad Prism® 6 (Graph Pad Software Inc., USA). The data were analysed by one-way ANOVA followed by Bonferroni's Multiple Comparison Test. Statistical significance was established at p-values < 0.05. Data were expressed as mean ± standard deviation (SD).

3. Results and discussion

3.1. Synthesis

FCAs were synthesized in two steps. The first step involved EDC coupling of the carboxylic acid group of fatty acids (oleic, linoleic and linolenic acids) and amine group of 3-aminopyridine. Formation of amide bond between the fatty acid and 3-aminopyridine was confirmed by the appearance of an IR peak near 1670 cm^{-1}. Also, the appearance of aromatic protons in the region δ 7.2–9.0 ppm in ^{1}H NMR and appearance of carbonyl peak near 170 ppm in ^{13}C NMR for all the compounds confirmed the successful conjugation of 3-aminopyridine and fatty acid. In the second reaction, fatty acid conjugated pyridinamines reacted with excess of methyl iodide in DCM at room temperature. After methylation, the carbonyl peak shifted to a higher frequency in the FTIR spectra. Appearance of the peak in the ^{1}H NMR at region near δ 4.5 ppm, integrating for three protons and peak at region δ 50 ppm in ^{13}C NMR confirmed the methylation. All the FCAs were also characterised by HRMS. The obtained masses were in complete agreement with the calculated masses hence confirming the formation of FCAs.

3.2. In vitro cytotoxicity

Biosafety is one of the prerequisite criteria for new materials to be employed as carriers of drug molecules (Choksakulnimitr et al., 1995). Hence, the FCAs were subjected for toxicity studies using human cell lines (A549, HEK-293 and Hep G2) to evaluate the biosafety. The test results displayed that the cell viabilities of the treated cells were in the range of 75.77 to 89.76% at all concentrations for all the three FCAs tested across all cell lines. The percentage cell viability ranged between 75.77 to 89.76% for OCA, 75.94 to 85.50 for LCA and 75.98 to 85.19 for LLCA respectively (Fig. 1). The FCAs showed no dose dependent toxicity towards all the cell lines studied across the concentration range. The results showed that the FCAs did not decrease the cell viabilities below 75% and can therefore be considered as biologically safe and non-toxic to mammalian cells (Cao et al., 2010).

Although quaternary ammonium compounds are known to be potent antimicrobial agents, they possess some degree of toxicity on mammalian cells (Docherty and Kulpa, 2005). Benzalkonium chloride a commercially available quaternary ammonium surfactant is one such example, known for anti-microbial properties. However, its application is limited due to inherent toxicity towards mammalian cells and its clinical use has been restricted to topical use only as per the FDA guidelines (FDA, 2016). Benzalkonium chloride is a widely used surfactant in the preparation of nanomedicines despite its associated cytotoxicity (Lewis and Irving, 2003; Zhang et al., 2009). In this study, the quaternary ammonium compounds derived from the biocompatible fatty acids (FCAs) displayed relatively low or negligible cytotoxicity. Therefore, these novel FCAs can be considered safe to demonstrate their potential applicability in medical nanotechnology. For further investigation, OCA was selected as a prototype for all the studies performed in this work.

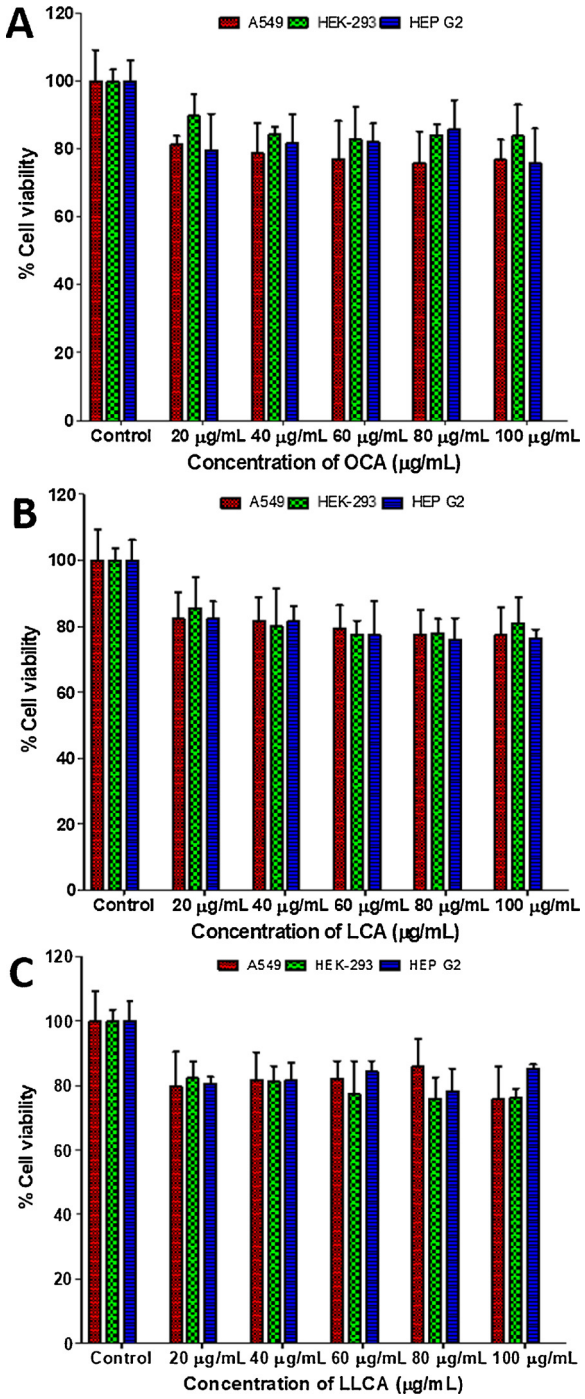

Fig. 1. Cytotoxicity assay displaying percentage cell viability after exposure of human cells (A549, HEK-293, HEP G2) to FCAs, (A) OCA, (B) LCA and (C) LLCA.

Table 3
Effect of different ratios of VCM and OCA employing different solvents for the optimization of formulation (mean ± SD n = 3).

Ratio (VCM: OCA)	Solvent	PS (nm)	PI	ZP (mV)	EE (%)
2:5	Methanol	94.99 ± 7.0	0.324 ± 0.03	13.9 ± 1.3	26.10 ± 2.1
1:10	Methanol	88.70 ± 6.0	0.351 ± 0.03	14.1 ± 1.6	32.14 ± 2.0
2:5	Acetone	191.2 ± 2.1	0.311 ± 0.01	14.4 ± 2.2	21.15 ± 1.0
1:10	Acetone	146.2 ± 1.4	0.157 ± 0.01	16.5 ± 1.3	39.32 ± 1.7
2:5	THF	142.7 ± 1.5	0.263 ± 0.01	17.8 ± 0.6	48.51 ± 1.1
1:10	THF	132.9 ± 2.5	0.167 ± 0.02	18.9 ± 1.2	61.24 ± 1.8
2:2.5	THF	127.4 ± 1.1	0.131 ± 0.01	15.8 ± 0.8	41.30 ± 1.3
1:5	THF	87.46 ± 1.0	0.095 ± 0.01	16.4 ± 1.0	43.69 ± 1.7

3.3. Fabrication of VCM loaded OCA vesicles

Self-assembly of amphiphilic molecules forming nano-carries such as spherical micelles, cylindrical micelles, vesicles and other more complex structures is a well-known phenomenon (Du and Chen, 2004). Among these nano-structures, vesicles have gained much attention because of their versatile nature of encapsulating both hydrophilic as well as hydrophobic moieties including small molecules, nucleic acids, dyes and antibacterial agents (Du and O'Reilly, 2009). VCM loaded OCA vesicles were formulated by self-assembling of OCA in PBS 7.4 using solvent evaporation technique. The spontaneous evaporation of solvent might have resulted in the self-assembly of OCA to form bilayered vesicular structures encapsulating hydrophilic VCM into the aqueous cores.

The formulations were prepared with several ratios of VCM: OCA in different solvents to optimize in terms of PS, PI, ZP and%EE (Table 3). The ratio of 1:10 VCM: OCA employing THF displayed satisfactory results in terms of lower particle size and PI, higher ZP and%EE. DLS revealed that, the drug loaded vesicles had a mean diameter of 132.9 ± 2.5 nm with narrow size distribution of 0.167 ± 0.02 and a positive ZP of 18.9 ± 1.2 mV.

The%EE and LC of VCM loaded OCA vesicles were found to be 61.24 ± 1.8% and 5.56 ± 0.02%. We assume that, this high entrapment could be due to the accumulation of hydrophilic VCM into the aqueous cores of vesicles. This result was comparable with previously reported studies showing high entrapment of VCM in aqueous cores of vesicles (Nicolosi et al., 2010; Omolo et al., 2017).

3.4. Surface morphology

TEM was employed to study the morphology of vesicles. Vesicles are known to have characteristic features of spherical and bilayered structures, where hydrophobic chains form the bilayered membrane and the hydrophilic head forms the internal core and external corona (Du and O'Reilly, 2009). TEM micrograph revealed that, the VCM loaded OCA vesicles had a spherical morphology with evident vesicular structures dispersed discretely and homogeneously (Fig. 2). Further, hydrophilic core and hydrophobic bilayered membrane with an extended hydrophilic external corona were clearly visible and were comparable with the previously reported images for vesicles (Mastrotto et al., 2013). The average particle size of VCM loaded OCA vesicles from TEM were found to be in the range of sizes obtained with DLS analysis.

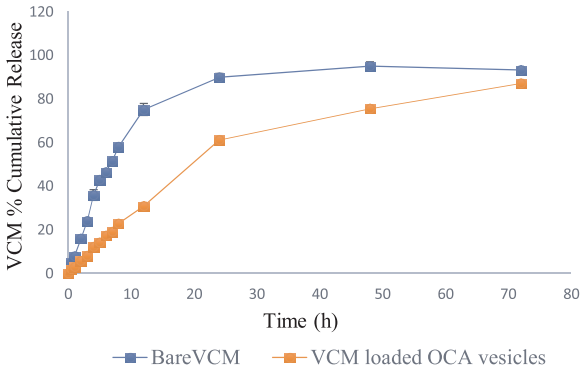

Fig. 3. *In vitro* drug release profiles of bare VCM and VCM loaded OCA vesicles.

3.5. In vitro drug release

The *in vitro* release profiles of bare VCM and VCM loaded OCA vesicles in PBS 7.4 are depicted in Fig. 3. The cumulative release for bare VCM and VCM from OCA vesicles at 12 h was 75% and 12% respectively. At the end of 24 h, almost 90% of bare VCM was released, while it took 72 h for the vesicles to release 87% of VCM, which is consistent with previously reported studies (Radovic-Moreno et al., 2012). These results indicate that, there was sustained release of drug from the formulation system compared to free drug, thus showing the promising application of OCA as a potential nano-carrier for prolonged drug activity.

Release kinetics of VCM loaded OCA vesicles in PBS 7.4 was investigated using various mathematical models (zero order, first order, Higuchi, Korsmeyer-Peppas, Hixon-Crowell and Weibull) to study the drug release profile (Table 4). As linearity of most of the equations can be successfully established using 60% of the initial release data, the maximum cumulative release percentage used for all the models was 60% (Duarte et al., 2006). Among all the models, the best fit model for VCM loaded OCA vesicles was Korsmeyer-Peppas with correlation coefficient (R^2) and root mean square error (RMSE) of 0.9988 and 0.6015 respectively (Table 4). To understand the VCM release behaviour, *'n'* exponent was determined which was found to be 0.930 indicating that the release mechanism was non-fickian or anomalous transport (Ritger and Peppas, 1987). This suggests that multiple

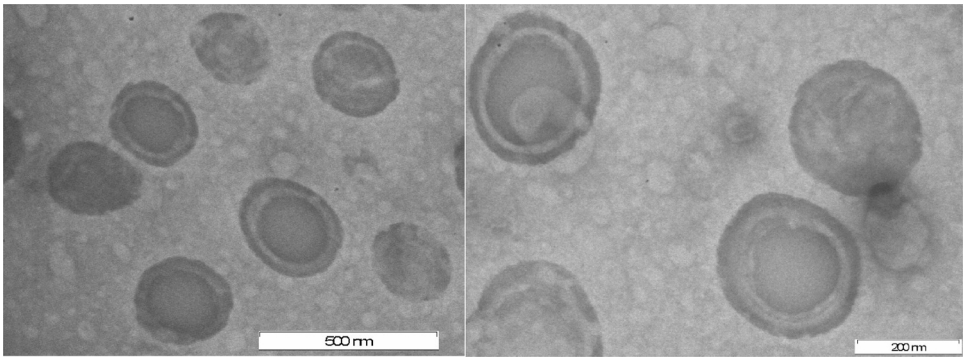

Fig. 2. TEM images displaying the morphology of bilayered vesicles.

Table 4
Drug release kinetics data using different mathematical models.

Model	Equation	R^2	RMSE	Release exponent (*n*)
Zero order	$Q = k.\ t + Q_0$	0.9952	1.1674	–
First order	$Q = Q_0.\ e^{kt}$	0.9846	2.0884	–
Higuchi	$Q = k.\ t^{½}$	0.8172	7.2022	–
Hixon-Crowell	$Q^{⅓} = kt + Q_0^{⅓}$	0.9940	1.3045	–
Weibull	$Q = 1\ \exp\ [-(t)^{a/b}]$	0.9969	1.0448	–
Korsmeyer-Peppas	$Q = k.\ t^n$	0.9988	0.6015	0.930

R^2 = linear regression coefficient, RMSE = Root mean square error.

mechanisms were involved in the release of VCM including diffusion (Arifin et al., 2006). The slow release of VCM from vesicles may be attributed to slow diffusion of drug from vesicles. The positive charge of inner and outer corona of vesicles could also have affected the drug diffusion by electrostatic or ionic interactions (Mosley et al., 2013). The mean dissolution time (MDT) values for bare VCM and VCM loaded vesicles were found to be 7.19 and 22.17 respectively suggesting that the release of VCM from vesicles was slower compared to bare VCM. From the obtained results for *in vitro* release and kinetics, VCM loaded OCA vesicles displayed sustained and controlled release trends and these systems may effectively control the infection with reduced frequency of dose.

3.6. In vitro antibacterial activity

In vitro antibacterial studies were performed for bare VCM, bare OCA, bare LCA, bare LLCA, and VCM loaded OCA vesicles. The studies were conducted against *S. aureus*, MRSA, *E. coli* and *P. aeruginosa* to determine MIC values (Table 5). The novel FCAs were more active against Gram positive. After 24 h, the MIC values for OCA, LCA and LLCA against *S. aureus* were 39.06 μg/mL, 39.06 μg/mL and 19.53 μg/mL respectively, whereas MIC value of 39.06 μg/mL remained the same for all the three fatty acid derivatives against MRSA. These trends were continued until 72 h for all the FCAs against both the strains suggesting the sustained bactericidal properties of novel FCAs. The MIC values for bare VCM against *S. aureus* and MRSA were 1.95 μg/mL and 7.8 μg/mL after 24 h respectively, whereas for VCM loaded OCA vesicles, the values remained the same against both *S. aureus* and MRSA with 1.95 μg/mL. However, bare VCM lost its activity after day 1 against both the strains while VCM loaded OCA vesicles continued to produce the same activity as day 1 after 72 h. From the above comparison, bare VCM and VCM loaded OCA vesicles displayed same activity against *S. aureus* at the initial time period of 24 h, however the latter was more efficient in sustaining the activity after 72 h. Against MRSA, VCM loaded OCA vesicles displayed enhanced and sustained activity compared to bare VCM after 72 h.

Table 5
MIC values for the FCAs, bare VCM and VCM loaded OCA vesicles against *S. aureus*, MRSA, *E. coli and P. aeruginosa*.

Bacteria	Time(h)	Bare VCM	Bare OCA	Bare LCA	Bare LLCA	VCM loaded OCA vesicles
MIC values (μg/mL)						
S. aureus	24	1.95	39.06	39.06	19.53	1.95
	48	NA	39.06	39.06	19.53	1.95
	72	NA	39.06	39.06	19.53	1.95
MRSA	24	7.8	39.06	39.06	39.06	1.95
	48	NA	39.06	39.06	39.06	1.95
	72	NA	39.06	39.06	39.06	1.95
E. coli	24	250	78.125	78.125	78.125	78.125
	48	250	78.125	78.125	78.125	78.125
	72	250	78.125	78.125	78.125	78.125
P. aeruginosa	24	NA	312.5	312.5	156.25	312.5
	48	NA	312.5	312.5	156.25	312.5
	72	NA	312.5	312.5	156.25	312.5

NA = No activity, n = 3.

The MIC values for all the tested samples against Gram negative bacteria remained the same as of day 1 throughout the study period of 72 h. The MIC value for bare VCM against *E. coli* was 250 μg/mL, while no activity was observed against *P. aeruginosa*. Based on a previous report, the lower efficacy of bare VCM against Gram negative bacteria was expected as it does not cross the outer membranes of these cells (Nicolosi et al., 2010). On the other hand, all FCAs had MIC values of 78.125 μg/mL against *E. coli* whereas, against *P. aeruginosa*, LLCA showed slightly better activity with MIC of 156.25 μg/mL compared to the MICs (312.5 μg/mL) of OCA and LCA. The VCM loaded OCA vesicles displayed MICs same as of OCA against both *E. coli* and *P. aeruginosa* indicating that VCM did not play any role in killing the bacteria. FCAs did not display exceptional antibacterial activity against *E. coli* and *P. aeruginosa*, however in contrast to the activity of bare VCM, they were found to be more potent than bare VCM against Gram negative bacteria.

The FIC values were determined to understand the combined effect of OCA and VCM in VCM loaded OCA vesicles against *S. aureus* and MRSA. Since bare VCM had lost its activity after 24 h, FIC values for both bare VCM and bare OCA were calculated at 24 h. The FIC values were found to be 1.04 and 0.29 for *S. aureus* and MRSA suggesting that there was indifference and synergism respectively (Table 6). Since VCM had very poor activity against Gram negative bacteria, FIC values were not determined.

Vancomycin is the drug of choice for the treatment of many infections caused by *S. aureus* strains which is credited to its ability of inhibiting the steps in peptidoglycan synthesis and assembly of NAM-NAG-polypeptide into the extending polypeptide chains (Kalhapure et al., 2014) while, pyridinium based amphiphiles act by disrupting the cell membrane integrity (Pendleton and Gilmore, 2015). Since VCM, a last resort for the treatment of *S. aureus* infections is under increasing threat of eventually acquiring resistance to *S. aureus* strains, a combination of VCM and pyridinium based amphiphiles could serve as a viable strategy to overcome resistance, producing significant sustained and synergistic activity. The study demonstrates that VCM can potentially show activity even at low doses. Thus, side effects such as nephrotoxicity that is caused due to high/frequent doses of VCM can be reduced or overcome (Bamgbola, 2016).

The overall conclusion is that the antibacterial activity of synthesized FCAs was found to be broad spectrum as compared to the antibiotic, VCM which is effective against Gram positive bacteria only. Further, they were more active against Gram positive bacteria than Gram negative bacteria. These results indicate that the mechanism of action could have been mainly due to electrostatic interactions between the cationic compounds (FCAs) and negative charge on bacterial cell membranes (Jennings et al., 2015). Similar to other quaternary ammonium compounds reported previously, FCAs synthesized in this study were also more active against Gram positive bacteria compared to Gram negative strains (Blois and Swarbrick, 1972). This difference in activity was attributed to the distinctive cell wall composition of Gram positive and Gram negative bacteria. According to a recent report, Gram negative bacteria are composed of two phospholipid cellular

Table 6
ΣFIC results of optimised formulation for the *in vitro* antibacterial activity against *S. aureus* and MRSA.

	ΣFIC		Results	
	S. aureus	MRSA	*S. aureus*	MRSA
VCM loaded OCA vesicles	1.04	0.29	Indifference	Synergy

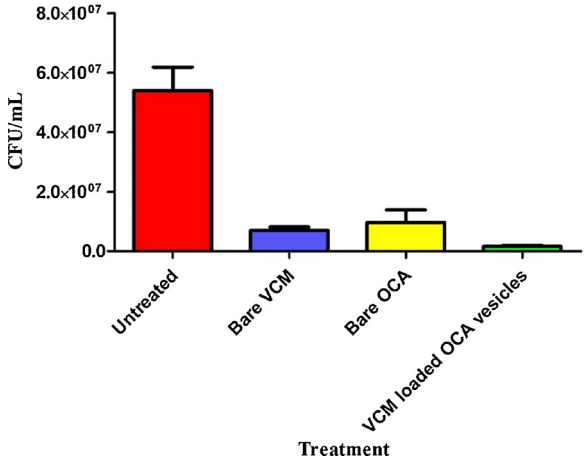

Fig. 4. MRSA burden in mice groups after 48 h.

membranes and a thin layer of peptidoglycan, while Gram positive bacteria possess only one phospholipid cellular membrane and a thick peptidoglycan layer. The presence of second phospholipid membrane in Gram negative strains was stated as a reason for reduced membrane lytic activity of quaternary ammonium compounds (Jennings et al., 2015). Another report suggests that cephalin, a phospholipid component present in Gram negative bacterial cell membranes neutralizes the bactericidal effect of quaternary ammonium compounds thus reducing their selectivity towards Gram negative bacteria (Blois and Swarbrick, 1972). Therefore, we assume that similar mechanisms might account for the better activity of FCAs against Gram positive than Gram negative bacterial strains tested in this study.

3.7. *In vivo* antibacterial activity

Since an *in vitro* synergism was observed for VCM loaded OCA vesicles against MRSA, an *in vivo* antibacterial study was performed against MRSA using a mouse infection model. The number of colony forming units (CFUs) were calculated for each group (treated and untreated) (Fig. 4) The highest MRSA burden was developed in un-treated mice group (7.7, 4.8 and 32.4 folds more than bare VCM, bare OCA and VCM loaded OCA vesicles respectively). Although, bare OCA showed less activity than bare VCM, the mean MRSA load found in bare VCM treated mice was comparable to bare OCA treated mice with a significant difference of $p > 0.05$, hence demonstrating the potential effects of OCA against Gram positive bacteria. The MRSA burden in VCM loaded OCA vesicles treated mice was significantly ($p = 0.01$) reduced (4.2-fold) compared to bare VCM displaying the superiority of these multi-functional vesicles. Similar trends were observed with *in vitro* antibacterial activity, suggesting that this enhanced activity could be due to synergism between VCM and OCA.

The histomorphological evaluations were performed on excised skin from the untreated, bare VCM, bare OCA and VCM loaded OCA vesicles groups to assess the morphological changes and skin integrity after 48 h MRSA infection. The H&E stained slides revealed that the untreated skin samples displayed evidence of tissue inflammation (as quantified by the swelling of the skin) and abscess formation (red arrows) (Fig. 5A). Although the bare VCM (Fig. 5B) and the bare OCA (Fig. 5C) groups displayed signs of swelling and abscess formation (abscess capsule area within the red lines), it was to a lesser extent to the untreated group (Fig. 5A). Interestingly, the VCM loaded OCA vesicles group displayed minimal signs of tissue inflammation and no evidence of abscess formation (Fig. 5D). The untreated, bare VCM and bare OCA groups presented with large quantities of white blood cells at the infection site, however this was evidently lower in the VCM loaded OCA vesicles group (Fig. 5D). The findings of the histomorphological analysis correlate directly with the CFU/ml calculated in the *in vivo* antibacterial study as the skin sample with the most number of recovered bacteria also presents with the highest degree of inflammation, abscess formation and presence of white blood cells. This is due to the greater immune response to the larger number of bacteria present at the infection site of the untreated group. The VCM loaded OCA vesicles group which displayed the lowest number of isolated bacteria presented with minimal signs of inflammation and no abscess formation, this could be due to a reduced immune response to a statistically lower number of isolated bacteria at the infection site. These findings further exhibit the antimicrobial superiority of the VCM loaded OCA vesicles.

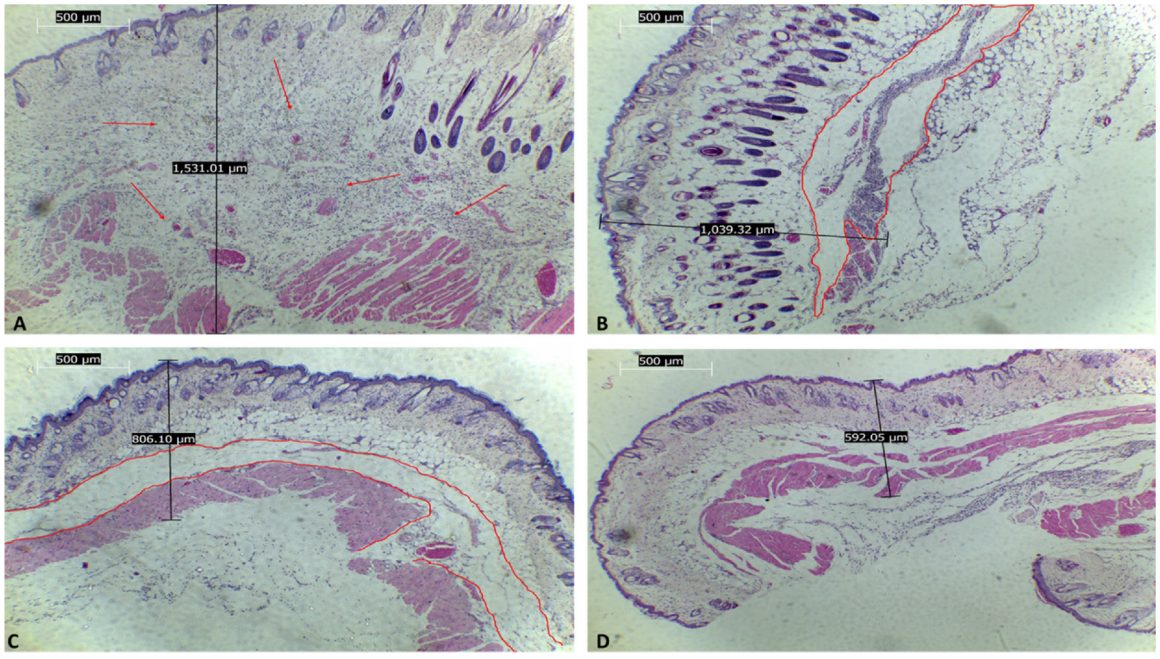

Fig. 5. Histomorphology of controls and treated: (A) Untreated (negative control), (B) Bare VCM treated (Positive control), (C) Bare OCA treated and (D) VCM loaded OCA vesicles treated.

Table 7
Effect of storage conditions and time on PS, PI and ZP of VCM loaded OCA vesicles (mean ± SD, n = 3).

Storage condition	4 °C	RT	4 °C	RT	4 °C	RT
Time (days)	PS (nm)		PI		ZP (mV)	
0	132.9 ± 2.5	132.9 ± 2.5	0.167 ± 0.02	0.167 ± 0.02	18.9 ± 1.2	18.9 ± 1.2
30	134.6 ± 3.0	175.4 ± 10.0	0.177 ± 0.01	0.214 ± 0.02	18.8 ± 1.2	17.7 ± 2.2
60	135.1 ± 2.7	186.6 ± 11.3	0.171 ± 0.01	0.249 ± 0.02	18.1 ± 1.3	16.8 ± 2.4
90	134.4 ± 2.4	191.1 ± 9.0	0.180 ± 0.01	0.250 ± 0.02	18.4 ± 1.3	16.2 ± 2.4

3.8. Stability studies

Stability studies revealed that, VCM loaded OCA vesicles were stable at 4 °C over a period of 90 days in terms of physical appearance, PS, PI and ZP with significant difference of ($p > 0.05$) (Table 7). However, vesicles stored at RT displayed significant variations ($p < 0.05$) over different time periods (Table 7). These results therefore confirm that the vesicles were stable at 4 °C.

4. Conclusion

We present in this study, the potential application of employing novel antibacterial materials that can self-assemble to form nano sized vesicles encapsulating VCM to treat infections caused by multi drug resistance bacteria, *S. aureus* and MRSA. All the FCAs were successfully synthesized, showed non-toxicity towards the tested mammalian cell lines and exhibited bactericidal activity against the tested bacterial strains. Self-assembled OCA vesicles encapsulating VCM were in the nano sized range with particle sizes less than 150 nm and a positive zeta potential. Drug loaded OCA vesicles displayed a high entrapment efficiency of > 60% for VCM. *In vitro* antibacterial studies revealed that, VCM loaded OCA vesicles improved the bacterial killing activity against both susceptible and resistant *S. aureus* compared to bare VCM. FCAs displayed greater activity than VCM against Gram negative bacteria, however when VCM was loaded into OCA vesicles, no improvement in the activity against Gram negative bacteria was observed. Further, the *in vivo* studies were in complete support of *in vitro* antibacterial activity confirming synergism against MRSA. We conclude that the synthesized novel FCAs can improve the antibacterial activities of encapsulated antibiotics and thus novel materials reported in this study may serve as a platform to develop such multifunctional nano-systems to treat bacterial infections.

Conflict of interest

The authors declare no conflict of interest.

Acknowledgment

The authors acknowledge the College of Health Sciences, University of KwaZulu-Natal (UKZN) and UKZN Nanotechnology Platform, National Research Foundation of South Africa (Grant No. 106040), Medical Research Council of South Africa for financial support. We acknowledge Biomedical Resource Unit and Microscopy and Microanalysis Unit at UKZN for letting us use the facilities.

References

Arifin, D.Y., Lee, L.Y., Wang, C.-H., 2006. Mathematical modeling and simulation of drug release from microspheres: implications to drug delivery systems. Adv. Drug Deliv. Rev. 58, 1274–1325.
Balouiri, M., Sadiki, M., Ibnsouda, S.K., 2016. Methods for in vitro evaluating antimicrobial activity: a review. J. Pharm. Anal. 6, 71–79.
Bamgbola, O., 2016. Review of vancomycin-induced renal toxicity: an update. Ther. Adv. Endocrinol. Metab. 7, 136–147.
Blois, D.W., Swarbrick, J., 1972. Interaction of quaternary ammonium bactericides with biological materials I: Conductometric studies with cephalin. J. Pharm. Sci. 61, 390–392.
Brahmachari, S., Debnath, S., Dutta, S., Das, P.K., 2010. Pyridinium based amphiphilic hydrogelators as potential antibacterial agents. Beilstein J. Org. Chem. 6, 859.
Cao, X., Cheng, C., Ma, Y., Zhao, C., 2010. Preparation of silver nanoparticles with antimicrobial activities and the researches of their biocompatibilities. J. Mater. Sci. Mater. Med. 21, 2861–2868.
Choksakulnimitr, S., Masuda, S., Tokuda, H., Takakura, Y., Hashida, M., 1995. In vitro cytotoxicity of macromolecules in different cell culture systems. J. Control. Release 34, 233–241.
Dash, S., Murthy, P.N., Nath, L., Chowdhury, P., 2010. Kinetic modeling on drug release from controlled drug delivery systems. Acta Pol. Pharm. 67, 217–223.
Debnath, S., Shome, A., Das, D., Das, P.K., 2010. Hydrogelation through self-assembly of Fmoc-peptide functionalized cationic amphiphiles: potent antibacterial agent. J. Phys. Chem. B 114, 4407–4415.
Docherty, K.M., Kulpa Jr, C.F., 2005. Toxicity and antimicrobial activity of imidazolium and pyridinium ionic liquids. Green Chem. 7, 185–189.
Du, J., Chen, Y., 2004. Organic–inorganic hybrid nanoparticles with a complex hollow structure. Angew. Chem. Int. Ed. 43, 5084–5087.
Du, J., O'Reilly, R.K., 2009. Advances and challenges in smart and functional polymer vesicles. Soft Matter 5, 3544–3561.
Duarte, A.R.C., Costa, M.S., Simplício, A.L., Cardoso, M.M., Duarte, C.M., 2006. Preparation of controlled release microspheres using supercritical fluid technology for delivery of anti-inflammatory drugs. Int. J. Pharm. 308, 168–174.
Eren, T., Som, A., Rennie, J.R., Nelson, C.F., Urgina, Y., Nüsslein, K., Coughlin, E.B., Tew, G.N., 2008. Antibacterial and hemolytic activities of quaternary pyridinium functionalized polynorbornenes. Macromol. Chem. Phys. 209, 516–524.
Safety and Effectiveness of Consumer Antiseptic Rub Products; Topical Antimicrobial Drug Products for Over-the-Counter Human Use; Proposed Amendment of the Tentative Final Monograph, 2016. https://www.fda.gov/downloads/AboutFDA/ReportsManualsForms/Reports/EconomicAnalyses/UCM510753.pdf.
Haldar, J., Kondaiah, P., Bhattacharya, S., 2005. Synthesis and antibacterial properties of novel hydrolyzable cationic amphiphiles. Incorporation of multiple head groups leads to impressive antibacterial activity. J. Med. Chem. 48, 3823–3831.
Hisey, B., Ragogna, P.J., Gillies, E.R., 2017. Phosphonium-functionalized polymer micelles with intrinsic antibacterial activity. Biomacromolecules 18, 914–923.
Huang, C.-M., Chen, C.-H., Pornpattananangkul, D., Zhang, L., Chan, M., Hsieh, M.-F., Zhang, L., 2011. Eradication of drug resistant Staphylococcus aureus by liposomal oleic acids. Biomaterials 32, 214–221.
Ilies, M.A., Seitz, W.A., Ghiviriga, I., Johnson, B.H., Miller, A., Thompson, E.B., Balaban, A.T., 2004. Pyridinium cationic lipids in gene delivery: a structure- activity correlation study. J. Med. Chem. 47, 3744–3754.
Jennings, M.C., Minbiole, K.P., Wuest, W.M., 2015. Quaternary ammonium compounds: an antimicrobial mainstay and platform for innovation to address bacterial resistance. ACS Infect. Dis. 1, 288–303.
Kalhapure, R.S., Mocktar, C., Sikwal, D.R., Sonawane, S.J., Kathiravan, M.K., Skelton, A., Govender, T., 2014. Ion pairing with linoleic acid simultaneously enhances encapsulation efficiency and antibacterial activity of vancomycin in solid lipid nanoparticles. Colloids Surf. B Biointerfaces 117, 303–311.
Kalhapure, R.S., Sonawane, S.J., Sikwal, D.R., Jadhav, M., Rambharose, S., Mocktar, C., Govender, T., 2015a. Solid lipid nanoparticles of clotrimazole silver complex: an efficient nano antibacterial against Staphylococcus aureus and MRSA. Colloids Surf. B Biointerfaces 136, 651–658.
Kalhapure, R.S., Suleman, N., Mocktar, C., Seedat, N., Govender, T., 2015b. Nanoengineered drug delivery systems for enhancing antibiotic therapy. J. Pharm. Sci. 104, 872–905.
Kunduru, K.R., Basu, A., Domb, A.J., 2016. Biodegradable Fatty Acid Polyesters.
Lee, J.S., Feijen, J., 2012. Polymersomes for drug delivery: design, formation and characterization. J. Control. Release 161, 473–483.
Leng, M., Hu, S., Lu, A., Cai, M., Luo, X., 2016. The anti-bacterial poly (caprolactone)-poly (quaternary ammonium salt) as drug delivery carriers. Appl. Microbiol. Biotechnol. 100, 3049–3059.
Lewis, R.J., Irving, N., 2003. Sax's Dangerous Properties of Industrial Materials. Van Nostrand Reinhold.
Mastrotto, F., Salmaso, S., Alexander, C., Mantovani, G., Caliceti, P., 2013. Novel pH-responsive nanovectors for controlled release of ionisable drugs. J. Mater. Chem. B 1, 5335–5346.
Mosley, G.L., Yamanishi, C.D., Kamei, D.T., 2013. Mathematical modeling of vesicle drug delivery systems 1: Vesicle formation and stability along with drug loading and release. J. Lab. Autom. 18, 34–45.
Nicolosi, D., Scalia, M., Nicolosi, V.M., Pignatello, R., 2010. Encapsulation in fusogenic liposomes broadens the spectrum of action of vancomycin against Gram-negative bacteria. Int. J. Antimicrob. Agents 35, 553–558.

Omolo, C.A., Kalhapure, R.S., Jadhav, M., Rambharose, S., Mocktar, C., Ndesendo, V.M., Govender, T., 2017. Pegylated oleic acid: a promising amphiphilic polymer for nano-antibiotic delivery. Eur. J. Pharm. Biopharm. 112, 96–108.
Pendleton, J.N., Gilmore, B.F., 2015. The antimicrobial potential of ionic liquids: a source of chemical diversity for infection and biofilm control. Int. J. Antimicrob. Agents 46, 131–139.
Radovic-Moreno, A.F., Lu, T.K., Puscasu, V.A., Yoon, C.J., Langer, R., Farokhzad, O.C., 2012. Surface charge-switching polymeric nanoparticles for bacterial cell wall-targeted delivery of antibiotics. ACS Nano 6, 4279–4287.
Ritger, P.L., Peppas, N.A., 1987. A simple equation for description of solute release I. Fickian and non-Fickian release from non-swellable devices in the form of slabs spheres, cylinders or discs. J. Control. Release 5, 23–36.
Sonawane, S.J., Kalhapure, R.S., Rambharose, S., Mocktar, C., Vepuri, S.B., Soliman, M., Govender, T., 2016. Ultra-small lipid-dendrimer hybrid nanoparticles as a promising strategy for antibiotic delivery: in vitro and in silico studies. Int. J. Pharm. 504, 1–10.
Testing, E.C.o.A.S., 2000. Terminology relating to methods for the determination of susceptibility of bacteria to antimicrobial agents. Clin. Microbiol. Infect. 6, 503–508.
Willyard, C., 2017. The drug-resistant bacteria that pose the greatest health threats. Nat. News 543, 15.
Zhang, J., Fan, Y., Smith, E., 2009. Experimental design for the optimization of lipid nanoparticles. J. Pharm. Sci. 98, 1813–1819.

CHAPTER 4. EXPERIMENTAL PAPER 2

4.1 Introduction

This chapter addresses Aim 2, Objectives 1-4, and is a first authored experimental article communicated in an ISI international journal: Colloids and Surfaces B: Biointerfaces (manuscript ID: COLSUB-S-19-01124) This article highlights the synthesis of novel HA-OLA conjugates, *in vitro* toxicity evaluation of synthesized compounds, formulation of VCM loaded polymersomes, and characterization of its physical and *in vitro* antibacterial properties.

Graphical abstract

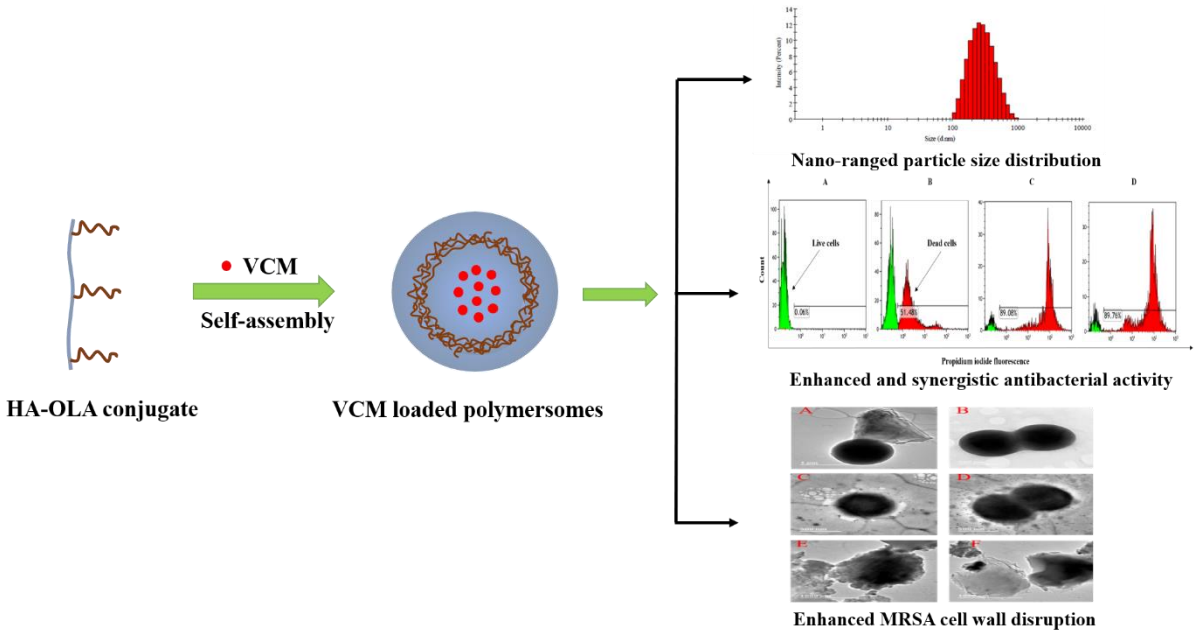

Self-assembled oleylamine grafted hyaluronic acid polymersomes for delivery of vancomycin against methicillin resistant *Staphylococcus aureus* (MRSA)

Pavan Walvekar, Ramesh Gannimani, Mohammed Salih, Sifiso Makhathini, Chunderika Mocktar, Thirumala Govender*

Discipline of Pharmaceutical Sciences, School of Health Sciences, University of KwaZulu-Natal, Private Bag X54001 Durban, 4000, South Africa.

*Corresponding Author: Private Bag X54001 Durban, 4000, KwaZulu-Natal, South Africa. Tel: 00 27 31 260 7358, Fax: 00 27 31 260 7792

Email: govenderth@ukzn.ac.za (T. Govender)

Abstract

MRSA infections are a major global healthcare problem associated with high morbidity and mortality. The application of novel materials in antibiotic delivery has efficiently contributed to the treatment of MRSA infections. The aim of the study was to develop novel hyaluronic acid-oleylamine (HA-OLA) conjugates with 25-50% degrees of conjugation, for application as a nano-drug carrier with inherent antibacterial activity. The biosafety of synthesized novel HA-OLA conjugates was confirmed by *in vitro* cytotoxicity assay. Drug carrying ability of HA-OLA conjugates was confirmed by 26.1-43.12% of vancomycin (VCM) encapsulation in self-assembled polymersomes. These polymersomes were dispersed in nano-sized range (196.1-360.9 nm) with a negative zeta potential. Vancomycin loaded polymersomes were to found have spherical and bilayered morphology. The VCM loaded polymersomes displayed sustained drug release for 72 h. *In vitro* studies showed moderate antibacterial activity for HA-OLA conjugates against both *S. aureus* and MRSA with minimum inhibitory concentration (MIC) of 500 µg/mL. The VCM loaded HA-OLA polymersomes displayed four-fold lower MIC (1.9 µg/mL) than free VCM (7.8 µg/mL) against MRSA. Furthermore, synergism was observed for VCM and HA-OLA against MRSA. Flow cytometry showed 1.8-fold higher MRSA cell death in the population for VCM loaded polymersomes relative to free drug, at concentration of 1.95 µg/mL. Bacterial cell morphology showed that the drug loaded polymersomes had stronger impact on MRSA membrane, compared to free VCM. These findings suggest that, HA-OLA conjugates are promising nano-carriers to function as antibiotic delivery vehicles for the treatment of bacterial/MRSA infections.

Introduction

Resistant strains of *Staphylococcus* bacteria are currently a significant factor contributing to deterioration of the health status in infected individuals, thus causing premature mortality[1]. Predominantly, MRSA has acquired resistance to virtually all potent antibiotics, making it extremely difficult to eliminate from the host, thus challenging current drug therapy[2]. Vancomycin (VCM) being the drug of choice to treat MRSA infections, has also capitulated to resistance to some of the isolates, known as vancomycin resistant *Staphylococcus aureus*[3]. Therefore, there is a need for novel and innovative approaches to treat MRSA infections effectively. In recent years, nano drug delivery systems have attracted large interest in the treatment of bacterial infections, because of their ability to target specific infection sites, thus increasing localized drug concentration; to provide sustained drug release, thus lowering the frequency of administration; and to improve physico-chemical properties of drugs etc. This can lead to improved therapeutic outcomes and patient compliance and can overcome drug resistance mechanisms[4]. Numerous antibiotic-loaded nano-systems are being reported for combating bacterial infections[5-7]. Therefore, antibiotic loaded nano-systems may efficiently overcome MRSA infections.

Among the various nano drug delivery systems, polymeric nano-systems have gained considerable interest to deliver therapeutic agents and treat many diseases. Polymeric nano-systems are considered to be more stable and reliable than other organic nano-platforms such as lipidic systems[8, 9]. For example, liposomes tend to lose their structural configuration upon storage thus resulting in leakage of encapsulated payloads. However, polymeric nano-systems are comparatively more robust and stable, and do not lose their integrity during long term storage. Furthermore, polymeric nano-systems can facilitate sustained/controlled, targeted and intracellular drug delivery to improve the therapeutic efficacy of encapsulated payloads[7, 10]. In addition to these advantages, polymers with surface functionalities can be easily structurally modified with other compounds to make graft or block copolymers that can suit various drug delivery applications. For example, hyaluronic acid was grafted with poly(L-histidine) for the preparation of pH responsive and tumor-targeted amphiphilic copolymer for use as a carrier for anticancer drugs[11].

Various naturally occurring, synthetic and semi-synthetic polymers such as chitosan, dextran, polylactic acid, polyglycolic acid, poly(lactic-co-glycolic acid), polyacrylic acid, methyl cellulose etc, have been used to construct nano-drug delivery systems to deliver therapeutic agents. These nano-systems have shown promising outcomes thus far in treating many diseases including bacterial infections[6]. Recently, hyaluronic acid (HA), a naturally occurring biodegradable hydrophilic polymer has captured considerable attention in designing various drug delivery nanotherapeutics. Many reports on HA-based nano-systems can be found in the literature to deliver anticancer drugs[12]. The application of HA to construct antibiotic loaded nano-systems may display improved and synergistic antibacterial activity because of its inherent bacteriostatic and antibiofilm effects against certain strains[13, 14]. Some evidences have also been documented where, polycarboxylic acids such as HA are shown to lower the pH of infection, thus creating an environment where pathogens find it difficult to survive[15]. Furthermore, HA is also known to possess wound healing, tissue regeneration and anti-inflammatory properties, which may help to cure dermal infections and facilitate quick recovery[16]. Recently, Zhu et al. reported HA-based nanogel loaded with chlorhexidine diacetate (an antibacterial agent) to demonstrate prolonged antimicrobial activity against *S. aureus* and *E. coli* followed by accelerated hemostasis and wound healing[16]. Therefore, there is a need for novel HA-based polymeric nano-systems to be used as antibiotic carriers to combat bacterial infections.

Self-assembling amphiphiles are considered as one of the most prominent and promising candidates for drug delivery applications[17]. HA is a completely hydrophilic polymer, and cannot self-organise to form nano-assemblies on its own. Therefore, an additional support is needed from a hydrophobic moiety to make it an amphiphile. Biodegradable hydrophobic long fatty chains are one class of compounds that have been frequently used to make amphiphiles[18]. Furthermore, long fatty chains have also been reported to enhance the activity of other antibacterial agents[19, 20]. The grafting of these hydrophobic long fatty chains with hydrophilic HA can make ideal amphiphilic drug cargoes. HA can be grafted with oleylamine (a long fatty chain) at certain degrees of conjugation to synthesize hyaluronic acid-grafted-oleylamine amphiphiles. To date, no HA-fatty amine conjugates have been used to deliver antibiotics.

Our research group has primarily been focussing on developing various novel nano-systems to deliver VCM for combating MRSA infections. Amongst, various other nano-systems, we have

developed polyacrylic acid, chitosan and dextran sulphate based polymeric nano-systems to deliver VCM, and fight MRSA infections[21-23]. In these findings, we have achieved decent entrapments for VCM with sustained and improved antibacterial activities against MRSA. In addition, these nano-formulations also enabled ease of preparation with good physical stability, which may enable the future commercialization of these VCM nano-systems. In continuation of our efforts to develop novel polymers, in this study, hydrophilic HA was grafted with hydrophobic oleylamine (OLA) to promote self-assembly and simultaneous encapsulation of VCM to combat MRSA infections. To the best of our knowledge, VCM has not been delivered using HA based polymeric nano-system to fight MRSA infections. Therefore, this research undertaken aimed to synthesize a novel amphiphile comprising of hydrophilic HA and hydrophobic oleylamine (fatty chain) for the formulation of self-assembled nano-carriers to deliver VCM and treat MRSA infections.

2. Materials and methods

Hydrochloride form of vancomycin was purchased from Sinobright Import & Export Co. Ltd. (China). 1-Ethyl-3- (3-dimethylaminopropyl)carbodiimide hydrochloride (EDC.HCl) was acquired from Carbosynth (UK). Oleylamine (≥ 98%) and Mueller Hinton Broth-2 (MHB) was procured from Sigma Aldrich (USA). N-Hydroxysuccinimide (NHS) was purchased from Sigma-Aldrich (Japan) Sodium hyaluronate (9.47 KDa) was purchased from Spec-Chem IND. INC. MTT (3-(4, 5-dimethylthiazol-2-yl)-2, 5-diphenyltetrazolium bromide) was purchased from Alfa Aesar (UK), Mueller Hinton Agar (MHA), Nutrient Agar and Nutrient Broth were obtained from Biolab (South Africa). The dialysis tube (MWCO 14,000 Da) was purchased from Sigma-Aldrich (USA) for drug release studies. Double distilled water obtained from a Direct-Pure EDI water system was used throughout the experiment. Gram positive bacteria, *Staphylococcus aureus* (*S. aureus*, ATCC 25923) & methicillin resistant *Staphylococcus aureus* (MRSA, ATCC 700699) were used to study the antibacterial activity.

2.1. Synthesis and characterization of HA-OLA conjugates

As sodium hyaluronate was not freely soluble in formamide, sodium salt of HA was converted to HA, to facilitate the reaction. Briefly, 2 g of sodium hyaluronate was dissolved in water, and 48 mL of 1 molar HCl was added slowly to the solution, followed by stirring for two hours. The obtained solution was freeze dried to obtain HA. Synthesis of HA-OLA with various degrees of

conjugation (50%, 33% and 25%) was planned to evaluate the self-assembling behaviour of HA after conjugation with OLA. Synthesis of HA-OLA conjugates were performed in one pot reaction as indicated in **Scheme 1**. EDC/NHS coupling chemistry was used to graft OLA to carboxylic acid groups of HA. Considering the molecular weight of HA, ~24 carboxylic were calculated per molecule. As OLA conjugated to 50% of carboxylic acids of HA became too hydrophobic, and did not self-assemble, it was not considered suitable for the present study. To synthesize 33% of conjugation, briefly, 500 mg of HA was allowed to completely dissolve in formamide, followed by sequential addition of 113 mg (8 equivalents) of OLA, 48.6 mg (8 equivalents) of NHS and 162 mg (16 equivalents) of EDC, and allowed to react for 48 h. The resulting reaction mixture was dialysed (MWCO = 3,500 Da) against water for two days to purify the polymer. Further, the polymer solution was freeze dried to obtain HA-OLA conjugates. To yield 25% of conjugation, the same procedure was followed, where OLA, NHS and EDC used were 84.8 mg (6 equivalents), 36.4 mg (6 equivalents) and 121.7 (12 equivalents) respectively. As twelve, eight and six carboxylic acids were targeted for conjugation, HA-OLA conjugates with 50%, 33% and 25% of conjugation were termed as HA-OLA12, HA-OLA8 and HA-OLA6 respectively. The HA-OLA conjugates were characterized by FTIR and ^{1}H NMR spectroscopy (D_2O).

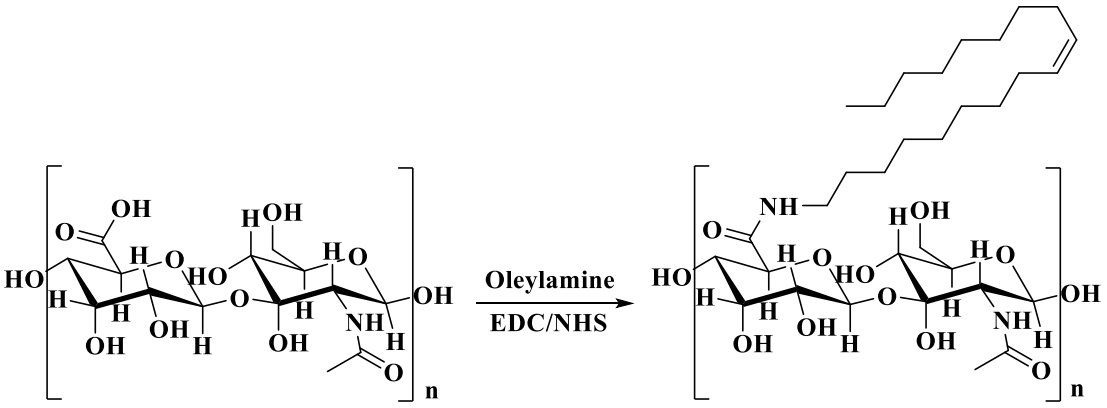

Scheme 1. Synthesis of HA-OLA conjugates

2.2. MTT assay

To evaluate the biosafety of the synthesized novel HA-OLA conjugates, MTT assay was performed on human embryonic kidney cells (HEK-293), human cervix adenocarcinoma (HeLa) cells and human breast adenocarcinoma cells (MCF-7) according to previously published

method[24]. Briefly, cell lines grown at 37 °C under humidified atmosphere of 5% CO_2 were seeded at a density of 3.0 x 10^3 cells in 96-well plates and incubated for 24 h. Thereafter, cells were treated with test compounds (HA-OLA6 and HA-OLA8) at various concentrations (20 - 100 µg/mL) and allowed to incubate for 48 h. Thereafter, the spent culture medium was replaced with 100 µL of fresh medium and 20 µL of MTT (5 mg/mL in PBS) in each well and incubated for 4 h, followed by the removal of the used medium and addition of 100 µL of DMSO to dissolve the MTT formazan crystals. The absorbance was recorded at 570 nm using a microplate spectrophotometer (Spectrostar nano, Germany). Untreated cells in the culture medium was used as negative control. The study was performed in pentaplicates, and the percentage cell viability was calculated as follows.

$$\%\ \text{Cell viability} = \left(\frac{\text{A570 nm treated cells}}{\text{A570 nm untreated cells}}\right) \text{X } 100\%$$

2.3. Preparation of VCM loaded HA-OLA polymersomes

The VCM loaded polymersomes were prepared using a probe ultrasonication technique[25]. Since, HA-OLA12 became highly hydrophobic, and did not self-assemble, it was therefore not included in the optimization process of polymersomes. Briefly, specified amounts of HA-OLA6 or HA-OLA8 conjugates were dispersed in 10 mL of water containing VCM (5/10 mg). The resulting mixture was ultrasonicated at 30% amplitude for 10 min under, cold water bath to obtain VCM loaded polymersomes of nano-sized range. Empty polymersomes were prepared using the same procedure by excluding VCM. All formulations in optimization process were prepared in triplicate.

2.4. Size, polydispersity index (PDI), zeta potential (ZP), morphology and stability

The determination of size, PDI and ZP of polymersomes was achieved through a zeta sizer (Nano ZS90, Malvern Instruments Ltd., UK) at 25 °C, without further dilution. Prior measurement, the polymersomes suspension were filtered through a 0.45 µm membrane filter to obtain a dust-free nano-system. Morphological characterisation of drug loaded polymersomes was investigated using a transmission electron microscopy (TEM - Jeol, JEM-1010, Japan). The samples were prepared and captured as previously reported[26].

A previously reported protocol was followed to assess the stability of polymersomes[25]. The stability of HA-OLA6 polymersomes in the presence of 10% FBS was measured by dynamic light

scattering (DLS) technique at 37 °C. HA-OLA6 polymersomes were dissolved in DMEM containing 10% FBS, and incubated in a shaking incubator at 100 rpm and 37 °C. The mean particle diameter (n=3) of polymersomes were obtained every 24 h for three consecutive days.

2.5. Entrapment efficiency (%EE) and drug loading capacity (DLC)

An ultrafiltration method was employed for the determination of %EE of VCM loaded polymersomes. Briefly, 2 mL of drug loaded polymersomes was placed in Amicon® Ultra-4 centrifugal filter tubes (MWCO, 10 kDa), and centrifuged at 3000 rpm at 25 °C for 30 min. The un-entrapped drug in the filtrate was assayed using reversed-phase high performance liquid chromatography (HPLC), Shimadzu Prominence DGU-20A3 with UV detection at 280 nm. A Nucleosil 120-5 C18 column (4×150 mm, 5 µm) was used, and the mobile phase consisted of acetonitrile:0.1% TFA in water (15:85 v/v). The flow rate and injection volume were 1 mL/min and 100 µL, respectively. The %EE and DLC were determined using the following equations[26].

$$\%\text{EE} = \left(\frac{\text{Amount of VCM in polymersomes}}{\text{Amount of VCM added}}\right) \text{X } 100$$

$$\%\text{DLC} = \left(\frac{\text{Amount of VCM in polymersomes}}{\text{Total weight of polymersomes}}\right) \text{X } 100$$

2.6. Differential scanning calorimetry (DSC)

DSC (Shimadzu DSC-60, Japan) was employed to study the thermal behaviours of free VCM, HA-OLA6, physical mixture (drug and the polymer) and lyophilized drug loaded polymersomes. Approximately, two mg of samples were transferred and sealed in an aluminium pan, which was further heated to 300 °C at a constant rate (10 °C/min) under a constant nitrogen flow (20 mL/min) using an empty pan as reference.

2.7. In vitro drug release

The release profiles of free VCM and VCM loaded polymersomes were studied using the dialysis bag method in PBS (pH 7.4) at 37 °C[27]. Both free VCM and VCM loaded polymersomes, each of 1 mL were loaded separately into dialysis bags (MWCO 14,000 Da). The loaded tubings were tightly sealed and dialyzed against 40 mL of PBS at 37 ± 0.5 °C in a shaking incubator at 100 rpm.

At defined time intervals, 3 mL samples were withdrawn from the dissolution media and replaced with an equal amount of fresh PBS to maintain a uniform volume and sink condition. The amount of VCM present in the samples was measured spectrophotometrically at 280 nm using HPLC (as specified in Section 2.5). The study was performed in triplicate. *In vitro* drug release kinetics and analysis were determined using DD Solver. Zero order, first order, Higuchi, Hixon-Crowell, Korsmeyer-Peppas and Weibull models. The parameters such as correlation coefficient (R^2), root mean square error (RMSE) and mean dissolution time (MDT) were calculated to determine the release kinetics and best fit model.

2.8. Antibacterial activity

2.8.1. In vitro antibacterial activity

The *in vitro* antibacterial effects of free VCM, free HA, HA-OLA6, HA-OLA8, and VCM loaded polymersomes (made up of HA-OLA6 and HA-OLA8) were studied against *S. aureus* and MRSA by determining MIC using broth dilution technique[28]. *S. aureus* and MRSA cultures were grown overnight in Nutrient Broth at 37 °C in a shaking incubator at 100 rpm. The overnight grown cultures were diluted with sterile distilled water to achieve a concentration equivalent to 0.5 MacFarland standard using a DEN-1B densitometer (Latvia). MHB (135 µL) was added to 96 well plates. Further, 135 µL of test samples were added in the first well and were serially diluted. The 0.5 MacFarland bacterial suspension were further diluted to 1:150 with sterile distilled water to achieve a final concentration equivalent to 5×10^5 colony forming units (CFU)/mL. The diluted bacterial culture (15 µL) was added to 96 well plates containing the mixture of MHB and the test samples. The plates were placed in a shaking incubator (100 rpm) at 37 °C for 24 h. MIC was determined as the lowest concentration that inhibited bacterial growth. The MIC was determined by spotting 10 µL of each broth on MHA plates followed by incubation for 24 h at 37 °C. The spotting was repeated for the next two days, i.e., at 48 h and 72 h. The study was performed in triplicate.

Σ Fractional Inhibitory Concentration (FIC) was used to study the combined effect of novel HA-OLA6 and VCM in VCM loaded polymersomes against both *S. aureus* and MRSA. ΣFIC was calculated on the basis of MIC data that was generated by *in vitro* antibacterial study. A previously reported method was followed to calculate the FIC[26]. The ΣFIC was calculated using the following equations and **Table S1** (Supplementary material).

FIC (VCM) = MIC of VCM in combination with HA-OLA6/MIC of HA-OLA6

FIC (HA-OLA6) = MIC of HA-OLA6 in combination with VCM/MIC of VCM

ΣFIC = FIC (VCM) + FIC (HA-OLA6)

2.8.2. Flow cytometry Bacterial cell viability

A flow cytometry assay was employed to study the cell viability of MRSA cells after treatment with free VCM and VCM-loaded polymersomes for 18 h[29]. The bacterial cultures were prepared as previously described in **Section. 2.8.1**. Sterile distilled water (135 µL) was added to the 96 well plate. Further, 135 µL of free VCM (positive control) and VCM-loaded polymersomes were added to the plate, and were serially diluted. Thereafter, bacterial suspension (15 µL) containing 5×10^5 CFU/mL was added at respective MICs of test samples, and incubated at 37 °C in a shaking incubator (100 rpm). To flowcytometry tubes containing 350 µL of the sheath fluid, free VCM and VCM loaded polymersomes treated broths were added and vortexed for five minutes. The tubes containing sheath fluid and test samples were further incubated for 30 min with 5 µL of propidium iodide (PI) and Syto9, which served as cell wall impermeable and permeable dyes, respectively. The fluorescence of PI was excited at 455 nm and collected through a 636 nm bandpass filter (red wavelength), whereas Syto9 excited at 485 nm, and collected at 498 nm (green wave length). Pure untreated MRSA cells were used as a negative control. A flow cytometer (BD FACSCanto II, Becton Dickinson, USA) was used for the experiment. Sheath fluid and sample flow rate were set at 16 mL/min and 0.1 mL/min, respectively. BD FACSDiva v8.0.1 (a flow cytometer software) was used to collect the data for fixed cells[30]. To analyse fluorescence-activated cell sorting, the voltage settings were, 731, 538, 444 and 451 for forward scatter, side scatter, PI and Syto9, respectively. The MRSA cells were initially gated using forward scatter, further, cells of appropriate size were gated and at least 10,000 cells were collected. The study for each sample was performed in triplicate, and position of the ‘live’ and ‘dead’ cells gates were determined. The detection threshold was set to 1,000 in side scatter analysis to avoid any background signal from particles smaller than bacteria[31].

2.8.3. Bacterial killing kinetics

Free VCM and VCM-PS6 were added at concentrations equivalent to five times the MIC to the MRSA culture (5×10^5 CFU/mL). Sterile water was added to MRSA broth, which served as a

control. Bacterial killing kinetics was monitored from 0 h to 24 h. At defined time periods (0, 1, 2, 4, 6, 8, 12 and 24 h), the samples were collected in sterile eppendorf tubes and serially diluted three times (1 : 10) with sterile water. The diluted broths were plated in triplicate on Mueller Hinton Agar plates, and incubated for 48 h at 37 °C. Thereafter, the total number of colonies were counted and converted to $\log_{10}$ values, followed by plotting a graph[32].

2.8.4. Bacterial cell morphology

VCM acts on the cell-wall of bacteria therefore, a membrane disruption study was undertaken using high resolution transmission electron microscopy (HRTEM). The study was performed for free VCM, VCM-PS6 and untreated MRSA, where, the former and latter served as positive and negative controls, respectively. Briefly, MRSA suspension (5×10^5 CFU/mL) was incubated with free VCM (500 µg/mL) and VCM-PS6 containing 500 µg/mL of VCM, at 1:1 ratio separately for 4 h. The test samples were fixed onto the surface of copper grids followed by drying. The images were captured using JEOL HRTEM 2100 (brightfield, darkfield, STEM diffraction).

2.9. Statistical analysis

The results obtained were reported as mean ± standard deviation (SD) and the data analysis was performed using GraphPad Prism®5 (Graphpad Software Inc., USA). Bonferroni's Multiple Comparison Test and One-way ANOVA were used to analyse the data and the difference was considered significant when $p < 0.05$.

3. Results and discussion

3.1. Synthesis

The conjugation of OLA to the carboxylic groups of HA was confirmed by FTIR and ^{1}H NMR studies. The spectra included in the supplementary material shows the comparative FTIR and ^{1}H NMR spectra of free HA and HA-OLA conjugates. The changes that appeared in the infrared vibrational frequencies of HA chemical bonds, provided a preliminary confirmation of the grafting of OLA to HA. The parent HA was characterised by the presence of peaks at 1725 cm$^-$1 and 1648 cm$^-$1 in the FTIR spectra, which corresponded to the carbonyl groups of carboxylic acids and acetamide bonds, respectively. After the grafting of HA with OLA, the peak at 1648 cm$^-$1 was shifted to 1643 cm$^-$1. In addition, the intensity of the peak was increased, which was due to the

increase in the number of amide bonds after the conjugation of OLA to HA. Both HA and HA-OLA conjugates contained broad peaks at ~3298 and sharp peaks at ~2923 cm^{-1}, which corresponded to OH and NH groups of amides respectively. These small shifts in bands were observed after the conjugation of OLA to HA. The results observed in FTIR were further verified by ^{1}H NMR studies. The appearance of new peaks at δ 0.903 and δ 1.30 in the ^{1}H NMR spectra of HA-OLA6 was attributed to the aliphatic protons of OLA, thus confirming the successful conjugation of OLA to HA.

3.2. MTT assay

Determining bio-safe dosages of novel materials is critical for any biomedical applications[33]. The *in vitro* cytotoxicity study demonstrated that both HA-OLA6 and HA-OLA8 displayed cell viability over 78% on HEK-293, HeLa and MCF-7, at all tested concentrations **(Fig. 1A and 1B**). The percentage cell viability of HA-OLA6 and HA-OLA8 ranged between 79.96 to 96.66%, 78.08 to 100.95% and 78.01 to 88.50% for HEK-293, HeLa and MCF-7, respectively, with no dose dependent toxicity observed at the tested concentrations. The percentage cell viability displayed on all tested cell-lines was above 75%, thus HA-OLA6 and HA-OLA8 can be considered as biologically safe and non-toxic to human cells[34].

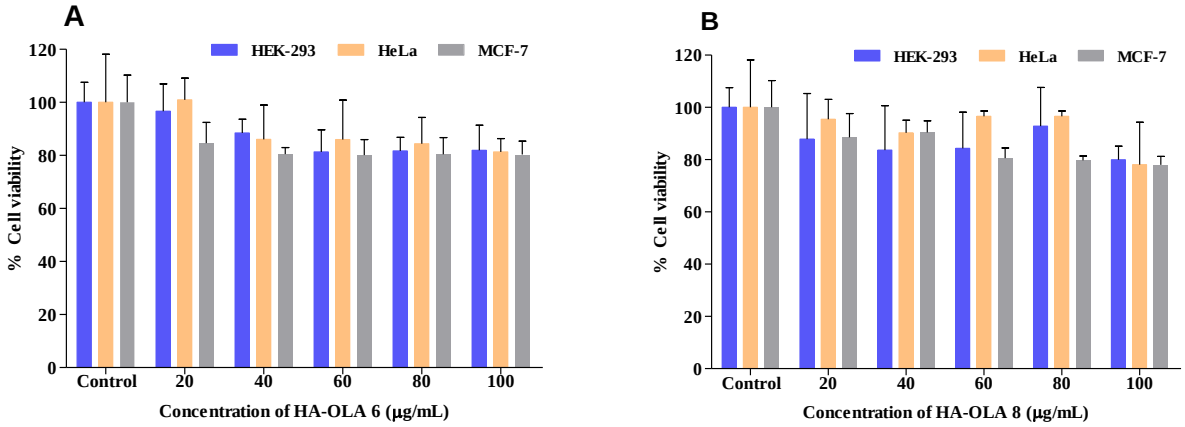

Fig.1. *In vitro* cytotoxicity of A) HA-OLA6 and B) HA-OLA8 on HEK-293, HeLa and MCF-7 (n=5).

3.3. Preparation of VCM loaded HA-OLA polymersomes

Self-assembled VCM loaded HA-OLA polymersomes were prepared using a simple probe ultrasonication technique without the use of any organic solvent, surfactant, stabilizer or emulsifier. HA and oleylamine serving as the hydrophilic backbone and grafted hydrophobic

chains, respectively, could have influenced the self-assembly of amphiphilic HA-OLA, under aqueous conditions to form polymeric vesicles (polymersomes), thereby encapsulating VCM in hydrophilic cores. This green approach to formulate polymersomes may circumvent the toxic effects of surfactants and residual organic solvents[35].

Several VCM loaded polymersomes were prepared using both HA-OLA6 and HA-OLA8 by varying the amounts of polymer and drug to optimize in terms of size, PDI, ZP and %EE. A combination of 5 mg and 20 mg of VCM and HA-OLA 6, respectively, showed satisfactory results with respect to size, PDI, ZP and %EE (**Table 1**). The results obtained from DLS revealed that, VCM (5 mg) loaded HA-OLA6 (20 mg) polymersomes (VCM-PS6) had a mean particle diameter of 248.7 ± 3.08 nm with a narrow size distribution of 0.189 ± 0.01 and a negative ZP of -17.6 ± 0.6 mV. The %EE and DLC of VCM-PS6 were found be 43.12 ± 2.18% and 8.62 ± 0.91% respectively, which were comparable with the reports for other VCM encapsulated vesicles[36, 37]. The polymersomes made up of HA-OLA8 were of smaller size compared to HA-OLA6 at all respective concentrations of polymer and drug. A similar trend was observed by Qui et.al, where, the diameter of micelles decreased with the increase in grafting of octadecylamine on HA[25]. Furthermore, polymersomes made up of HA-OLA8 displayed lower %EE compared to VCM-PS6 at all respective concentrations of polymer and drug (Supplementary material, **Table S2**). We assume that, smaller particle size and increased hydrophobicity in HA-OLA8, due to the presence of greater number of oleylamines might have reduced the encapsulation of hydrophilic VCM. Since, VCM-PS6 exhibited good results in terms of size and %EE compared to other formulations, it was therefore considered as the optimized formulation to perform other studies.

The surface morphology of VCM-PS6 was studied using TEM imaging. The images revealed a bilayered vesicular morphology with particles being spherical, and dispersed discretely and homogeneously **(Fig.2A)**. The polymersomes were found to be in the size range obtained with DLS **(Fig.2B)**.

The stability of nanoparticles in serum environment is important, as serum proteins can interact with them and may adversely affect *in vivo* efficacy[11]. The stability of polymersomes was investigated by measuring the change in their particle size as a function of time in the presence of a complete medium with FBS at 37 °C. As shown in **Fig. 2C**, the polymersomes were found to be stable after incubation in FBS for 72 h, with average diameter remaining almost the same on all

three days with no significant difference ($p > 0.05$). The results indicate that the hydrophilic anionic shell present in HA-OLA6 polymersomes might have prevented the adsorption of serum proteins on polymersomes[25].

Table 1. Effect of various concentrations of VCM and HA-OLA6 on formulation optimization (n = 3).

VCM	HA-OLA6	Size (nm)	PDI	ZP	%EE
5	10	201.4 ± 3.25	0.196 ± 0.01	-20.4 ± 1.84	33.12 ± 2.11
5	20	248.7 ± 3.08	0.189 ± 0.01	-17.6 ± 0.61	43.12 ± 2.18
5	40	339.5 ± 3.37	0.222 ± 0.01	-18.8 ± 1.42	41.04 ± 1.85
10	10	203.7 ± 3.81	0.181 ± 0.01	-19.2 ± 0.89	27.68 ± 2.41
10	20	251.3 ± 1.21	0.202 ± 0.01	-18.4 ± 1.26	36.48 ± 2.06
10	40	360.9 ± 5.84	0.225 ± 0.01	-18.5 ± 1.11	38.34 ± 4.74

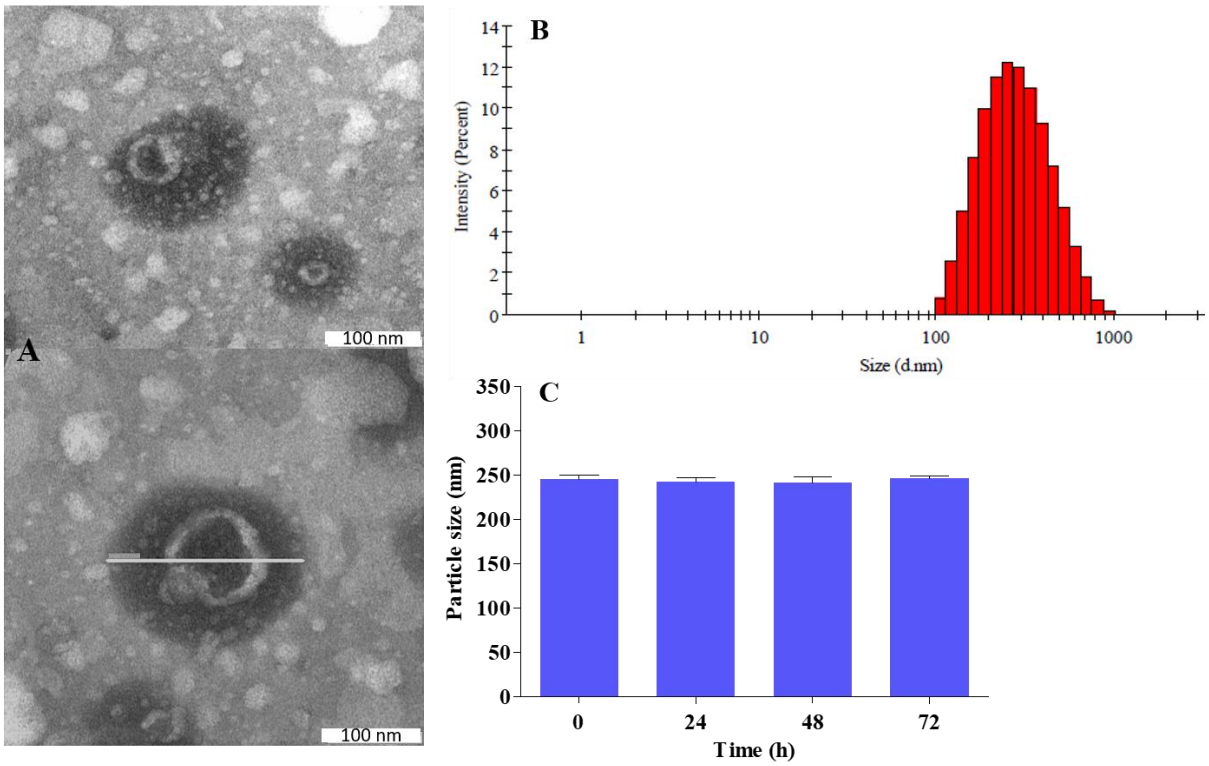

Fig. 2. A) TEM images of VCM-PS6 showing bilayered morphology. B) Size distribution of VCM-PS6 determined by DLS. C) Stability of HA-OLA6 polymersomes in 10% FBS (n=3).

3.4. Differential scanning calorimetry (DSC)

DSC studies were performed to confirm the loading of VCM into HA-OLA6 polymersomes. The thermal behaviour of VCM, HA-OLA6, physical mixture of VCM and HA-OLA6 and lyophilised drug loaded formulation were studied **(Fig. 3)**. As many chemical and physical transitions are associated with consumption or generation of heat, an abrupt change in the thermal behaviour may indicate a possible interaction between the excipients[38, 39]. A broad endothermic peak was observed for free VCM at 129.96 °C, which displayed its thermal decomposition, while for HA-OLA6, a similar peak was noticed at 203.93 °C. Two separate endothermic peaks with slightly upward shifts were observed for VCM and HA-OLA6 mixture at 137.25 °C and 208.68 °C respectively, whereas, the thermogram of VCM loaded HA-OLA6 polymersomes (VCM-PS6) did not display any thermal peaks for neither VCM nor HA-OLA6. This disappearance of VCM suggested that the drug was encapsulated into the polymersomes in non-crystalline form[40].

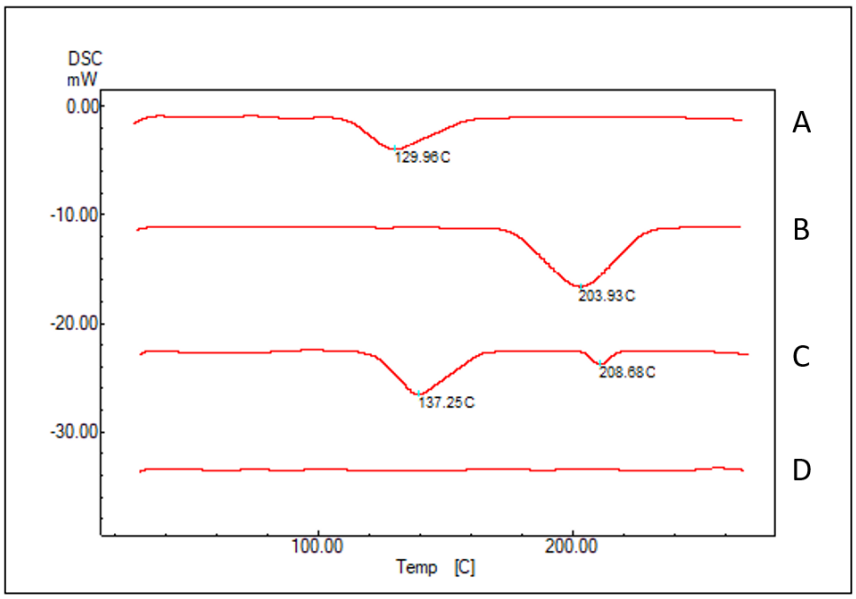

Fig.3. Thermograms of (A) Free VCM; (B) HA-OLA6; (C) physical mixture of VCM and HA-OLA6 and (D) Lyophilized VCM-PS6.

3.5. In vitro drug release

The drug release behaviour of free VCM and VCM-PS6 were studied in PBS 7.4, and are represented in **Fig. 4**. The cumulative percentage release for free VCM and VCM from polymersomes at 12 h was 75% and 57%, respectively, displaying ~22% of difference in the release pattern between free VCM and VCM in polymersomes, respectively. After 24 h, almost 90% of free VCM was released, whereas, it took 72h for the polymersomes to release same amount of drug. Although, the release profiles of free VCM and VCM from polymersomes were comparable at initial hours, a sustained drug release was observed with nano-formulation after 6 h. The initial quick release could have been governed by diffusion and greater concentration gradient of drug, whereas, sustained drug release might have been due to polymer erosion and degradation[41]. From these observations, it was evident that, polymersomes made from HA-OLA6 were able to release the encapsulated VCM in a sustained manner, compared to free drug. Considering, the ability of polymersomes to release VCM in a slow manner, this formulation could provide required lethal doses of encapsulated antibiotic in bacterial microenvironment for a prolonged period of time to facilitate improved and sustained antibacterial activity. Furthermore, this sustained release of VCM may also overcome the development of resistance.

Various mathematical models were used to understand the release kinetics of VCM from HA-OLA6 polymersomes **(Table 2)**. Among the studied mathematical models, the release of VCM from polymersomes was found to fit in Weibull model with a higher co-relation coefficient of 0.994 and a lower root mean square error of 2.433. The '*n*' exponent (0.488), that was obtained from Korsmeyer-Peppas equation indicated that the release mechanism was anomalous or non-fickian transpot[42]. Apart from drug diffusion, polymer erosion and degradation may have significant roles in releasing VCM slowly from polymersomes. The MDT values calculated for the release of free VCM and VCM polymersomes were 9.76 and 15.06, respectively, indicating slower release of VCM from polymersomes.

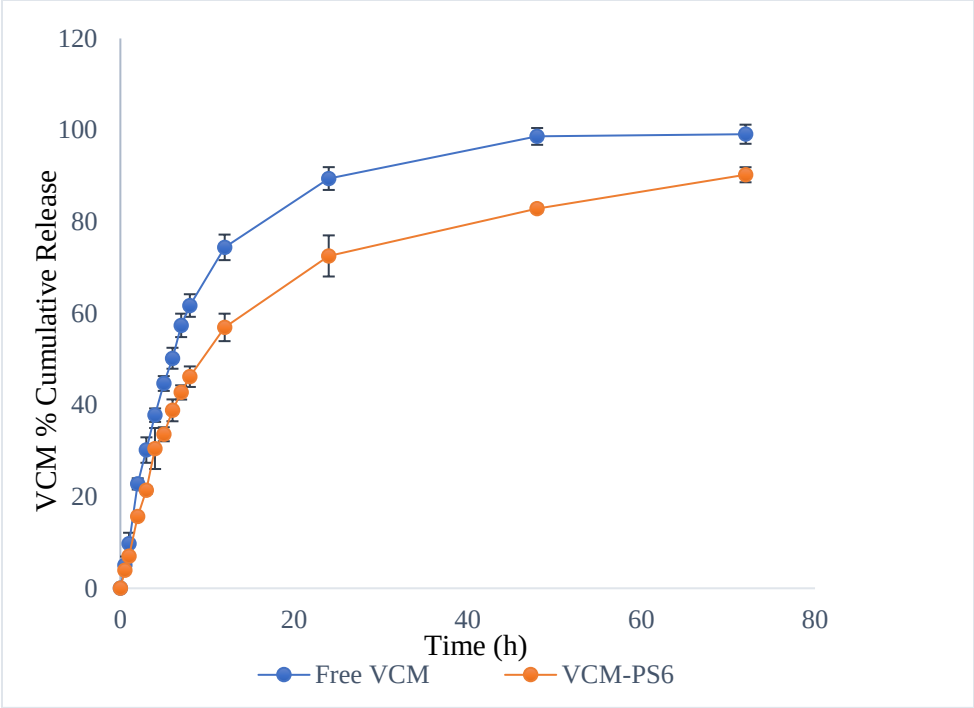

Fig. 4. *In vitro* drug release profiles of free VCM and VCM-PS6

Table 2. Various mathematical models for drug release from VCM-PS6

Model	Equation	R^2	RMSE	Release exponent (*n*)
Zero order	$Q = k.\ t + Q_0$	0.2724	24.581	-
First order	$Q = Q_0 . e^{kt}$	0.9579	5.9115	-
Higuchi	$Q = k.\ t^{½}$	0.9100	8.6468	-
Hixon-Crowell	$Q^{⅓} = kt + Q_0^{⅓}$	0.9045	8.9037	-
Korsmeyer-Peppas	$Q = k\ .\ t^n$	0.9460	6.2425	0.488
Weibull	$Q = 1 \exp - (t)^{a/b}]$	0.9940	2.4334	-

3.6. Antibacterial activity

3.6.1. In vitro antibacterial activity

The *in vitro* antibacterial studies were performed for free VCM, free HA, HA-OLA6 and optimized drug loaded formulation, i.e., VCM-PS6 against *S. aureus* and MRSA **(Table 3)**. Since OLA is an antibacterial enhancer, MIC values were determined for HA-OLA8 and VCM (5 mg) loaded HA-OLA8 (20 mg) polymersomes (VCM-PS8) as well. There was no antibacterial activity observed

for free HA against the tested strains of *S. aureus* and MRSA. Interestingly, the novel amphiphilic polymers synthesized in this study, HA-OLA6 and HA-OLA8 displayed moderate antibacterial activities against both *S. aureus* and MRSA with MIC values of 500 µg/mL, over the studied period of 72 h. The MIC values for free VCM against *S. aureus* and MRSA were 1.95 and 7.8 µg/mL, respectively at 24 h. Although, the MIC values for VCM-PS6 and VCM-PS8 remained same as free VCM against *S. aureus*, enhanced activities were observed against MRSA with MIC values of 1.95 µg/mL, displaying 4-fold improvement. At 48 h, free VCM started to lose its potential antibacterial activity, displaying an increased MIC value (250 µg/mL) against *S. aureus* and complete bacterial growth against MRSA. At the end of day three, free VCM had no activity against both *S. aureus* and MRSA. In contrast, VCM-PS6 and VCM-PS8 retained the activity of VCM at 48 h and 72 h against both bacterial strains with MIC values (1.95 µg/mL), remaining same as day one. From these results, both VCM-PS6 and VCM-PS8 showed better activity than free VCM against the tested bacterial strains. The nano-formulations preserved the antibacterial potency of VCM for three days against both strains, while free VCM lost its activity after 24 h. The improved and sustained antibacterial activity of VCM loaded polymersomes can be attributed to slow and controlled release of VCM in bacterial environment over a prolonged period of time. This sustained antibacterial potential of VCM-PS6 and VCM-PS8 can efficiently control infection with reduced frequency of dose and adverse effects. Although, HA-OLA6 and HA-OLA8 were not as potent as VCM, they were able to improve the antibacterial activity of VCM against both *S. aureus* and MRSA. Therefore, the grafted polymers synthesized in this study can make promising nano-carriers to deliver antibiotics and treat MRSA infections.

Table 3. MIC values of free VCM, free HA, HA-OLA 6, HA-OLA8, VCM-PS6 and VCM-PS8

Time (h)	24	48	72	24	48	72
	S. aureus (µg/mL)			MRSA (µg/mL)		
Free VCM	1.95	250	NA	7.8	NA	NA
Free HA	NA	NA	NA	NA	NA	NA
HA-OLA6	500	500	500	500	500	500
HA-OLA8	500	500	500	500	500	500
VCM-PS6	1.95	1.95	1.95	1.95	1.95	1.95
VCM-PS8	1.95	1.95	1.95	1.95	1.95	1.95

NA = No activity, n = 3

To understand the combined effect of HA-OLA6 and VCM in VCM loaded HA-OLA6 polymersomes (VCM-PS6) against *S. aureus* and MRSA, FIC values were calculated. As free VCM had lost its potential activity at the end of 24 h, FIC values for both free VCM and free HA-OLA6 were determined at 24 h. The calculated FIC values for VCM-PS6 were found to be 1.01 and 0.25 against *S. aureus* and MRSA, indicating that there was indifference and synergistic antibacterial activity respectively **(Table S3,** supplementary material**)**.

3.6.2. Flow cytometry Bacterial cell viability

The rapid cell viability of MRSA cells was analysed using a Flow cytometry technique[29]. The MRSA cells were incubated with free VCM and VCM-PS6. The bacterial cells, upon incubation with antibiotics, change their morphology and cell-division cycle, which can be measured using special dyes. PI, a cell-wall non-permeant dye and Syto9, a non-selective cell wall permeant dye were used to detect dead and live cells, respectively[43]. Kaluza-2.1 (Beckman Coulter USA) flow cytometer software was used to analyse the data. Two gates were created to differentiate viable cells (green) and dead cells (red). VCM acts by interfering with the cell wall integrity, which enables the uptake of PI in bacterial cells. The PI inside the cell, intercalate the DNA showing a shift in PI fluorescence, indicating bacterial cell death. Whilst, untreated MRSA showed ~100% viable cells, the bacteria treated with free VCM and VCM-PS6 showed a shift in PI fluorescence, where two distinct populations of live and dead bacteria were observed **(Fig. 5 1)**. The free VCM **(Fig. 5 1 C)** and VCM-PS6 **(Fig. 5 1 D)** showed 88.7 ± 1.21% and 89.2 ± 0.60% dead MRSA cells in the population, after treating at their MICs of 7.8 and 1.95 µg/mL respectively. However, the MRSA treated with free VCM at a concentration same as of MIC of VCM-PS6 (1.95 µg/mL), had reduced killing percentage of bacterial cells, i.e., 51.22 ± 1.21% ($p < 0.05$) **(Fig. 5 1 B)**. VCM-PS6 proved to be more efficient than free VCM at concentration of 1.95 µg/mL, showing 1.8-fold more dead cells. These results further supported the antibacterial superiority of VCM-PS6.

3.6.3. Bacterial killing kinetics

Time-kill curve for free VCM and VCM-PS6 at 5 x MIC against MRSA is presented in **Fig. 5 ll**. Rapid bactericidal activity was observed for VCM-PS6 after eight hours of exposure, displaying 3-log reduction (99.9% clearance). In contrast, free VCM displayed slow killing rate (2-log

reduction) after 24 h treatment. A complete bacterial inhibition was not observed for free VCM over the studied period of 24 h. It was worth noting that, VCM-PS6 at four times lower concentration than free VCM, achieved bactericidal activity within eight hours of treatment. This may lead to rapid elimination of bacteria, thus reducing the dose and course of treatment.

3.6.4. Bacterial cell morphology

The ability of free VCM and VCM-PS6 to disrupt bacterial cell membrane was determined by assessing the morphological changes/differences induced in MRSA cells after four hours of treatment. The HRTEM images showed that, untreated MRSA, which was used as negative control exhibited smooth and integrated cell membrane with intact cocci (**Fig. 5 lll A and 5 lll B**). The MRSA cells that were treated with VCM alone displayed a deformed and impaired cell membrane after four hours (**Fig. 5 lll C and 5 lll D**). In contrast, after same incubation period, the MRSA cells treated with VCM-PS6 were damaged and ruptured intensely (**Fig. 5 lll E and 5 lll F**). The closer view of VCM-PS6 treated cells revealed that, the drug loaded formulation had a strong impact on the integrity of MRSA cell membrane. Furthermore, the membrane and shape of cocci was completely altered with distinguished perforations and leakage of cytosol (**Fig. 5 lll E and 5 lll F**). VCM-PS6 were found to be more potent than free VCM in disrupting MRSA membrane. These results corroborate well with *in vitro* antibacterial activity, flow cytometry analysis and bacterial killing kinetics.

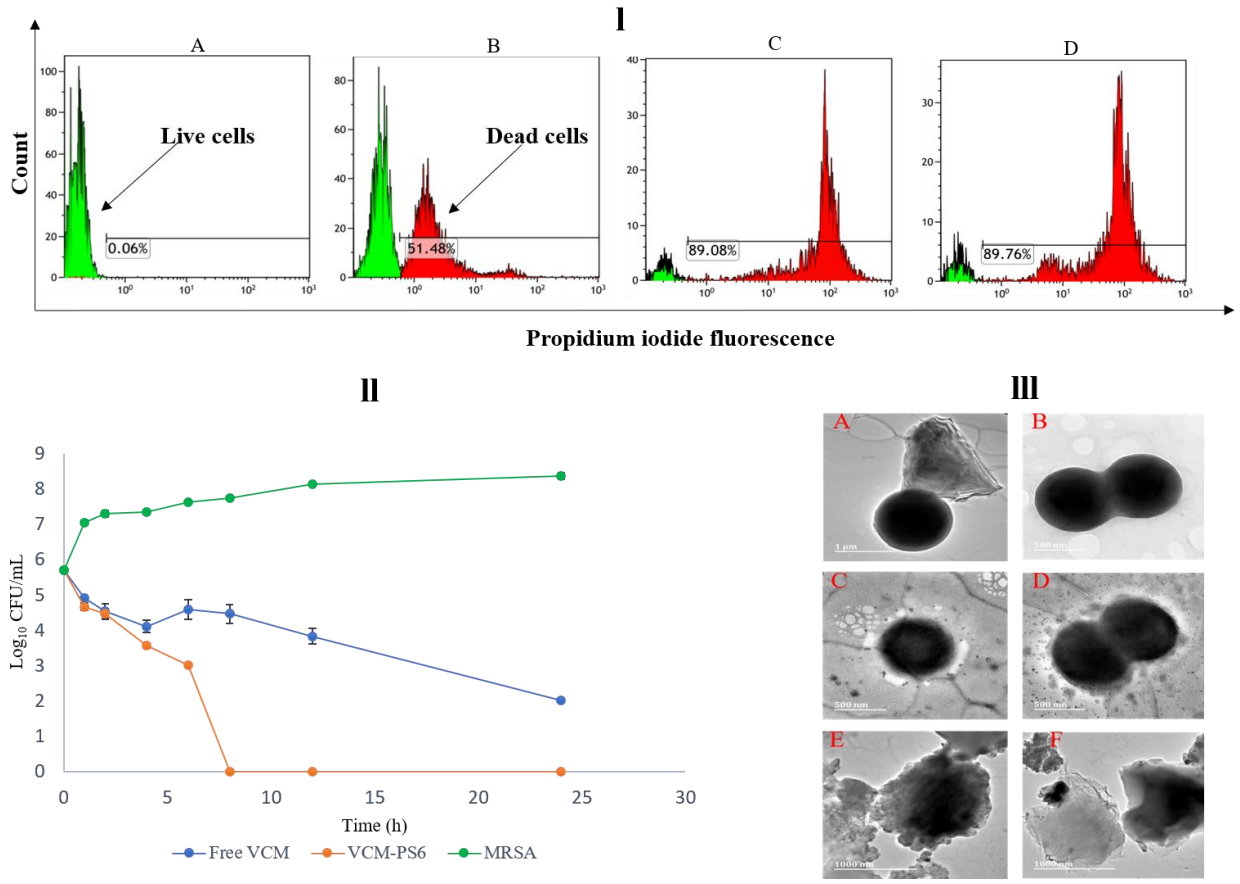

Fig. 5. (l) MRSA cell counts vs PI uptake histogram where, A represents untreated MRSA (live cells); B, C and D represents percentage of dead cells in the population after incubation with free VCM at MIC of 1.95 µg/mL, free VCM at its MIC (7.8 µg/mL) and VCM-PS6 at its MIC (1.95 µg/mL) respectively; (ll) Bacterial killing kinetics of MRSA exposed to 5 x MIC of free VCM, VCM-PS6 and sterile water; (lll) HRTEM images showing morphological differences of untreated MRSA (A and B); VCM treated MRSA (C and D) and VCM-PS6 treated MRSA (E and F).

4. Conclusions

Recently, there has been a surge of interest to develop novel drug carrier systems for antibiotic delivery. In this study, conjugates of HA and OLA were synthesized depending on various percentage of conjugation. The novel HA-OLA conjugates were proven to be bio-safe on the cell lines tested and exhibited moderate antibacterial activity against *S. aureus* and MRSA. VCM loaded HA-OLA6 polymersomes (VCM-PS6) were dispersed in nano-sized range with particle sizes < 250 nm and entrapment efficiency of 43.12 ± 2.18%. The polymersomes exhibited slow and sustained release for VCM throughout the studied period of 72 h. The *in vitro* antibacterial

activity against MRSA revealed that, VCM-PS6 had 4-fold enhanced activity, compared to free VCM. Furthermore, synergism was observed for VCM and HA-OLA6 against MRSA. The antibacterial studies using flow cytometry revealed that, VCM-PS6 showed 1.8-fold more dead cells of MRSA, compared to free VCM, when samples were treated at MIC of 1.95 µg/mL. Bacterial cell morphology showed that, VCM loaded polymersomes had a stronger impact on MRSA membrane disruption compared to free VCM. These results indicate that, VCM-PS6 was more potent than free VCM against MRSA in all performed antibacterial studies. In summary, these findings suggest that, HA-OLA conjugates can make promising antibiotic nano-carriers to combat multi-drug resistant bacterial strains. In addition, these novel conjugates can be further explored to encapsulate other classes of pharmacologically active agents to manage various disease conditions effectively.

Conflict of interest

The authors declare no conflict of interest.

Acknowledgment

The authors acknowledge the College of Health Sciences, University of KwaZulu-Natal (UKZN) and UKZN Nanotechnology Platform, National Research Foundation of South Africa (Grant No. 106040) and Medical Research Council of South Africa for financial support. We acknowledge Microscopy and Microanalysis Unit and Department of Human Physiology at UKZN for use of facilities and Ms. Charlotte Ramadhin for proof reading.

References:

[1] T. Foster, Staphylococcus, in: S. Baron (Ed.) Medical Microbiology 1996.
[2] D.C. Kaur, S.S. Chate, Study of antibiotic resistance pattern in methicillin resistant Staphylococcus aureus with special reference to newer antibiotic, J. Glob. Infect. Dis, 7 (2015) 78.
[3] A. Gupta, S. Mumtaz, C.-H. Li, I. Hussain, V.M. Rotello, Combatting antibiotic-resistant bacteria using nanomaterials, Chem. Soc. Rev, 48 (2019) 415-427.
[4] L. Zhang, F. Gu, J. Chan, A. Wang, R. Langer, O. Farokhzad, Nanoparticles in medicine: therapeutic applications and developments, Clin. Pharmacol. Ther, 83 (2008) 761-769.
[5] M.-H. Xiong, Y. Bao, X.-Z. Yang, Y.-H. Zhu, J. Wang, Delivery of antibiotics with polymeric particles, Adv. Drug Deliv. Rev, 78 (2014) 63-76.
[6] A.J. Huh, Y.J. Kwon, "Nanoantibiotics": a new paradigm for treating infectious diseases using nanomaterials in the antibiotics resistant era, J. Control. Release, 156 (2011) 128-145.
[7] W. Gao, S. Thamphiwatana, P. Angsantikul, L. Zhang, Nanoparticle approaches against bacterial infections, Wiley. Interdiscip. Rev. Nanomed. Nanobiotechnol, 6 (2014) 532-547.

[8] H. Pinto-Alphandary, A. Andremont, P. Couvreur, Targeted delivery of antibiotics using liposomes and nanoparticles: research and applications, Int. J. Antimicrob. Agents, 13 (2000) 155-168.
[9] W.S. Cheow, K. Hadinoto, Factors affecting drug encapsulation and stability of lipid–polymer hybrid nanoparticles, Colloids Surf. B Biointerfaces, 85 (2011) 214-220.
[10] U.S. Toti, B.R. Guru, M. Hali, C.M. McPharlin, S.M. Wykes, J. Panyam, J.A. Whittum-Hudson, Targeted delivery of antibiotics to intracellular chlamydial infections using PLGA nanoparticles, Biomaterials, 32 (2011) 6606-6613.
[11] L. Qiu, Z. Li, M. Qiao, M. Long, M. Wang, X. Zhang, C. Tian, D. Chen, Self-assembled pH-responsive hyaluronic acid–g-poly (l-histidine) copolymer micelles for targeted intracellular delivery of doxorubicin, Acta Biomater, 10 (2014) 2024-2035.
[12] J.M. Wickens, H.O. Alsaab, P. Kesharwani, K. Bhise, M.C.I.M. Amin, R.K. Tekade, U. Gupta, A.K. Iyer, Recent advances in hyaluronic acid-decorated nanocarriers for targeted cancer therapy, Drug Discov. Today, 22 (2017) 665-680.
[13] P. Pirnazar, L. Wolinsky, S. Nachnani, S. Haake, A. Pilloni, G.W. Bernard, Bacteriostatic effects of hyaluronic acid, J. Periodontol, 70 (1999) 370-374.
[14] L. Drago, L. Cappelletti, E. De Vecchi, L. Pignataro, S. Torretta, R. Mattina, Antiadhesive and antibiofilm activity of hyaluronic acid against bacteria responsible for respiratory tract infections, APMIS, 122 (2014) 1013-1019.
[15] B.S. Nagoba, N.M. Suryawanshi, B. Wadher, S. Selkar, Acidic environment and wound healing: a review, Wounds : a compendium of clinical research and practice, 27 (2015) 5-11.
[16] J. Zhu, F. Li, X. Wang, J. Yu, D. Wu, Hyaluronic Acid and Polyethylene Glycol Hybrid Hydrogel Encapsulating Nanogel with Hemostasis and Sustainable Antibacterial Property for Wound Healing, ACS Appl. Mater. Interfaces, 10 (2018) 13304-13316.
[17] A. Rösler, G.W. Vandermeulen, H.-A. Klok, Advanced drug delivery devices via self-assembly of amphiphilic block copolymers, Adv. Drug Deliv. Rev, 64 (2012) 270-279.
[18] J.-P. Douliez, C. Gaillard, Self-assembly of fatty acids: from foams to protocell vesicles, New J. Chem, 38 (2014) 5142-5148.
[19] A. Desbois, K. Lawlor, Antibacterial activity of long-chain polyunsaturated fatty acids against Propionibacterium acnes and Staphylococcus aureus, Mar. Drugs, 11 (2013) 4544-4557.
[20] T. Kitahara, N. Koyama, J. Matsuda, Y. Aoyama, Y. Hirakata, S. Kamihira, S. Kohno, M. Nakashima, H. Sasaki, Antimicrobial activity of saturated fatty acids and fatty amines against methicillin-resistant Staphylococcus aureus, Biol. Pharm. Bull, 27 (2004) 1321-1326.
[21] D.R. Sikwal, R.S. Kalhapure, S. Rambharose, S. Vepuri, M. Soliman, C. Mocktar, T. Govender, Polyelectrolyte complex of vancomycin as a nanoantibiotic: Preparation, in vitro and in silico studies, Mater. Sci. Eng. C, 63 (2016) 489-498.
[22] R.S. Kalhapure, M. Jadhav, S. Rambharose, C. Mocktar, S. Singh, J. Renukuntla, T. Govender, pH-responsive chitosan nanoparticles from a novel twin-chain anionic amphiphile for controlled and targeted delivery of vancomycin, Colloids Surf. B Biointerfaces, 158 (2017) 650-657.
[23] D. Hassan, C.A. Omolo, R. Gannimani, A.Y. Waddad, C. Mocktar, S. Rambharose, N. Agrawal, T. Govender, Delivery of Novel Vancomycin Nanoplexes for Combating Methicillin Resistant staphylococcus aureus (MRSA) Infections, Int. J. Pharm, (2019).
[24] C.A. Omolo, R.S. Kalhapure, N. Agrawal, S. Rambharose, C. Mocktar, T. Govender, Formulation and Molecular Dynamics Simulations of a Fusidic Acid Nanosuspension for

Simultaneously Enhancing Solubility and Antibacterial Activity, Mol. Pharm, 15 (2018) 3512-3526.
[25] L. Qiu, M. Zhu, Y. Huang, K. Gong, J. Chen, Mechanisms of cellular uptake with hyaluronic acid—octadecylamine micelles as drug delivery nanocarriers, RSC Adv, 6 (2016) 39896-39902.
[26] P. Walvekar, R. Gannimani, S. Rambharose, C. Mocktar, T. Govender, Fatty acid conjugated pyridinium cationic amphiphiles as antibacterial agents and self-assembling nano carriers, Chem. Phys. Lipids, 214 (2018) 1-10.
[27] S.J. Sonawane, R.S. Kalhapure, S. Rambharose, C. Mocktar, S.B. Vepuri, M. Soliman, T. Govender, Ultra-small lipid-dendrimer hybrid nanoparticles as a promising strategy for antibiotic delivery: In vitro and in silico studies, Int. J. Pharm, 504 (2016) 1-10.
[28] M. Balouiri, M. Sadiki, S.K. Ibnsouda, Methods for in vitro evaluating antimicrobial activity: A review, J. Pharm. Anal, 6 (2016) 71-79.
[29] N.M. O'Brien-Simpson, N. Pantarat, T.J. Attard, K.A. Walsh, E.C. Reynolds, A Rapid and Quantitative flow cytometry method for the analysis of membrane disruptive antimicrobial activity, PLoS One, 11 (2016) e0151694.
[30] A.R.C. Duarte, M.S. Costa, A.L. Simplício, M.M. Cardoso, C.M. Duarte, Preparation of controlled release microspheres using supercritical fluid technology for delivery of anti-inflammatory drugs, Int. J. Pharm, 308 (2006) 168-174.
[31] S. Renggli, W. Keck, U. Jenal, D. Ritz, Role of autofluorescence in flow cytometric analysis of Escherichia coli treated with bactericidal antibiotics, J. Bacteriol, 195 (2013) 4067-4073.
[32] P. Vaudaux, A. Gjinovci, M. Bento, D. Li, J. Schrenzel, D.P. Lew, Intensive therapy with ceftobiprole medocaril of experimental foreign-body infection by methicillin-resistant Staphylococcus aureus, Antimicrob. Agents Chemother, 49 (2005) 3789-3793.
[33] S. Choksakulnimitr, S. Masuda, H. Tokuda, Y. Takakura, M. Hashida, In vitro cytotoxicity of macromolecules in different cell culture systems, J. Control. Release, 34 (1995) 233-241.
[34] X. Cao, C. Cheng, Y. Ma, C. Zhao, Preparation of silver nanoparticles with antimicrobial activities and the researches of their biocompatibilities, J. Mater. Sci. Mater. Med, 21 (2010) 2861-2868.
[35] I. Hussain, N. Singh, A. Singh, H. Singh, S. Singh, Green synthesis of nanoparticles and its potential application, Biotechnol. Lett, 38 (2016) 545-560.
[36] J. Liu, Z. Wang, F. Li, J. Gao, L. Wang, G. Huang, Liposomes for systematic delivery of vancomycin hydrochloride to decrease nephrotoxicity: Characterization and evaluation, Asian J. Pharm, 10 (2015) 212-222.
[37] M. Jadhav, R.S. Kalhapure, S. Rambharose, C. Mocktar, S. Singh, T. Kodama, T. Govender, Novel lipids with three C18-fatty acid chains and an amino acid head group for pH-responsive and sustained antibiotic delivery, Chem. Phys. Lipids, 212 (2018) 12-25.
[38] G. Höhne, W.F. Hemminger, H.-J. Flammersheim, Differential Scanning Calorimetry, Springer Science & Business Media 2013.
[39] G. Ceschel, R. Badiello, C. Ronchi, P. Maffei, Degradation of components in drug formulations: a comparison between HPLC and DSC methods, J. Pharm. Biomed. Anal, 32 (2003) 1067-1072.
[40] C.G. Pupe, M. Villardi, C.R. Rodrigues, H.V.A. Rocha, L.C. Maia, V.P. de Sousa, L.M. Cabral, Preparation and evaluation of antimicrobial activity of nanosystems for the control of oral pathogens Streptococcus mutans and Candida albicans, Int. J. Nanomedicine, 6 (2011) 2581.

[41] J. Ritsema, E. Herschberg, S. Borgos, C. Løvmo, R. Schmid, Y. Te Welscher, G. Storm, C.F. van Nostrum, Relationship between polarities of antibiotic and polymer matrix on nanoparticle formulations based on aliphatic polyesters, Int. J. Pharm, 548 (2018) 730-739.
[42] P.L. Ritger, N.A. Peppas, A simple equation for description of solute release I. Fickian and non-fickian release from non-swellable devices in the form of slabs, spheres, cylinders or discs, J. Control. Release, 5 (1987) 23-36.
[43] M. Fittipaldi, A. Nocker, F. Codony, Progress in understanding preferential detection of live cells using viability dyes in combination with DNA amplification, J. Microbiol. Methods, 91 (2012) 276-289.

CHAPTER 5, CO-AUTHORED PAPERS

5.1 Introduction

In addition to the first authored experimental papers in Chapters, 3 and 4 focusing on the aims 1 and 2. I have also been involved in other research project within our group as a team member. This project also focused on the broad aim of novel nano-based strategies to effectively treat bacterial infections. This chapter therefore includes one co-authored experimental paper, which has been communicated in ISI international journal, Nanotechnology (Impact Factor = 3.404) with manuscript id: NANO: 121995.

CHAPTER 6: CONCLUSION

6.1 General conclusions

Resistance to antibiotics has reached extreme levels throughout the world, with available treatment options gradually becoming ineffective to treat multi-drug resistant bacteria. Nano-drug delivery approaches are showing considerable potential to improve the efficacy of existing antibiotics to treat bacterial infections. The severity of bacterial resistance demands advanced materials to design novel drug delivery systems, that can improve pharmacokinetic properties of drugs and contribute to enhance their antibacterial efficacy. The broad aim of this study was to design and synthesize advanced materials to formulate nano-systems and explore their potential for targeting and treating bacterial infections. The specific research aims of this study were therefore to: (1) Synthesize novel fatty acid based pyridinium cationic amphiphiles (FCAs), and employ them to deliver VCM via polymersomes against *S. aureus* and MRSA infections. (2) Synthesize novel hyaluronic acid-oleylamine (HA-OLA) conjugates, and explore their potential to deliver VCM via polymersomes against *S. aureus* and MRSA infections.

The main conclusions generated from the research data are summarised below:

Aim 1

- Three novel FCAs namely, oleic acid based cationic amphiphile (OCA), linoleic acid based cationic amphiphile (LCA) and linolenic acid based cationic amphiphile (LLCA) were successfully synthesized, and their successful synthesis and structures were confirmed using FT-IR, ^{1}H and ^{13}C NMR and HRMS.

- The cytotoxicities of synthesized compounds were studied using MTT assay on three different mammalian cell lines i.e., adenocarcinoma alveolar basal epithelial cells (A549), liver hepatocellular carcinoma (Hep G2) cell lines and human embryonic kidney cells 293 (HEK-293). The results showed that the synthesized FCAs were bio-safe.

- Amongst three FCAs, oleic based cationic amphiphilic (OCA) was employed to demonstrate the applicability of these novel materials as nano-carriers. VCM loaded OCA vesicles were successfully formulated., and exhibited particle size, PDI and ZP of 132.9 ± 2.5 nm, 0.167 ± 0.02 and 18.9 ± 1.2 mV respectively, with 61.24 ± 1.8% of drug entrapment being achieved. The VCM release from OCA vesicles was found to be sustained compared to bare VCM.

- *In vitro* antibacterial study showed that the novel OCA, LCA and LLCA displayed bactericidal activity against the tested Gram positive and Gram negative bacterial strains. However, they were more active against Gram positive bacteria compared to Gram negative. VCM loaded OCA vesicles displayed four-fold lower minimum inhibitory concentration (MIC) against MRSA compared to the free drug. Furthermore, synergism was observed for VCM and OCA against MRSA. An *in vivo* skin infection mouse model showed four-fold reduced MRSA burden in the VCM loaded OCA vesicles treated mice groups compared to bare VCM, thus confirming the synergistic activity between VCM and OCA.

Aim 2

- Three novel hyaluronic acid-oleylamine (HA-OLA) conjugates were synthesized depending on degree of substitution. The conjugates were named according to the number of oleylamines used for conjugation, i.e., HA-OLA6 and HA-OLA8. FT-IR and ^{1}H NMR analysis confirmed the successful synthesis and structure of polymer-lipid conjugates.

- Cytotoxicity studies performed using an MTT assay on three mammalian cell lines, HEK-293, human cervix adenocarcinoma (HeLa) and human breast adenocarcinoma (MCF-7) revealed that the synthesized HA-OLA conjugates were biosafe.

- The VCM loaded polymersomes (VCM-PS6) were found to have particle size, PDI, ZP and %EE of 248.7 ± 3.08 nm, 0.189 ± 0.01, -17.6 ± 0.6 mV and 43.12 ± 2.18% respectively. The *in vitro* VCM release from polymersomes was sustained compared to free VCM.

- From *in vitro* antibacterial studies, HA-OLA conjugates showed moderate activity against both *S. aureus* and MRSA, with MIC values of 500 µg/mL. VCM-PS6 showed four-fold lower MIC values (1.95 µg/mL) against MRSA compared to the free VCM (7.8 µg/mL). Furthermore, synergism was observed for VCM and HA-OLA6 against MRSA. The flow cytometry study showed 1.8-fold more dead cells of MRSA in the population when samples were treated with the drug loaded polymersomes than the free VCM at a concentration of 1.95 µg/mL of the drug. The images from HRTEM revealed that, VCM-PS6 had a stronger impact on MRSA membrane compared to free drug.

The findings of this study therefore confirmed that the synthesized novel materials were biosafe for biomedical applications. These molecules displayed great potential as nano-carriers to encapsulate antibiotics (VCM), and treat *S. aureus* and MRSA infections more efficiently than the free drug. In addition to their ability to encapsulate therapeutic agents, these novel materials also showed antibacterial effects against the tested strains of bacteria, and synergistic effects with VCM against MRSA.

The studies presented in Chapter 5 as a co-author on other publications by the group also confirmed the potential of novel antimicrobial peptides for bacterial membrane specificity and treatment of bacterial infections.

6.2 Significance of the findings in the study

The newly synthesized materials and designed nano-formulations, VCM loaded OCA vesicles and VCM-PS6 were successfully employed to address the limitations associated with conventional dosage forms of antibiotics and antibacterial resistance. The significance of the findings in this study include the following:

New pharmaceutical products: This study has generated new pharmaceutical materials, i.e., FCAs (OCA, LCA and LLCA) and HA-OLA conjugates (HA-OLA6 and HA-OLA8) and new medicines i.e., VCM loaded OCA vesicles and VCM-PS6. These novel nano-systems were able to enhance the antibacterial activity of encapsulated antibiotic (VCM) against MRSA. Therefore, these nano-systems can stimulate pharmaceutical industries to manufacture cost-effective superior medicines.

Improved patient therapy and disease treatment: The newly designed VCM loaded OCA vesicles and VCM-PS6 nano systems were formulated successfully with improved antibacterial potential against *S. aureus* and MRSA. These novel nano-systems lowered the MIC of the loaded drugs significantly, and can effectively control the infection with reduced dosing frequency without affecting therapeutic outcomes. These findings therefore prove the potential of these novel nano-systems in improving patient therapy and treatment of bacterial infections, and thereby ultimately improving quality of patients as well as saving lives.

Creation of new knowledge to the scientific community: The various studies and their findings have contributed to the pharmaceutical sciences knowledge database in several ways. These include the following:

- New synthetic pathways, characterisation and determination of the toxicity profiles of novel FCAs and HA-OLA conjugates were developed. The *in vitro* and *in vivo* evaluation of drug loaded nano-systems can add to the conception of new knowledge.

- Formulation and process parameters of VCM loaded OCA vesicles and VCM-PS6 were identified using various experimental techniques.

- By combining novel materials having intrinsic antibacterial activity and an antibiotic, a strategy for achieving synergistic antibacterial activity in nano-vesicular form was described.

- In the case of VCM loaded OCA vesicles study, the results generated from antimicrobial activity through *in vitro* MIC determination and *in vivo* antibacterial infection models successfully showed *in vitro* and *in vivo* correlation of developed novel nano-drug delivery system.

Stimulation of new research: The research findings of the various studies and the successful development of VCM loaded OCA vesicles and VCM-PS6 can stimulate new research areas, including the following:

- The newly synthesized FCAs and HA-OLA conjugates can be utilized for delivering other classes of drugs to treat various disease conditions, such as cancer, HIV/AIDS, fungal infections, gene therapy related diseases, metabolic diseases etc.

- Besides bacterial infections, VCM loaded OCA vesicles and VCM-PS6 can also assist to treat other diseases that are associated with bacterial infections.

- The ability of newly developed FCAs and HA-OLA conjugates to produce synergism with antibiotics against bacterial strains could stimulate research to develop such multifunctional nano-systems to treat bacterial infections.

- Delivery of antibiotics using an antibacterial nano-carrier can contribute to combination therapy to combat bacterial infections more effectively.

6.3 Recommendations for future studies

Although, VCM loaded OCA vesicles and VCM-PS6 displayed great prospects as novel nano-drug delivery systems to eradicate the problem of bacterial resistance, additional studies are

necessary to further explore and improve their potential to ensure eventual regulatory approval for patient use.

The following studies are proposed:

- In the case of VCM loaded OCA vesicles, there is a need for MD simulations to show the binding affinity of OCA to negatively charged bacterial membranes.
- Quaternary ammonium compounds have also been reported as fungicides, therefore, FCAs synthesized in this study can be tested for their anti-fungal effects. Further, these compounds can also be used as nano-carriers for anti-fungal drugs.
- As oppositely charged molecules are known to make various complexes, the positive charge of FCAs can be utilized to prepare other nano-based systems such as nanoplexes, comb-like structures etc.
- The successfully developed vesicles and polymersomes for vancomycin delivery can be loaded with different classes of antibiotics and tested against various bacterial strains to evaluate their synergism and advantages over different antibiotics.
- Simultaneous delivery of multiple antibiotics from these nano-systems can be explored to achieve enhanced and synergistic activities.
- Encapsulation of multiple hydrophilic as well as hydrophobic drugs in these vesicular nano-systems can be explored.
- Application of these amphiphiles as surfactants to stabilize other nanoparticulated systems such as, solid lipid nanoparticles, polymeric nanoparticles etc, can be studied.
- Hyaluronic acid has specificity towards certain cancer cells, therefore, HA-OLA conjugates can be explored for their cancer targeting ability. Furthermore, anticancer drugs can be loaded into HA-OLA nano-system for enhanced and improved therapeutic activity.
- Long-term stability studies using ICH guidelines to assess the physical and chemical stability of optimised formulations must be undertaken to confirm their shelf life.

- *In vivo* intravenous infection model, bioavailability and pharmacokinetic studies followed by clinical trials on both the developed nano-systems could be performed in order to achieve approval for market introduction.

- *In vivo* acute, intermediate and long-term toxicity study models can be performed to determine the full toxicological profile of the material and the formulations reported in this study.

- A method for the bulk production of the nano-systems presented in this study could be developed in order to enable their applications for pharmaceutical industries.

6.4 Conclusion

The findings of this study therefore specifically demonstrate the potential of the newly developed FCAs and HA-OLA conjugates as nano-carriers having inherent antibacterial activity as well as their drug delivery potential, for improving the treatment of *S. aureus* and MRSA infections. This current research has therefore made significant contributions to nano-based approaches to overcome limitations of current/conventional dosage forms. The study further directed way towards synthesis of novel antibacterial amphiphiles to develop multifunctional nano-systems to treat bacterial infections. The understanding of novel antibacterial materials and nano-technology to address the current global antibiotic drug therapy crisis will be dependent on future intensive and multidisciplinary research. This strategic approach will play a vital role towards improving treatment of bacterial infections as well as other diseases that are associated with bacterial infections, thereby saving lives and improving the quality of lives of communities.

Supplementary material for Experimental paper 1

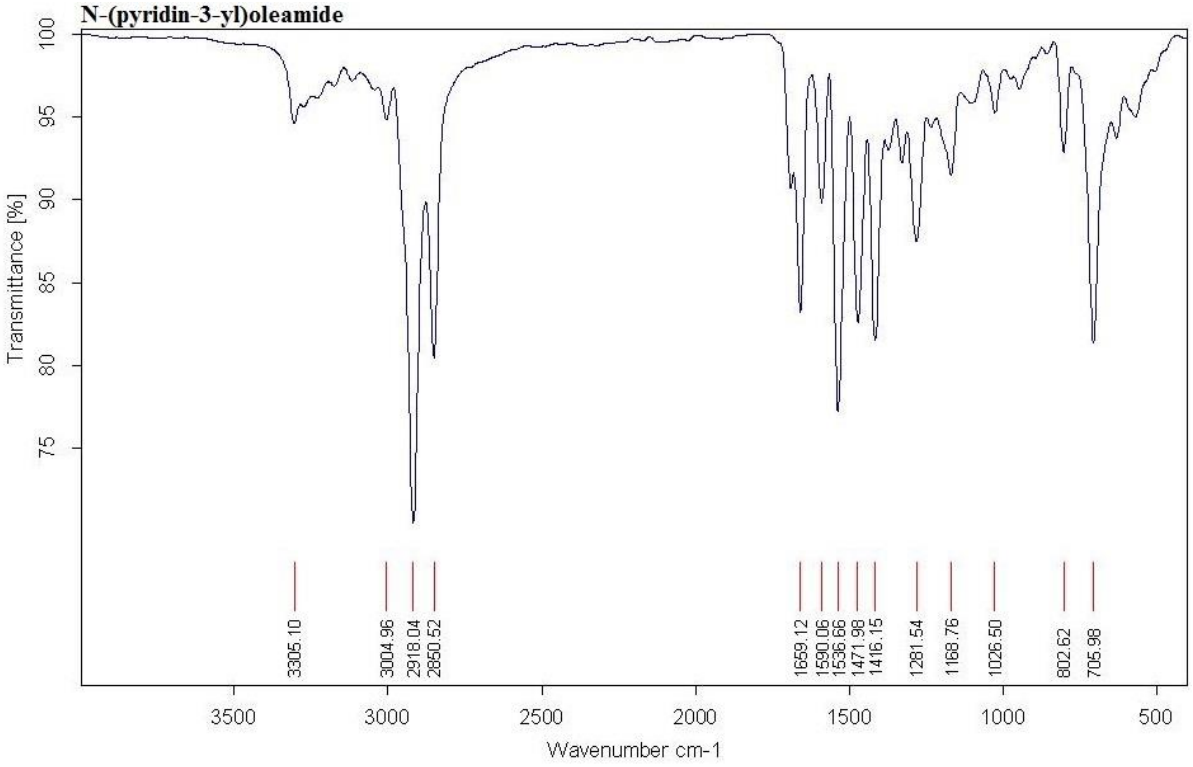

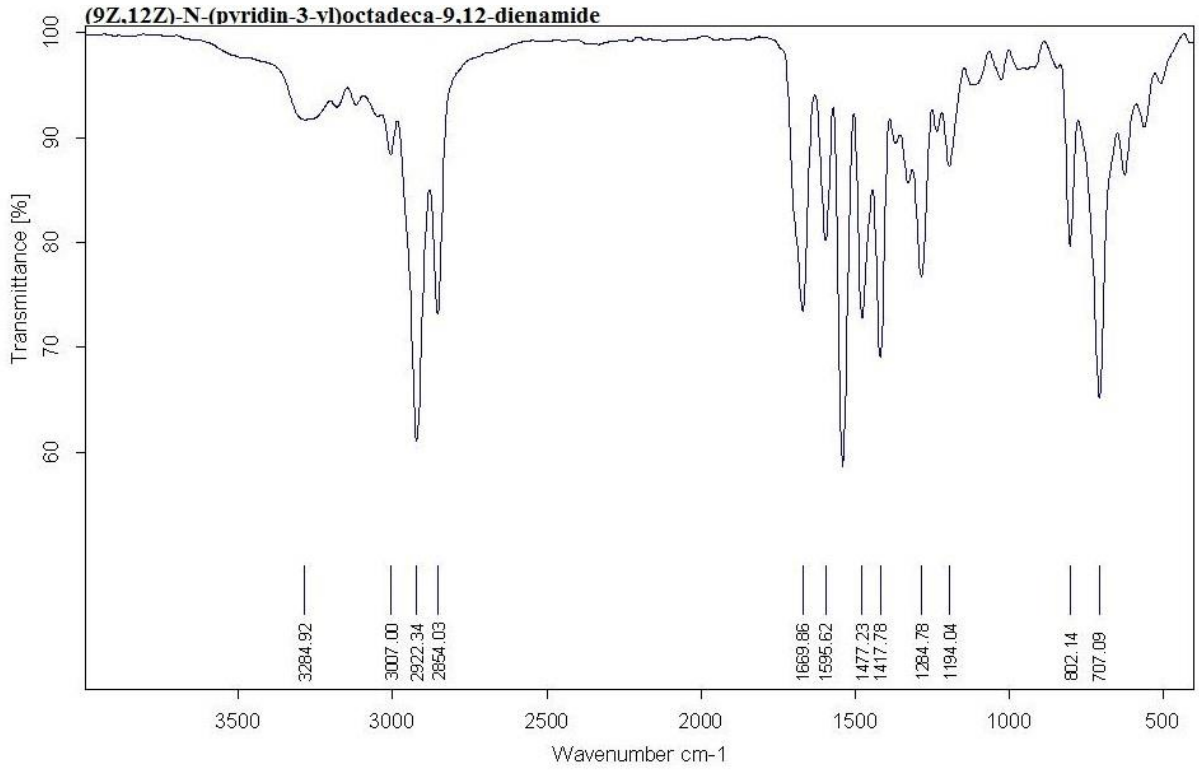

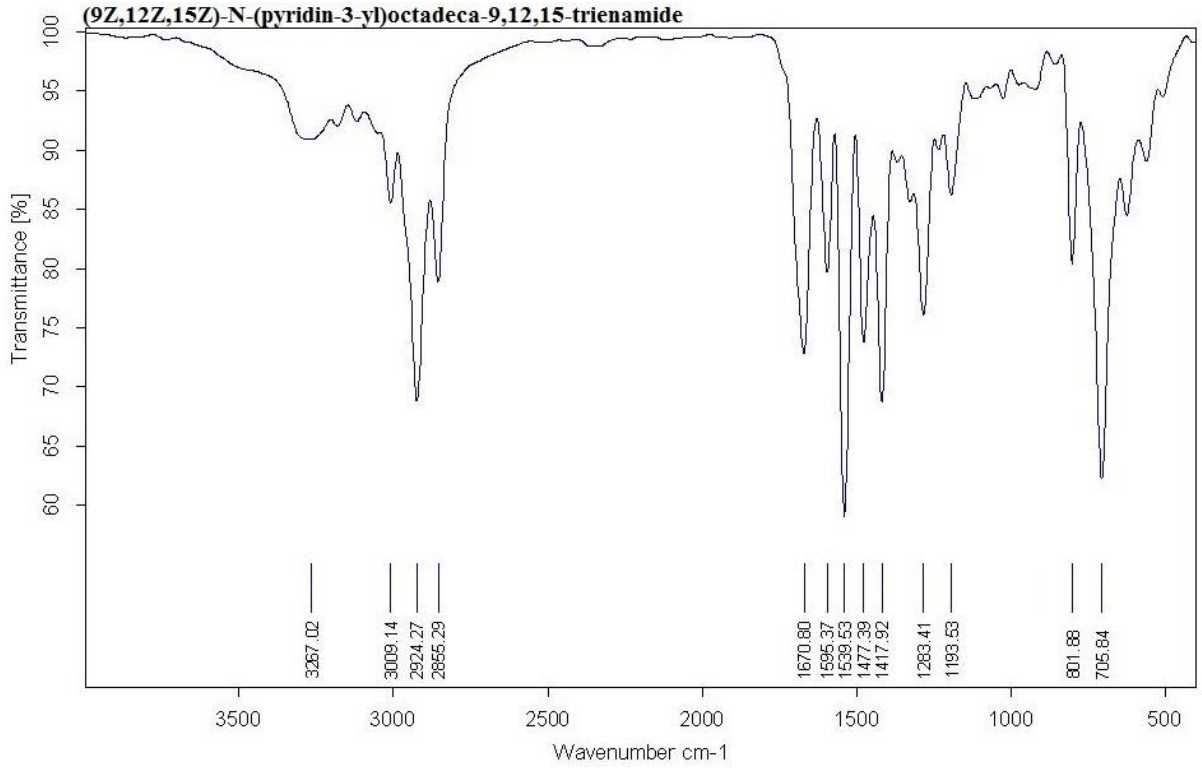
(9Z,12Z,15Z)-N-(pyridin-3-yl)octadeca-9,12,15-trienamide
Transmittance [%]
100
95
90
85
80
75
70
65
60
3267.02
3009.14
2924.27
2855.29
1670.80
1595.37
1539.53
1477.39
1417.92
1283.41
1193.53
801.88
705.84
3500
3000
2500
2000
1500
1000
500
Wavenumber cm-1

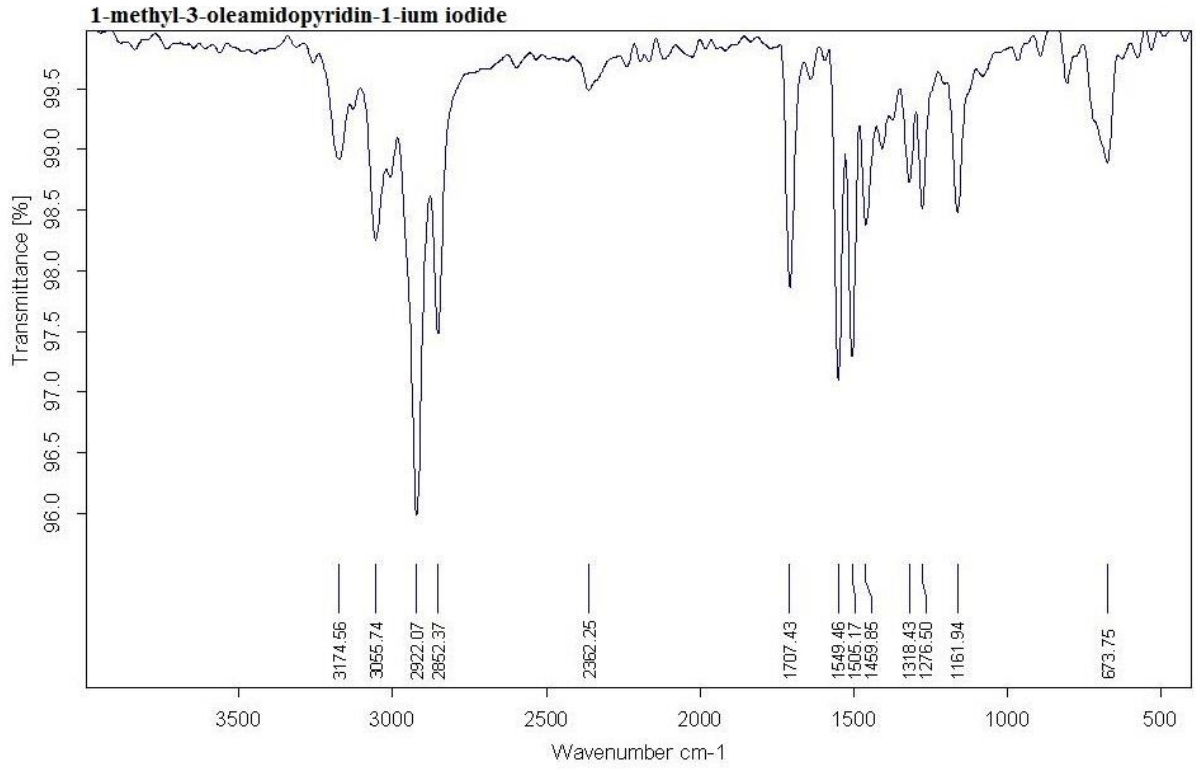
1-methyl-3-oleamidopyridin-1-ium iodide
Transmittance [%]
99.5
99.0
98.5
98.0
97.5
97.0
96.5
96.0
3174.56
3055.74
2922.07
2852.37
2362.25
1707.43
1549.46
1505.17
1459.85
1318.43
1276.50
1161.94
673.75
3500
3000
2500
2000
1500
1000
500
Wavenumber cm-1

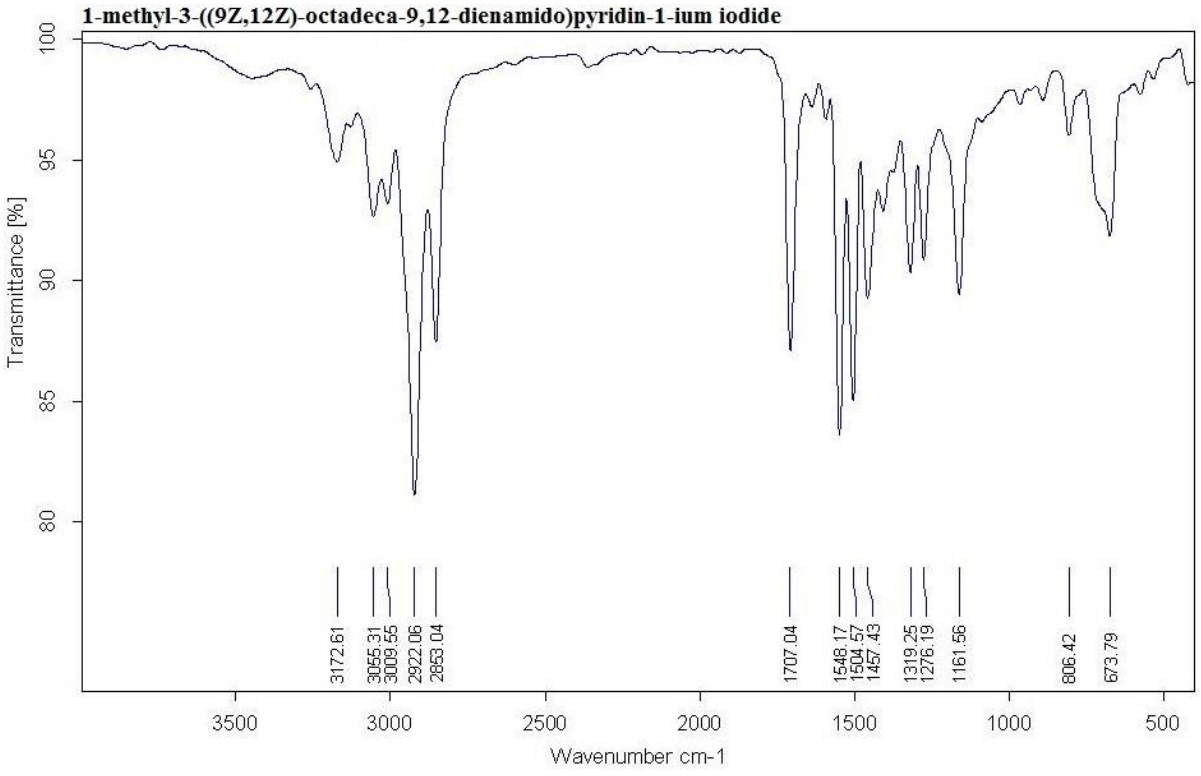
1-methyl-3-((9Z,12Z)-octadeca-9,12-dienamido)pyridin-1-ium iodide
Transmittance [%]
100
95
90
85
80
3172.61
3055.31
3009.55
2922.06
2853.04
1707.04
1548.17
1504.57
1457.43
1319.25
1276.19
1161.56
806.42
673.79
3500
3000
2500
2000
1500
1000
500
Wavenumber cm-1

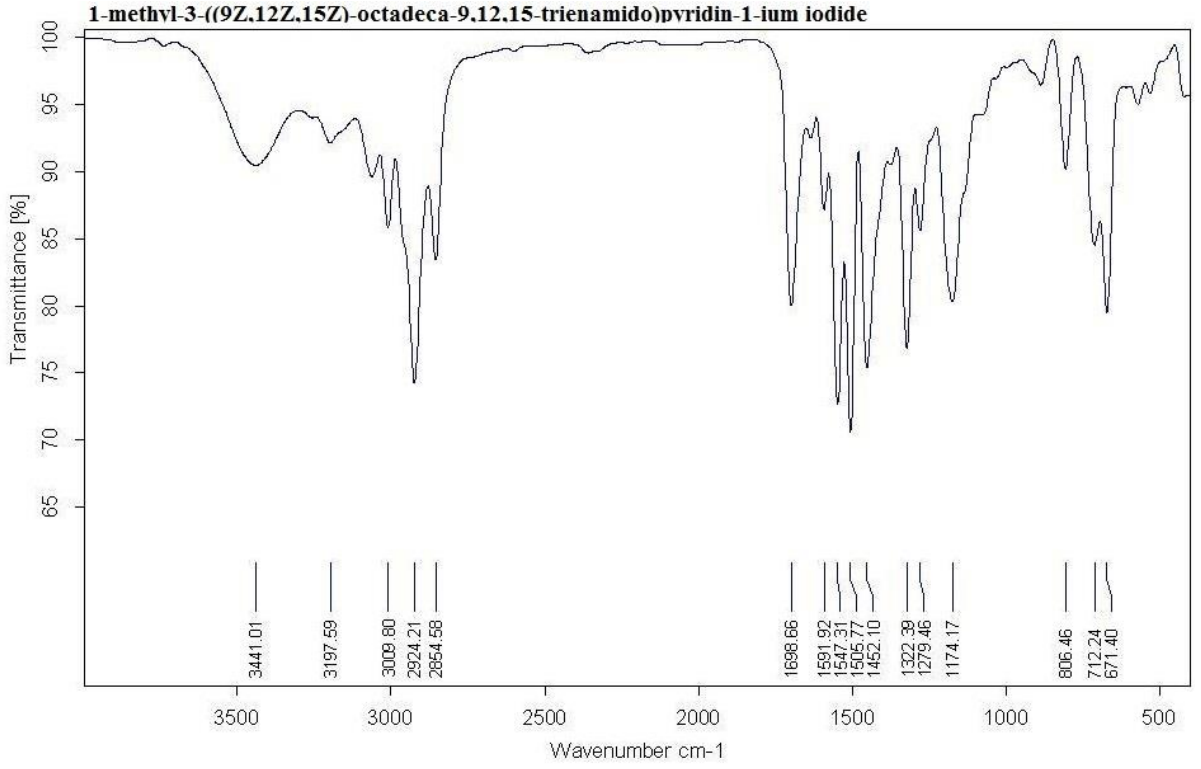
1-methyl-3-((9Z,12Z,15Z)-octadeca-9,12,15-trienamido)pyridin-1-ium iodide
Transmittance [%]
100
95
90
85
80
75
70
65
3441.01
3197.59
3009.80
2924.21
2854.58
1698.66
1591.92
1547.31
1505.77
1452.10
1322.39
1279.46
1174.17
806.46
712.24
671.40
3500
3000
2500
2000
1500
1000
500
Wavenumber cm-1

N-(pyridin-3-yl)oleamide

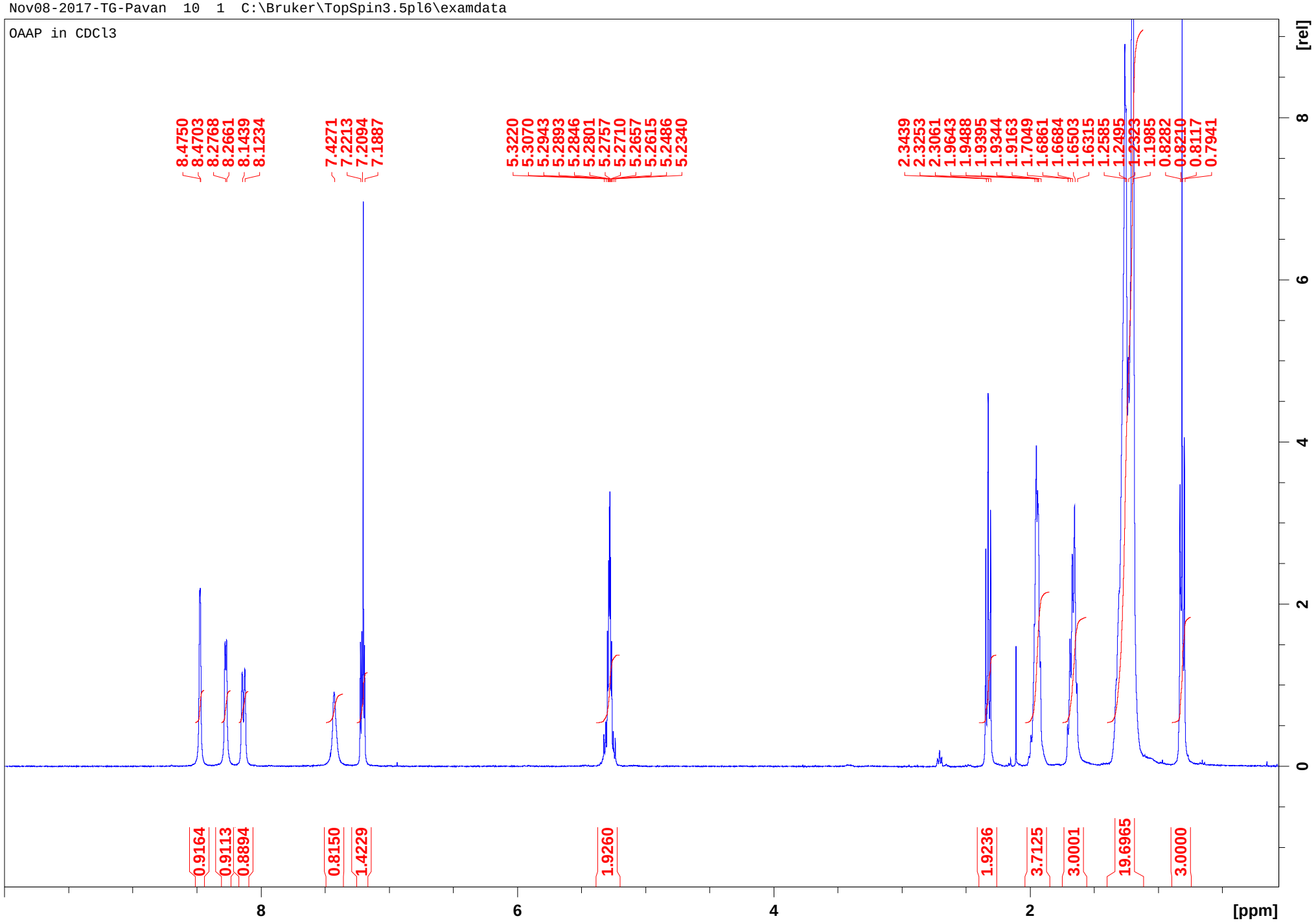

(9Z,12Z)-N-(pyridin-3-yl)octadeca-9,12-dienamide

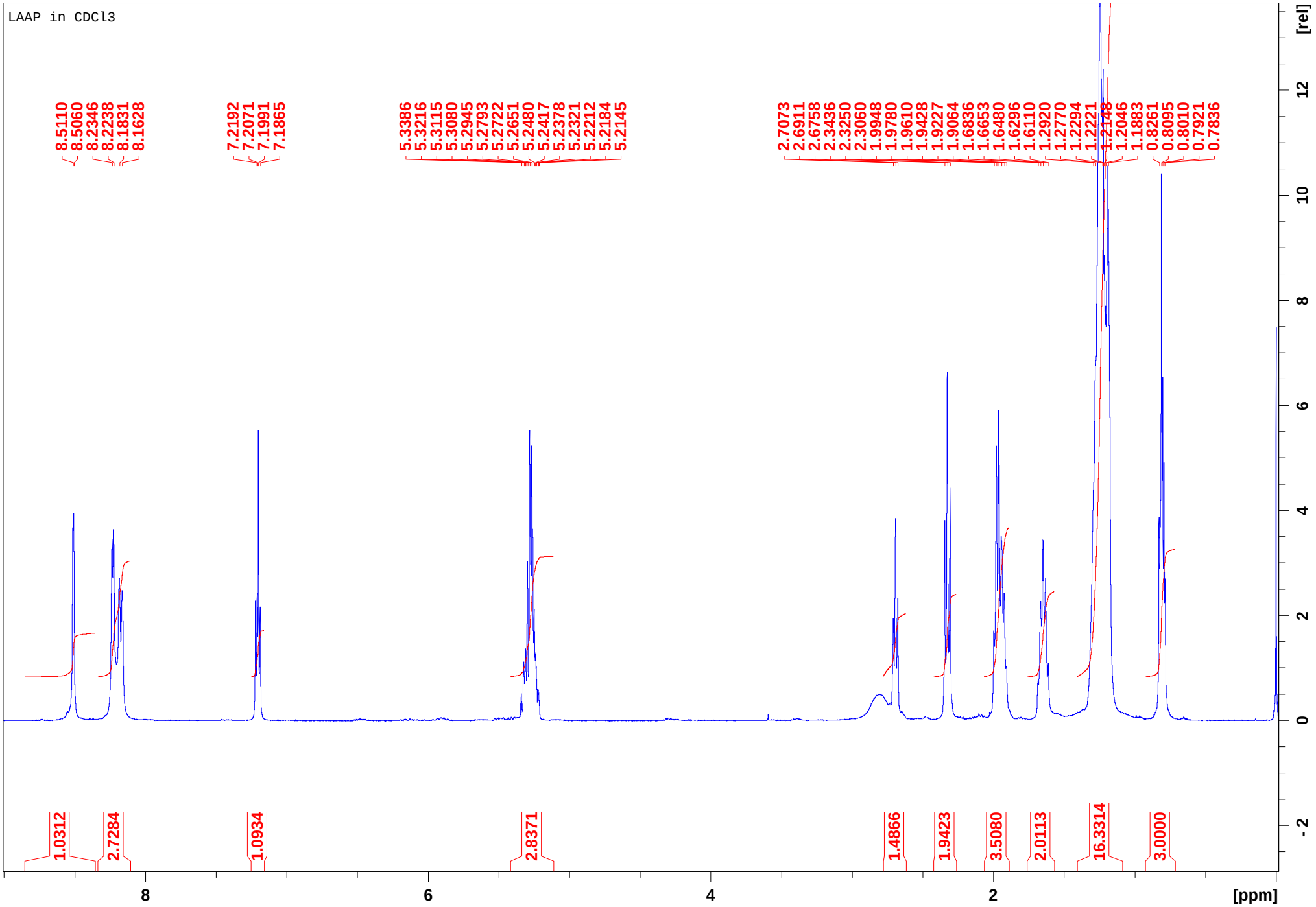

(9Z,12Z,15Z)-N-(pyridin-3-yl)octadeca-9,12,15-trienamide

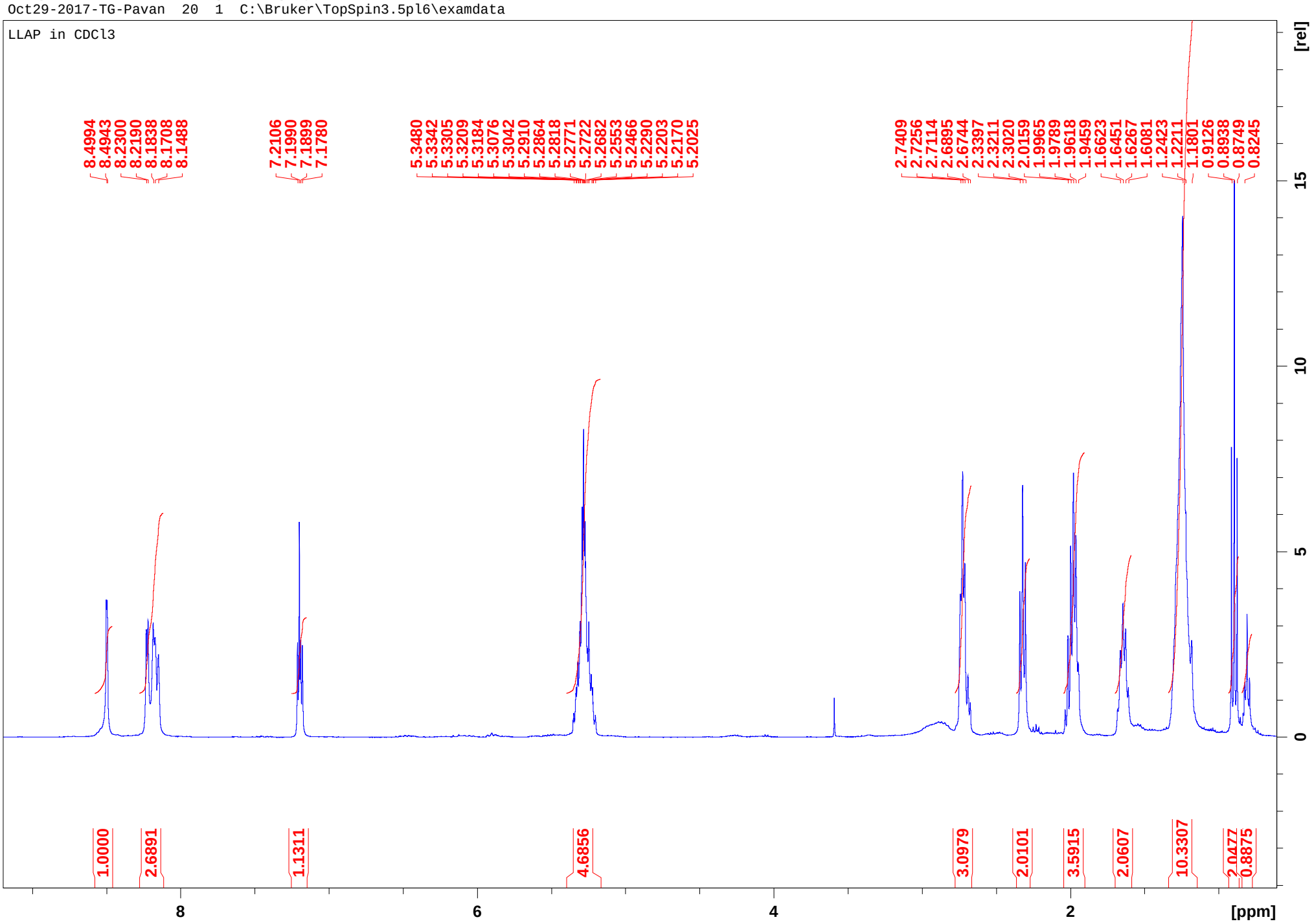

1-methyl-3-oleamidopyridin-1-ium iodide

Nov08-2017-TG-Pavan 20 1 C:\Bruker\TopSpin3.5pl6\examdata

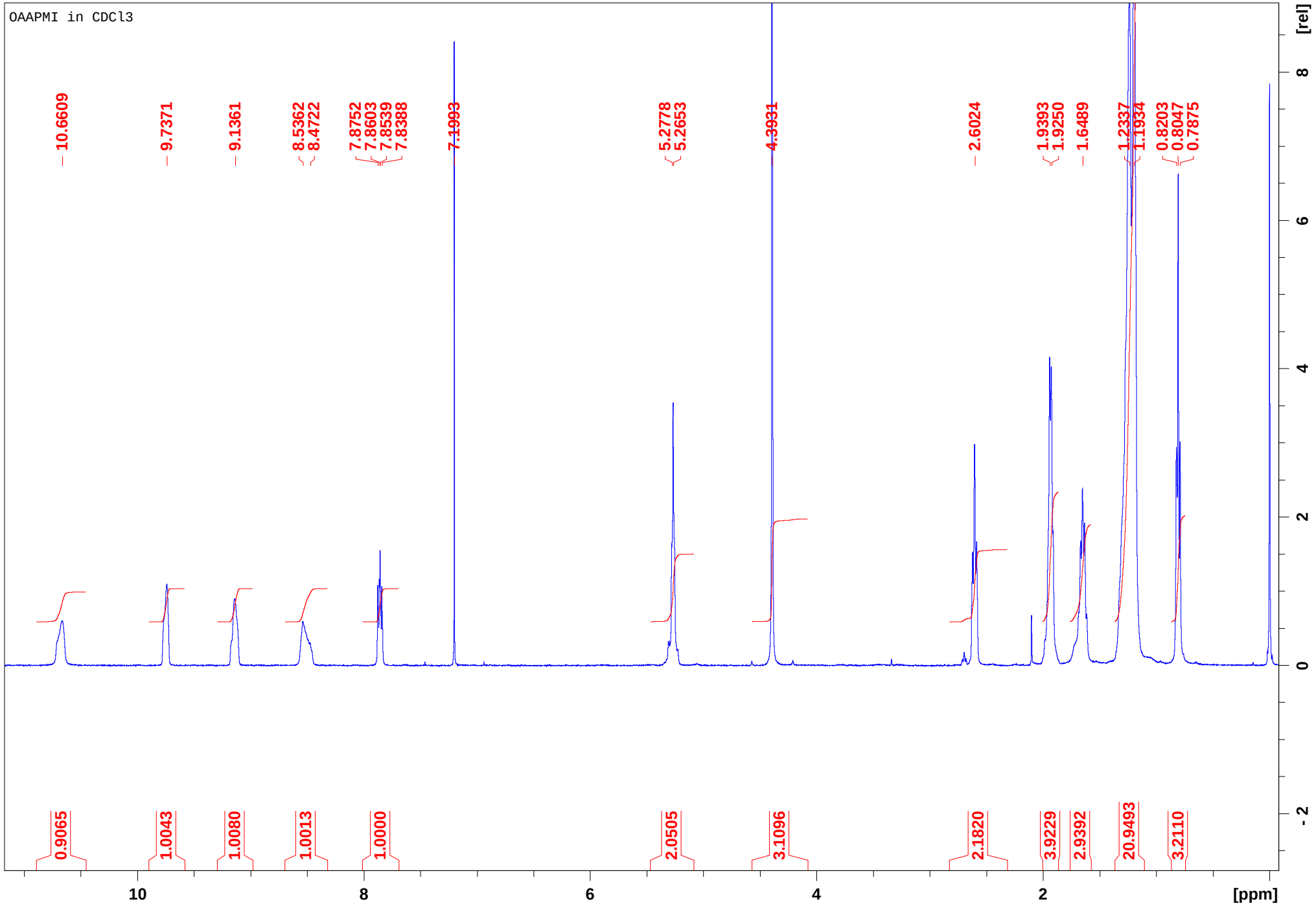

1-methyl-3-((9Z,12Z)-octadeca-9,12-dienamido)pyridin-1-ium iodide

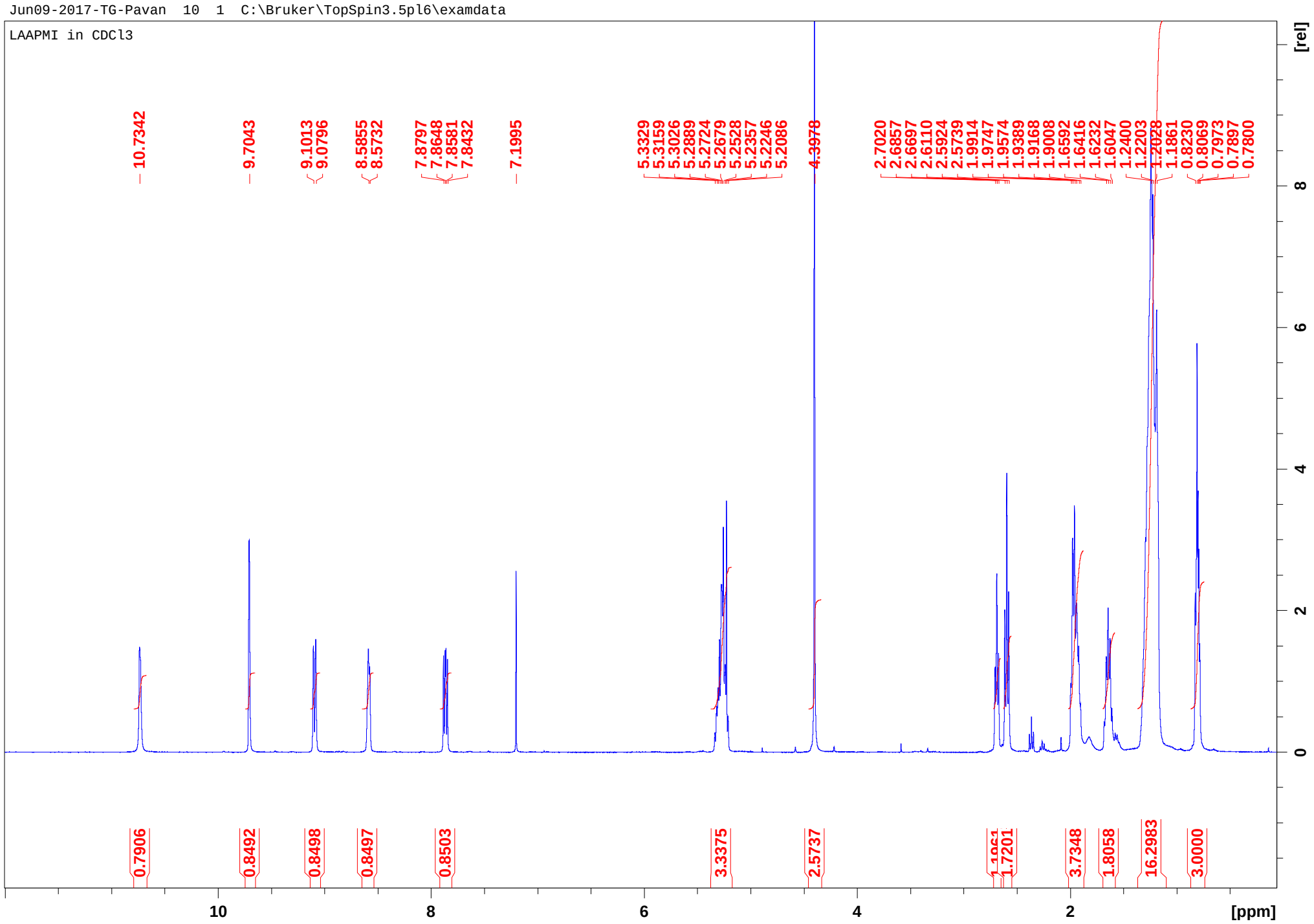

1-methyl-3-((9Z,12Z,15Z)-octadeca-9,12,15-trienamido)pyridin-1-ium iodide

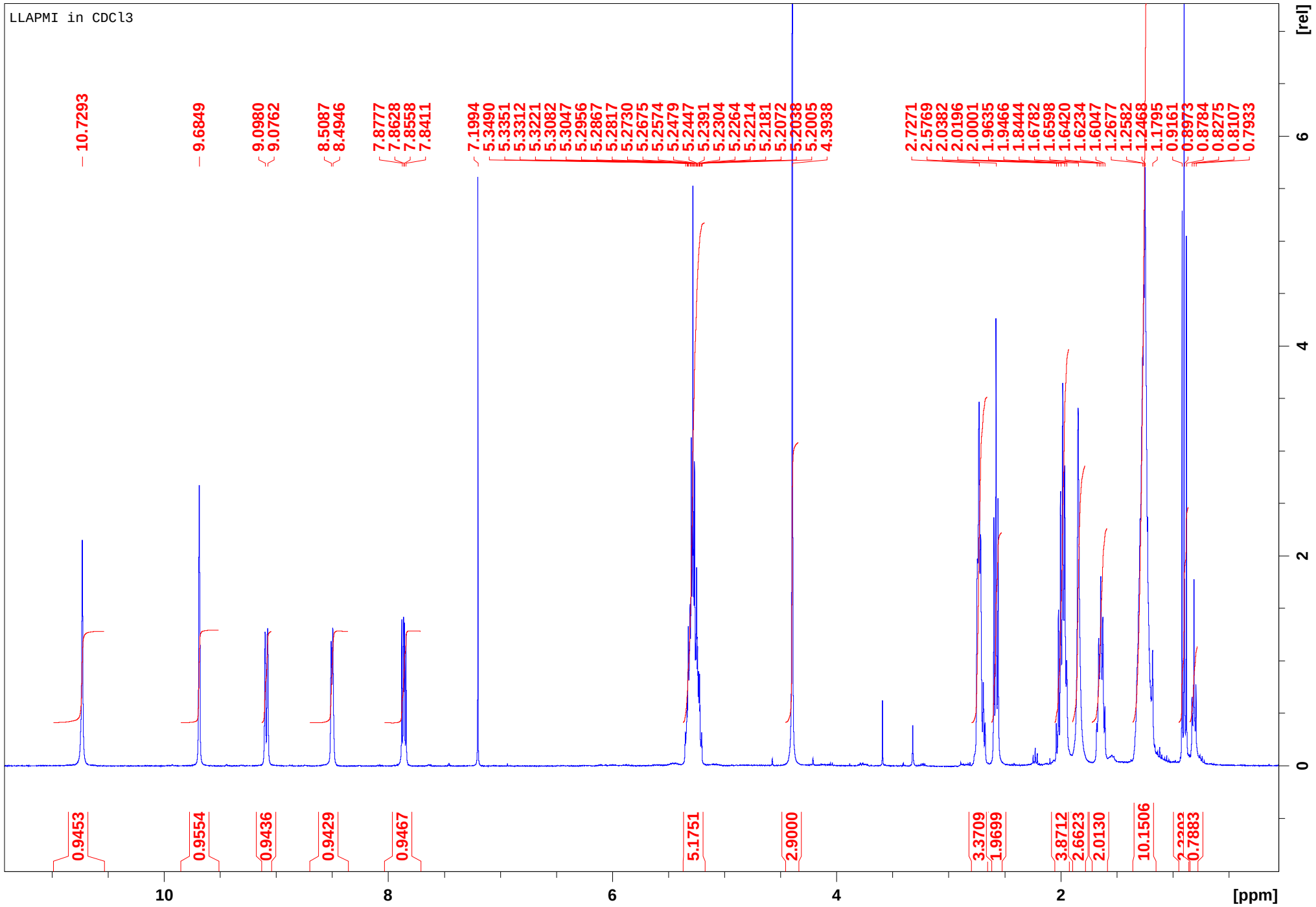

N-(pyridin-3-yl)oleamide

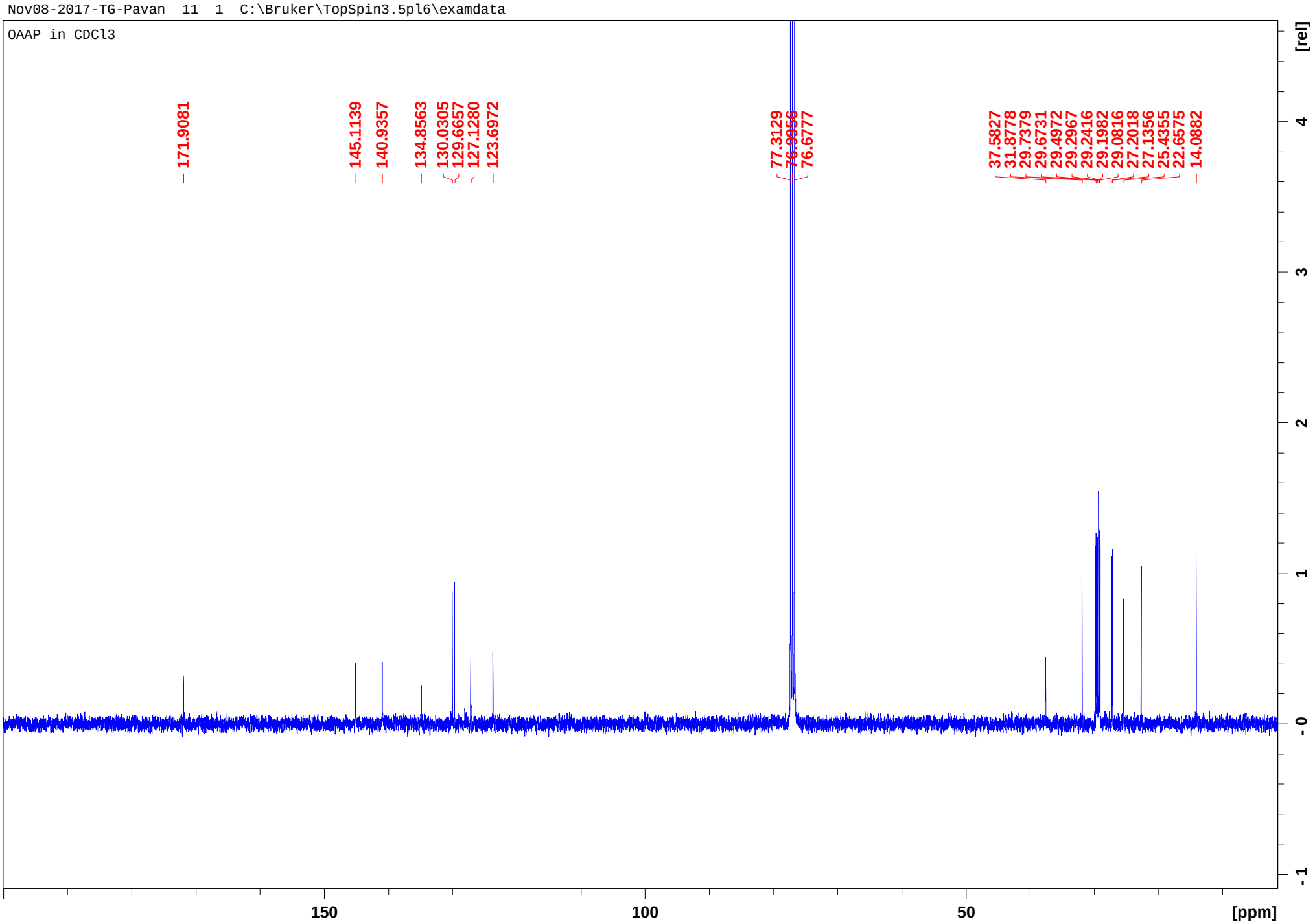

(9Z,12Z)-N-(pyridin-3-yl)octadeca-9,12-dienamide

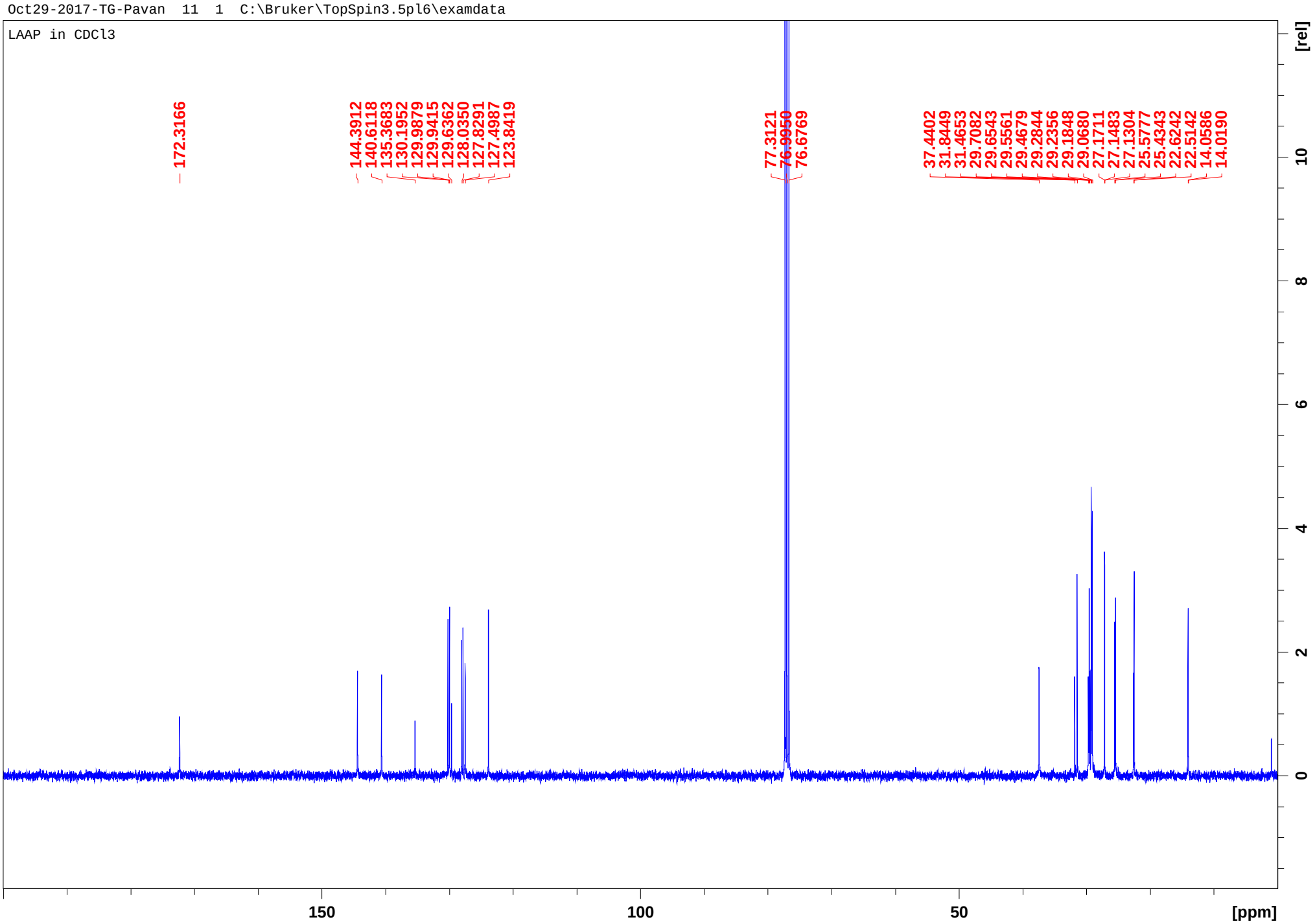

(9Z,12Z,15Z)-N-(pyridin-3-yl)octadeca-9,12,15-trienamide

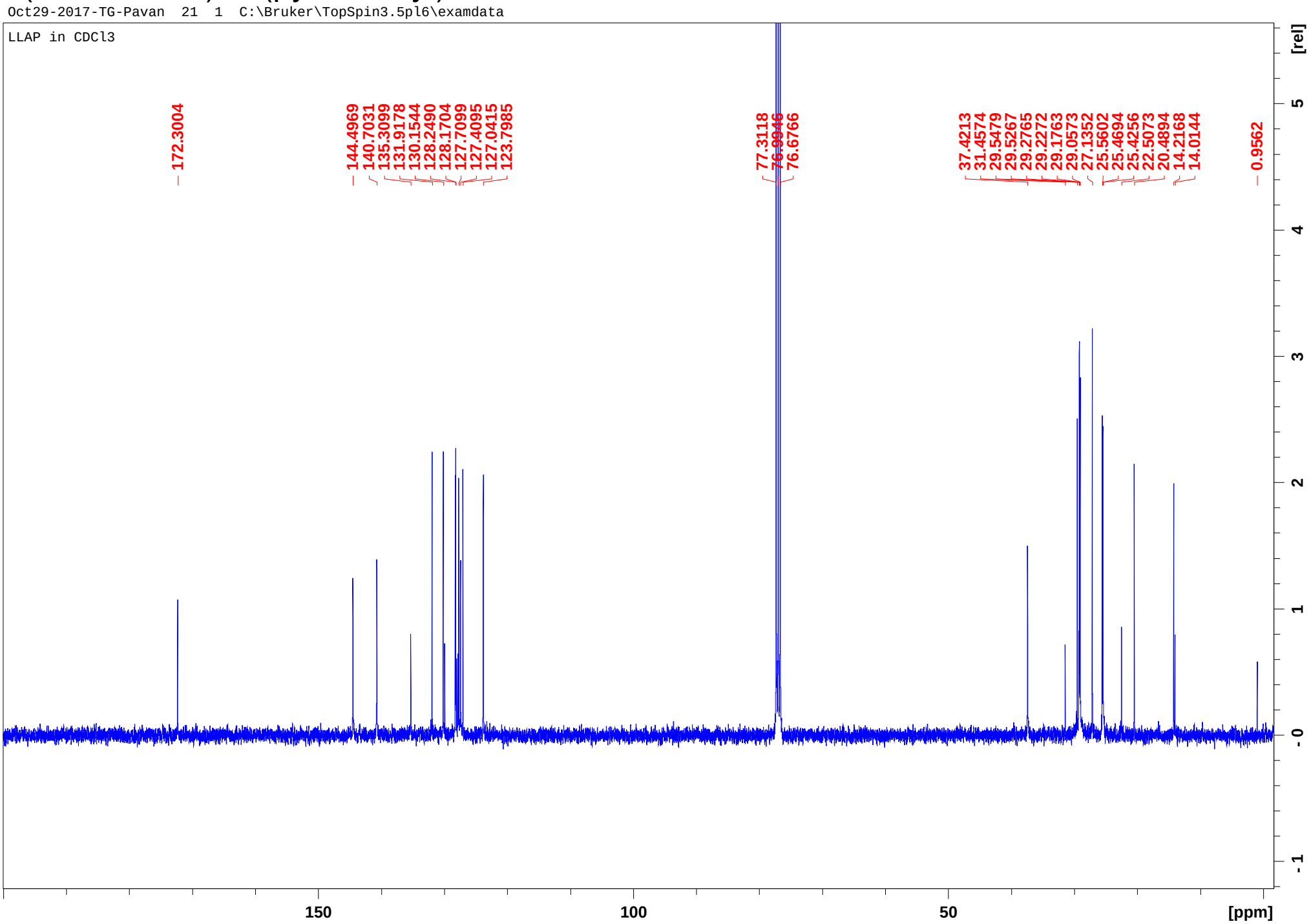

1-methyl-3-oleamidopyridin-1-ium iodide

Nov08-2017-TG-Pavan 21 1 C:\Bruker\TopSpin3.5pl6\examdata

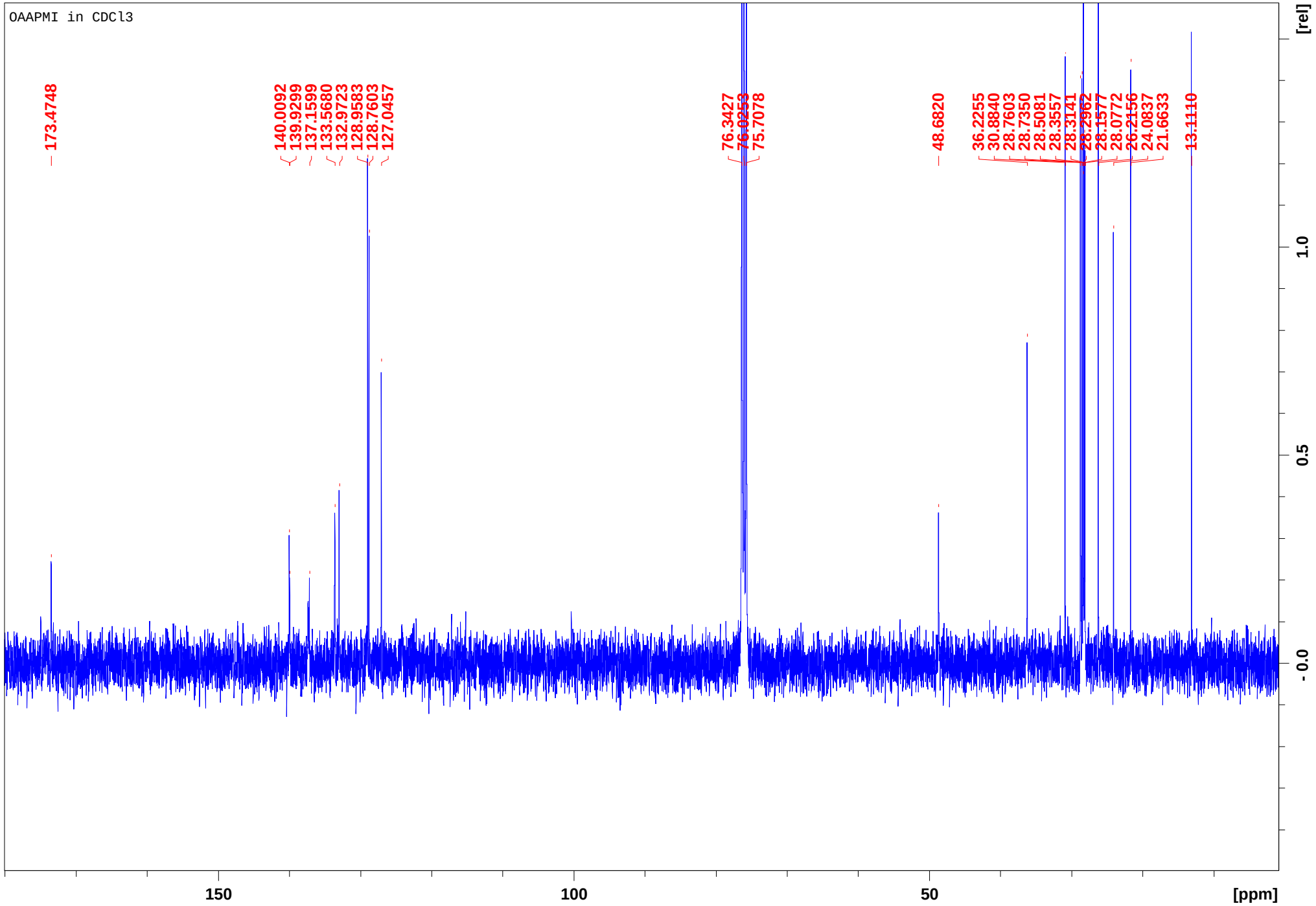

1-methyl-3-((9Z,12Z)-octadeca-9,12-dienamido)pyridin-1-ium iodide

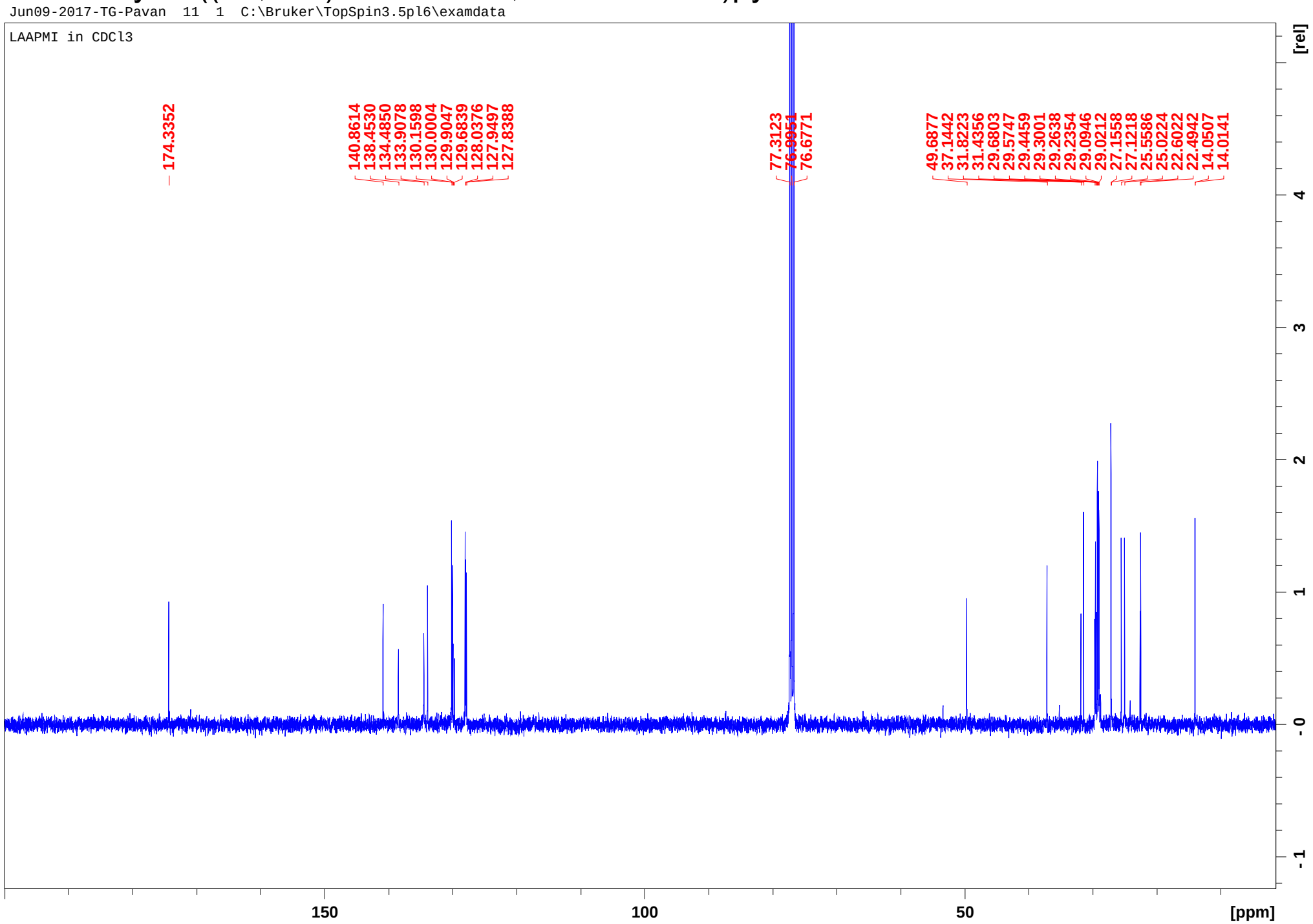

1-methyl-3-((9Z,12Z,15Z)-octadeca-9,12,15-trienamido)pyridin-1-ium iodide

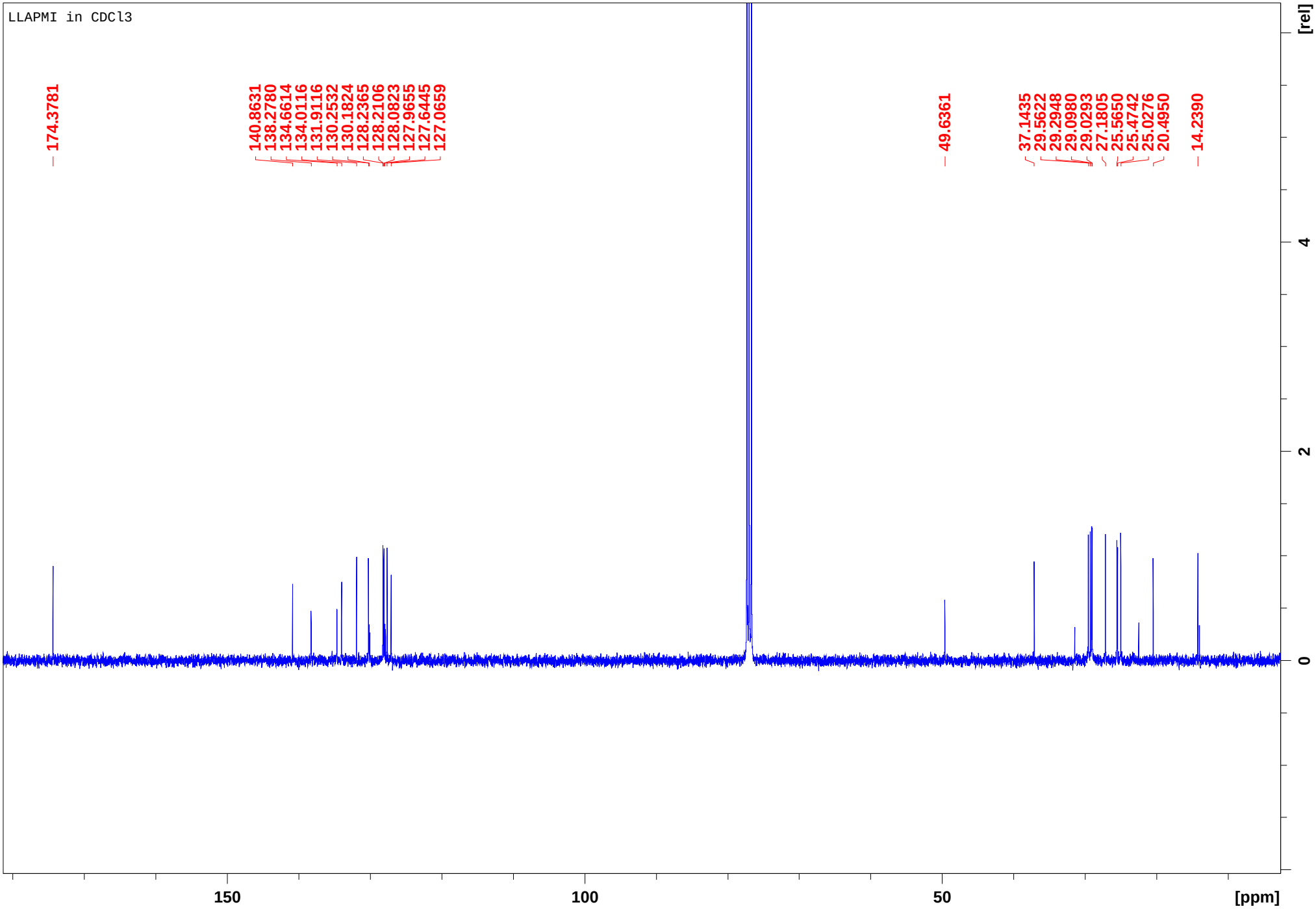

Single Mass Analysis

Tolerance = 5.0 PPM / DBE: min = -1.5, max = 50.0
Element prediction: Off
Number of isotope peaks used for i-FIT = 2

Monoisotopic Mass, Even Electron Ions
13 formula(e) evaluated with 1 results within limits (up to 20 closest results for each mass)
Elements Used:
C: 20-25 H: 35-40 N: 0-5 O: 0-5 Na: 1-1

P1 45 (1.483) Cm (1:61)
TOF MS ES+

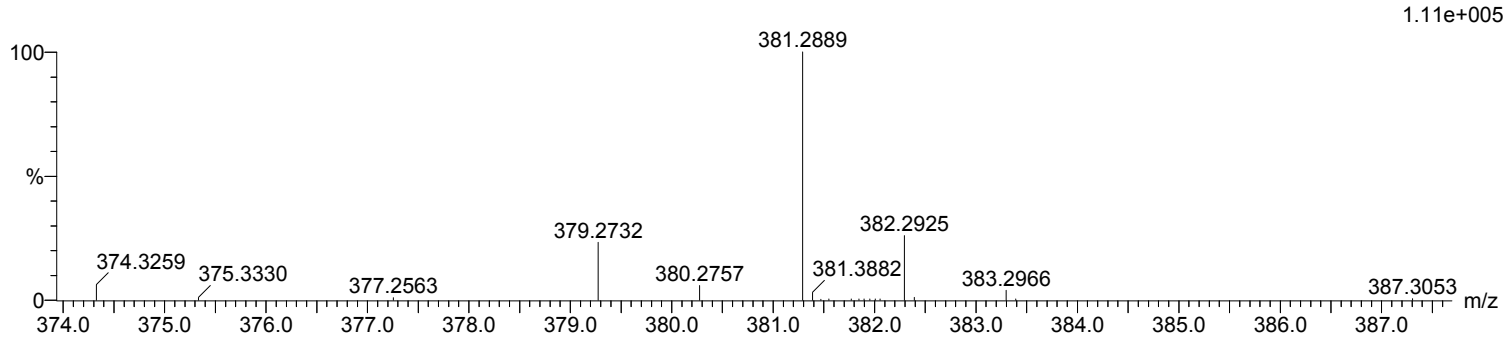

Minimum:				-1.5			
Maximum:		5.0	5.0	50.0			
Mass	Calc. Mass	mDa	PPM	DBE	i-FIT	i-FIT (Norm)	Formula
381.2889	381.2882	0.7	1.8	5.5	139.3	0.0	C23 H38 N2 O Na

Single Mass Analysis

Tolerance = 5.0 PPM / DBE: min = -1.5, max = 50.0
Element prediction: Off
Number of isotope peaks used for i-FIT = 2

Monoisotopic Mass, Even Electron Ions
14 formula(e) evaluated with 1 results within limits (up to 20 closest results for each mass)
Elements Used:
C: 20-25 H: 35-40 N: 0-5 O: 0-5 Na: 1-1

P2 11 (0.338) Cm (1:61)
TOF MS ES+

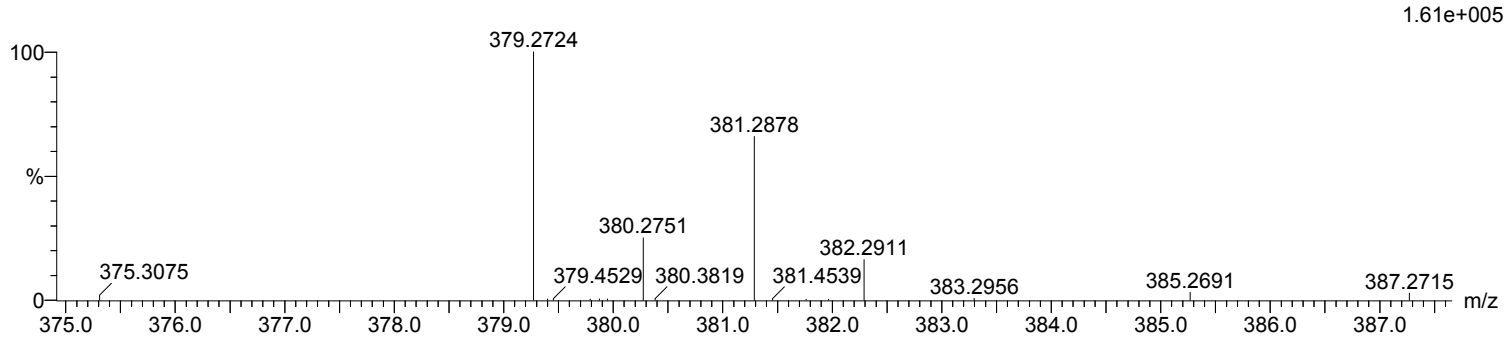

Minimum:				-1.5			
Maximum:		5.0	5.0	50.0			
Mass	Calc. Mass	mDa	PPM	DBE	i-FIT	i-FIT (Norm)	Formula
379.2724	379.2725	-0.1	-0.3	6.5	91.6	0.0	C23 H36 N2 O Na

Single Mass Analysis

Tolerance = 5.0 PPM / DBE: min = -1.5, max = 50.0
Element prediction: Off
Number of isotope peaks used for i-FIT = 2

Monoisotopic Mass, Even Electron Ions
14 formula(e) evaluated with 1 results within limits (up to 20 closest results for each mass)
Elements Used:
C: 20-25 H: 30-35 N: 0-5 O: 0-5 Na: 1-1

P3 45 (1.485) Cm (1:61)
TOF MS ES+

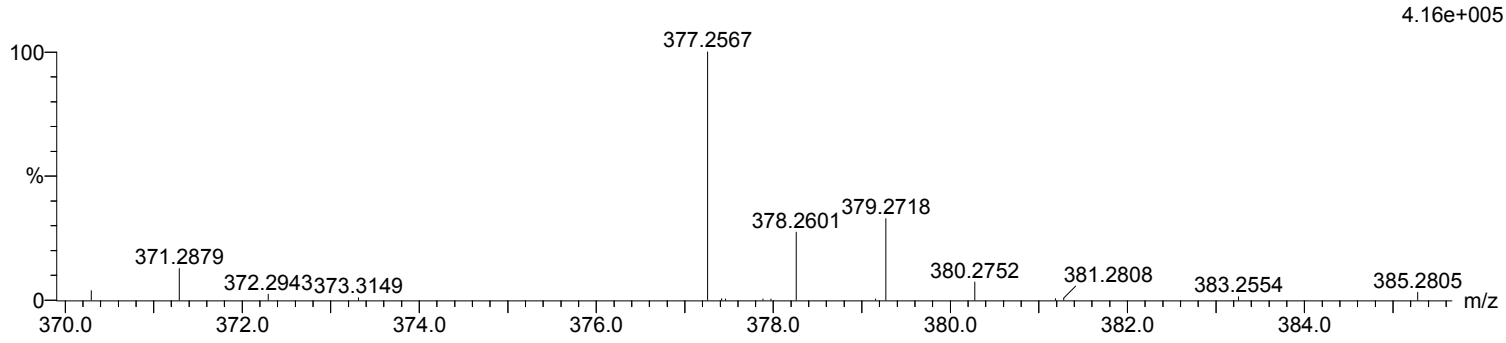

Minimum:				-1.5			
Maximum:		5.0	5.0	50.0			
Mass	**Calc. Mass**	**mDa**	**PPM**	**DBE**	**i-FIT**	**i-FIT (Norm)**	**Formula**
377.2567	377.2569	-0.2	-0.5	7.5	70.6	0.0	C23 H34 N2 O Na

Single Mass Analysis

Tolerance = 5.0 PPM / DBE: min = -1.5, max = 100.0
Element prediction: Off
Number of isotope peaks used for i-FIT = 2

Monoisotopic Mass, Even Electron Ions
14 formula(e) evaluated with 1 results within limits (up to 20 best isotopic matches for each mass)
Elements Used:
C: 20-25 H: 40-45 N: 0-5 O: 0-5

PW-1 15 (0.473) Cm (1:61)
TOF MS ES+

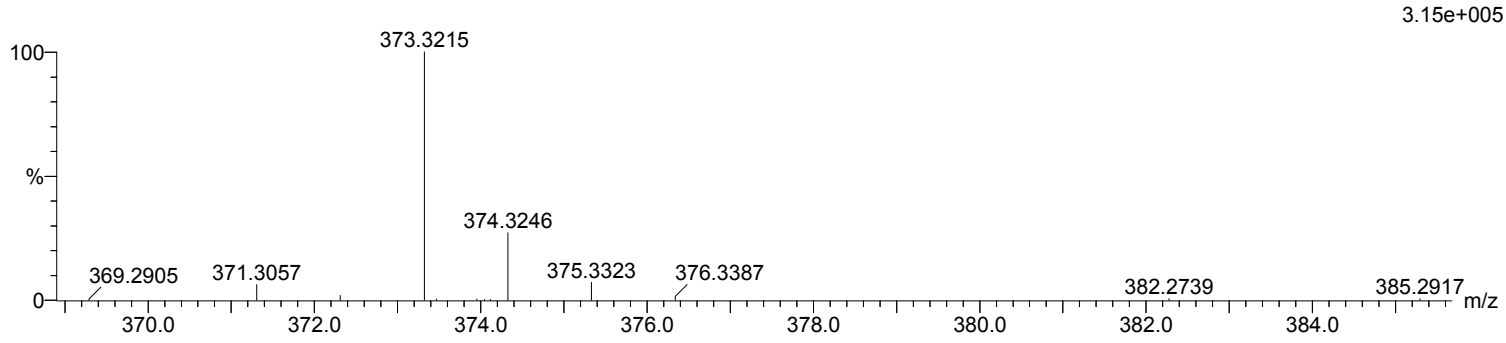

Minimum:				-1.5			
Maximum:		5.0	5.0	100.0			
Mass	Calc. Mass	mDa	PPM	DBE	i-FIT	i-FIT (Norm)	Formula
373.3215	373.3219	-0.4	-1.1	5.5	69.9	0.0	C24 H41 N2 O

Single Mass Analysis

Tolerance = 5.0 PPM / DBE: min = -1.5, max = 100.0
Element prediction: Off
Number of isotope peaks used for i-FIT = 2

Monoisotopic Mass, Even Electron Ions
13 formula(e) evaluated with 1 results within limits (up to 20 best isotopic matches for each mass)
Elements Used:
C: 20-25 H: 35-40 N: 0-5 O: 0-5

PW-2 14 (0.439) Cm (1:61)
TOF MS ES+

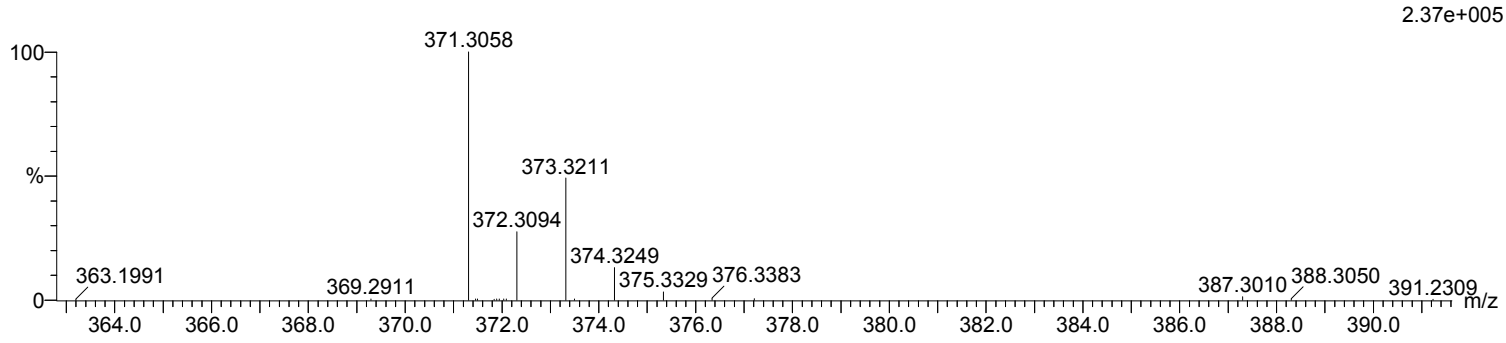

Minimum:				-1.5			
Maximum:		5.0	5.0	100.0			
Mass	Calc. Mass	mDa	PPM	DBE	i-FIT	i-FIT (Norm)	Formula
371.3058	371.3062	-0.4	-1.1	6.5	105.4	0.0	C24 H39 N2 O

1-methyl-3-((9Z,12Z,15Z)-octadeca-9,12,15-trienamido)pyridin-1-ium iodide

Single Mass Analysis

Tolerance = 5.0 PPM / DBE: min = -1.5, max = 100.0
Element prediction: Off
Number of isotope peaks used for i-FIT = 2

Monoisotopic Mass, Even Electron Ions
15 formula(e) evaluated with 1 results within limits (up to 20 best isotopic matches for each mass)
Elements Used:
C: 20-25 H: 35-40 N: 0-5 O: 0-5

PW-3 2 (0.034) Cm (1:61)
TOF MS ES+

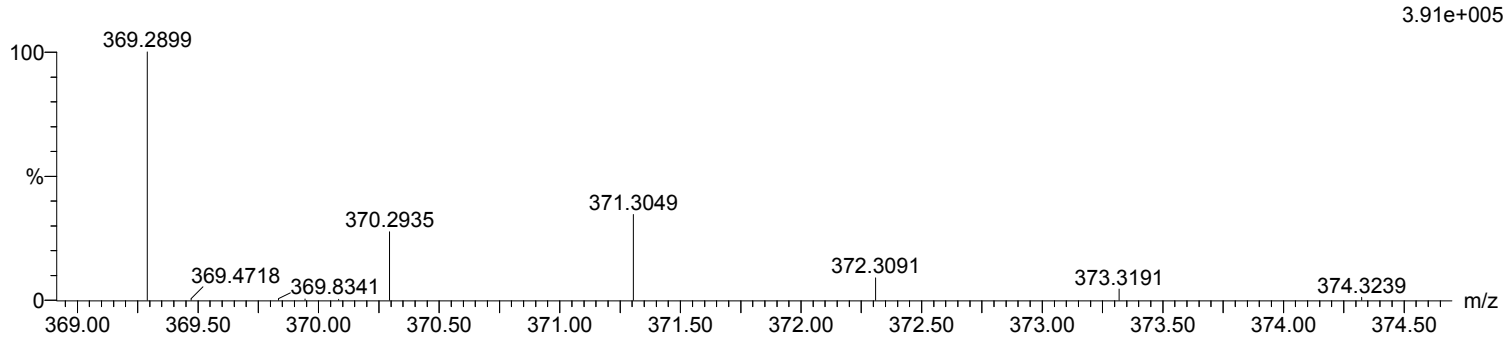

Minimum:				-1.5			
Maximum:		5.0	5.0	100.0			
Mass	Calc. Mass	mDa	PPM	DBE	i-FIT	i-FIT (Norm)	Formula
369.2899	369.2906	-0.7	-1.9	7.5	70.6	0.0	C24 H37 N2 O

Supplementary material for Experimental paper 2

Table S1. FIC index interpretation

Index	Synergy	Additive	Indifference	Antagonism
FIC	≤ 0.5	> 0.5-1	> 1 to < 2	≥ 2

Table S2. Effect of various concentrations of VCM and HA-OLA8 on formulation optimization (n = 3)

VCM	**HA-OLA8**	**Size (nm)**	**PDI**	**ZP**	**%EE**
5	10	196.1 ± 4.99	0.261 ± 0.01	-18.8 ± 2.05	26.1 ± 3.14
5	20	211.5 ± 3.48	0.247 ± 0.01	-15.1 ± 1.24	33.8 ± 1.01
5	40	276.8 ± 2.05	0.289 ± 0.01	-18.3 ± 1.02	29.1 ± 0.84
10	10	198.6 ± 5.35	0.277 ± 0.01	-18.7 ± 2.22	29.4 ± 4.52
10	20	209.6 ± 2.96	0.240 ± 0.01	-20.1 ± 1.21	27.7 ± 2.22
10	40	271.5 ± 1.79	0.283 ± 0.01	-17.7 ± 0.96	26.5 ± 1.81

Table S3. ΣFIC results of VCM-PS6 for the *in vitro* antibacterial activity against *S. aureus* and MRSA.

	ΣFIC		Results	
	S. aureus	MRSA	*S. aureus*	MRSA
VCM-PS6	1.01	0.25	Indifference	Synergy

FTIR SPECTRA

Hyaluronic acid (HA)

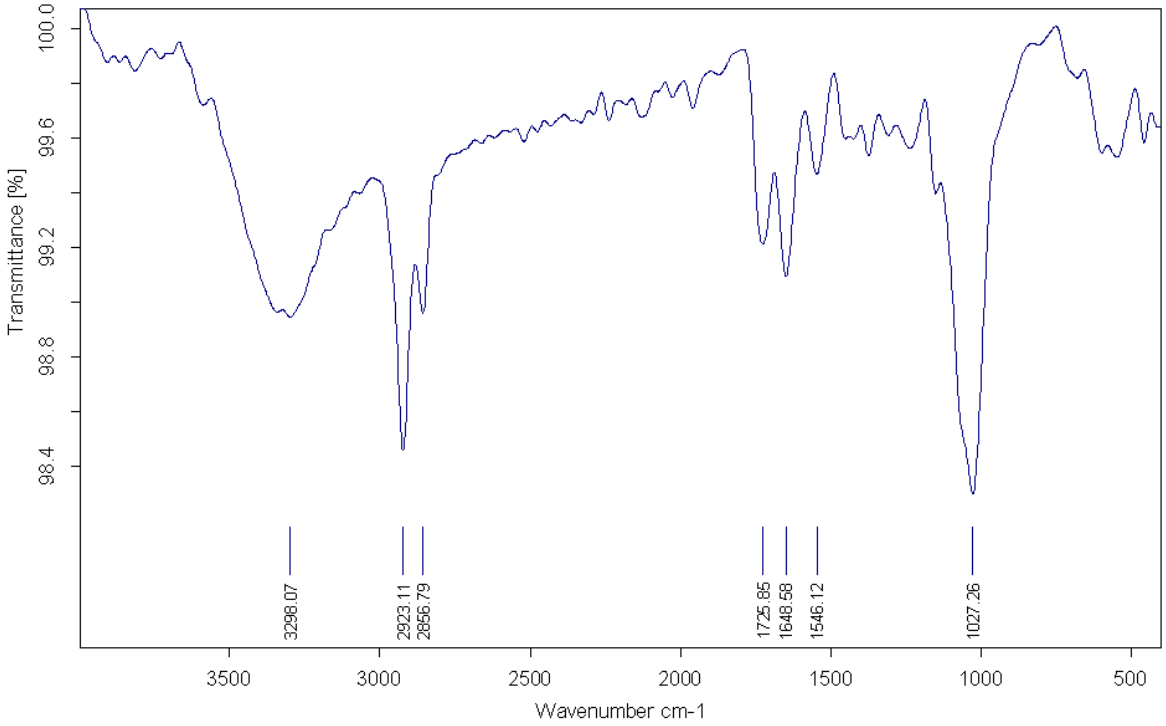

Hyaluronic acid-Oleylamine6 (HA-OLA6)

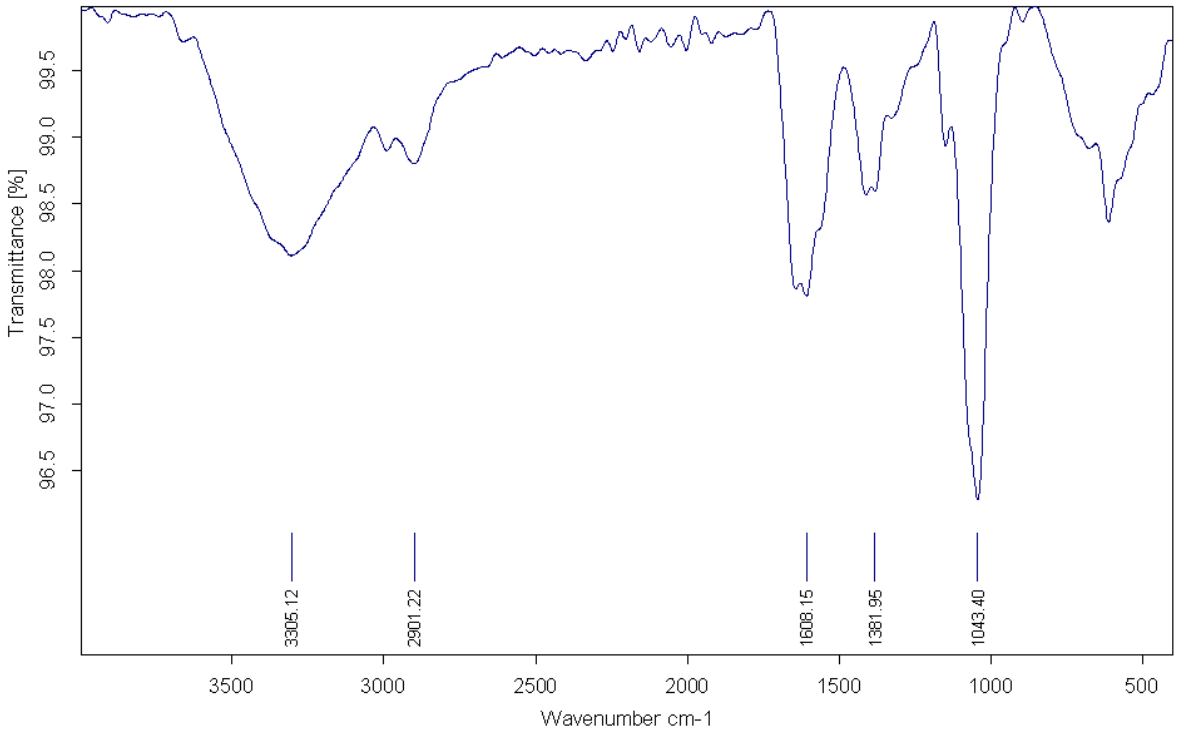

Hyaluronic acid-Oleylamine8 (HA-OLA8)

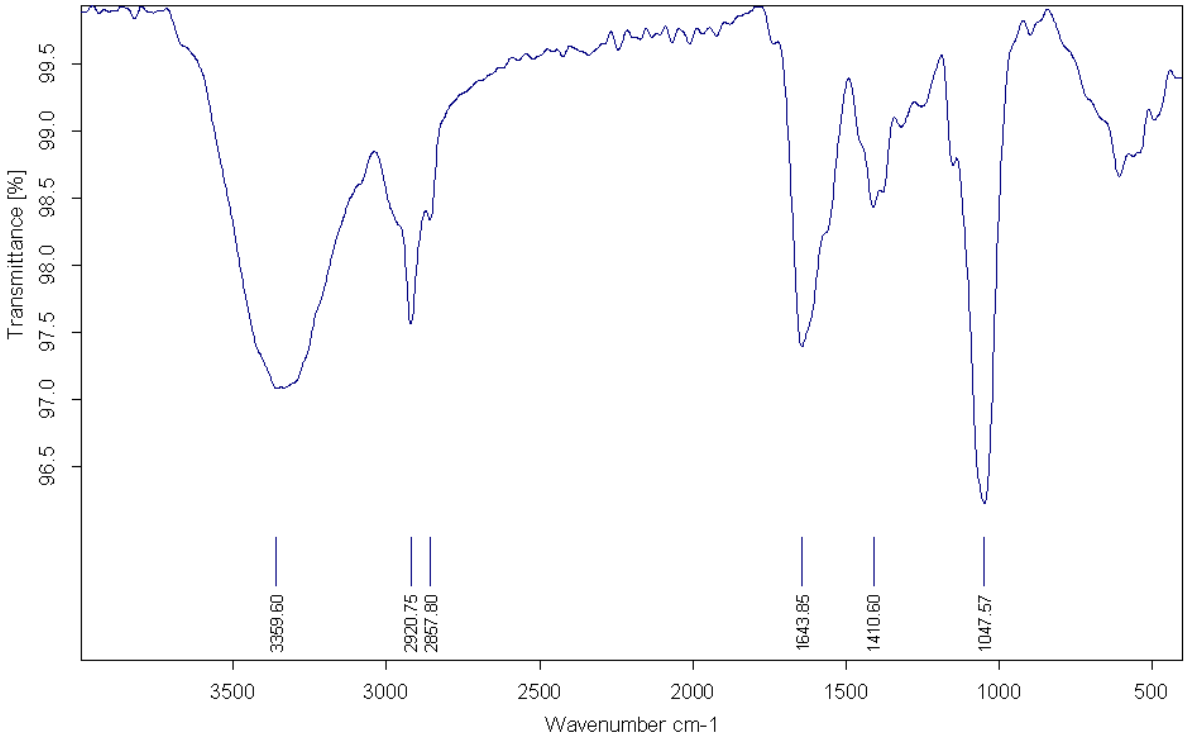

^{1}H NMR SPECTRA

Hyaluronic acid (HA)

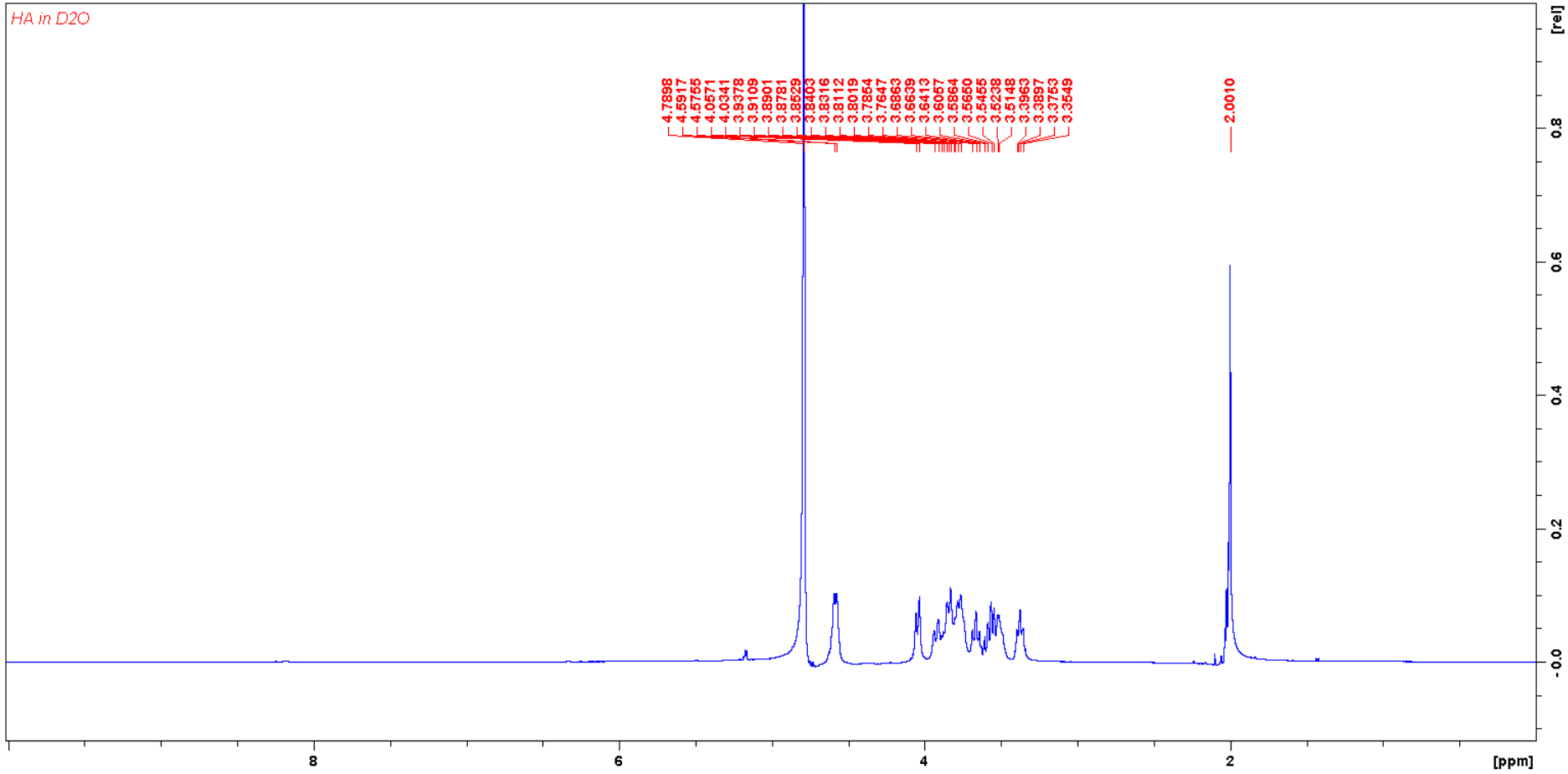

Hyaluronic acid-Oleylamine6 (HA-OLA6)

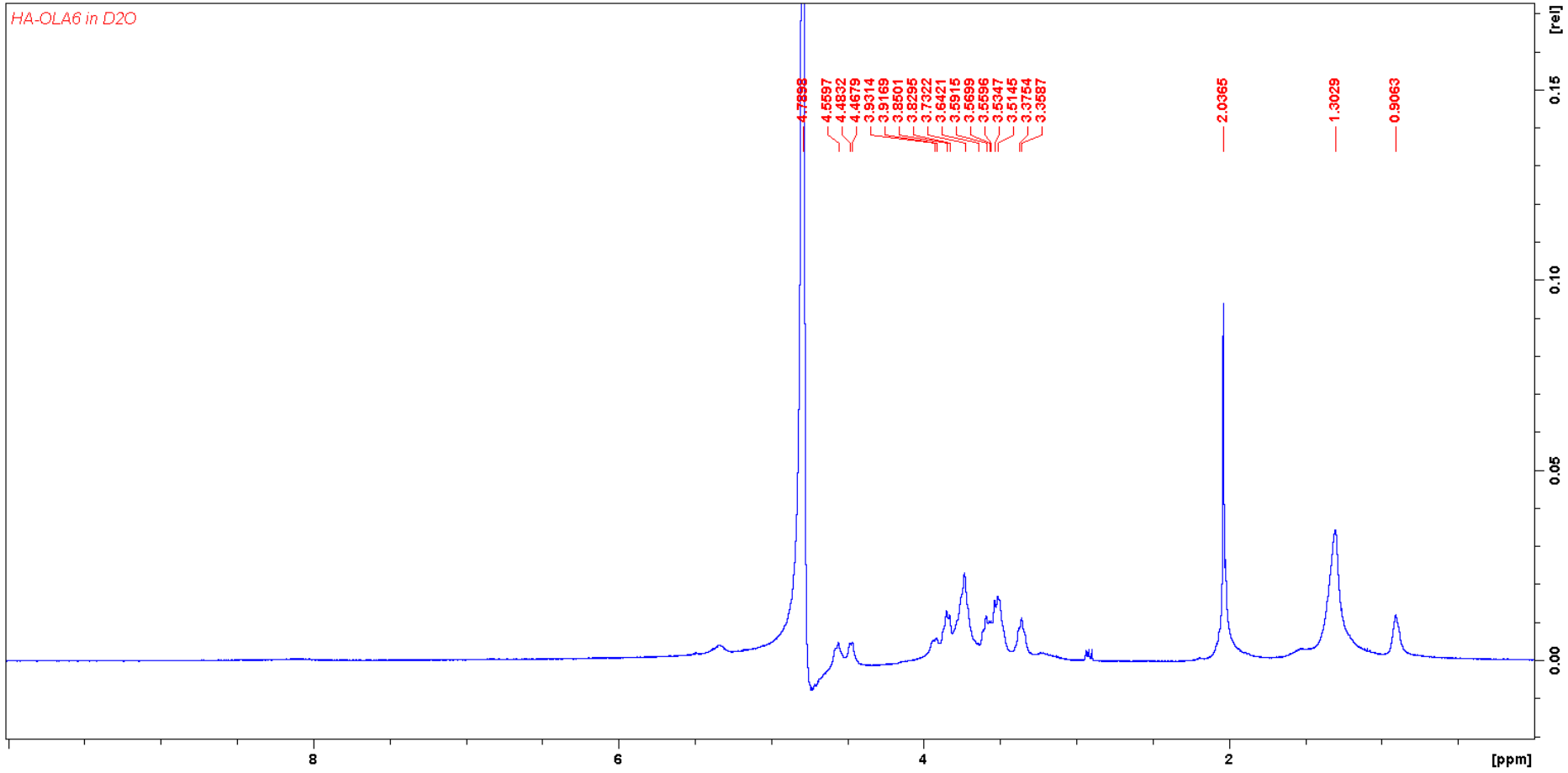

Hyaluronic acid-Oleylamine8 (HA-OLA8)

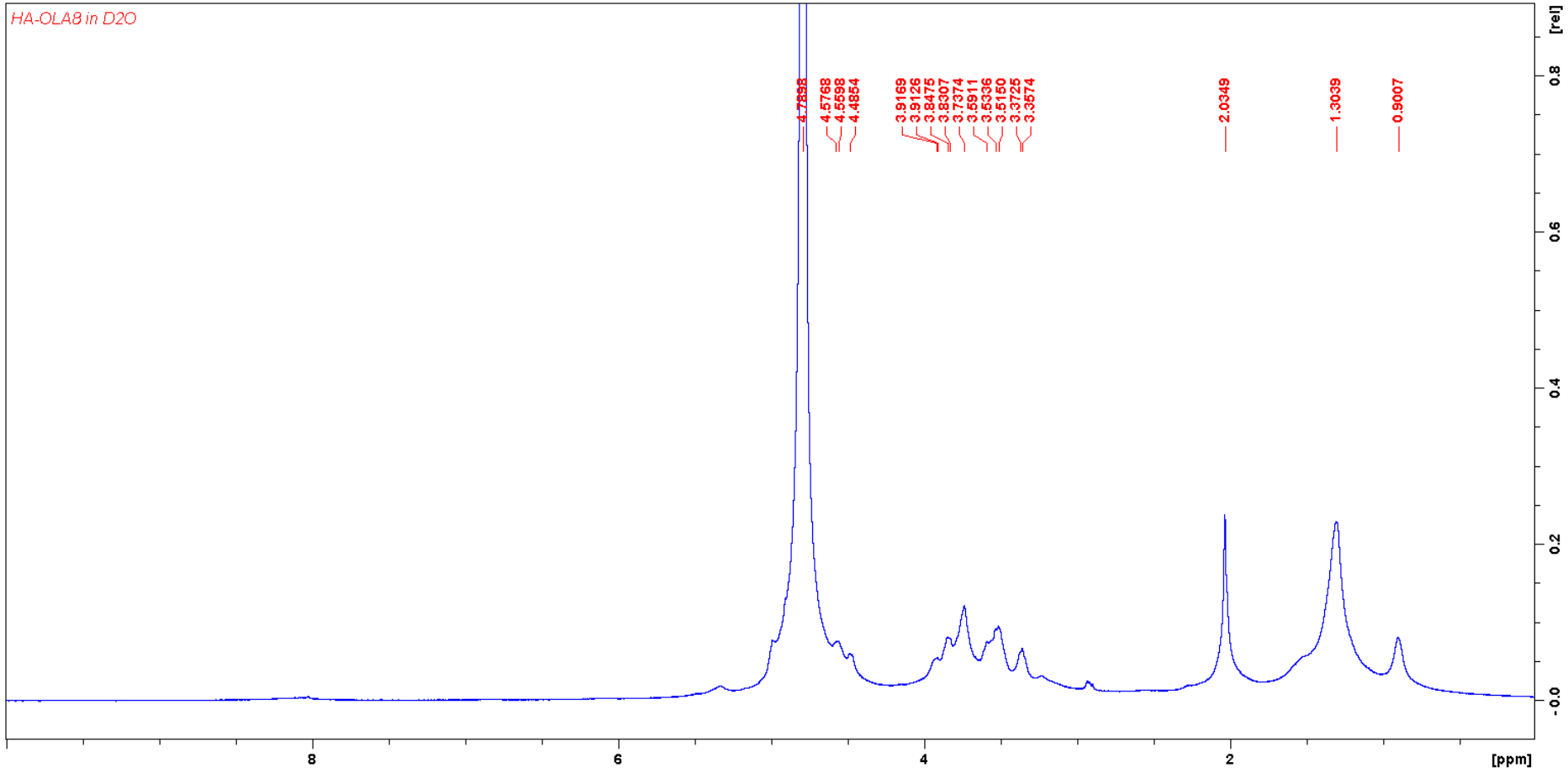

Submissions Being Processed for Author Thirumala Govender, Ph.D.

Page: 1 of 1 (1 total submissions)

Display 10 results per page.

Action	Manuscript Number	Title	Initial Date Submitted	Status Date	Current Status
View Submission		Self-assembled oleylamine grafted hyaluronic acid polymersomes for delivery of vancomycin against methicillin resistant Staphylococcus aureus (MRSA)	May 09, 2019	May 09, 2019	Submitted to Journal

Page: 1 of 1 (1 total submissions)

Display 10 results per page.

<< Author Main Menu

Submission Confirmation

Print

Thank you for your submission

Submitted to
Nanotechnology

Manuscript ID
NANO-121995

Title
Supramolecular Lipidation of Novel Antimicrobial Peptides Enhances Antimicrobial Activity Against Methicillin-Resistant Staphylococcus aureus (MRSA)

Authors
Faya, Mbuso
Hazzah, Heba. A
Omolo, Calvin A.
Agrawal, Nikhil
Maji, Ruma
Walvekar, Pavan
Mocktar, Chundereka
Nkambule, Bongani
Albericio, Fernando
de la Torre, Beatriz G.
Govender, Thiru

Date Submitted
09-May-2019

Author Dashboard